BERGISCHE
UNIVERSITÄT
WUPPERTAL

Mobilization, Methylation, and Ethylation of Mercury in Contaminated Floodplain Soils under Controlled Laboratory Redox Conditions as Influenced by Potential Immobilizing Agents as well as Mobilization of Mercury under Field Conditions

Dissertation
zur Erlangung eines Doktorgrades
(Dr.-Ing.)

in der
Fakultät für Architektur und Bauingenieurwesen
der
Bergischen Universität Wuppertal

vorgelegt von
Felix Beckers
aus Herdecke

Wuppertal 2018

The PhD thesis can be quoted as follows:

urn:nbn:de:hbz:468-20200218-105208-2
[http://nbn-resolving.de/urn/resolver.pl?urn=urn%3Anbn%3Ade%3Ahbz%3A468-20200218-105208-2]

DOI: 10.25926/n4rq-qd34
[https://doi.org/10.25926/n4rq-qd34]

Eingereicht am: 17.10.2018
Prüfung am: 26.02.2019

Prüfungskommission:

Erster Gutachter:
Univ.-Prof. Dr.-Ing. agr. Jörg Rinklebe
LuFG Boden- und Grundwassermanagement
Bergische Universität Wuppertal

Zweiter Gutachter:
Prof. Pablo León Higueras
Institut für Angewandte Geologie
Universität Kastilien-La Mancha, Spanien

Vorsitzender:
Univ.-Prof. Dr.-Ing. Andreas Schlenkhoff
LuFG Wasserwirtschaft und Wasserbau
Bergische Universität Wuppertal

Weiteres Mitglied:
Univ.-Prof. Dr.-Ing. Steffen Anders
LuFG Werkstoffe im Bauwesen
Bergische Universität Wuppertal

"A work as this is never finished, one must simply declare it finished, when one has, within limits of time and circumstances, done what is possible."

"So eine Arbeit wird eigentlich nie fertig, man muss sie für fertig erklären, wenn man nach Zeit und Umständen das Möglichste getan hat."

(Johann Wolfgang von Goethe)

Table of content

Abbreviations

AAS	Atomic absorption spectrometry
AED	Atomic emission detector
AG Boden	Arbeitsgemeinschaft Boden
BAM	Bundesanstalt für Materialforschung und -prüfung
BC	Biochar based material
BC200	Biochar pyrolyzed at 200 °C
BC500	Biochar pyrolyzed at 500 °C
BBodSchV	Bundes-Bodenschutz- und Altlastenverordnung
CEC_{eff}	Effective Cation-exchange capacity
C/N	Carbon/nitrogen ratio
CS	Contaminated soil
CS+BC	Contaminated soil + biochar based material (biochar)
CS+BC200	Contaminated soil + biochar pyrolyzed at 200 °C
CS+BC500	Contaminated soil + biochar pyrolyzed at 500 °C
CS+SBFL	Contaminated soil + sugar beet factory lime
CV-AFS	Cold vapor atomic fluorescence spectrometry
DIC	Dissolved inorganic carbon
DN	Dissolved nitrogen
DOC	Dissolved organic carbon
EC	Electrical conductivity
e.g.	*Exemple gratia* (for example)
E_H	Redox potential
EtHg	Ethylmercury
EtHgCl	Ethylmercury chloride
$(Et)_3PbCl$	Triethyllead chloride
$(Et)_4Pb$	Tetraethyllead
FeRB	Iron-reducing bacteria
FLm	Mollic Fluvisol
GC-AED	Gas chromatograph-atomic emission detector
GLA-SA	Geologisches Landesamt Sachsen-Anhalt
GLmk	Calcic-Mollic Gleysol
GW	Groundwater
Hg(0)	Elemental mercury
Hg_t	Total mercury
ICP-OES	Inductively coupled plasma optical emission spectrometry

i.e.	*Id est* (that is)
IUSS	International Union of Soil Science
IUSS-FAO	International Union of Soil Science – Food and Agriculture Organization
LAU	Landesamt für Umwelt
LCF	Linear combination fitting
MC	Microcosm
MeHg	Methylmercury
N	Number of samples
NIST	National Institute of Standards and Technology
OC	Organic carbon
OM	Organic matter
p	Probability
PDMS	Polydimethylsiloxane
pH	$-\log_{10}[H^+]$, measure of hydrogen ion concentration
PLFA	Phospholipid fatty acids
PTFE	Polytetrafluorethylen
PVC	Polyvinyl chloride
PWP	Pore water pressure
r	Pearson's correlation coefficient
rpm	Revolutions per minute
RSD	Relative standard deviation
SBFL	Sugar beet factory lime
SOB	Sulfur-oxidizing bacteria
SPME	Solid phase microextraction
SRB	Sulfate-reducing bacteria
$SUVA_{254}$	Specific UV absorbance at 254 nm
TC	Total carbon
UIT	Umwelt- und Ingenieurtechnik GmbH Dresden
U.S. EPA	U.S. Environmental Protection Agency
XANES	X-ray absorption near-edge structure

List of tables

List of figures

Summary

Mercury (Hg) is an important pollutant in soils and sediments and its species are highly toxic for humans. Soil components such as minerals and dissolved organic carbon (DOC) provide binding sites for Hg species. The amount and the chemical structures of the binding sites determine the concentration of dissolved Hg in soil solution which is furthermore influenced by several parameters including redox potential (E_H), pH value, amount of DOC, chemistry of sulfur (S), chloride (Cl^-), and iron (Fe). The impact and relative importance of these parameters on the mobility and speciation of Hg is not fully understood. This is particularly true for floodplain soils where flooding induces substantial biogeochemical changes affecting Hg mobilization. Amendments can be used to immobilize dissolved Hg species including highly toxic methylmercury (MeHg).

Therefore, the general objective of this work was to systematically and experimentally quantify the impact of flooding events with their associated E_H and pH changes on the release of Hg_t and the release and formation of Hg species. Furthermore, the capability of different amendments such as biochars and sugar beet factory lime (SBFL) to impede Hg mobilization and to hamper the formation of MeHg and ethylmercury (EtHg) was examined. The presence of sulfate-reducing bacteria (SRB) as important Hg methylators was investigated via quantification of specific phospholipid fatty acids (PLFAs).

The approach of the current thesis is based on laboratory experiments utilizing biogeochemical microcosms to simulate flooding and on a field study conducted by means of soil hydrological monitoring stations. By this it was aimed to verify whether results gained by the laboratory experiments are in accordance with those achieved in the field study.

Contaminated Wupper River floodplain soil was flooded in the course of the microcosm experiments. In a first microcosm experiment mobilization of Hg_t and the release and formation of MeHg and EtHg in the contaminated soil (CS) was studied as well as the impact of the amendments biochar based material (BC) and sugar beet factory lime (SBFL) on these processes. Released Hg_t concentrations of CS were very high (5.4-41.9 µg/l). Biochar based material and SBFL as amendments for CS proved to be appropriate to diminish the Hg_t mobilization even under dynamic redox conditions. SBFL efficiently reduced soluble Hg_t of CS by 65% while BC resulted in a reduction by 21%. No perceivable influence of BC and SBFL on MeHg and EtHg concentrations was detected. The higher methylation efficiency in CS+SBFL indicated by the $MeHg/Hg_t$ ratio counterbalanced the benefit of lower Hg_t release. The stimulation of microbial growth including SRB by SBFL deduced from PLFA abundances appears to be the reason for this finding. In general, the mobiliza-

tion of Hg_t, MeHg, and EtHg decreased with increasing E_H irrespective of soil treatment. A strong positive correlation between Hg_t and DOC was found in CS and CS+BC probably based on the strong interaction of Hg with thiol groups of DOC. Furthermore, Hg_t correlated positively with pH and SO_4^{2-} and negatively with Fe, Mn, and PO_4^{3-} (in CS solely). There was no apparent effect of Cl^- on Hg mobility. With SBFL as amendment such correlations were not observed which can be explained by the efficient Hg adsorption to the lime's high content in calcium carbonate. However, EtHg correlated well with Hg_t and MeHg in CS+SBFL. Canonical discriminant analysis (CDA) clearly corroborated the finding that both amendments, BC and SBFL, significantly changed the soil's biogeochemistry with SBFL provoking a more pronounced and distinct change.

The addition of pine cone biochars produced via pyrolysis at 200 °C (BC200) and 500 °C (BC500) to CS in the course of the second microcosm experiment showed little impact on the release of Hg_t and on the release and formation of MeHg and EtHg. However, under highly reduced conditions at a redox potential around -110 mV, Hg_t concentrations were considerably lower in treatments with BC200 (16 µg/l) and BC500 (14 µg/l) compared to CS (28 µg/l). Similar results were found at a E_H of -122 mV when biochar based material (BC) was used to immobilize Hg_t. The redox potential correlated negatively with pH in the slurry of CS and also of biochar amended CS. For CS a significant positive correlation between Hg_t and pH and a strong negative relationship between Hg_t and E_H was determined. The alteration of E_H resulted in a substantial Hg_t release from CS with Hg_t concentrations between 1.8-52.0 µg/l which exceed those in natural fresh water systems by far.

Besides Hg_t also EtHg correlated negatively with E_H while the concentrations of MeHg did not correlate with E_H. EtHg concentrations appear closely related to Hg_t concentrations. Interestingly, Hg methylation in CS and the treatments was determined at higher E_H than expected, i.e. between -50 mV and 100 mV. Correspondingly, we observed a decline in the SO_4^{2-} to Cl^- ratio as an indicator of SO_4^{2-} reduction by Hg methylating SRBs. Ethylmercury patterns compared between CS and the treatments differed only slightly pointing at best to a weak influence of the biochars on EtHg dissolution/formation. A significant relationship between pH and MeHg concentrations was found exclusively for CS+BC500. Increased pH correlated positively with MeHg. Positive correlations between Hg_t and DOC were found for CS and the treatments with BC200 and BC500. Total Hg concentrations in CS and the treatments were negatively correlated with Cl^-.

The field study was conducted at the Saale-Elbe confluence by establishing two soil hydrological monitoring stations. The data gathered from this field study are difficult to inter-

pret. It was observed that rising water levels during flooding result in fast and significant E_H changes which, however, did not exhibit a direct impact on Hg(II) concentrations. Possibly, the alterations were too fast to attain respective Hg adsorption/desorption equilibria. Another problem is that Hg(II) concentrations in precipitation samples were in the same range as those from soil solutions obtained from different depths of the Saale 1 and 2 sites. Consequently, the origin of Hg(II) in the soil solution samples which can be either precipitation or soil derived remains unclear.

The main conclusions are: (1) Results from the laboratory and field studies show that flooding events and their associated geochemical alterations including concomitant E_H reductions result in higher Hg mobilization. (2) Soil amendments are suitable to immobilize dissolved Hg_t. However, SBFL was more efficient in this respect than the tested biochars. It has to be examined whether this is also true for different soils and conditions, in particular in acidic or high salt environments. (3) Phospholipid fatty acid profiles indicate that SRB were the primary Hg methylators in the microcosm experiments and that SRB are capable to methylate Hg at higher E_Hs than expected. (4) Ethylation of Hg seems to be favored at E_H 0 mV.

Zusammenfassung (Summary in German)

Quecksilber (Hg) stellt eine bedeutsame Kontamination in Böden und Sedimenten dar und seine Verbindungen sind für den Menschen höchst toxisch. Bodenbestandteile wie mineralische Komponenten und gelöster organischer Kohlenstoff (DOC) bieten Bindungsstellen für Quecksilberspezies. Anzahl und chemische Struktur verfügbarer Bindungsstellen bestimmen die Konzentration von frei gelöstem Hg in der Bodenlösung. Sie wird von verschiedenen Parametern wie dem Redoxpotential (E_H), dem pH-Wert und der DOC-Menge sowie der Konzentration an Chlorid (Cl^-) und Eisen (Fe) beeinflusst. Der Einfluss und die relative Bedeutung dieser Parameter in Bezug auf die Mobilität und Speziierung von Hg ist nur unzureichend bekannt. Dies trifft insbesondere für Auenböden zu, wo Überflutungen zu maßgeblichen biogeochemischen Veränderungen im Boden führen, die die Hg-Mobilisierung beeinflussen. Bodenzusätze können eingesetzt werden, um gelöstes Hg zu immobilisieren, darunter auch das hochtoxische Methylquecksiber (MeHg).

Die allgemeine Zielsetzung dieser Arbeit war es daher, den Einfluss von Überflutungen und der damit assoziierten geochemischen Veränderungen auf die Mobilisierung und Bildung von Hg-Spezies systematisch und experimentell zu untersuchen. Des Weiteren wurde das Potential von Bodenzusätzen wie Biokohle (BC) und Zuckerrübenfabrik-Kalk (SBFL) untersucht, die Hg-Mobilisierung sowie die Bildung von MeHg und Ethylquecksilber (EtHg) zu unterdrücken. Das Vorkommen sulfatreduzierender Bakterien (SRB) als bedeutende Hg-Methylierer sollte mittels Quantifizierung spezifischer Phospholipid-Fettsäuren (PLFA) nachgewiesen werden.

Die methodische Vorgehensweise der vorliegenden Dissertation basiert auf Laborexperimenten unter Nutzung biogeochemischer Mikrokosmen zur Simulation von Überflutungen und auf einer Feldstudie unter Nutzung hydrologischer Messstationen. Schließlich sollte überprüft werden, inwieweit Ergebnisse der experimentellen und der Feldstudien miteinander in Übereinstimmung gebracht werden können.

Kontaminierter Boden aus der Wupper-Überflutungszone (CS) wurde in Mikrokosmen-Experimenten unter Simulation einer Überflutung eingesetzt. In einem ersten Experiment wurde die Mobilisierung von Hg_t sowie die Freisetzung und Bildung von MeHg und EtHg im kontaminierten Boden (CS) sowie der Einfluss der Zusätze BC (biochar based material) und SBFL auf diese Prozesse untersucht. Die freigesetzten Hg_t-Konzentrationen waren sehr hoch (5.4-41.9 µg/l). BC und SBFL stellten sich als geeignete Zusätze zur Verringerung der Hg_t-Konzentration selbst unter dynamischen Redoxbedingungen heraus.

SBFL reduzierte Hg_t im CS effizient um 65% während BC nur zu einer Verminderung um 21% führte. Ein deutlicher Einfluss von BC und SBFL auf MeHg und EtHg konnte nicht verzeichnet werden. Die höhere Methylierungsrate in CS+SBFL, angezeigt durch das höhere MeHg/Hg_t-Verhältnis, wirkte dem positiven SBFL-Einfluss durch verminderte Hg_t-Freisetzung entgegen. Vermutlicher Hintergrund ist die Stimulation des mikrobiellen Wachstums einschließlich der SRB durch SBFL, welches über die analysierten PLFA nachgewiesen wurde. Generell nimmt die Mobilisierung von Hg_t, MeHg und EtHg mit steigendem E_H unabhängig von der Bodenbehandlung ab. Eine deutlich positive Korrelation zwischen Hg_t und DOC wurde sowohl in CS als auch in CS+BC gefunden, was wahrscheinlich auf der starken Interaktion zwischen Hg und Thiolgruppen des DOC beruht. Weiterhin korrelierte Hg_t positiv mit dem pH und SO_4^{2-} und negativ mit Fe, Mn und PO_4^{3-} (nur in CS). Ein offensichtlicher Effekt von Cl^- auf die Hg-Mobilität war nicht nachweisbar. Mit SBFL als Zusatz wurden solche Korrelationen nicht beobachtet, was durch die effiziente Hg-Adsorption an das im SBFL in hohem Anteil vorkommende Calciumkarbonat erklärt werden kann. Allerdings korreliert in CS+SBFL Hg_t mit MeHg sehr gut. Die kanonische Diskriminanzanalyse bestätigte den Befund, dass beide Zusätze – BC und SBFL – die biogeochemischen Eigenschaften des Bodens signifikant verändert haben, wobei SBFL zu distinkten und deutlicheren Effekten führte als BC.

Die Zugabe von Kieferzapfen-Biokohlen, die bei einer Pyrolysetemperatur von 200 °C (BC200) bzw. 500 °C (BC500) hergestellt und im Verlauf des zweiten Mikrokosmenexperimentes verwendet wurden, zeigte nur geringen Einfluss auf die Freisetzung von Hg_t sowie auf die Freisetzung und Formation von MeHg und EtHg. Unter stark reduzierenden Bedingungen bei einem E_H von etwa -110 mV waren die Hg_t-Konzentrationen in den Behandlungen mit BC200 (16 µg/l) und BC500 (14 µg/l) deutlich geringer als in CS (28 µg/l). Bei der Verwendung von BC im Rahmen des ersten Mikrokosmen-Experimentes wurde ein vergleichbares Ergebnis bei einem E_H von -122 mV erzielt. Das Redoxpotential korrelierte sowohl in der Aufschlämmung von CS als auch in den Aufschlämmungen der behandelten Böden negativ mit den pH-Werten. Für CS zeigte sich eine positive Korrelation zwischen Hg_t und pH und eine deutlich negative Beziehung zwischen Hg_t und E_H. Die Veränderungen des E_H führte zu einer beträchtlichen Hg_t-Freisetzung in CS mit Hg_t-Konzentrationen zwischen 1,8 und 52,0 µg/l, welche die Konzentrationen in natürlichen Frischwassersystemen bei weitem überschreiten.

Neben Hg_t korrelierte auch EtHg negativ mit dem E_H, während MeHg-Konzentrationen nicht mit dem E_H korrelierten. Die EtHg-Konzentrationen scheinen eng mit den Hg_t-

Konzentrationen zusammenzuhängen. Interessanterweise fand Hg-Methylierung in CS und den behandelten Böden unter höherem E_H statt als erwartet, das bedeutet zwischen -50 mV und 100 mV. Übereinstimmend fanden wir eine Absenkung des Sulfat/Chlorid-Verhältnisses, welches als Indikator für Sulfatreduzierung durch Hg-methylierende SRB herangezogen werden kann. Die Konzentrationsverläufe von EtHg in CS und den behandelten Böden weichten nur geringfügig voneinander ab, was auf einen schwachen Einfluss der Biokohlen auf die EtHg-Freisetzung oder -Bildung hindeutet. Ein signifikanter Zusammenhang zwischen pH und MeHg-Konzentrationen wurde nur in CS+BC500 detektiert. Der Anstieg des pH korrelierte positiv mit MeHg-Konzentrationen. Außerdem wurden positive Zusammenhänge zwischen Hg_t und DOC in CS und den BC200 und BC500 behandelten Böden gefunden. Die Konzentration von Gesamtquecksilber in CS und den behandelten Böden korrelierten negativ mit Cl^-.

Die Feldstudie wurde mittels zweier bodenhydrologischer Intensivmessstationen am Zusammenfluss von Saale und Elbe durchgeführt. Die erhobenen Daten sind schwierig zu interpretieren. Es wurde beobachtet, dass ansteigende Wasserstände während Überflutungen zu schnellen und deutlichen Änderungen des E_H in den Bodenlösungen führen können, welche keinen direkten Einfluss auf die Hg(II)-Konzentrationen zeigten. Möglicherweise waren die Änderungen zu schnell, um entsprechende Hg-Adsorptions-/Desorptionsgleichgewichte zu erreichen. Ein weiteres Problem ist, dass die Hg(II)-Konzentrationen in den Niederschlagsproben vergleichbar mit denen der Bodenlösungen von Saale 1 und Saale 2 waren. Die Herkunft von Hg(II) in der Bodenlösung blieb unklar, da sowohl der Niederschlag als auch der Boden selbst als Quellen in Betracht zu ziehen sind.

Die wichtigsten Ergebnisse sind: (1) die Ergebnisse aus dem Labor und der Feldstudie zeigen, dass Überflutungen und die mit ihnen einhergehenden geochemischen Veränderungen, wie E_H-Absenkungen, zu einer höheren Hg-Mobilisierung führen. (2) Bodenzusätze sind geeignet, gelöstes Hg_t zu immobilisieren. Diesbezüglich war SBFL effektiver als die getesteten Biokohlen. Es sollte untersucht werden, ob dies auch für unterschiedliche Böden und Bedingungen zutrifft, insbesondere in sauren und sehr salzigen Umgebungen. (3) Phospholipidfettsäure-Profile deuten an, dass die Methylierung von Hg in den Mikrokosmenexperimenten hauptsächlich durch SRB erfolgte und dass SRB dies auch unter höheren E_H-Werten als erwartet vollziehen. (4) Hg-Ethylierung scheint bei einem E_H von 0 mV begünstigt zu sein.

1. Introduction

1.1 General aspects

Due to geological processes or caused by anthropogenic activities soils can contain substances, particularly toxic ones, with an impact on the environment including animals and plants and on human health. The food chain and the drinking water constitute potential pathways by which soil contaminants find their way into the human body. Therefore, it is important to know the mechanisms by which contaminants are bound to and released from soil components and how these processes can be controlled. On this background, mercury (Hg) in its different chemical and highly toxic forms or species will be considered here.

1.2 Properties of mercury

Mercury is a heavy, glistening, silvery-white metal with a faint bluish tinge and the only metal that is liquid at room temperature. It is relatively stable, dense and has high surface tension. Below its melting point, Hg is a white solid and in its gaseous state, it is a colorless vapor. Elemental mercury is highly volatile so that a saturated atmosphere of Hg vapor contains approximately 18 mg Hg/m^3 at 24.0 °C (Satoh, 2013). The volatility of Hg further increases with rising temperature and accounts for its presence in the atmosphere in appreciable amounts (Wang et al., 2004; Sigler and Lee, 2006; Zhang et al., 2016). Both properties of elemental Hg, volatility and also its solubility in water (Table 1-1) are important with respect to dispersal in the environment and exposure to humans. Mercury has seven stable isotopes (Meija et al., 2010; Beckers and Rinklebe, 2017), a property which can be exploited for analytical purposes (Blum et al., 2014; Yin et al., 2016; Washburn et al., 2017).

General properties of elemental mercury are listed in the following Table 1-1.

Table 1-1: General properties of elemental mercury. Data from (Adriano, 2001; Eisler, 2006; Meija et al., 2010; Zheng et al., 2012).

Property	**Value**
atomic number	80
standard atomic weight	200.5924(8)
melting point	-38.8 °C
boiling point	356.7 °C
density	13.534 g/cm^3
specific gravity	13.55
vapor pressure	1.22 x 10^{-3} mm at 20 °C 2.8 x 10^{-3} mm at 30 °C
aqueous solubility	5.6 x 10^{-7} g/l at 25 °C

Mercury may be present in three oxidation states: 0 (elemental or metallic mercury), I (monovalent or mercurous mercury), and II (divalent or mercuric mercury). The properties and chemical behavior of Hg depend on the oxidation state. Metallic mercury and Hg(II) are stable under normal environmental conditions while mercurous mercury is not stable since it dismutates into Hg(0) and Hg(II) (Schuster, 1991; Schroeder and Munthe, 1998); Hg(0) and Hg(II) are the two main naturally occurring oxidation states. Nevertheless, both Hg(I) and Hg(II) form numerous inorganic and organic chemical compounds (Zheng et al., 2012). The chemical and physicochemical properties of these compounds may vary considerably (Table 1–2). Accordingly, Hg species abundance varies between different environmental compartments: More than 95% of the Hg encountered in the atmosphere is elemental Hg vapor (Stein et al., 1996; Zhang et al., 2013; Megaritis et al., 2014). Most Hg in water, soils, and sediments is in the inorganic Hg(II) form while (mono)methylmercury (MeHg; CH_3Hg^+) is dominant in biota.

Table 1-2: Properties of several mercury compounds (modified from Zheng et al., 2012).

	Name	Molar weight [g/mol]	Melting point [°C]	Boiling point [°C]	Decomposition / sublimate temperature [°C]	Density [g/cm³]	Aqueous solubility [g/l at 25 °C]
Hg(0)	Elemental mercury	200.59	-38.8	356.7	n.a.	13.534	5.6×10^{-7}
Hg_2Cl_2	Mercurous chloride	472.09	525	n.a.	383	7.15	0.002
$HgCl_2$	Mercuric chloride	271.50	277	302	n.a.	5.43	28.6
Hg_2SO_4	Mercurous sulfate	497.24	n.a.	n.a.	n.a.	7.56	0.51
$HgSO_4$	Mercuric sulfate	296.66	n.a.	n.a.	450	6.47	Decomposes
HgS	Mercury sulfide	232.66	n.a.	446-583	580	8.10	Insoluble
HgO	Mercuric oxide	216.59	n.a.	356	500	11.14	Insoluble
Hg_2Br_2	Mercurous bromide	560.99	405	n.a.	340-350	7.307	3.9×10^{-4}
$Hg\text{-}Br_2$	Mercuric bromide	360.44	237	322	n.a.	6.03	Slightly soluble
Hg_2l_2	Mercurous iodide	654.98	n.a.	n.a.	140	7.7	Slightly soluble
Hgl_2	Mercuric iodide	454.4	259	350	n.a.	6.36	0.06
Hg_2F_2	Mercurous fluoride	439.18	n.a.	n.a.	570	8.73	Decomposes
HgF_2	Mercuric fluoride	238.59	645	650	645	8.95	Soluble, reacts
$Hg_2(NO_3)_2$	Mercurous nitrate	525.19	n.a.	n.a.	70 (dihydrate)	4.8 (dihydrate)	Slightly soluble, reacts
$Hg(NO_3)_2$	Mercuric nitrate	324.7	79	n.a.	n.a.	4.3	Soluble
$Hg(CN)_2$	Mercuric cyanide	252.63	320	n.a.	n.a.	3.996	Soluble

n.a.: not available

1.3 Mercury in the environment

1.3.1 Natural and anthropogenic sources of mercury

Mercury is a naturally occurring rare element with ubiquitous appearance in the environment; including soils and all types of rocks, in at least trace concentrations, especially enriched in volcanic regions. More than 95 minerals of Hg are known; the most abundant Hg compound is HgS, which occurs in three polymorphs: cinnabar, metacinnabar, and extremely rare hypercinnabar (Hazen et al., 2012; IMA, 2018). Nearly all Hg mined is extracted from cinnabar (α-HgS, 86.2% Hg) ores. However, commercial mining operations have exploited deposits of corderoite ($Hg_3Cl_2S_2$, 81.7% Hg), livingstonite ($HgSb_4S_8$, 21.2% Hg), metacinnabar (β-HgS, 86.2% Hg), and native mercury as well (Jasinski, 1995).
Mercury accumulation and cycling in the environment is influenced by both natural and anthropogenic activities (Beckers and Rinklebe, 2017). The Hg content of most igneous rocks is typically lower than 0.2 mg/kg (Adriano, 2001). In general, higher Hg contents can be found in rocks which are rich in organic matter (OM), i.e., clay rocks (Gworek et al., 2016). Due to this, sedimentary rocks often tend to contain more Hg than igneous rocks (Adriano, 2001; HDOH, 2012). Mercury has a strong affinity for OM, especially organic thiols, and it thus concentrates in black shales and coal and is also found in petroleum and natural gas deposits (Wilhelm, 2001; Hazen et al., 2012). It might be stated that the average Hg contents in soils of the world range from a few µg/kg to some hundred µg/kg (Beckers and Rinklebe, 2017). Mercury concentrations in plants vary significantly and depend on the ability of the plants to take up Hg (e.g. Rothenberg et al., 2012). Furthermore, it is suggested that a range of specific local environmental factors strongly influence the accumulation of Hg in plants and that they may outbalance the importance of local soil Hg contents (Siegel et al., 1987; Overesch et al., 2007; Hang et al., 2016). Extremely high Hg concentrations have been found in mushrooms (e.g. Melgar et al., 2009; Falandysz et al., 2015; Falandysz, 2017), which are among others considered as suitable and sensitive bioindicators for Hg in ecosystems (Kabata-Pendias, 2011; Lodenius, 2013; Bargagli, 2016).
Mercury concentrations in uncontaminated natural waters vary by the type of waterbody and location. In general, pure fresh water systems show wide ranges of Hg concentrations due to their diversity. However, the concentration range in river waters (1.0-5.0 ng/l) is not that large as these waterbodies commonly exhibit strong fluctuations and are subject to

dilution effects. The Hg concentrations in lake waters show a wide variation 0.2-80 ng/l, while Hg concentrations in groundwater are usually in the range 0.1-16 ng/l. The variation in rain is very pronounced and is in the range of 5.0-90 ng/l (Leopold et al., 2010). Mercury concentrations in contaminated waters can be significantly higher than in uncontaminated natural waters.

Mercury has wide applications in science, industry, and agriculture. Anthropogenic activities continue to release large amounts of Hg into the environment. World production, i.e. mining and processing of primary Hg ores plus by-production from mining of other metals, decreased to 2.035×10^3 tons per year in 1994 and has remained fairly constant since then (Hylander and Meili, 2003; UNEP, 2006). Although alternative solutions are implemented Hg has a major role as a process or product ingredient in several industrial sectors. Its biggest consumers in higher income countries are chlor-alkali industry, electrical and control instruments industry, laboratory products (e.g. barometers, thermometers, and vacuum pumps), dentistry (dental amalgams), and compact fluorescent as well as other energy-efficient lamps. In lower income countries, but not exclusively, there is also a demand for Hg in the vinyl chloride monomer production, artisanal and small-scale gold mining, batteries, cosmetic and skin-lightening creams, paints as well as in agriculture and forestry as ingredient of various types of pesticides (UNEP, 2006; Hazen et al., 2012). Mercury has been released in many ways into the environment in connection with its use including the release from Hg-containing car switches when the automobile is scrapped for recycling, from coal-fired powerplant emissions, and from incinerated Hg-containing medical devices. Horowitz et al. (2014) noted that small-scale gold mining in developing countries is presently the largest use of Hg globally and is continuing to grow. The particularly toxic species MeHg has been used in some fungicides but has no industrial purposes and basically occurs naturally where environmental conditions favor Hg net methylation (Hunter et al., 1940; Bakir et al., 1973; Beckers and Rinklebe, 2017).

Recently, the increasing awareness of Hg toxicity has led to the replacement of Hg in many areas. An international effort to ban Hg mining was made in line with the “Minamata Convention on Mercury”, a multilateral agreement to protect the human health and the environment from anthropogenic emissions and releases of Hg and Hg compounds (UNEP, 2013).

1.3.2 Mercury in soils and sediments and its emission to atmosphere

In general, sorption, fate, and mobility of Hg in soils are determined by a range of factors including soil composition such as soil texture, contents of OM, pedogenic (hydr)oxides and other organic and inorganic complexing agents as well as the specific stability of the bond between Hg and a ligand, the chemical form of Hg, pH and the redox potential (E_H) (e.g. Biester et al., 2002; Reis et al., 2010; Frohne et al., 2012; Gruba et al., 2014). Metallic Hg (Hg^0 or Hg(0)) may occur naturally as a large fraction of total Hg (Hg_t, the sum of all Hg species) content in soils in mineralized areas with a considerable flux of gaseous Hg(0) from geological sources, or may be found in the liquid form in soils and sediments seriously contaminated by local industry (Schlüter, 2000; Biester et al., 2002; Skyllberg, 2012; Kabata-Pendias and Szteke, 2015). However, as a matter of E_H/pH conditions and the presence of strong Hg sorbents in most soils and sediments divalent mercury (Hg(II)) is usually the most common Hg state in soils (Schlüter, 2000) and sediments (Chen et al., 2015; Leng et al., 2015; Amde et al., 2016). Divalent Hg reveals a high affinity to soil OM (Skyllberg et al., 2003; Ravichandran, 2004; Skyllberg et al., 2006). In consequence, high Hg contents are often accompanied by high organic carbon values (Wallschläger et al., 1998a; Wallschläger et al., 1998b; O'Driscoll et al., 2011; Obrist et al., 2011). Accordingly, higher levels of Hg between 1 and 2 mg/kg are frequently found in organic-rich, forest and peaty soils, in areas used for paddy cultivation (Clifford et al., 2010) as well as in floodplain soils (e.g. Devai et al., 2005; Overesch et al., 2007; Rinklebe et al., 2009; Rinklebe et al., 2010; Frohne and Rinklebe, 2013). According to Gabriel and Williamson (2004) the second major sorbent of Hg in terrestrial environments next to OM are inorganic oxides. Several factors exert influence on the adsorption: The pH is one of the most important factors controlling adsorption of Hg since it affects both surface charge characteristics of soil particles and metal speciation in solution. Another important factor influencing the fate of Hg within the soil and sediment profile is its complexation by dissolved organic carbon (DOC) (Wallschläger et al., 1996). Generally, DOC concentrations increase with increasing soil pH (Adriano, 2001). Accordingly, Yin et al. (1996) were able to show that adsorption of Hg(II) was significantly reduced at low pH when soil was treated with hydrogen peroxide to oxidize OM.

The adsorption of MeHg by soils is subject to the influence of the same factors that control the adsorption of inorganic Hg(II) (Adriano, 2001). Non-adsorbed Hg remains in soil solution. The speciation of water-soluble Hg in soil is still not fully understood. It is estimated that complexes of Hg oxides, chlorides, oxychlorides and sulfates are the dominant Hg

forms in soil solutions (Yin et al., 2013). These compounds are mobile Hg species which may be subject to both physical (leaching, erosion, and volatilization) and biochemical transformations (methylation, photochemical and biological reduction) and may precipitate or be taken up by organisms (Morel et al., 1998; Yin et al., 2013).

Leopold et al. (2010) stated that any Hg released into the environment undergoes biogeochemical transformation processes and may, therefore, be converted into the highly toxic compound MeHg. The formation of MeHg is mainly microbially mediated. Today, it is accepted that Hg methylation occurs primarily under anaerobic conditions and that sulfate-reducing bacteria (SRB) mainly govern this methylation process (Jeremiason et al., 2006; Feyte et al., 2012; Tjerngren et al., 2012a; Hsu-Kim et al., 2013; Parks et al., 2013; Janssen et al., 2016). Organic-rich floodplain soils have been identified as places of Hg methylation and sources for enhanced MeHg contribution to adjacent streams (e.g. Devai et al., 2005; Stoor et al., 2006). In line with the presence of decomposable OM, particulate organic carbon and DOC were reported to be related to Hg methylation (Ullrich et al., 2001; Matsuyama et al., 2016). Furthermore, temperature, sulfide concentrations, nutrients, and salinity may affect Hg methylation by influencing the supply of bioavailable Hg(II) and/or the activity of Hg-methylating organisms (Liang et al., 2013; Matsuyama et al., 2016). Next to the microbial alias biotic methylation of Hg there are also abiotic pathways for the formation of MeHg. Three exclusively chemical reactions have been identified in laboratory experiments, namely methylation by methylcobalamin (Bertilsson and Neujahr, 1971), transmethylation involving other methylated metals, and oxidative methylation (Hintelmann, 2010). Among these reactions the latter two and also the methylation by extracts of humic substances, particularly fulvic acid (e.g. Rogers, 1977; Nagase et al., 1984; Weber, 1993), are of potential relevance for abiotic Hg methylation. However, the environmental relevance of abiotic Hg methylation still needs to be quantified while the ability to differentiate abiotic from biotic methylation needs to be improved.

Knowledge on the formation and behavior of ethylmercury (EtHg; $CH_3CH_2Hg^+$) in the natural environment is limited since sensitive and reliable methods for the analysis of this highly toxic Hg compound were not present until recently (Mao et al., 2010; Kodamatani and Tomiyasu, 2013; Lusilao-Makiese et al., 2016). Hintelmann (2010) stated that EtHg is not very persistent in the environment and readily decomposes. Contrarily, it appears to occur widely in the environment, as indicated by EtHg contents found in soil samples (Mao et al., 2010). However, information on its microbial formation is lacking (Hintelmann, 2010).

In general, Hg can be mobilized by volatilization, leaching, and/or partial plant uptake in the terrestrial environment. Mercury discharge from soils via leaching to groundwater is considered to be almost negligible (Fritsche et al., 2008). In contrast, volatilization of Hg(0) in particular is thought to constitute a potentially important factor for the release of Hg from soils (Grigal, 2003; Rinklebe et al., 2009; Rinklebe et al., 2010). In fact, volatilization of Hg from soils and rocks contributes significantly to the atmospheric Hg pool (e.g. Zhang et al., 2001; Gustin, 2003). It may be concluded that the magnitude of Hg emissions from soil is related to its Hg content, while various factors, among them irradiation, soil moisture, temperature, air Hg concentration, relative humidity, wind speed, turbulence, atmospheric oxidants, soil characteristics, Hg speciation in soil, soil microbial community structure and activity influence diel and seasonal patterns. Both natural as well as anthropogenic processes contribute to the total atmospheric Hg load. Gaseous elemental Hg is efficiently transported over long distances with air masses and moves between the continents, thereby reaching even isolated regions (Beckers and Rinklebe, 2017). It is assumed that the Hg contents in soils and sediments have already increased 3 to 10 times solely due to the combustion of fossil fuels and subsequent atmospheric dispersion of released Hg during the post-industrial era (Xu et al., 2015). Many floodplain soils accumulate substantial amounts of Hg via anthropogenic activities and transport within the watershed (e.g. Gosar and Žibret, 2011; Frohne and Rinklebe, 2013; Manceau et al., 2015). However, floodplain soils can act both as sink and source of Hg (Flanders et al., 2010; Rinklebe et al., 2010; Han et al., 2012). Particularly organic-rich floodplain soils which provide an energy-rich organic substrate for bacterial metabolism and exhibit low oxygen conditions during flooding have been recognized as Hg methylation sites and sources for enhanced MeHg input to adjacent streams (Roulet et al., 2001; Lazaro et al., 2016; Beckers and Rinklebe, 2017).

1.3.3 Ecological and health effects of mercury

Soil contamination with Hg is a challenging issue for human and environmental health since Hg compounds are more toxic than compounds of any other nonradioactive heavy element (Tipping et al., 2010; UNEP, 2013; MacDonald et al., 2016). The particularly toxic species MeHg basically occurs naturally where environmental conditions favor the net methylation of Hg (Hunter et al., 1940; Bakir et al., 1973; Beckers and Rinklebe, 2017) and Hg methylation is a key step in the transfer of Hg into the food chain. Hintelmann

(2010) stated that the MeHg production is basically the product of microbial activity and Hg(II) bioavailability, and that it is therefore suggested that in many aquatic environments, most MeHg is generated in sediments. However, demethylation rates in sediments are also very pronounced and the high turnover of MeHg in sediments leads to a standing MeHg pool, which is suggested to constitute at most 1% of the Hg_t (Hintelmann, 2010; Randall et al., 2013). In contrast, demethylation activity is almost absent in water, making the small amounts of MeHg transferred from sediments into the overlying water very persistent in this compartment (Hintelmann, 2010). It is suggested that MeHg generally makes up 0.1 to 5% of the Hg_t content in surface waters while higher percentages may be found in anoxic waters where MeHg may constitute one of the dominant Hg species (Crump and Trudeau, 2009). The concern about MeHg in aquatic environments arises from its toxicity and the fact that this Hg species bioaccumulates and biomagnifies particularly in the aquatic environment threatening human health due to human consumption of primarily fish or fish predators (Lavoie et al., 2013; Llop et al., 2014; Nakamura et al., 2014). Accumulation of MeHg in rice plants is probably one of the most concerning aspects of Hg in economic crops. Compared to aquatic environments bioaccumulation and biomagnification of Hg are less evident in terrestrial ecosystems and usually do not pose a threat to human health (Beckers and Rinklebe, 2017). Unlike MeHg, EtHg is not known to (bio)accumulate (Hintelmann, 2010). In general, chemical species of Hg differ considerably in their toxicokinetics (i.e., absorption, distribution, metabolism, and excretion) and toxicodynamics. Elemental Hg is primarily taken up by inhalation while MeHg is efficiently absorbed in the gastrointestinal tract. Intoxication by inorganic Hg salts is usually rare, but the ingestion of mercuric salts is potentially fatal. Contrary to Hg vapor and MeHg the primary target organ of inorganic mercury compounds is the kidney and not the central nervous system or the placenta (Jeevanaraj et al., 2016; Beckers and Rinklebe, 2017).

1.3.4 Mercury immobilization in soils (for remediation)

Strategies to either remove Hg or to efficiently immobilize it by transforming it into its most stable and least toxic forms in situ are required (Cassina et al., 2012; Wang et al., 2013; Ullah et al., 2015; Xu et al., 2015). One possible way to diminish Hg mobility in soil is the use of soil amendments (Zhu et al., 2015; Shu et al., 2016a; Šípková et al., 2016). Organic amendments are considered to be particularly suitable as they might reveal a high potential to immobilize Hg and simultaneously fertilize the soil (Wang et al., 2012; Shu et

al., 2016a). Much soil Hg is usually bound to reduced sulfur functional groups (thiol, disulfide, and disulfane) of soil OM in an oxidized form such as Hg(II) (Xia et al., 1999; Skyllberg, 2012; Eckley et al., 2015). Therefore, carbon-rich biochar which can be cost-efficiently produced via pyrolysis of agricultural bio-waste under oxygen limitation and which has the potential to promote plant growth and stimulate ecological restauration is one possible amendment (Ahmad et al., 2014; Ahmad et al., 2017; Igalavithana et al., 2017). Its potential to remove Hg from solution (Kong et al., 2011) and from combustion flue gas (e.g. Klasson et al., 2014; Yang et al., 2016; Shen et al., 2017), to reduce the MeHg levels in rice grains (Shu et al., 2016b), or to immobilize MeHg in soil (Shu et al., 2016a) has already been demonstrated. However, to our best knowledge, information on the effect of biochar on the retention of total Hg (Hg_t), and the Hg species MeHg, and EtHg in soil during systematically controlled E_H changes is missing up to date.

Sugar beet factory lime (SBFL) is another low-cost sorbent for potentially toxic elements. Lime is one of the main stabilizing agents used for *in situ* stabilization/solidification of Hg in soils and known to reduce Hg uptake by plants (Heeraman et al., 2001; Azevedo and Rodriguez, 2012; Xu et al., 2015). In general, sugar beet factories produce large volume lime piles due to the application of considerable quantities of calcium oxide during the sugar beet juice purification process (Loginova et al., 2012). The applicability of SBFL to immobilize trace elements other than Hg in soils has been demonstrated (Shaheen and Rinklebe, 2015; Shaheen et al., 2015; Shaheen and Rinklebe, 2017). However, information on the potential of SBFL to stabilize Hg_t, MeHg, and EtHg in flooded soils is missing. In particular, their release kinetics from contaminated floodplain soils under varying redox conditions are still not fully understood.

1.4 Research justification

As Hg is an important pollutant in soils and sediments there is a need to understand its geochemical behavior such as release kinetics and adsorption/desorption in frequently flooded soils (Beckers and Rinklebe, 2017). The impact of several parameters such as E_H, pH, DOC, chemistry of sulfur (S), chloride (Cl^-), iron (Fe), and Hg_t content in soil on the mobility and speciation of Hg has been studied in some detail (Pelcová et al., 2010; Christensen et al., 2018; Zhu et al., 2018). However, there is a need to simultaneously analyze the above mentioned parameters and Hg_t under controlled conditions to recognize correlations and to identify interdependencies. Frohne et al. (2012) used an automatic bio-

geochemical microcosm system to simulate flooding events and to investigate the impact of E_H and other influencing parameters on Hg mobilization. It was shown that controlled E_H variations appear to affect Hg mobilization and methylation on the background of concomitant changes in DOC, sulfur cycle, and microbial community structure whereas E_H and pH values as well as concentration of dissolved Fe and Cl^- appeared to be less influential. Based on the chemistry of Hg interactions with DOC and other organic and inorganic soil components as well as on published results concerning Hg removal from aqueous solutions by means of biochar (Liu et al., 2018b) it is supposed that Hg can be immobilized in soils by amendments exploiting similar chemical reactions. The latter include reactions with sulfhydryl and carboxyl groups as well as electrostatic interactions and surface precipitation with inorganic materials. Of particular importance is the affinity of Hg for reduced sulfur functional groups. In order to cover various possible interaction types we selected two types of amendments with different proportions of organic and inorganic components, BC and SBFL. Their effects on Hg release, mobilization, methylation, and ethylation were planned to be investigated. Methylmercury is particularly toxic for humans and is formed in the soil environment primarily in the course of SRB-dependent metabolism. These bacteria are suggested to exhibit characteristic patterns of phospholipid fatty acids (PLFA) which were quantified to draw conclusions on the soil's SRB community.

Biochars are manufactured at different temperatures leading to products with varying chemical and physical properties and thus differing efficiency to interact with Hg species. In this respect, Liu et al. (2016) and Liu et al. (2017) who applied biochars pyrolyzed at high (600 °C, 700 °C) and low (300 °C) temperatures obtained contradictory results. On the one hand, Liu et al. (2016) stated that BC produced at 600 and 700 °C was more effective to immobilize Hg than low temperature BC. On the other hand, they found in a subsequent publication that low temperature BC was more effective in this respect (Liu et al., 2017).

Due to the existing gaps in knowledge and the published contradictory results the present work explored the influence of various amendments on Hg concentrations and Hg species formation in soil solutions under controlled redox conditions including reevaluation of effects obtained with biochars pyrolyzed at different temperatures (chapter 4 and 5). It is questioned whether the different effects of the biochar types on Hg binding can be explained by their distinct chemical properties i.e. the amount of functional groups which decreases with increasing pyrolysis temperature in biochar production.

In chapter 6, it is attempted to identify the parameters which control Hg release under field conditions by means of two soil hydrological monitoring stations. Therefore, parameters similar to that in the microcosm experiments were determined. By this, it was possible to compare the results to a certain degree and recognize differences which may help to improve our understanding of the examined processes and further improve experimental set-ups for future research.

2. General and specific objectives

The general objective of this work was to experimentally and systematically quantify the impact of flooding events by microcosm experiments and field studies, respectively. It was aimed to determine associated E_H and pH changes, the release of Hg_t as well as the release and formation of Hg species in floodplain soils, and to identify the influence of diverse biogeochemical factors and the underlying processes as specified below. Additionally, different soil amendments were tested for their abilities as immobilizing agents to reduce the concentrations of Hg_t, MeHg, and EtHg in soil solution.

Two laboratory experiments simulating floodings in biogeochemical microcosms and one field study monitoring the impact of floodings were conducted in order to meet these objectives.

The specific objectives were:

- to systematically quantify the impact of pre-defined redox conditions on the release dynamics of Hg_t, MeHg, and EtHg in a contaminated floodplain soil non-treated as well as, separately, treated with:
    1. commercially available biochar based material and commercial by-product SBFL
    2. biochar pyrolyzed either at 200 °C (BC200) or 500 °C (BC500) in the laboratory
- to identify the underlying redox-driven processes mechanistically with particular emphasis on parameters which are thought to affect Hg methylation
- to evaluate the efficiency of the soil amendments biochar based material, SBFL, BC200, and BC500 as immobilizing agents to reduce the concentrations of Hg_t, MeHg, and EtHg in soil solution
- to identify linkages between shifts in Hg species and changes in soil microbial community structure as determined by phospholipid fatty acid (PLFA) analysis
- to quantify the impact of flooding and changing redox conditions on the release dynamics of Hg(II) under field conditions
- to verify whether results gained by the laboratory experiments are in accordance with those achieved in the field

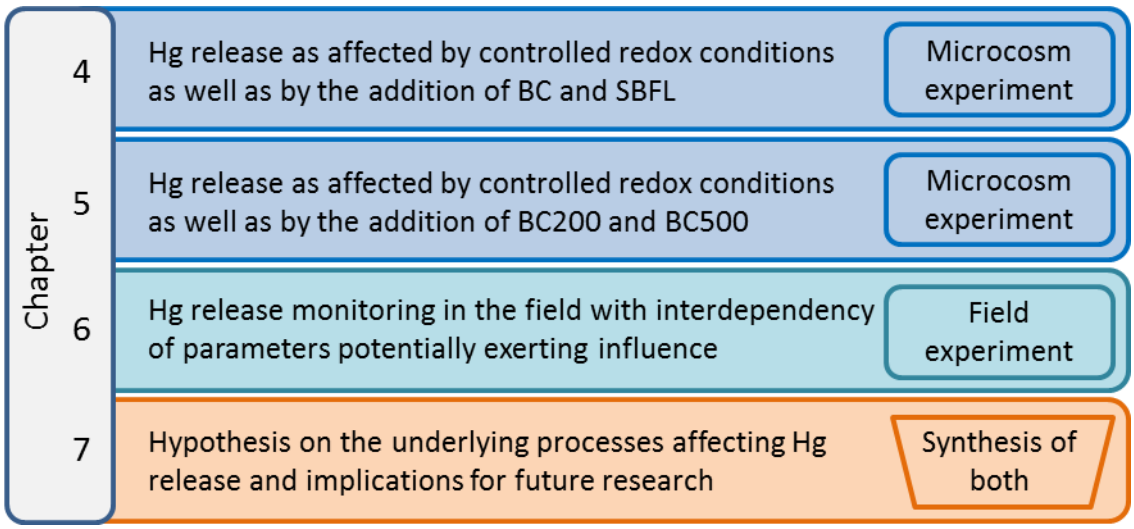

Figure 2-1: Graphical outline of the thesis.

3. Materials and methods

3.1 Study and sampling sites

The two study areas selected for the current thesis are situated in Germany in Hg-polluted floodplain ecosystems. Considerable Hg contents up to 47.78 mg/kg have been found in soil samples of both study areas (Frohne and Rinklebe, 2013) which substantially exceeds the applicable action value (2 mg/kg) of the German Federal Soil Protection and Contaminated Sites Ordinance (BBodSchV, 1999) in relation to plant quality for the soil – plant transfer of metals on grasslands.

3.1.1 Wupper River

The Wupper River sampling site is located at the lower course of the Wupper River (near to its confluence into the Rhine River) in the state of North Rhine-Westphalia (2568987 E, 5659539 N; 51°4´0.449´´N, 6°59´0.718´´E). The Wupper River is approximately 116 km long and its catchment area covers 813 km² (MKULNV, 2014). The sampling site is used as grassland and periodically inundated by the Wupper River, usually in spring time. The area is located in a region of high annual precipitation (774 mm). The mean discharge of the Wupper River is 14 m³/s (Wichern et al., 2006).

The valley of the Wupper River has been used for industry, agriculture and as a settlement area for centuries (LUA NRW, 2005). Substantial amounts of Hg reside in floodplain soils especially downstream of the urban area of Wuppertal (Gaida and Radtke, 1990; Schenk and Gaida, 1994). The high Hg content in the soil of the Wupper River sampling site is most likely the result of discharge from the metal industry such as electroplating, the production and use of Hg containing fungicides, the production of Hg thermometers, and the textile industry, particularly from dye factories, during the last centuries in the proximity of the river leading to the contamination of the water, the sediments, and the floodplains of the Wupper River (Schenk, 1994; Frohne et al., 2012; Frohne and Rinklebe, 2013). Today, atmospheric deposition of Hg is of particular importance in this region. The emission of Hg into the air in North Rhine-Westphalia is mainly the result of the coal industry (MKULNV, 2014).

A soil profile within the floodplain had been excavated before and was described in detail (Frohne and Rinklebe, 2013). The soil was classified as Eutric Fluvisol according to IUSS (2015). The Hg_t content of the soil horizon within 26 to 40 cm was 41.0 mg/kg. Therefore,

about 400 kg soil material was collected from this depth from a 4 m^2 area and homogenized in one composite sample. The soil sample was further homogenized, air-dried, crushed, ground and sieved through a 2 mm sieve in the laboratory and used for several analyses: Soil properties of this contaminated Wupper soil (CS) were determined following standard methods described in Blume et al. (2011). Soil pH was measured according to DIN EN 15933 (2012). Subsamples of CS, and the amendments BC, SBFL, BC200, and BC500 were digested in a microwave system (MLS 1200 Mega, MLS GmbH, Leutkirch, Germany) to determine (pseudo)total metal concentrations (U.S. EPA Method 3051A, 2007) which were measured by inductively coupled plasma optical emission spectrometry (ICP-OES) (Ultima 2, Horiba Jobin Yvon, Unterhaching, Germany). Total Hg was determined with atomic absorption spectrometry (AAS) using a DMA-80 direct mercury analyzer (MLS GmbH, Leutkirch, Germany). The Hg species MeHg and EtHg were analyzed using gas chromatography with atomic emission detection (GC-AED) (HP 6890, Agilent, Waldbronn, Germany - jas 2350, jas GmbH, Moers, Germany). Additional information on chemical species of Hg in soil was obtained by X-ray absorption near-edge structure (XANES) spectroscopy. Mercury L_{III}-edge XANES of the soil sample and reference Hg standard compounds were collected at the beamline (BL) 1W1B in Beijing Synchrotron Radiation Facility (BSRF, China). The fine powder ($\leq$ 74 µm, passed the soil to 200 mesh screen) of soils was pressed into a 1 mm thick tablet for the X-ray absorption near-edge structure (XANES) spectroscopy analysis. The BL1W1B was equipped with a Si (111) double-crystal monochromator that was detuned to minimize the harmonic content of the beam. Energy was scanned from –150 to 500 eV relative to the Hg L_{III}-edge (typical energy peak 12,284 eV). The reference compounds, including HgS, Hg-Cys, and MeHg-Cys, were recorded in transmission mode. The soil samples were detected in fluorescence mode using a 19-elemental Ge solid detector. The data of spectra were normalized by using ATHENA software. More detailed information on analytical procedures including quality control is provided in Chapter 3.5.

Major properties of the soil are given in Table 3-1.

Table 3-1: Properties and chemical composition of the contaminated soil (CS).

	Unit	CS
Basic properties		
pH [H_2O]		6,4
EC	[dS/m]	n.d.[a]
Silt	[%]	92
Clay		2
Total nitrogen		0,35
Total carbon		7,06
Total organic carbon		7,05
Total carbonates		0,04
Contents		
Hg_t	[mg/kg]	31,2
MeHg		0,44
EtHg	[µg/kg]	0,10
Al	[g/kg]	18,5
Fe		43,8
Mn		0,87
S		0,99

[a] n.d. = not determined

Silt dominated the soil texture. The soil was slightly acidic (pH 6.4) and had a high organic carbon (OC) content. The total content of Hg in CS was 31.19 mg/kg while MeHg and EtHg contents were 0.44 mg/kg and 0.10 µg/kg, respectively (Table 3-1). Normalized XANES Hg L_{III}-edge spectra of the soil sample and the standard compounds HgS, Cysteine-Hg-Cysteine, and MeHg-Cysteine obtained at beamline 1W1B are shown in Figure 3-1. We analyzed the XANES spectra by least square linear combination fitting (LCF). The LCF numerical results of the soil sample are given in Table 3-2. It provides the percentage of each standard Hg form of the total Hg in the soil sample. The LCF results indicate that HgS, MeHg-Cysteine, and Cysteine-Hg-Cysteine like forms are the main three components in the soil. The LCF results imply that HgS is the predominant Hg species in the soil. Based on the LCF results its relative proportion was 53% while MeHg-S like species accounted for 28% and S-Hg-S like species for 17%.

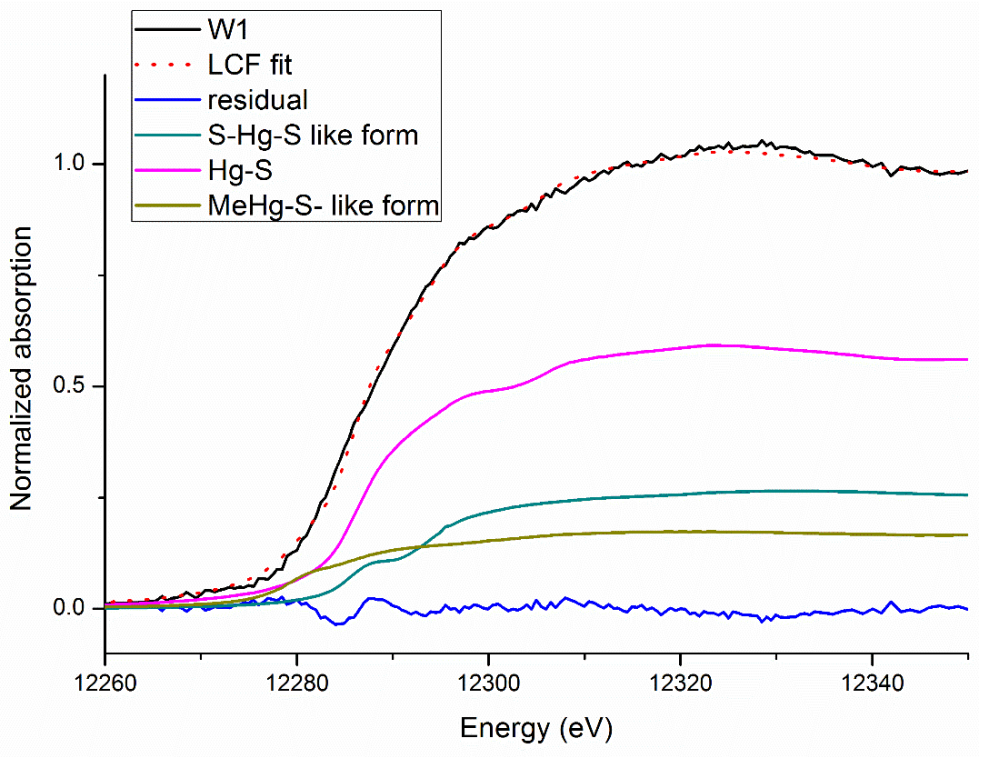

Figure 3-1: Normalized Hg L_{III} near-edge spectra of the Wupper soil sample W1. The least square linear combination fitting (LCF) of XANES spectra from W1 was performed using a series of Hg standard compounds. The black line shows sample W1 XANES spectra. The red dot line shows the LCF result. The pink line shows the standard Hg compound of HgS. The green line shows the standard organic Cys-Hg-Cys bonding form. Brown line shows the standard of MeHg-Cys. The blue line shows the acceptable LCF residual.

Table 3-2: Hg L_{III} XANES least square linear combination fitting results of the Wupper soil sample.

Standard	Weight (SD)	R-factor
Hg-S	0.538 (0.030)	0.00128
S-Hg-S	0.177 (0.011)	0.00128
MeHg-S	0.284 (0.035)	0.00128

SD = standard deviation.

3.1.2 Saale-Elbe confluence

The selected study area in the state of Saxony-Anhalt encompasses two study sites Saale 1 and Saale 2 with a distance of 28 m between them. These sites are located at the confluence of the Saale River into the Elbe River (700811 E, 5759540 N; 51°57'0.9324"N, 11°55'19.8624"E) within the nature reserve Steckby-Lödderitzer Forst in the vicinity of Breitenhagen. A detailed map of the study sites has been adapted from Swaton (2001) (Fig. 3-2).

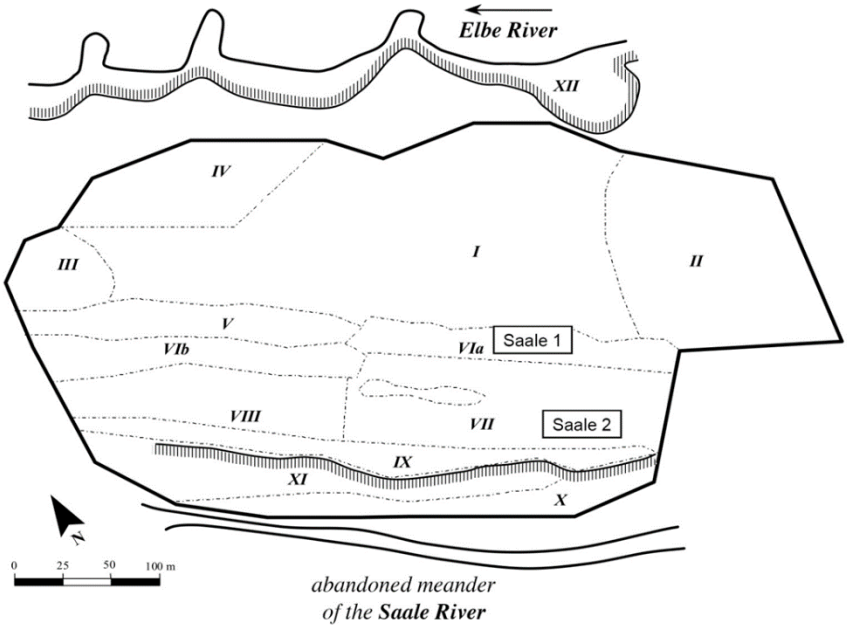

Figure 3-2: The study area in the vicinity of the confluence of the Saale and Elbe Rivers. The locations of the two soil hydrological monitoring stations are marked by the description fields "Saale 1" and "Saale 2". Roman numerals indicate geomorphological units: I = low terrace; II = terrace flattening to southeast; III = terrace flattening to northwest; IV = terrace flattening to Elbe River; V = slope to floodplain; VIa = flood channel; VIa = flood channel with kolks; VII = floodplain with kolk channel; VIII = inclined floodplain; IX = upper slope of floodplain; X = littoral zone abandoned meander of the Saale River; XI = elevation abandoned meander of the Saale River; XII = littoral zone Elbe River. Figure adapted from Swaton (2001).

Selection of the study sites at the Saale-Elbe confluence is based on previous studies and large-scale conventional soil mapping (Swaton et al., 2003; Devai et al., 2005; Rinklebe et al., 2010). Flooding of the study sites by the Saale and Elbe rivers occurs periodically either by snowmelt in winter and spring or caused by heavy rainfalls during spring and summer (Rinklebe et al., 2009). The region is characterized by a mean annual precipitation of 473 mm and an annual air temperature of 8.7 °C (Frohne and Rinklebe, 2013). Lengths of the Elbe and Saale rivers are 1,094 km and 413 km, respectively, and their catchment

areas amount to 148,268 km² and 24,079 km² (Claus et al., 2015; Arroyo-Abad et al., 2016). The source of the Saale River is situated close to Zell im Fichtelgebirge. Discharge averages are 570 m³/s for the Elbe River and 115 m³/s for the Saale River (Frohne and Rinklebe, 2013). The study area is a woodland habitat.

Two soil profiles had been excavated at the study sites earlier and were characterized in detail: According to IUSS (2015) the soil profile at the study site Saale 1 can be defined as Calcic-Mollic Gleysol (GLmk) while the soil at Saale 2 is classified as Mollic Fluvisol (FLm). Swaton (2001) determined high Hg contents of up to 48 mg/kg in these soil profiles which can be attributed primarily to emissions of the former chlor-alkali industry and the acetaldehyde production located within the Elbe River catchment. Before 1990 inadequately purified sewage has been dumped into the Elbe and Saale rivers. The amount of discharged pollutants has markedly decreased since 1990 due to the closure of large industrial facilities (Swaton, 2001). However, Hg pollution principally originating from former emissions of the chlor-alkali industry and the acetaldehyde production within the catchments caused persistently high Hg contents in floodplain soils and sediments (Müller and Furrer, 1994; Zerling et al., 2003; Frohne and Rinklebe, 2013; Krüger, 2016). Chlor-alkali plants were operated in Ústí nad Labem and Neratovice in the former Czechoslovakia as well as in in the former German Democratic Republic in Bitterfeld (Mulde River) Osternienburg, and Schkopau near Halle (Saale River), with the latter being the largest (Hintelmann and Wilken, 1995; Krüger, 2016). Additionally, one acetaldehyde factory located in Schkopau contributed to the Hg emissions (Krüger et al., 1999). In fact, Swaton (2001) found the highest Hg contents in the upper 20 cm of the study area in a sample collected from the elevation of the abandoned meander of the Saale River (XI, Fig. 3-2). It has been supposed that the heavily industrialized area in the Bitterfeld/Halle/Leipzig (burning of lignite coal) triangle was once the main source of anthropogenic Hg emissions to the atmosphere in Europe (Ebinghaus et al., 1995). Next to these large point sources agricultural Hg inputs in the course of the past application of Hg containing pesticides such as Agronal and Falisan likely contributed to the Hg contents (Schinkel, 1985; Dusek et al., 2005). Furthermore, effluents of urban areas and municipal waste dumps, as well as the use of mineral fertilizers, sewage sludge and manure have or still do contribute to the Hg contents of the study site (Devai et al., 2005; Rinklebe et al., 2007; AMAP/UNEP, 2013). Similarly, atmospheric deposition and Hg release by geogenic sources contribute to the accumulation of Hg (Rinklebe et al., 2007).

Major parameters of the soil profiles are given in Table 3-3.

Table 3-3: Parameters of the soil profiles.

Depth [cm]	Symbol of horizon	Texture	Sand [%]	Silt [%]	Clay [%]	Humus [%]	OC [%]	pH in $CaCl_2$	C/N	CEC_{eff} [1)] [cmolc/kg]	kf-value [cm/d] [2) 3)]	Hg_t [mg/kg]
Saale 1												
0-15	aoAh	Ls2	35	44	20	12	6.99	5.8	14.7	26.3	4115 [2)]	13.6-15.0
15-50	aoAh-M-Go	Lu	27	51	21	10.7	6.23	5.7	17	25.9	4076 [2)]	16.5-48.0
50-73	II aoAh-M-oGo	Ls2	31	45	24	6.9	4.03	6.5	14.8	22.3	2258 [2)]	8.4-19.0
73-120	III aoAh-M-oGo	Tu3	15	51	33	3.6	2.08	6.8	11.8	22.6	16 [2)]	4.9-27.0
Saale 2												
0-10	aoAxh	Lu	14	51	35	12.5	7.29	5.9	13	35.1	25 [3)]	5.0
10-40	aM-oAxh	Lu	11	57	32	10.4	6.04	5.9	15.1	31.5	25 [3)]	7.0-21.0
40-50	aoGo-M-oAxh	Lu	16	52	32	7.3	4.22	6.3	13.7	27.2	25 [3)]	5.0
50-75	aoGo-M	Lu	6	61	33	8.7	5.06	7.1	14.5	33.4	25 [3)]	3.0-7.0
75-130	II aoGo-M	Lu	11	56	33	6.6	3.87	7.3	14.7	30	25 [3)]	3.0-19.0

1) = estimated according to (Ad-hoc-Arbeitsgruppe Boden, 2005)
2) = determined by GLA-SA
3) = estimated according to (Ad-hoc-Arbeitsgruppe Boden, 2005)

3.2 Materials

3.2.1 Biochar (biochar based material)

The biochar based material used in the microcosm experiment with commercially available or commercial by-product materials is a commercially available fertilizer product named "TERRA PRETA" which was obtained from TERRA PRETA GmbH, Berlin, Germany. The material is composed of bio-charcoal, humus, clay, alumina, shell limestone, perlite, microorganisms, and organic fertilizer. For conciseness it is called "biochar" (BC) here.

3.2.2 Sugar beet factory lime

The sugar beet factory lime (SBFL) used in the microcosm experiment is a commercial by-product material. It was acquired by Prof. Sabry Shaheen from the sugar beet factory in El-Hamoul, Egypt, operated by the Delta Sugar Company. The SBFL was alkaline (pH = 8.7), contained large amounts of total carbonates, total sulfur (S), aluminium (Al), and iron (Fe), while contents of Hg_t, MeHg, and EtHg were found to be low or below the detection limit.

3.2.3 Biochar (pyrolyzed pine cone)

Fallen pine cones were collected at the Kangwon National University, Chuncheon, South Korea, and dried in a greenhouse before the biochar production. The dried pine cone was ground and sieved through a 2 mm sieve. Biochar production was carried out by a heating program in a muffle furnace (LT, Nabertherm, Germany) under limited supply of air. The heating rate was 7 ˚C/min, and the holding time at the desired temperature (200 ˚C or 500 ˚C) was 2 h. The biochar was cooled down to 30 ˚C inside the muffle furnace (Igalavithana et al., 2017). By this, two biochars were produced, pyrolyzed either at 200 °C (BC200) or 500 °C (BC500).

Major properties of the soil and the soil amendments are given in Table 3-4.

Table 3-4: Properties and chemical composition of the contaminated soil (CS), biochar (BC), sugar beet factory lime (SBFL), and biochar pyrolyzed at 200 °C (BC200) or 500 °C (BC500), respectively.

	Unit	CS	BC	SBFL	BC200	BC500
Basic properties						
pH [H_2O]		6.4	7.3	8.7	4.2[a]	6.8[a]
EC	[dS/m]	n.d.[b]	n.d.	n.d.	0.001[a]	0.001[a]
Silt	[%]	92	n.d.	n.d.	n.d.	n.d.
Clay		2	n.d.	n.d.	n.d.	n.d.
Total nitrogen		0.35	6.11	n.d.	1.03[c]	1.81[c]
Total carbon		7.06	28.7	n.d.	69.7[c]	74.6[c]
Total organic carbon		7.05	26.6	2.19	n.d.	n.d.
Total carbonates		0.04	6.77	82.5	n.d.	n.d.
Total hydrogen		n.d.	n.d.	n.d.	2.13[c]	2.62[c]
Total oxygen		n.d.	n.d.	n.d.	27.1[c]	20.9[c]
hydrogen/carbon		n.d.	n.d.	n.d.	0.42	0.37
oxygen/carbon		n.d.	n.d.	n.d.	0.21	0.29
Contents						
Hg_t	[mg/kg]	31.2	0.08	0.04	0.03	0.01
MeHg		0.44	b.d.l.[d]	b.d.l.	n.d.	n.d.
EtHg	[µg/kg]	0.10	b.d.l.	b.d.l.	n.d.	n.d.
Al	[g/kg]	18.5	12.4	1.71	n.d.	n.d.
Fe		43.8	8.50	0.85	n.d.	n.d.
Mn		0.87	0.30	0.08	n.d.	n.d.
S		0.99	2.20	2.03	n.d.	n.d.
Additional properties						
Mobile matter	[%]	n.d.	n.d.	n.d.	62.4	10.0
Ash		n.d.	n.d.	n.d.	0.8	9.0
Resident matter		n.d.	n.d.	n.d.	35.6	79.6
Surface area	m^2/g	n.d.	n.d.	n.d.	0.47[e]	193.0[e]
Average pore volume	$\times 10^{-3}$ m^3/g	n.d.	n.d.	n.d.	2.38[f]	10.2[f]
Average pore diameter	nm	n.d.	n.d.	n.d.	45.1[f]	2.44[f]

[a] 1:20 ratio of biochar to deionized water
[b] n.d. = not determined
[c] moisture and ash free
[d] b.d.l. = below detection limit
[e] Brunauer-Emmett-Teller (BTE) method
[f] Barret-Joyner-Halender (BJH) method

3.2.4 Chemicals, reagents and reference materials

The quality of the measurements was ensured by using high quality chemicals and reagents and controlled by means of analytical standards and certified reference materials.
Ultrapure water was produced in the laboratory via a Milli-Q® Reference water purification system (Merck KGaA, Darmstadt, Germany).

Table 3-5: Chemical reagents.

Chemical/reagent	**Producer**
PlasmaPURE Hydrochloric Acid (34 – 37% HCl))	SCP SCIENCE (Canada)
Nitric acid 65% for analysis EMSURE® Reag. Ph Eur, ISO (max. 0.0000005% Hg)	Merck (Germany)
Hydrogen peroxide 30% (Perhydrol®) for analysis EMSURE® ISO	Merck (Germany)

Table 3-6: Analytical standards and reference materials.

Reference material	**Producer**
BRM#09b and BRM#12	The Federal Institute for Materials Research and Testing (BAM, Germany)
SRM 1575a	The National Institute of Standards and Technology (NIST, USA)
IAEA-405 and IAEA-433	The International Atomic Energy Agency (IAEA, Austria)
CRM 580 (old name) ERM®- CC580 (new name)	The Community Bureau of Reference (BCR, Belgium) Institute for Reference Materials and Measurements (IRMM, Belgium)
CertiPur®	Merck KGaA (Germany)
N5377	Sigma-Aldrich Co. (Sigma, Germany)
CRM47885	Sigma-Aldrich Co. (Supelco®, Germany)
47080-U	Sigma-Aldrich Co. (Supelco®, Germany)

3.3 Automated biogeochemical microcosm system

An automated biogeochemical microcosm system was used to simulate flooding in the laboratory. Two microcosm experiments were conducted by means of this system: One experiment in which the contaminated soil (CS), the contaminated soil + biochar (CS+BC), and the contaminated soil + sugar beet factory lime (CS+SBFL) were flooded and a second experiment, which was performed with the contaminated soil (CS), the contaminated soil + biochar 200 (CS+BC200), and the contaminated soil + biochar 500 (CS+BC500). The biogeochemical microcosm system enables to set and maintain pre-defined redox windows by automatically flushing the slurry, obtained by continuous stirring of the flooded soil, with O_2 or N_2 (Fig. 3-3). Therefore, it was possible to study the impact of dynamic redox conditions on the mobilization of Hg_t, MeHg, and EtHg within single microcosms containing CS, CS+BC, CS+SBFL, CS+BC200, or BC500 under controlled conditions. The automated biogeochemical microcosm system has been utilized in several studies (e.g. Frohne et al., 2011; Rinklebe et al., 2016a; Rinklebe et al., 2016b; Shaheen et al., 2016; Beiyuan et al., 2017). A technical description of the system is provided in Yu and Rinklebe (2011).

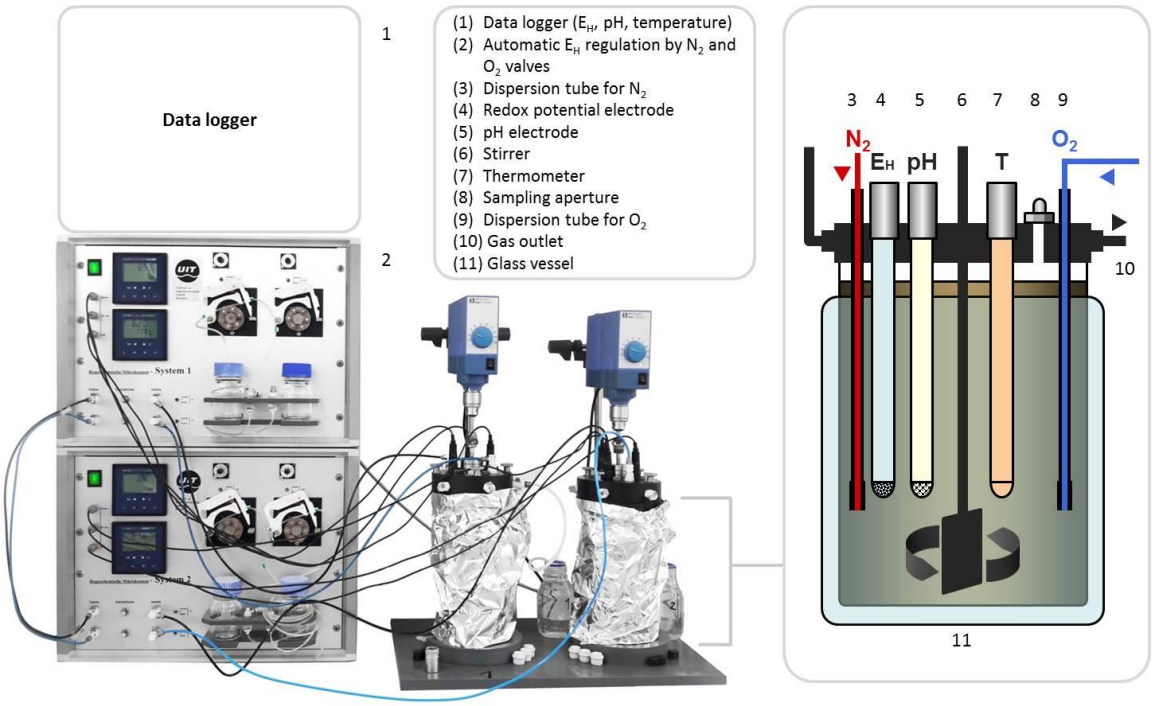

Figure 3-3: Automated biogeochemical microcosm system.

The range of E_H values typically measured in wetland soils, such as floodplain soils, is from 700 mV to -300mV (DeLaune and Reddy, 2005; Reddy and DeLaune, 2008; Yu and Rinklebe, 2011). Soils are commonly classified as oxidized soils at E_H values > 400 mV or > 350 mV (Karathanasis et al., 2003; DeLaune and Reddy, 2005; Dorau and Mansfeldt, 2016). Other classifications are often not closely confined. Here, the redox condition ranges were adopted from Bohn (1971): The E_H range 100 to 400 mV is classified as moderately reduced soils. Reduced soils are between -100 and 100 mV, and highly reduced soils are at E_H -100 to -300 mV.

3.3.1 Soil treatment with biochars and SBFL

For the microcosm experiment with the addition of commercially available or commercial by-product materials contaminated Wupper soil (CS) was amended with biochar based material (BC) and sugar beet factory lime (SBFL): Both, BC and SBFL, were separately applied to the soil at a rate of 10 g/kg soil. The soil and the amendments were mixed thoroughly and subsequently used for a pot experiment (Shaheen and Rinklebe, 2015; Shaheen et al., 2015). After the experiment, the soil was dried, crushed, and stored in the laboratory for ten months allowing a proper aging. Thus, the total time was about one year after mixture before the soil was used for the redox experiment, which is called BC & SBFL experiment for conciseness here. Major properties of the used amendments BC and SBFL are given in Table 3-4.

For the microcosm experiment with the addition of laboratory-produced biochars two subsamples of the contaminated Wupper soil were amended with either BC200 or BC500. Both, BC200 and BC500, were applied to the subsamples at a rate of 80 t/ha. The soil and the amendments were mixed thoroughly, subsequently maintained at 70% water holding capacity and incubated at 25 °C for 40 days. After the incubation, the soil was spread for air-drying and subsequently used for the redox experiment, which is called BC200 & BC500 experiment for conciseness here.

3.3.2 Experiments under pre-set redox conditions

For the BC & SBFL experiment CS, CS+BC, and CS+SBFL were each separately added into three independent biogeochemical microcosms (replications) and inundated. Thus, 9 microcosm systems (MCs) were used, allowing three replicates of each of these soils in order to obtain replications that cover the natural soil heterogeneity.

The MCs were filled with 200 g air-dried soil mixed with 1600 mL of water collected from the Wupper River to obtain a ratio 1:8. The achieved slurry was continuously stirred to reach homogeneous conditions. Ten g grinded wheat straw (34.6 % carbon) was added for each MC as an additional carbon source for soil microorganisms after 24 hours of incubation. The straw contained (in mg/kg): 49.8 aluminum, 1.6 copper, 63.3 iron (Fe), 4.5 manganese (Mn), 268.8 sulfur (S), and 11.8 zinc (Zn). Contents of total Hg (Hg_t) and other potentially toxic elements were below the detection limit of cold vapor atomic fluorescence spectrometry (CV-AFS) and inductively coupled plasma optical emission spectrometry (ICP-OES) (see below). The straw addition was repeated after 48 hours. Similar to the straw 5 g of glucose was added after 24 hours of incubation to each MC. Another 10 g of glucose (two times 5 g) was added per MC six days after the incubation. These amendments and the continuously flushing of the MCs with nitrogen (N_2) efficiently decreased redox potential (E_H) levels.

Redox conditions (in mV) were changed stepwise from highly (-142 in CS, -138 in CS+BC, and -260 in CS+SBFL) to moderately reduced conditions (311, 303, and 310, respectively) during the experiment. Seven pre-defined redox windows (E_H windows) were sampled within this range.

After the sampling around E_H -125 mV in CS and CS+BC as well as -205 mV in CS+SBFL E_H-values were gradually increased by adding synthetic air (at low E_H) or oxygen (at higher E_H) since the E_H could not be further lowered by means of N_2 supply. In general, the E_H was controlled by the supply of oxygen (O_2) or N_2 in the described way. Different E_H-windows were set, reached, and kept stable by automatically flushing the slurry with O_2 or N_2, respectively. Redox potential was maintained for approximately 24 hours within each of these pre-set E_H-windows. Subsequently, samples were collected from the MCs before moving to the next E_H-window. Redox potential, pH, and temperature in each MC were automatically recorded every ten minutes by a data logger. The pH of MC No. 3 in CS was not recorded regularly due to a technical error of the pH-electrode. For this MC, pH was measured by a manual device at the moment of sampling and these values were used for statistical analyses (Fig. 0-1, Appendix A). Therefore, the number of

samples (N) for the pH values was 7,400 in CS, 10,296 in CS+BC, and 10,329 in CS+SBFL (Table 0-1, Appendix A). The total incubation period was 24 days (576 hours) at room temperature.

For the BC200 & BC500 experiment CS, CS+BC200, and CS+BC500 were added into four biogeochemical microcosms each in order to obtain replications that cover the natural soil heterogeneity. Thus, twelve biogeochemical microcosms were used in total. The MCs were filled with 210 g air-dried soil mixed with 1680 mL of water collected from the Wupper River. The achieved slurry was continuously stirred to achieve homogeneous conditions. Twenty g of the above-mentioned grinded wheat straw and 5 g of glucose were directly added to each MC as an additional carbon source for soil microorganisms. Another 5 g of glucose were added after 45 hours of incubation to each MC. These amendments and the continuously flushing of the MCs with N_2 efficiently decreased E_H levels similar to the BC & SBFL experiment. In general, the operational procedure of the BC & SBFL and the BC200 & BC500 experiment was identical. Therefore, differences of the BC200 & BC500 experiment are mentioned here solely. Nine redox windows were set in line with this experiment covering the range between -300 mV and 300 mV. However, the buffering capacity of the soil limited the effective range to ~ -150 to 307 mV. Lower windows were set after the highest redox window had been sampled. By this the windows 100 mV and 200 mV were sampled twice. Thus, using the redox condition ranges classified by Bohn (1971) redox conditions in the course of the experiment varied between highly and moderately reduced conditions.

3.3.3 Slurry sampling and processing

In the course of the BC & SBFL experiment slurry samples with a volume of 50 ml were collected approximately 24 h after reaching each new E_H-window by using a syringe connected with a Teflon tube of about 20 cm length. Next to each sampling a quantity of 7 ml was transferred into new glass bottles and stored at 2-8 °C for the analysis of MeHg and EtHg. The remaining slurry sample material was immediately centrifuged at 4000 rpm for 15 min and the supernatants were subsequently filtered under N_2-atmosphere through a 0.45 µm Millipore membrane (Whatman Inc., Little Chalfont, UK). This filtrate was divided into different subsamples for analysis. The solid material which remained in the centrifuge tubes was collected and stored at -20 °C until phospholipid fatty acid (PLFA) analysis.

In the course of the BC200 & BC500 experiment 65 ml of slurry were collected. Subsequent to each sampling samples were transferred and processed in a glove box (MK3 Anaerobic Work Station, Don Whitley Scientific, Shipley, UK) under anaerobic conditions (0–0.1% O_2). First, a quantity of 7 ml was transferred into new glass bottles and stored at 2-8 °C for the analysis of MeHg and EtHg. The remaining slurry sample material was immediately centrifuged at 5000 rpm for 15 min and the supernatants were subsequently filtered under N_2-atmosphere through a 0.45 µm nylon filter membrane (Thermo Scientific, Rochester, USA).

3.4 Soil hydrological monitoring stations at the Saale-Elbe confluence

Two soil hydrological monitoring stations were established at the study sites to examine the solubility of Hg in the soil solution with regard to variable chemical and physical parameters. Devices for groundwater monitoring and for sampling were integrated in the monitoring stations. This allows to directly measure control factors in the soil solution such as water level, pH-value, temperature and conductivity and to take groundwater samples either event-driven or at defined time intervals. Each monitoring station is divided in several self-sufficient modules. Module 1: measurement of soil humidity, soil temperature, water tension (at 3 different depths) and sampling of soil solution (at 3 different depths including 3 repeats); module 2: automatic sampling of groundwater with direct measurement of temperature, pH-value, redox potential and conductivity; module 3: central data acquisition. Each module is equipped with a separate photovoltaic solar power device.

Each measuring field of the stations is equipped with a suction cup which can provide three replicates of soil solution each in three different depths (Table 3-7). The measurement sensors are installed in the middle of the respective soil horizon. Water levels were measured via pressure determinations by means of multi-sensor modules (UIT, 2002) or by sonic water level meters, respectively. Soil humidity was determined by the FDR technique (Delta-T Devices Typ ML1-UM-2). For measurement of soil temperature sensors of tolerance class A according to DIN in four wire technique (Sensortyp PT 1000) with a measuring range from -30 °C to 80 °C and a resolution of 0.1 °C were used. Water tension was determined in the upper soil depth by means of needle sensor tensiometers with a diameter of 10 mm and in the lower depths by means of standard tensiometers with a diameter of 35 mm. Ceramic suction cups (type SK 2) with a pore diameter of 2.5 µm and a di-

ameter of 50 mm were used for extraction of soil solution. The suction head consists of > 90% Al_2O_3 and about 10% of SiO_2, Fe_2O_3 and TiO_2 as additional constituents. The air entry pressure is approximately 1 bar, the porosity amounts to 45 volume % and the saturated hydraulic conductivity comes to 8.6 x 10^{-6} cm/sec. The cladding tubes consist of PVC (UIT, 2002). The soil hydrological monitoring stations are equipped with rain gauges for sampling. Starting with summer 2002, the monitoring stations were additionally equipped with air temperature sensors. Daily means of precipitation and air temperature were provided by LAU Saxony-Anhalt (station Dessau).

Table 3-7: Equipment of the soil hydrological monitoring stations, examined types of floodplain soils as well as installation depths.

Study site	**Soil type**	**Parameter (instrument)**	**Depth [cm]**
Saale 1	Calcic-Mollic Gleysol	soil temperature (PT 100) soil humidity (TDR) water tension (tensiometer) soil solution (suction cup) groundwater (sonic water level meter)	30, 60, 100 500
Saale 2	Mollic Fluvisol	soil temperature (PT 100) soil humidity (TDR) water tension (tensiometer) soil solution (suction cup) groundwater (sonic water level meter)	25, 60, 100 500

3.5 Analytical procedures

3.5.1 Total mercury analysis

In the course of the BC & SBFL microcosm experiment a 10 ml subsample of slurry sample filtrate was filled into borosilicate glass bottles with PTFE-lined caps and preserved with 200 µl 0.2 M bromine monochloride solution (BrCl) (U.S. EPA Method 1631, 2002). Prior to bottling borosilicate glass bottles were rinsed with acid (10% HNO_3), 0.2 M bromine monochloride solution (BrCl) (U.S. EPA Method 1631, 2002) and ultrapure water (via Milli-Q® Reference, Merck, Darmstadt, Germany). The obtained subsamples were used for the determination of Hg_t and stored at 2-8 °C until analysis. Total Hg was measured using cold vapor atomic fluorescence spectrometry (CV-AFS) (mercur duo plus, Analytik Jena, Jena, Germany). A 7-point calibration curve was generated by preparing deionized water diluted Hg standard solutions from a 1000 mg/l Hg standard solution (CertiPur,

Merck) and by means of a blank sample. The instrument drift was controlled by the analysis of an intern reference sample every 10 samples. It was found to be satisfying for all measurements. The detection limit was 50 ng/l for CS and CS+BC samples and 27 ng/l for CS+SBFL samples. Each sample was measured three times. The relative standard deviation of these repeated measurements was below 5% for all samples.

During the BC200 & BC500 microcosm experiment Hg_t sample processing was basically identical to the BC & SBFL experiment while Hg_t was measured with atomic absorption spectrometry (AAS) using a DMA-80 direct mercury analyzer (MLS GmbH, Leutkirch, Germany). Quality of the measurements was controlled by means of certified reference materials obtained from the Federal Institute for Materials Research and Testing (BAM, Germany) BRM#09b: Hg: 1.02 (0.85–1.19) mg/kg, BRM#12: Hg: 8.86 (8.48–9.24) mg/kg, and material obtained from the National Institute of Standards and Technology (NIST, USA) SRM 1575a: 0.0399 (0.0392–0.0406) mg/kg. All recoveries fell within the designated range.

3.5.2 Mercury species analysis

The unfiltered 7 ml subsamples from microcosm slurry sampling (see Chapter 3.3.3) were shipped on dry ice to the UFZ Helmholtz Centre for Environmental Research in Leipzig where MeHg and EtHg were determined using gas chromatography with atomic emission detection (GC-AED). Mercuric mercury was additionally quantified in one sample. A quantity of 2 ml of the sample was spiked with 4 ml buffer solution (pH 4.5) and 20 µl Na-propylborate solution (2% in tetrahydrofuran) and subsequently stirred for 10 min. The Hg species were enriched from the aqueous phase by solid phase microextraction (SPME) in the headspace mode onto a 100 µm polydimethylsiloxane (PDMS) fibre for 30 min at 30 °C. Thermal desorption was achieved directly in the injector of the gas chromatograph for 1 min at 200°. The refined samples were stored at 15 °C until analysis and processed automatically by a multipurpose sampler (MPS2, GERSTEL, Mülheim an der Ruhr, Germany). The Hg species were analyzed with a gas chromatograph Hewlett-Packard 6890 (Agilent, Waldbronn, Germany) equipped with a HP1 column (30m x 0.25 mm x 0.25 µm) using helium (He) as carrier gas and a microwave-induced plasma atomic emission detector (jas 2350, jas GmbH, Moers, Germany). The Hg emission line 254 nm was examined. The detection limits were 0.8 ng Hg/l for MeHg and 2 ng Hg/l for EtHg. The quality of

analyses was controlled using the reference materials IAEA-405, IAEA-433, and CRM 580.

For the Saale-Elbe confluence study area Hg(II) in precipitation, soil solutions, and groundwater was determined by the method described above with the following modifications concerning sample processing: (1) manual SPME, (2) no temperature control for samples, (3) 1 ml sample was mixed with 2 ml of buffer.

3.5.3 Multi-element analysis

A 10 ml subsample of the slurry sample filtrate was stabilized by the addition of 100 µl 65% HNO_3 and used for the determination of Fe, Mn, S, and other elements by inductively coupled plasma optical emission spectrometry (ICP-OES) (Ultima 2, Horiba Jobin Yvon, Unterhaching, Germany). Analyses of multi-element standards (CertiPur, Merck) were routinely included into the quality control. Maximum allowable relative standard deviation between replicates was 5 %. Additionally, a test of recovery was carried out at five different concentration levels (1000, 100, 50, 25, and 12.5 µg/l) as an internal quality control. The average relative standard deviation (RSD) was less than 3 %. The detection limits were 6.2 µg/l for Fe, 1.4 µg/l for Mn, and 60 µg/l for S. Maximum allowable relative standard deviation between replicates was 5 %.

3.5.4 Dissolved organic carbon, DIC, SO_4^{2-}, Cl^-, and PO_4^{3-} analysis

A second 10 ml subsample of slurry sample filtrate was stored in a freezer at -20 °C until analysis. This subsample was used for determination of DOC, DIC, SO_4^{2-}, Cl^-, and PO_4^{3-}: Dissolved organic and inorganic carbon was measured with a C/N-analyzer (multi N/C 2100 S, Analytik Jena, Jena, Germany). Measurements included two replicates for each sample with a detection limit of 1 mg/l. Sulfate, Cl^-, and PO_4^{3-} were determined using 5 ml of the subsample and an ion chromatograph (Personal IC 790, Metrohm, Filderstadt, Germany) with a Metrosep A Supp 4 - column (Metrohm, Filderstadt, Germany). A 2-point calibration was conducted. The detection limit was 0.03 mg/l.

3.5.5 Phospholipid fatty acid analysis

The solid material which remained in the centrifuge tubes was collected and the material of the replicates was merged and homogenized. These composite samples were stored at -20 °C until phospholipid fatty acid (PLFA) analysis.

Phospholipid fatty acid analysis was used to assess the microbial community and to identify changes in the SRB community in the solid phase collected from CS, CS+BC, and CS+SBFL at the initial E_H (subsequent to flooding of the soils), at the time highest MeHg concentrations were measured in the liquid phase, and at high E_H (at the end of the experiment). Phospholipid extraction and PLFA analysis were performed on 2 g of frozen soil samples following the standard procedure described by White et al. (1979) and Frostegård et al. (1991). The PLFAs were designated according to Feng et al. (2003b). Additional details on the method are provided in Rinklebe and Langer (2006; 2013) and Langer and Rinklebe (2009).

In the course of the BC200 & BC500 experiment PLFA analysis was performed for each sampled E_H-window.

3.5.6 PLFAs considered to identify the sulfate-reducing bacteria community

Divers fatty acids have been found in sulfate-reducing bacteria (SRB) but only a few are recognized biomarkers. However, several genera of SRB possess significant proportions of specific PLFA with unusual structures that are suitable biomarkers (Lovley et al., 1993; Londry et al., 2004). The fatty acids i17:1ω7c and 10Me16:0 are narrowly distributed or constitute only small amounts in bacteria other than SRB while they are the major fatty acids of the genera *Desulfovibrio* (i17:1ω7c) and *Desulfobacter* (10Me16:0) (Macalady et al., 2000). However, the methyl-branched fatty acids 10Me16:0 and 10Me18:0 can be found in both SRB and actinomycetes (Sundh et al., 1997) and research by Dowling et al. (1986) indicated that the presence of 10Me16:0 in absence of high levels of 10Me18:0 has the potential to act as a specific biomarker for the SRB genus *Desulfobacter*. Thus, SRB that possess 10Me16:0 do not contain considerable quantities of 10Me18:0 while actinomycetes possess relatively large amounts of 10Me18:0 with some of them containing 10Me16:0 but in lower amounts (Kroppenstedt and Kutzner, 1978; Sundh et al., 1997). Moreover, Macalady et al. (2000) complied available information on PLFA abundances within 100 isolated SRB strains and found that the fatty acid 10Me18:0 has been detected

in marine *Desulfobacter* sp. Strain 3ac10 solely among the 16 *Desulfobacter* isolates considered. Hence, it seems likely that 10Me16:0 is indicating the presence of the SRB genus *Desulfobacter* whenever its concentrations are higher than those of 10Me18:0 or when 10Me18:0 is not detected (Smith et al., 1986; Sundh et al., 1997). Edlund et al. (1985) found that i17:1ω7c was the major component in five of six *Desulfovibrio* species. Similar results were obtained by Vainshtein et al. (1992) who revealed that iso-branched 17:1, and, in many cases, iso-15:0 were the predominant PLFAs in eighteen type strains of the genus *Desulfovibrio*. This was particularly true for the "classical" desulfovibrios, among them *Desulfovibrio* desulfuricans a well-known Hg-methylating bacterium (Vainshtein et al., 1992; Parks et al., 2013; Wang et al., 2016). Contrary to i17:1ω7c iso-15:0 is not regarded as a SRB specific biomarker but as a common biomarker for bacteria (Vestal and White, 1989). However, Sundh et al. (1997) found a strong positive correlation between i17:1ω7c and i15:0 in peat samples and concluded that both fatty acids originate from desulfovibrios. In some studies 10Me16:0 and i17:1ω7c were the only fatty acids considered as SRB biomarkers (e.g. Boon et al., 1996; Sundh et al., 1997; Yu and Ehrenfeld, 2010). Nevertheless, the unusual fatty acid 17:1ω6 is a major component of the SRB genus *Desulfobulbus* and can be used as indicator for its presence (Parkes and Calder, 1985; Vestal and White, 1989; Lovley et al., 1993). *Desulfobulbus* species do not possess branched fatty acids but consist of straight-chain saturated and monounsaturated fatty acids such as 15:0, 15:1, and 17:1 (Lovley et al., 1993; Macalady et al., 2000). Last named fatty acids are known to be widely distributed among bacterial taxa (Macalady et al., 2000). They may still be useful indicators of *Desulfobulbus* in the presence of 17:1ω6 due to the knowledge of their high abundance in this genus. Similarly, odd carbon number branched fatty acids coexist with the biomarker i17:1ω7c in *Desulfovibrio* which may in certain cases increase the indication for the presence of this genus (Jiang et al., 2012). Next to i15:0 (e.g. Sundh et al., 1997) a15:0 (Vainshtein et al., 1992), i17:0, and a17:0 (Jiang et al., 2012; Vetter et al., 2012) may support the indication for *Desulfovibrio*. Furthermore, Macalady et al. (2000) found that *Desulfobacter* isolates contain high relative amounts of the cyclopropyl fatty acids cy17:0 and cy19:0 next to the biomarker 10Me16:0. Both, cy17:0 and cy19:0, have been suggested as biomarkers for anaerobic bacteria and indicators of Gram-negative bacteria but cy19:0 was also found in substantial amounts in a Gram-positive strain which has influenced the interpretation on these fatty acids (Vestal and White, 1989; Schoug et al., 2008; Frostegård et al., 2011; Derrien et al., 2014).

3.5.7 BC200 & BC500 ultraviolet (UV) absorbance at λ = 254 nm

In the course of the BC200 & BC500 experiment a part of the remaining filtrate was used to determine the ultraviolet (UV) absorbance at λ = 254 nm spectrophotometrically (Dr. Lange CADAS 200, Hach Lange GmbH, Düsseldorf, Germany) to calculate the specific UV absorbance at 254 nm ($SUVA_{254}$) by dividing UV absorbance at 254 nm relative to a Milli-Q reference by the DOC concentration of the sample (Weishaar et al., 2003).

3.6 Calculations, statistical analysis, and graphics

During the BC & SBFL and BC200 & BC500 microcosm experiments E_H and pH values had been automatically recorded in a data logger every 10 minutes. These data served as the underlying dataset to calculate the mean values of E_H and pH levels for 3, 6, 12, and 24 hours prior to sampling (Microsoft Excel 2010). Correlation analyses were performed between these E_H/pH values and the mean concentrations of Hg_t, MeHg, EtHg, DOC, SO_4^{2-}, Cl^-, PO_4^{3-}, Fe, and Mn which were computed by dividing the sum of analysis results for the individual replications by the number of MCs used per soil type (Microsoft Excel 2010). The closest correlations were found for the results 6 hours before sampling and were therefore used for statistics. The programs IBM SPSS Statistics 25 and GraphPad Prism 5 were used for descriptive statistics and calculating correlations. GraphPad Prism 5 and Origin 2015G were used to create graphics. Canonical discriminant analysis (CDA) and principal component factor analyses were performed with IBM SPSS Statistics 25. The latter were carried out using principal components for factor extraction, followed by the varimax rotation procedure to make components easier to interpret. Component plots in rotated space were used to provide a visual representation of factor analyses loadings plotted in a 2-dimensional space.

Data from the soil hydrological monitoring stations was processed by means of the programs IBM SPSS Statistics 25 (graphics, statistics, correlations), Microsoft Excel 2010 (descriptive statistics), GraphPad Prism 5 (graphics, descriptive statistics), and Origin 2015G (3D bar graphs).

4. Mobilization of mercury species under dynamic redox conditions in a contaminated Wupper floodplain soil as influenced by biochar and sugar beet factory lime

4.1 Short introduction Chapter 4

Mobilized Hg species in soil solution are subject to transport and may enter the food chain. With respect to the toxicity of Hg species this is of major concern for human health. It is therefore of interest to explore methods capable to immobilize such toxic Hg species. The two amendments BC and SBFL were investigated for this purpose by utilization of microcosms under controlled redox conditions. It is suggested that Hg species are attracted to specific binding sites, preferably such resulting in a strong binding and thus Hg immobilization. The selected amendments, BC and SBFL, differ largely in their chemical composition and in types of functional groups which can potentially interact with Hg. Roughly, interaction of Hg with BC or SBFL is governed by organic or inorganic components, respectively. The aim of the present study is therefore to study the capability and efficiency of the two different amendments to bind soluble Hg species. Concept and methodology of this chapter are illustrated in Figure 4-1.

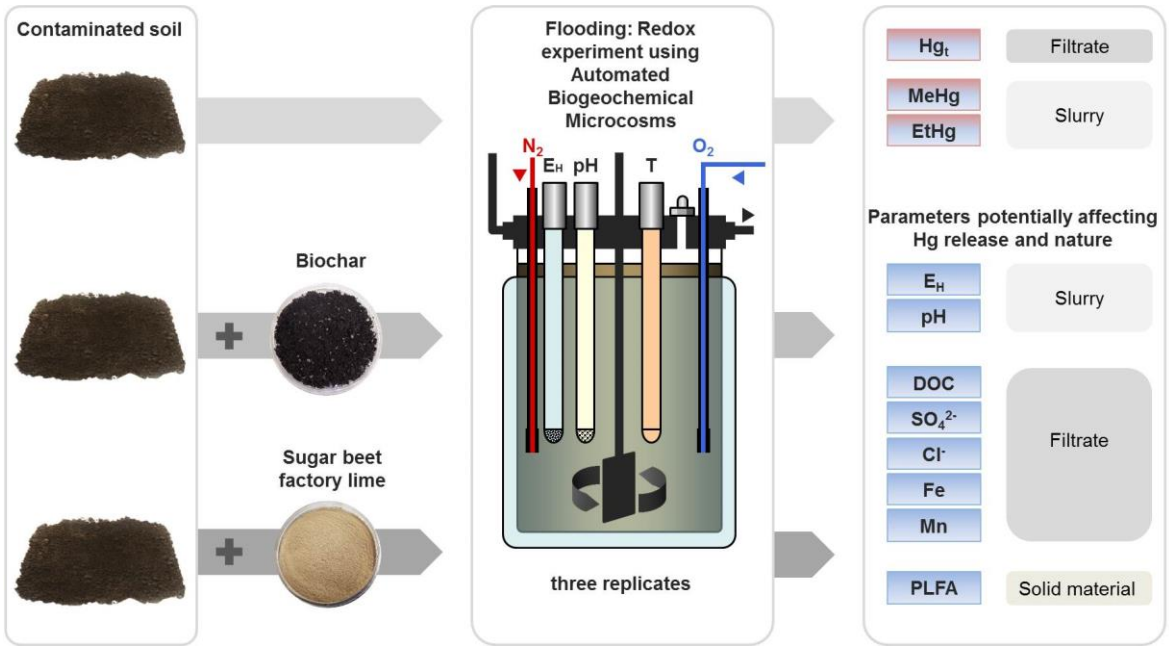

Figure 4-1: Graphical sketch illustrating the experimental design of the microcosm experiment to study the effects of biochar and sugar beet factory lime on Hg mobility and Hg species formation considering the influence and interdependency of several parameters which potentially affect Hg mobility.

4.2 Results and Discussion

4.2.1 Soil E_H and pH

The E_H (E_H all; data measured every 10 min during the experiment) in the slurries of CS and the treatments (CS+BC and CS+SBFL) varied between highly reduced conditions and moderately reduced conditions (Fig. 4-2, Table 0-1).

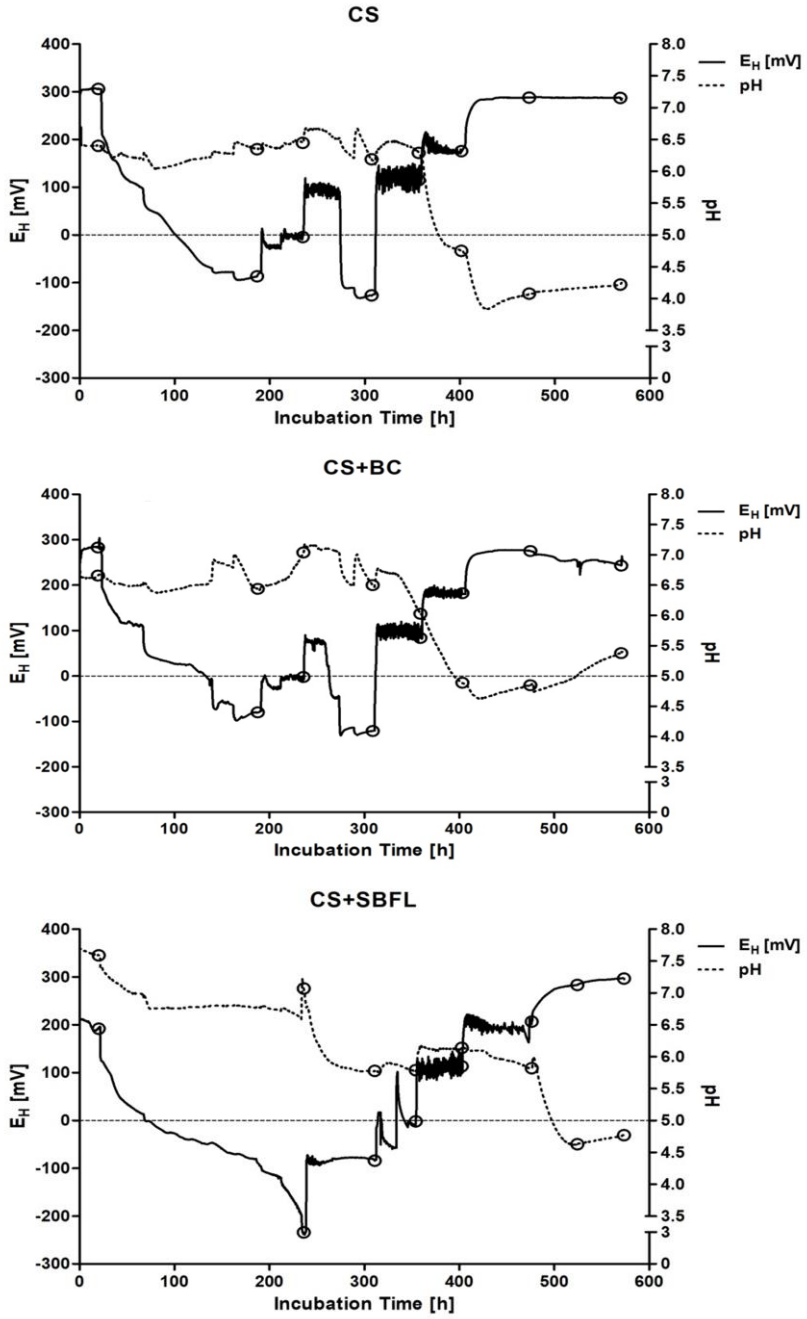

Figure 4-2: Development of redox potential E_H (solid line), pH (dashed line), and sampling points (circles) in soil slurry (data every 10 min, averages were reported for an underlying dataset (n ≈ 10,330) of three replicate samples) in the microcosms of untreated contaminated soil (CS), CS treated with biochar (CS+BC), and CS treated with sugar beet factory lime (CS+SBFL).

The pH (pH all) values ranged between extremely acidic to neutral (CS), slightly alkaline (CS+SBFL), and moderately alkaline (CS+BC) (Table 0-1). The pH in the slurry of CS and the treatments was inversely related to E_H (r = -0.77; $p < 0.01$; n = 7,400 in CS; r = -0.56; $p < 0.01$; n = 10,293 in CS+BC; and r = -0.54; $p < 0.01$; n = 10,329 in CS+SBFL) (Fig. 4-2). The inverse relationship between pH and E_H might be attributed to the consumption of protons required for the reduction of NO_3^-, Mn^{4+}, Fe^{3+}, and SO_4^{2-} (Yu et al., 2007; Reddy and DeLaune, 2008). In general, pH results indicate that the application of both BC and SBFL to CS increased the pH in soil slurry (Fig. 4-2, Table 0-1).

4.2.2 Impact of E_H/pH changes on mobilization of Hg_t, MeHg, and EtHg in CS, CS+BC, and CS+SBFL

The considerable contents of Hg in the studied soil rendered the possibility of substantial Hg releases in the course of flooding and E_H/pH changes. From the LCF results we can deduce that most of Hg_t in the soil is present in the form of divalent mercury (Hg(II)) which is generally the dominant Hg species in soil (Amde et al., 2016; Beckers and Rinklebe, 2017). Next to the high Hg(II) content, MeHg content of the soil was very high, while EtHg content was similar to contents reported from the Florida Everglades (Cai et al., 1997; Mao et al., 2010; Kim et al., 2015).

Released Hg_t concentrations in CS (5.4-41.9 µg/l) are very high considering concentrations of dissolved Hg_t that can be found in natural uncontaminated river waters (0.001-0.005 µg/l), lake waters (0.0002-0.08 µg/l), groundwaters (0.0001-0.016 µg/l), and rain (0.005-0.09 µg/l) (Leopold et al., 2010). They were higher than concentrations found in Hg mine water runoff in Texas (0.0079-0.014 µg/l) (Gray et al., 2015) and comparable to concentrations determined in Hg mine drainage in California (ranging up to 280 µg/l) (Rytuba, 2000). Thus, flooding of the soil and alteration of E_H released substantial amounts of Hg_t which exceeded the Maximum Contaminant Level for Hg in drinking water (2 µg/l) recommended by the U.S. Environmental Protection Agency (U.S. EPA, 2009) and the trigger value for the assessment of the soil – groundwater pathway (1 µg/l) of the BBodSchV (1999). However, it has to be considered that the loss of soil structure and the continuous stirring of the flooded soil may have favored Hg release.

The mobilization of Hg_t, MeHg, and EtHg in CS and in CS+BC was generally high at low E_H and decreased with increasing E_H (Fig. 4-3). Consequently, several significant negative correlations between Hg species and E_H were determined (Table 0-2, Appendix A).

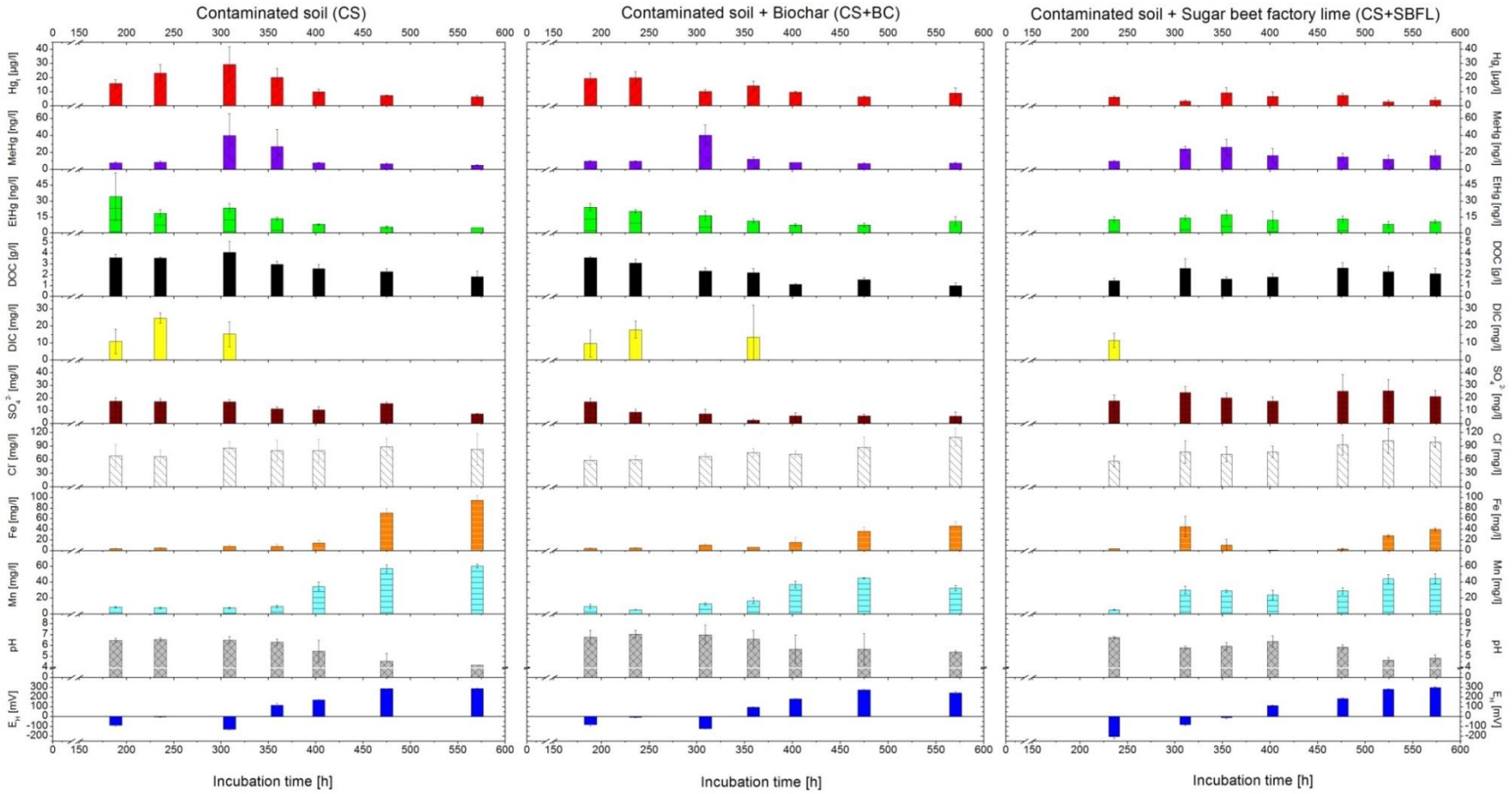

Figure 4-3: Impact of pre-defined E_H-conditions on release dynamics of total Hg (Hg_t), methylmercury (MeHg), ethylmercury (EtHg), dissolved organic carbon (DOC), dissolved inorganic carbon (DIC), sulfate (SO_4^{2-}), chloride (Cl^-), iron (Fe), manganese (Mn), and pH in a contaminated soil (CS) compared with a contaminated soil treated with biochar (CS+BC) and a contaminated soil treated with sugar beet factory lime (CS+SBFL). Columns represent mean and whiskers represent standard deviation of three replicates using biogeochemical microcosm systems.

The addition of BC and SBFL particularly influenced the release of Hg_t and partially changed the time when highest concentrations were measured.

In CS, the concentrations of dissolved Hg_t slightly increased from E_H -88 mV to -128 mV while increasing the E_H resulted in lower concentrations at E_H 119 mV. In CS+BC Hg_t concentrations were lower at an E_H of -122 mV indicating that the added BC curtailed the dissolution of Hg_t at this E_H (Fig. 4-3). Thus, we found a distinct difference in Hg_t release between CS and CS+BC at an E_H of about -125 mV. The pattern of dissolved Hg_t in CS+SBFL differed from those in CS and CS+BC and Hg_t concentrations were generally lower (Fig. 4-3, Table 0-1). The highest measured concentration was 15 µg/l and consequently constituting 35% and 59% of the maximum Hg_t concentrations found in CS and CS+BC, respectively. The lowest sampled E_H in CS+SBFL (-204 mV) was significantly lower than those sampled in CS (-128 mV) and CS+BC (-122 mV) (Fig. 4-3). The concentration of Hg_t in CS+SBFL remained in the same order of magnitude (3-9 µg/l) despite E_H fluctuations. These findings indicate that the SBFL amendment diminished the release of Hg_t from CS.

The amendment of CS with BC decreased the maximum Hg_t concentration (Table 0-1). The addition of SBFL was more efficient; the Hg_t concentration range was considerably lower. Still, Hg_t concentrations in both CS+BC and CS+SBFL exceeded the trigger value for the assessment of the soil – groundwater pathway of the BBodSchV (1999).

The pattern of Hg_t concentrations in CS+BC was of particular interest. It seems that the added BC curtailed Hg mobilization primarily at one particular E_H (Fig. 4-3). Under highly reduced conditions at an E_H of around -125 mV Hg_t concentration in CS+BC was reduced by 65% compared to CS while little deviations between CS and CS+BC Hg_t concentrations were found for the following E_H windows. This suggests that BC provided redox sensitive binding sites for Hg. One possible explanation are BC associated disulfide bridges which turned into two thiol groups under highly reduced conditions providing strong binding sites for Hg lowering dissolved Hg_t concentrations. Mercury could have been released again with changing E_H due to the redox sensitivity of the disulfide bridges. Such disulfide-dithiol sites exist in biological systems and are part of enzyme-based microbial Hg resistance (Robinson and Tuovinen, 1984; Barkay et al., 2003).

The amendment of CS with SBFL resulted in lower Hg_t concentrations irrespective of E_H window (Fig. 4-3). The bulk material SBFL mainly consists of lime whose chemical composition depends on its origin. Calcium oxide (CaO) is usually the main constituent of lime while silicon dioxide (SiO_2), Al_2O_3, Fe_2O_3, MgO, and calcium carbonate ($CaCO_3$) are pre-

sent in variable amounts (Panda et al., 2012; Kiliç, 2013; Zumrawi and Hamza, 2014; Sarsam et al., 2017). However, the main constituent of carbonated lime, such as SBFL, is $CaCO_3$, which accounted for more than 80% of SBFL (Shaheen and Rinklebe, 2017). Sorption of various metal ions such as Cd^{2+}, Mn^{2+}, Zn^{2+}, and Co^{2+} on $CaCO_3$ has been shown (Comans and Middelburg, 1987). In this context, two reactions were identified: an initial rapid uptake and a subsequent slow precipitation, i.e. a more stable incorporation of the metal into the crystal lattice (Comans and Middelburg, 1987; Papadopoulos and Rowell, 1988). Calcium carbonate has been successfully utilized to remove Hg from coal flue gas (Hutson et al., 2008) or oil field brine (Fazlollahi et al., 2014). Furthermore, other constituents of lime, such as SiO_2 exposing hydroxyl groups (≡Si-OH) (Tiffreau et al., 1995), iron oxides (Bonnissel-Gissinger et al., 1999), and CaO (binding $HgCl_2$) (Guo et al., 2007; Sasmaz and Wilcox, 2008) are capable to bind Hg. Heeraman et al. (2001) showed that lime amendment significantly reduced Hg mobilization in soils. Moreover, calcareous soils were found to release less bioavailable Hg compared to acidic soils (Frey and Rieder, 2013). Apparently, the binding sites of SBFL had a strong potential to reduce Hg_t in CS+SBFL at all E_Hs studied in the experimental conditions.

The highest MeHg concentrations in CS were found at E_H values of -128 mV (40 ng/l) and 119 mV (27 ng/l), and similar patterns were observed in CS+BC and CS+SBFL (Fig. 4-3, note the E_H). In general, a clear increase in MeHg was found at an E_H around -100 mV in CS and the treatments. Such increase at the given E_H was probably related to Hg methylation rather than MeHg release. In CS+SBFL MeHg concentrations were comparatively low at E_H -204 mV, indicating that the prevailing conditions at this particular low E_H did not seem to favor MeHg release or Hg methylation. On the other hand, we may conclude that an E_H above -90 mV was probably too high for optimal Hg methylation, since the MeHg results for CS at -88 mV and CS+BC at -80 mV were also relatively low. Following this assumption, methylation peaked between -204 and -90 mV in CS and the treatments, and decreased thereafter, which would explain why we found a higher MeHg concentration in CS+SBFL compared to CS and CS+BC at E_H window 0 mV (Fig. 4-3). On the other hand, the highest measured MeHg concentration in CS+SBFL was almost half as high as in CS, and variations of dissolved MeHg in CS+SBFL were not as pronounced as in CS and CS+BC (Table 0-1, Fig. 4-3).

Correlations between MeHg and Hg_t were missing in CS and CS+BC (Table 0-2), probably due to the strong in- and decrease of the MeHg concentrations and the low Hg_t concen-

tration at E_H ~ -125 mV in CS+BC (Fig. 4-3). In CS+SBFL, a modest positive correlation between MeHg and Hg_t was found, which is relatively rarely observed, as the amount of bioavailable Hg in Hg_t may vary, and since it is suggested that MeHg production is rather limited by microbial methylation potential than by Hg bioavailability (Frohne et al., 2012; Feng et al., 2014; Bowman et al., 2015). Consequently, Frohne et al. (2012) assumed that Hg_t has limited utility as a predictor of Hg net methylation. Despite the fact that Hg methylation is primarily taking place under anaerobic conditions, significant correlations between MeHg and E_H are usually missing (DeLaune et al., 2004; Sunderland et al., 2006; Frohne et al., 2012). Consistently, a significant negative correlation between MeHg and E_H was only found in CS+BC (Table 0-2).

The highest dissolved EtHg concentration in CS was measured at E_H -88 mV. However, the high relative standard deviation indicates that the general pattern in CS was not significantly different from those in CS+BC and CS+SBFL. In general, EtHg concentrations in CS and CS+BC were around 20 ng/l for samples collected at E_H values below 0 mV (Fig. 4-3). Concentrations decreased slightly with increasing E_H. Consequently, significant negative correlations between EtHg and E_H were detected in CS and CS+BC (Table 0-2). Mean EtHg concentrations were similar in CS, CS+BC, and CS+SBFL. Also, no significant decrease in EtHg was detected due to the amendment of CS with BC or SBFL (Table 0-1). A relation between EtHg and E_H was missing in CS+SBFL. Instead, strong positive correlations were found between EtHg and Hg_t in CS+SBFL and CS+BC (Table 0-2). The absence of this correlation in CS might be due to the high EtHg concentration determined for the sampling at E_H -88 mV.

Ethylmercury contents found in soils of the Florida Everglades in absence of obvious anthropogenic sources indicate that biotic and abiotic alkylation may provoke widespread existence of EtHg in the environment (Cai et al., 1997; Mao et al., 2010). Formation of EtHg has been found in tissues of common dwarf garden pea (*Pisum sativum*) after exposure to elemental Hg vapor; and the presence of EtHg in St. Clair River sediments has been explained by ethylmercury chloride formation when high-octane gasoline containing tetraethyllead was combined with an aqueous solution of mercuric chloride (Fortmann et al., 1978; Jernelöv and Wennergren, 1980). The lack of knowledge on EtHg formation and environmental fate is also due to the fact that EtHg concentrations in environmental samples other than soil are frequently below the detection limit (Beckers and Rinklebe, 2017). However, it has been noted that EtHg is not very persistent and readily decomposes in the

environment (Hintelmann, 2010). This suggests that concentrations determined in the course of our experiment are rather a product of EtHg formation than of legacy EtHg release.

Positive correlations were found for Hg_t and pH in CS and CS+SBFL (Table 0-2). Divalent mercury shows a different behavior than most other divalent metals as its extent of adsorption is greatest in acidic media (Barrow and Cox, 1992; Yin et al., 1996; Sarkar et al., 1999; Pelcová et al., 2010). It seems that Hg adsorption is particularly high at pH 3 (Pelcová et al., 2010; Xu et al., 2014). Increasing concentrations of Cl^- may reduce Hg adsorption and sorption maximum may move to higher pH (Barrow and Cox, 1992). This effect of Cl^- may not always be observed, as it depends on various parameters such as Hg species and concentration, soil organic matter content, Cl^- and sulfide concentration (Yin et al., 1996; Pelcová et al., 2010; Xu et al., 2014). Our results were similar to those of Pelcová et al. (2010) who also found decreasing Hg adsorption with increasing pH. However, linear relationships between Hg_t and pH are uncommon (Xu et al., 2014). Latter authors observed enhanced Hg desorption from soil at pH 5 and 11 but generally found that pH adjustment was insufficient for Hg removal since only up to 0.3% of soil Hg_t was mobilized at these pH values. Thus, the diminished Hg_t concentration in CS+SBFL was probably the result of diverse binding sites of the liming material rather than of pH changes.

Based on the finding that intracellular accumulation and toxicity of Hg(II) in model bacteria *E. coli* HMS174 were both significantly enhanced with decreasing pH under anaerobic conditions, it has been suggested that increased concentrations of Hg(II) within methylating bacteria due to declining pH values would probably enhance methylation activity (Golding et al., 2008). Consistently, strong negative relationships between MeHg and pH are frequently reported (e.g. Ullrich et al., 2001) but were not found in our experiment (Table 0-2). Mercury methylation is principally driven by microbial activity, and it is accepted that it occurs primarily under anaerobic conditions and that SRB mainly govern this process (Compeau and Bartha, 1985; Beckers and Rinklebe, 2017). In fact, MeHg and SO_4^{2-} have been used as indicators of seasonal redox changes with high MeHg during low SO_4^{2-} being indicative of reducing conditions (Ekström et al., 2016). However, not all bacteria of the SRB phylogenetic tree methylate Hg (Barkay and Wagner-Döbler, 2005; Parks et al., 2013), and certain strains of iron-reducing bacteria are also capable of methylating Hg, while methanogens that are known to rather demethylate MeHg may become the primary methylators under specific environmental conditions (Fleming et al., 2006; Hamelin

et al., 2011; Beckers and Rinklebe, 2017). Sulfate-reducing bacteria perform SO_4^{2-} reduction under highly reduced conditions at E_Hs between -100 and -1000 mV (Dominique et al., 2007; Fritsche et al., 2014). This is in good agreement with our finding that the concentrations of MeHg in CS and CS+BC sharply increased at an E_H of around -125 mV (Fig. 4-3). The ratio of SO_4^{2-} to Cl^- can be used as an indicator for SO_4^{2-} reduction (Alpers et al., 2014). According to the latter authors, a decreasing ratio may indicate SO_4^{2-} reduction which in turn may be attributed to the SRB. However, significant negative correlations between MeHg and (SO_4^{2-}/Cl^-) were not detected. The ratio of MeHg to Hg_t is assumed to reflect the methylation efficiency (Frohne et al., 2012; Alpers et al., 2014). Low MeHg/Hg_t rates are associated either with low Hg methylation or high demethylation rates (Remy et al., 2006). The highest methylation efficiencies in CS and CS+BC were found at an E_H of around -125 mV which falls within the range of SO_4^{2-} reduction (DeLaune and Reddy, 2005) and supports the hypothesis that Hg methylation took place and was mediated by SRB in our experiment. In CS the efficiency increase was about 3.7 fold, while it was about 8 fold in CS+BC. In CS the methylation efficiency remained elevated at E_H 119 mV, decreased thereafter and persisted fairly constant afterwards. In CS+BC the methylation efficiency had already declined at E_H 96 mV and remained constant thereafter. The methylation efficiency in CS+SBFL was highest at E_H -80 mV and its preceding increase was about 4.6 fold. The methylation efficiency in CS+SBFL was generally higher than in CS and CS+BC: The highest methylation efficiency in CS+SBFL was about 5.3 times higher compared to CS and about 1.9 times higher compared to CS+BC. Methylmercury concentrations are the result of ongoing methylation and demethylation processes (Lambertsson and Nilsson, 2006; Lazaro et al., 2016). Therefore, MeHg concentrations found under reduced or moderately reduced conditions in our experiment may be partly explained by the persistence of MeHg proportions after major net methylation of Hg had been taken place earlier when E_H fell below -100 mV. According to Hintelmann (2010), most MeHg in many aquatic environments is generated in the sediments, since MeHg production is basically the product of microbial activity and Hg(II) bioavailability. At the same time demethylation rates within sediments are also very pronounced, leading to a standing MeHg pool, which is suggested to constitute at most 1% of the Hg_t (Hintelmann, 2010; Randall et al., 2013). In contrast, demethylation activity is almost absent in water, making the little MeHg transferred from sediments into the overlying water very persistent in this compartment (Hintelmann, 2010). However, our MeHg results for CS and CS+BC indicate that

comparatively high MeHg concentrations can be depleted within two days following controlled E_H changes.

The positive correlations found between EtHg and pH in CS and CS+BC are in good agreement with Pelcová et al. (2010), who found that EtHg adsorption to river sediments was highest at pH 3-4.

4.2.3 Impact of DOC, SO_4^{2-}, Cl^-, PO_4^{3-}, Fe, and Mn changes on mobilization of Hg_t, MeHg, and EtHg in CS, CS+BC, and CS+SBFL

A strong correlation between Hg_t and DOC was found in CS and CS+BC (Fig. 4-3, Table 0-2). Positive correlations between Hg_t and DOC were reported from numerous aquatic ecosystems (e.g. Picado and Bengtsson, 2012; Hinkle et al., 2013; Johannesson and Neumann, 2013) since DOC is generally regarded as the predominant ligand for both Hg_t and MeHg in oxic (sulfide-free) waters (Ravichandran, 2004; Gorski et al., 2008; Chadwick et al., 2013). This link is principally attributed to the strong affinity of Hg_t for reactive (reduced) thiol functional groups within DOC (Ravichandran, 2004; Tsui and Finlay, 2011; Frohne et al., 2012). However, as indicated by the absence of a similar correlation in CS+SBFL, a positive correlation may not always be detected, since the binding is controlled by a small fraction of dissolved organic matter molecules which contain these thiol groups (Ravichandran, 2004). According to the latter author it is most likely to be found when Hg_t is mainly derived from wetlands and soils, where Hg_t is discharged and co-transported bound to organic carbon, as has been reported by Wallschläger et al. (1996). This pattern is in good agreement with our findings in CS and CS+BC. In both CS and CS+BC correlations between either Hg_t or DOC with Fe or Mn are negative, indicating that the release of Hg_t or DOC at low E_H was not governed by the reductive dissolution of particulate Fe and Mn oxyhydroxides (Fig. 4-3, Table 0-2). Instead, it seems that fine biologically decomposed organic matter with associated Hg entered the aqueous phase upon flooding of the soil. Figure 4-4 shows the strong influence of E_H and DOC on Hg_t mobilization in CS and the changing pattern due to the addition of BC and SBFL, respectively.

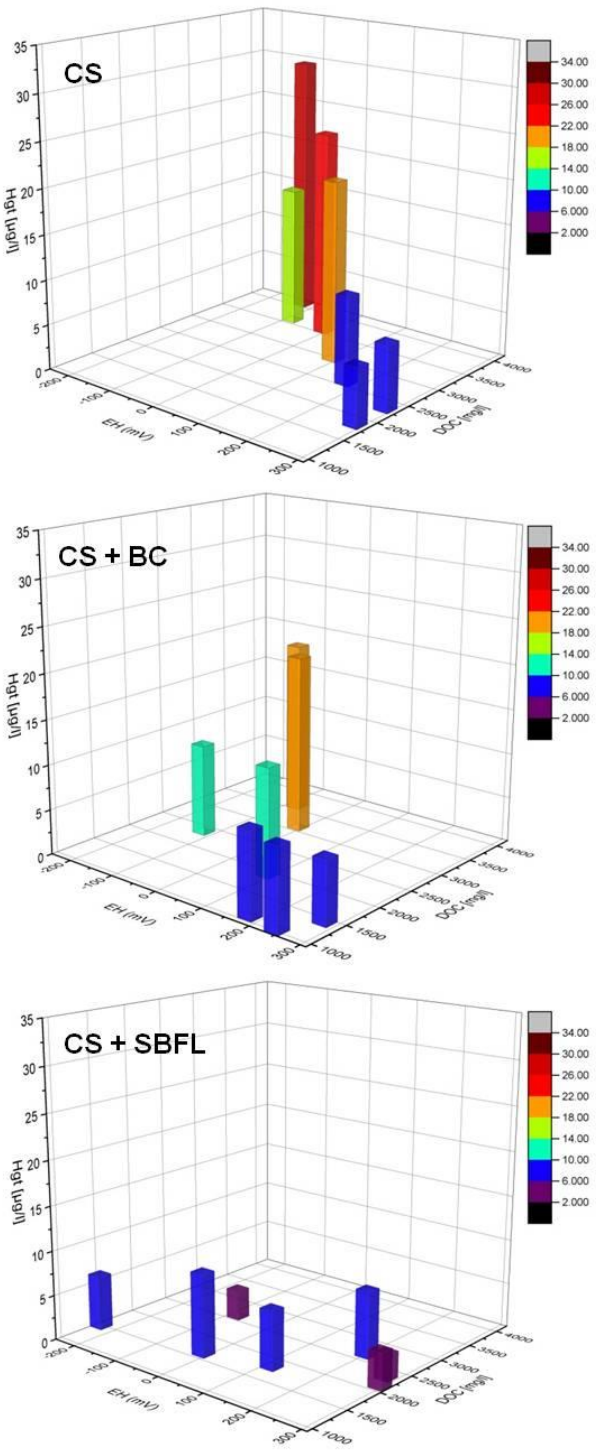

Figure 4-4: Dependency of Hg_t concentrations in soil solution from redox potential (E_H) and DOC displayed in a three-dimensional coordinate system. Bars show means of data obtained for CS, CS+BC, and CS+SBFL. Bar colors correspond to the concentrations indicated by the color scale.

In CS+SBFL, a strong relation between the release of Hg_t and DOC is unlikely since a correlation between both parameters is missing. Positive correlations between DOC and EtHg were found in CS and CS+BC. In general, similar correlations of Hg_t and EtHg with the other parameters were found in CS and CS+BC: Negative correlations were found with Fe, Mn, and PO_4^{3-} (in CS solely), while positive correlations were detected with pH, DOC,

and SO_4^{2-}. We may suggest that the analogous correlations in CS and CS+BC may not necessarily indicate that the release or formation of EtHg is related to one of these parameters, since the only correlations found for EtHg in CS+SBFL were those with Hg_t and MeHg (Table 0-2). However, congruent with the relation found in our experiment, Pelcová et al. (2010) observed that the adsorption of EtHg to sediments decreased with SO_4^{2-} addition. Contrarily, in CS+SBFL an analogous correlation was missing and EtHg concentrations were comparable to CS and CS+BC, while SO_4^{2-} concentrations were considerably higher (Fig. 4-3, Table 0-2). Pelcová et al. (2010) increased the SO_4^{2-} concentration in solution to 50 and 200 mg/l, respectively, and found only slight differences in EtHg adsorption between these two concentrations. Thus, we may suggest that SO_4^{2-} differences between CS and the treatments had little effect on EtHg concentrations measured in solution.

Chloride is a potentially important inorganic ligand for Hg in terrestrial and aquatic ecosystems (Frey and Rieder, 2013; Jiménez-Moreno et al., 2013). Its concentrations may influence both the formation and the stability of MeHg (Beckers and Rinklebe, 2017). It has been indicated that abiotic and biotic demethylation of MeHg are more effective in ecosystems containing higher Cl^- concentrations such as marine ecosystems than in freshwater ones (Compeau and Bartha, 1984; Jiménez-Moreno et al., 2013). Furthermore, the presence of Cl^- may curtail dimethylmercury formation (Perrot et al., 2013). However, a clear influence of changing Cl^- concentrations on Hg release or the formation of organic Hg species could not be determined in our experiment (missing correlation; Table 0-2). This is in good agreement with other studies which examined the influence of Cl^- on Hg mobilization (Yin et al., 1996; Pelcová et al., 2010; Xu et al., 2014). The effect of changing Cl^- concentrations on Hg depends on diverse parameters, including Hg species and concentration, OM content, Cl^- and sulfide concentration, and pH (Pelcová et al., 2010). Our results indicate that concentrations of dissolved Hg_t were higher at lower Cl^- and higher DOC concentrations in CS and CS+BC (Fig. 4-5). Higher Cl^- concentrations may provoke the formation and precipitation of Hg_2Cl_2, thereby removing dissolved Hg (Kim et al., 2004; Chen et al., 2017).

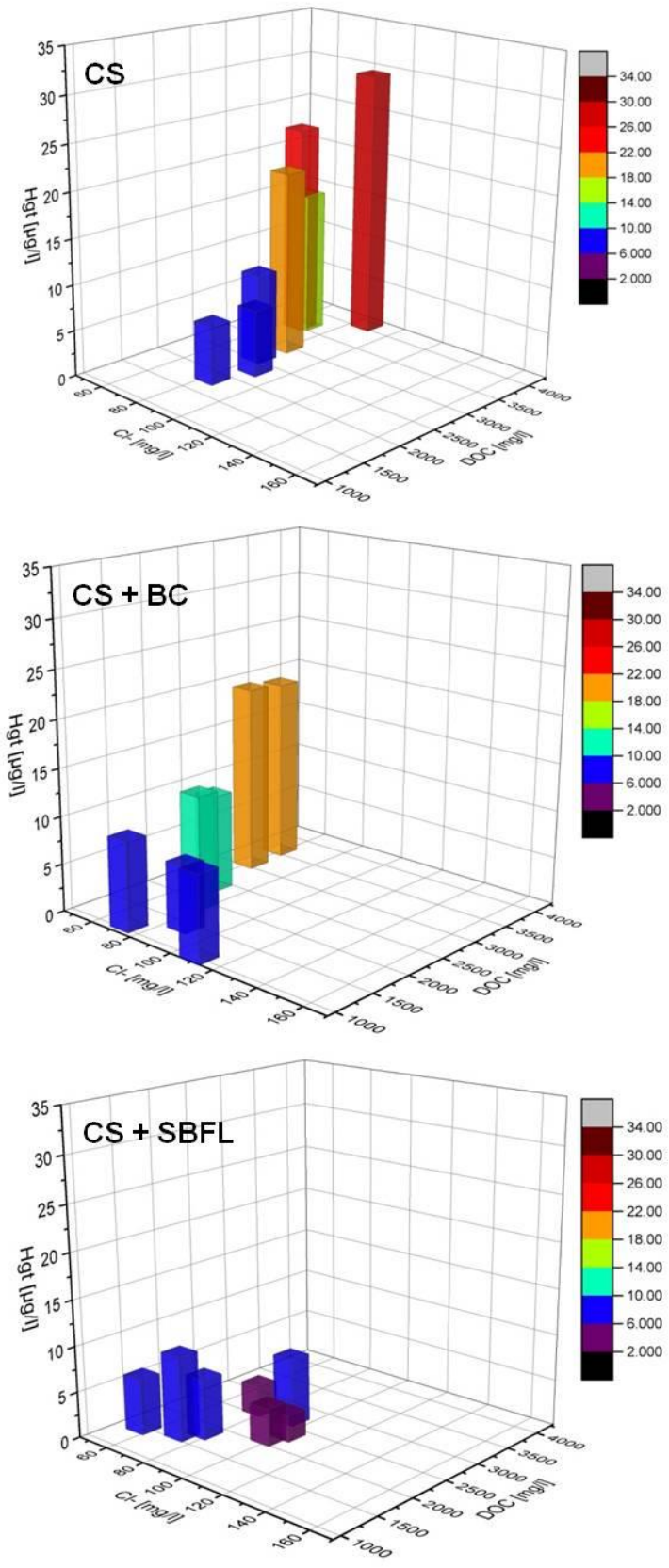

Figure 4-5: Dependency of Hg_t concentrations in soil solution from chloride concentrations (Cl^-) and DOC displayed in a three-dimensional coordinate system. Bars show means of data obtained for CS, CS+BC, and CS+SBFL. Bar colors correspond to the concentrations indicated by the color scale.

Phosphate is seen as a proxy for organic matter (OM) mineralization, and it is suggested that the relation between MeHg and PO_4^{3-} indicates that the MeHg production is linked to the availability and remineralization of OM (Cossa et al., 2009; Lehnherr, 2014). Thus, biological production would promote both higher MeHg and PO_4^{3-} concentrations in solution (Cossa et al., 2009). The significant positive correlation found for MeHg and PO_4^{3-} in CS+BC may therefore indicate biological production (Table 0-2).

We performed factor analyses for CS and the treatments (Fig. 4-6) to evaluate associations between the measured parameters and to identify hidden multivariate data structures. We extracted two factors. These factors explained 71.77% of the total variance in CS (60.55% Component No. 1 and 11.22% Component No. 2), 70.89% in CS+BC (57.67% Component No. 1 and 13.22% Component No. 2), and 62.97% in CS+SBFL (39.66% Component No. 1 and 23.31% Component No. 2), respectively.

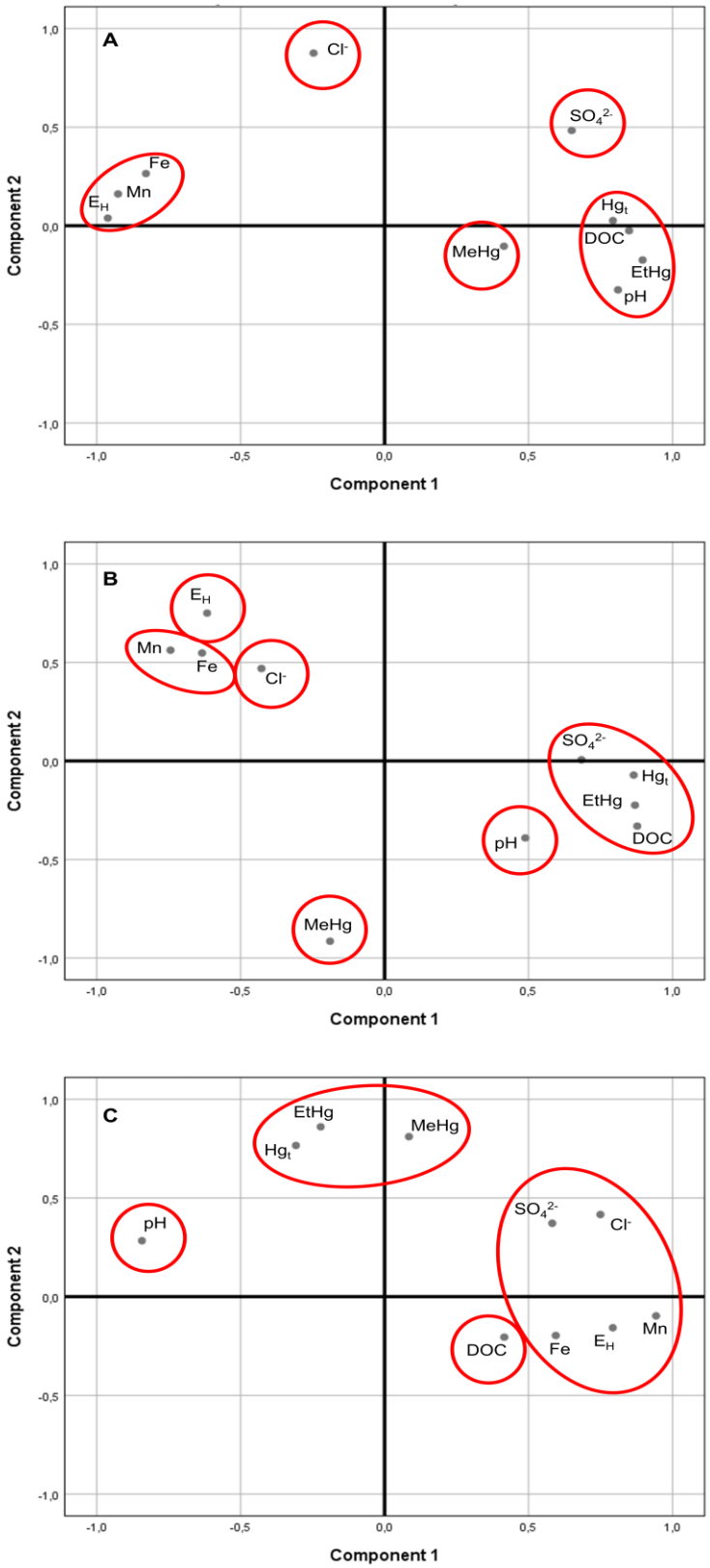

Figure 4-6: Factor analysis of the contaminated soil (A), the contaminated soil + biochar (B), and the contaminated soil + sugar beet factory lime (C). Kaiser-Meyer-Olkin (KMO) measures were 0.606 for CS, 0.689 for CS+BC, and 0.559 for CS+SBFL, respectively.

Figure 4-6A demonstrates that Hg_t, EtHg, DOC, and pH had high loadings on Component No. 1 in CS, which indicates a similar behavior of these parameters. Iron, Mn, and E_H showed an opposite behavior with high negative loadings on Component No. 1, which is in good agreement with the correlation patterns and our argumentations above. Thus, Hg_t, EtHg, DOC, and pH decreased with rising E_H, while Fe and Mn increased. Chloride was the only variable with a high loading on Component 2, while SO_4^{2-} and particularly MeHg loaded rather on Component 1 but were presumably best explained by other components. In CS+BC Hg_t, EtHg, and DOC behaved very similar and clustered along with SO_4^{2-} (Fig. 4-6B). Iron and Mn grouped together, and their cluster differentiated from the first mentioned cluster, indicating dissimilar biogeochemical behavior. The E_H was relatively close to Fe and Mn but loaded high on Component 2. Contrarily, MeHg had a high negative load on Component 2, illustrating the opposite behavior to E_H. The pH and Cl^- were not grouped with other parameters. In CS+SBFL Hg_t and EtHg were clustered together suggesting a comparable biogeochemical behavior in our experiment (Fig. 4-6C). Here, MeHg was grouped with Hg_t and EtHg. Iron and Mn clustered with E_H, while pH and DOC were free-standing. Summarizing, the results of the factor analyses indicate similarities in the biogeochemical behavior of Hg_t and EtHg as well as Fe and Mn, regardless of whether CS was amended or not. It seems that the BC amendment particularly influenced Cl^-, SO_4^{2-}, pH, and MeHg, while there was little effect on other parameters when compared to CS. The added SBFL had a more pronounced effect on the interrelationships of the parameters.

We used CDA to identify significant differences in the parameters among CS, CS+BC, and CS+SBFL, and to determine those parameters with the highest discriminatory power. Figure 4-7 shows the results of the CDA, illustrating that there is a clear discrimination in the biogeochemical behavior between CS and the treatments. Function 1 is able to explain 74.3% of the variability of the biogeochemical behavior between CS and the treatments; Function 2 can explain 25.7% and both functions together 100.0%.

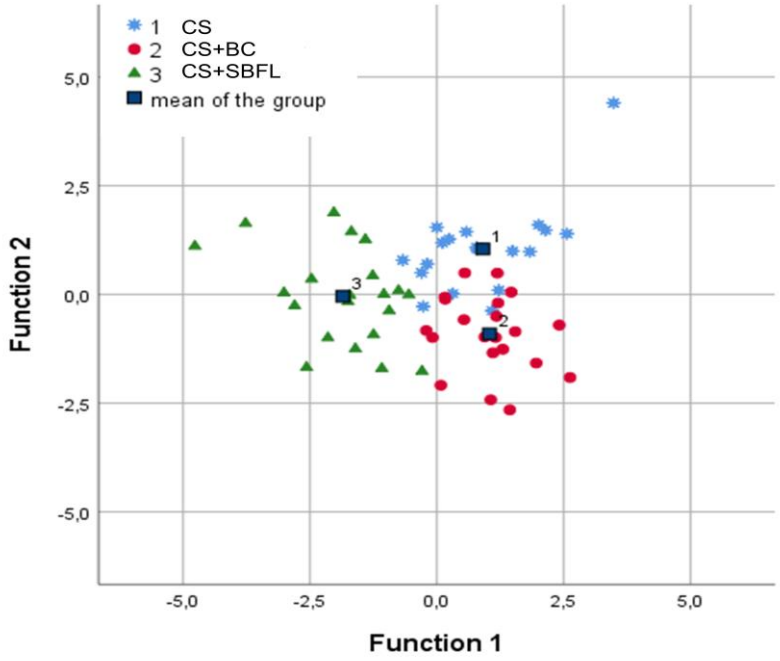

Figure 4-7: The canonical discriminant analysis (CDA) illustrates the different biogeochemical properties of the contaminated soil (CS), the contaminated soil + biochar (CS+BC), and the contaminated soil + sugar beet factory lime (CS+SBFL).

Function 1 discriminates CS and the treatments into two groups; CS and CS+BC on the one hand and CS+SBFL on the other hand. Function 2 segregates CS and CS+BC in two groups. The standardized canonical discriminant coefficient shows that the parameters SO_4^{2-} and Hg_t are most important for the discrimination of CS and the treatments based on Function 1. Based on Function 2 EtHg, Hg_t, and DOC are the most responsible parameters for discrimination. The CDA results clearly corroborate the finding that both amendments changed the biogeochemical pattern in the soil, with SBFL provoking a more distinct change.

4.2.4 Impact of E_H/pH changes on the microbial community

In summary, 61 PLFAs were identified but we focused on fatty acids with carbon numbers between C_{12} and C_{20} as bacteria have been shown to have fatty acids mainly in this range (White et al., 1996; Jiang et al., 2012) (Fig. 0-2, Appendix A). The results for the PLFAs considered for the SRB were similar to the picture obtained for the range C_{12} and C_{20} (Figs. 4-8 and 0-2).

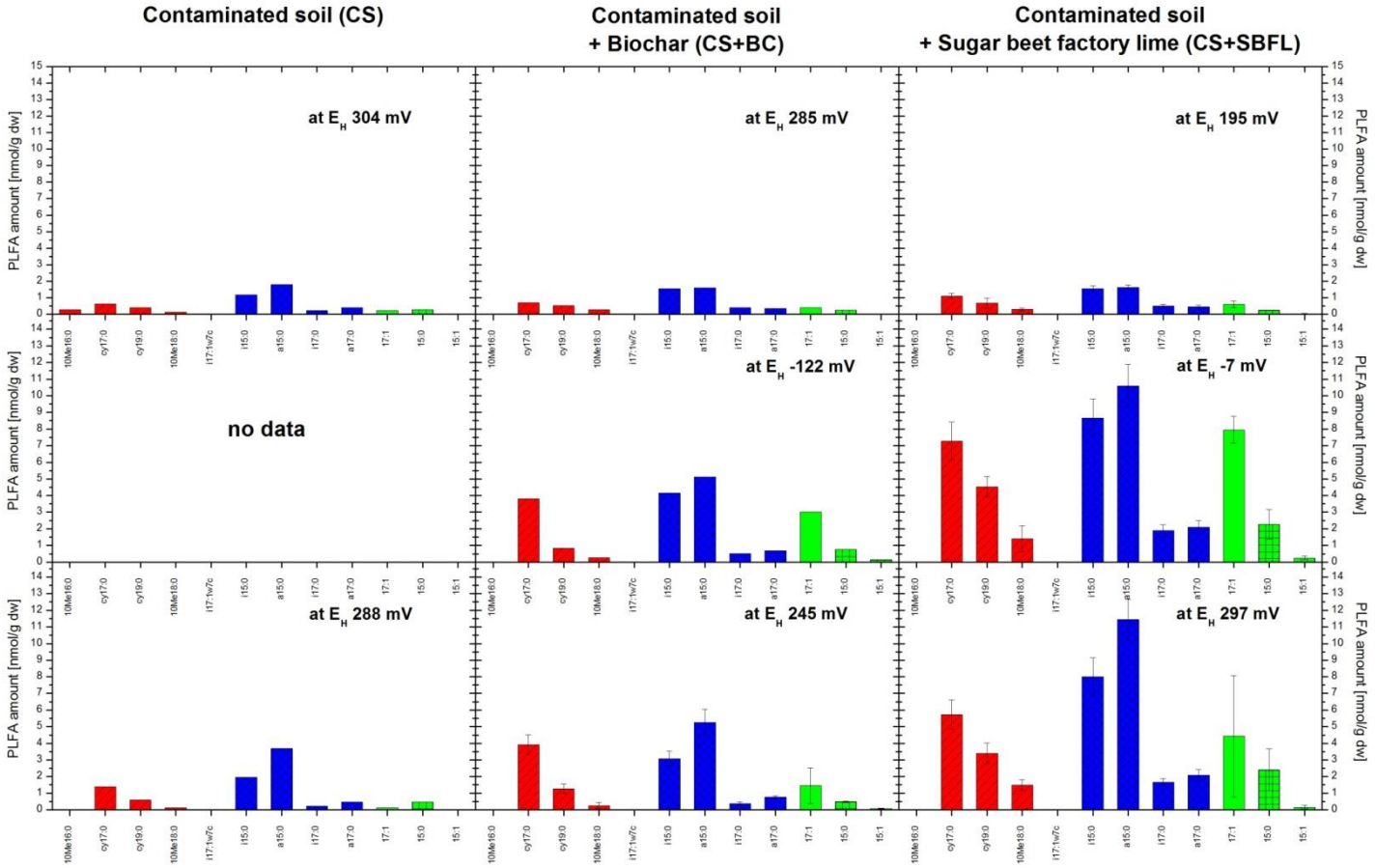

Figure 4-8: SRB PLFA amounts as influenced by soil treatment and changing E_H/pH. The PLFAs considered to identify the SRB genera *Desulfobacter* (red), *Desulfovibrio* (blue), and *Desulfobulbus* (green) are particularly 10Me16:0, i17:1ω7c, and 17:1ω6 (part of the summed aggregate 17:1). Hatched columns indicate potentially useful indicators. The amount of the PLFA 10Me16:0 should be higher than that of 10Me18:0 to indicate the SRB genus *Desulfobacter*.

The PLFA amounts at the time of the initial sampling were substantially lower than those determined at low E_H and at higher E_H at the end of the experiment. In general, there was a considerable increase in PLFA amount after flooding of the soils. It is well established that rewetting of dried soils is usually followed by a "pulse" or "flush" of soil respiration and that bacterial growth rates in rewetted soils exceed those in continually moist soils several hours after rewetting and for a given period of time (Birch, 1958; Meisner et al., 2013; Sun et al., 2015). Comparing CS and the treatments it was found that both amendments, BC and SBFL, stimulated microbial growth as inferred from PLFA profiles, even though data for CS at low E_H are missing. We may suggest that the general pattern in CS and the treatments was similar with growing PLFA biomass after flooding of the soil and slightly decreasing abundances at high E_H at the end of the experiment. The influence of SBFL on microbial growth was higher compared to BC.

In general, anaerobic respiration yields less energy for the microorganisms compared to respiration of oxygen which may favor the increase of PLFA biomass at higher E_H (Froelich et al., 1979; Jurtshuk Jr., 1996; Antler et al., 2013). The fact that we found high PLFA abundance at low E_H may be explained by the wetting "pulse" which was probably enhanced by our addition of straw and glucose as an additional carbon sources for soil microorganisms aiming to promote redox processes. The PLFA biomass at higher E_H at the end of the experiment was surprisingly in the similar order of magnitude as at low E_H. We expected a higher PLFA biomass here, however, the relatively lower PLFA biomass might be attributed to a slow reaction of the microbial community on the changing E_H conditions. A lag phase might have occurred in the course of the shifting microbial community structure from anaerobic to aerobic microorganisms (Maier, 2009; Rolfe et al., 2012).

The amounts of PLFAs considered for the SRB found within the initial samplings in CS and the treatments were very similar (Fig. 4-8). Small amounts of the suggested *Desulfobacter* biomarker fatty acid 10Me16:0 were determined in CS while this PLFA was not detected in the treatments. However, the use of the fatty acid 10Me16:0 as *Desulfobacter* biomarker is disputed.

Parkes et al. (1993), who investigated changes in viable counts of SRB and PLFA induced by different substrate additions, found that increases in SRB due to acetate addition determined by viable counts were reflected by a slight increase of the fatty acids 16:0 and 16:1ω7. The genus *Desulfobacter* oxidizes acetate preferentially or even exclusively (Boschker et al., 2001) but the biomarker PLFA for *Desulfobacter*-type SRB 10Me16:0 was not stimulated in the study of Parkes et al. (1993). Similarly, results of other studies

indicated that 10Me16:0 should be used with care as a specific biomarker for *Desulfobacter*, as they suggest that substantial amounts of 10Me16:0 might rather be attributed to other bacteria such as *Desulfobacterium autotrophicum* (Vainshtein et al., 1992; Oude Elferink et al., 1998; Boschker et al., 2001). Parkes et al. (1993) suggested that the increases in 16:0 and 16:1ω7 may have been due to *Desulfobacter* or some other acetate utilizing SRB, as high concentrations of 16:1ω7 were reported in *Desulfobacter*-like 'fat vibrio' and *Desulfotomaculum acetoxidans* before (Dowling et al., 1986).

The *Desulfovibrio* biomarker i17:1ω7c was neither detected in CS nor in the treatments. The fatty acid 17:1ω6, which was considered as indicator for the genus *Desulfobulbus*, could not be determined individually but as part of the summed aggregate 17:1. The variations of this PLFA between CS and the treatments at the initial sampling were rather small. The amounts of 17:1 in CS+SBFL were slightly higher compared to CS and CS+BC.

Substantial increases of specific PLFAs were determined at low E_H when concentrations of MeHg in the slurry were particularly high. Considerable increases of the PLFAs cy17:0, i15:0, a15:0, and 17:1 were found in both treatments. Additionally, fatty acid cy19:0 showed a clear increase in CS+SBFL. The biomarker PLFAs 10Me16:0 and i17:1ω7c were again neither found in CS+BC nor in CS+SBFL. However, even though the abundance of 17:1 was about 2.6 times higher in CS+SBFL MeHg concentrations were about 1.5 times lower in CS+SBFL compared to CS+BC. This may be explained by possible differences in 17:1ω6 ratios within the summed aggregate 17:1 in CS+BC and CS+SBFL but is most likely a result of the combination of specific bacterial abundances with other biotic and abiotic influencing factors that may alter formation, persistence, and degradation of MeHg within the slurries. Another explanation for the higher MeHg concentrations in CS+BC results from the findings of Parkes et al. (1993): We may suggest that the absence of the fatty acid 10Me16:0 does not necessarily indicate the absence of the genus *Desulfobacter* as the fatty acid 16:0 and the summed aggregate 16:1 (including 16:1ω7) showed higher abundances in CS+BC at low E_H compared to CS+SBFL, which may signify the presence of the genus *Desulfobacter* and may therefore explain the higher concentrations of MeHg in CS+BC (Figs. 0-2 and 4-3). However, Jiang et al. (2012) mentioned that contents of 16:0 and 16:1ω7 are not expected to be higher than biomarker PLFAs when derived from SRB. Further information on 16:0 and 16:1ω7 is provided in the Appendix A.

The PLFA amounts detected at higher E_H in CS and the treatments at the end of the experiment show the same trend already observed in the course of the initial and the sampling at low E_H: PLFA abundances were lowest in CS and highest in CS+SBFL. The fatty acid

10Me16:0 was again missing in the treatments but was not found in CS as well. The summed aggregate 17:1 showed a comparatively strong decrease due to the changing E_H irrespective of treatment while other PLFA abundances remained fairly constant.

In summary, our PLFA results support the hypothesis that SRB might have been methylators of Hg in the course of our experiment. Specific biomarker PLFAs were rarely (10Me16:0), not (i17:1ω7c), or only determined as part of a summed aggregate (17:1ω6). Nevertheless, other PLFAs that may serve as indicators of the presence of SRB genera such as cy17:0, i15:0, and a15:0 showed higher abundances at the time MeHg concentrations were found to be highest. Moreover, our results support the hypothesis that the use of 10Me16:0 as specific biomarker for *Desulfobacter* is debatable. We may rather presume that the presence of the genus *Desulfobacter* could have been indicated by the abundance of the PLFAs 16:0 and 16:1ω7 (part of the summed aggregate 16:1 in Fig. 0-2) as also suggested by Parkes et al. (1993).

4.3 Conclusions

The mobilization of Hg_t, MeHg, and EtHg was generally higher at low E_H and decreased with increasing E_H irrespective of soil treatment. Co-dissolution of Hg and DOC upon flooding may have contributed to this. Both amendments diminished the Hg_t mobilization from a contaminated floodplain soil even under dynamic redox conditions. However, the added BC was principally efficient in curtailing Hg_t release around E_H -125 mV, which may limit its applicability to a small E_H range. Sugar beet factory lime was more efficient in curtailing Hg_t release, since less than half of Hg_t was found in solution compared to CS. It probably reduced Hg_t mobilization by different binding sites; thereby the incorporation of Hg into the crystal lattice might have occurred. The higher methylation efficiency in CS+SBFL, indicated by the MeHg/Hg_t rate, counterbalanced the benefit of lower Hg_t release. No perceivable influence of BC and SBFL on MeHg and EtHg concentrations was detected during our experiment.

The MeHg results may suggest that Hg methylation was the main process leading to substantial increases in MeHg concentrations at particular conditions rather than release from the solid phase. Methylmercury concentrations in CS, CS+BC, and CS+SBFL peaked within the range of SO_4^{2-} reduction at an E_H between -204 and -90 mV. Therefore, SRB are suggested to be responsible for a significant part of methylation in CS and the treatments. The abundances of several PLFAs that may indicate the presence of SRB increased at low-

er E_H supporting this hypothesis. The MeHg results for CS and CS+BC indicate that comparatively high MeHg concentrations may have formed and may have been depleted within a short period of time following controlled E_H changes into and out of the range of SO_4^{2-} reduction. This finding should be validated considering its implications for risk assessments. In general, future research should deeper elucidate the role of SRB and their contribution to Hg methylation. Within this context, the use of microbial molecular techniques under dynamic redox conditions remains a challenge. Moreover, Hg contents and composition of the solid phase should be determined to identify geochemical changes. Also, the impact of E_H retention times should be systematically studied to identify their influence on biogeochemical processes. Furthermore, experiments with lower DOC concentrations should be conducted. Finally, other types of low cost soil amendments should be tested for their ability to immobilize Hg while simultaneously impeding the formation of MeHg or EtHg under dynamic redox conditions in the laboratory and in the field.

5. Mobilization of mercury species under dynamic redox conditions in a contaminated Wupper floodplain soil as influenced by two different types of biochar

5.1 Short introduction Chapter 5

Potential Hg binding sites of biochars include for example sulfhydryl and carboxyl groups. Dependent on the temperature regime for biochar production the resultant biochars differ in their chemical and physical properties. Chemical structures which potentially mediate Hg binding to biochar can be altered in their abundance by the pyrolysis temperature resulting in overall differing binding capacity for Hg between the biochar types. We used BC200 and BC500, manufactured at 200 °C and 500 °C, respectively to investigate their effects on Hg binding and how they differ in their efficiency to bind Hg. A number of parameters and chemical compounds which have an effect on or interfere with Hg immobilization were quantified such as pH, E_H, and DOC as well as some anions and metals. Also, speciation of Hg was studied in greater detail considering MeHg and EtHg in addition to Hg_t and linkages between shifts in Hg species and changes in soil microbial community structure as determined by PLFA analysis were investigated. The theoretical and methodological background is summarized in the following Figure 5-1.

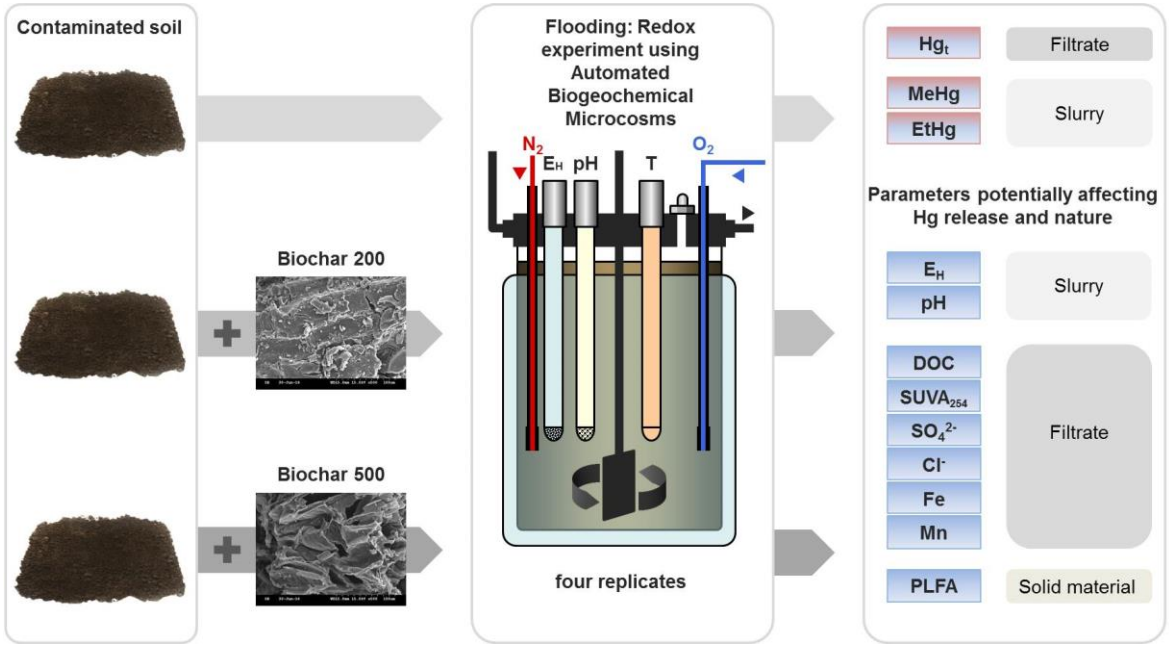

Figure 5-1: Graphical sketch illustrating the experimental design of the microcosm experiment to study the effects of different biochars on Hg mobility and Hg species formation considering the influence and interdependency of several parameters which potentially affect Hg mobility.

5.2 Results and Discussion

5.2.1 Soil E_H and pH

The observed E_H values (E_H all) in the slurries of CS and the biochar treatments (CS+BC200 and CS+BC500) fell within the range of highly reduced and moderately reduced conditions (Table 0-3, Appendix B, Fig. 5-2).

The pH (pH all) values in the slurries varied between very strongly acidic to neutral (CS and CS+BC500) and slightly alkaline (CS+BC200) (Table 0-3). The pH in the slurry of CS and the biochar treatments showed an opposite behavior to E_H (Fig. 5-2). Therefore, the correlation between soil E_H and pH was negative for the overall trends ($r = -0.68$; $p < 0.01$; $n = 11{,}856$ in CS; $r = -0.72$; $p < 0.01$; $n = 11{,}910$ in CS+BC200; and $r = -0.79$; $p < 0.01$; $n = 11{,}353$ in CS+BC500; data not shown) as well as for the data collected when the microcosms (MCs) were sampled ($r = -0.70$; $p < 0.00001$; $n = 36$ in CS, $r = -0.77$; $p < 0.00001$; $n = 36$ in CS+BC200, and $r = -0.85$; $p < 0.00001$; $n = 36$ in CS+BC500).

The inverse relationship of pH and E_H was expected, presumably due to the consumption of protons required for the reduction of NO_3^-, Mn^{4+}, Fe^{3+}, and SO_4^{2-} (Yu et al., 2007; Reddy and DeLaune, 2008). The results indicate that the application of both BC200 and BC500 to CS exerted no significant influence on the pH in soil slurry, with only a slightly lower pH found in CS+BC500 (Table 0-3).

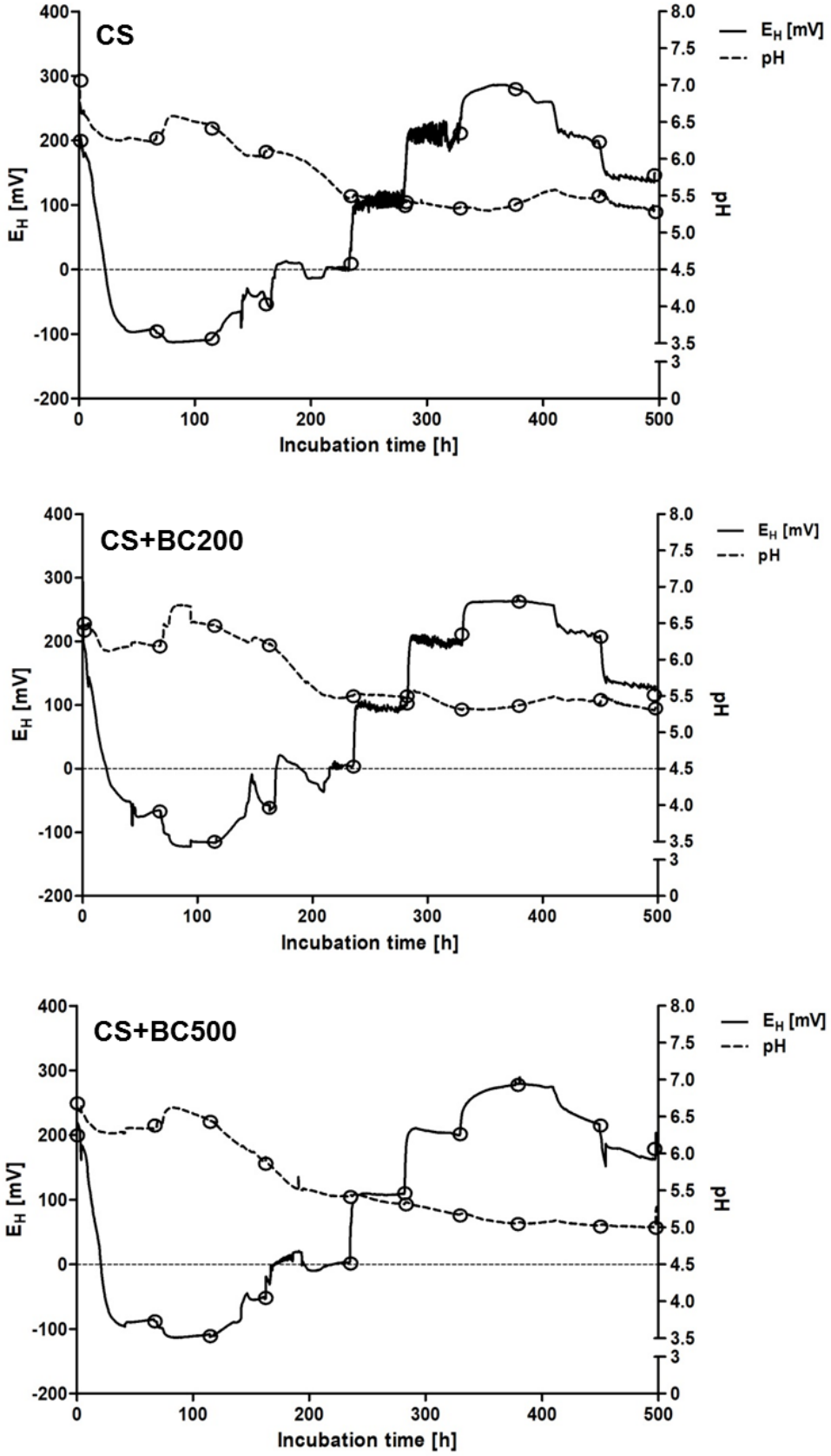

Figure 5-2: Development of redox potential E_H (solid line), pH (dashed line), and sampling points (circles) in soil slurry (data every 10 min, averages were reported for an underlying dataset (n ≈ 11,915) of four replicate samples) in the microcosms of untreated contaminated soil (CS), CS treated with biochar pyrolyzed at 200 °C (CS+BC200), and CS treated with biochar pyrolyzed at 500 °C (CS+BC500).

5.2.2 Impact of E_H/pH changes on mobilization of Hg_t, MeHg, and EtHg in CS, CS+BC200, and CS+BC500

The mobilization of Hg_t in CS was particularly high under low redox conditions (Fig. 5-3). Hence, the highest concentrations of dissolved Hg_t were determined for the first two samplings at E_H -92 mV (29 µg/l) and -110 mV (28 µg/l).

The high mean concentration found for the second sampling at E_H -110 mV was significantly affected by one of the four CS MCs in which the Hg_t concentration increased up to 52 µg/l. The average 6 hour E_H value for this MC was slightly lower (4-5 mV) compared to the other MCs in which Hg_t declined even though E_H values were lower than during the first sampling. Here, the pH may have had an effect: The pH value of the MC (6.9) was higher than in the other MCs (6.5; 6.3; 6.3). Mercuric mercury (Hg(II)) shows a different behavior than most other divalent metals as its extent of adsorption is greatest in acidic media (Barrow and Cox, 1992; Yin et al., 1996; Sarkar et al., 1999; Pelcová et al., 2010). The close link between Hg_t dissolution and pH in CS is supported by a significant positive correlation (Table 0-4, Appendix B).

However, it is unlikely that the pH was the main influencing factor. Xu et al. (2014) observed enhanced Hg desorption at pH 5 and 11 but generally found that pH adjustment was insufficient for Hg removal since no more than 0.3% of soil Hg_t was mobilized at these pH values in their soil washing experiments. In our study, the relationship between Hg_t and E_H in CS was also strong. We found an inverse relationship with decreasing Hg_t concentrations when E_H increased. Correspondingly, Hg_t concentrations were found to be higher at the last two samplings when E_H had been lowered again (Fig. 5-3, Table 0-4). Moreover, the lowest mean Hg_t concentration (3 µg/l) was determined for the highest mean E_H (282 mV).

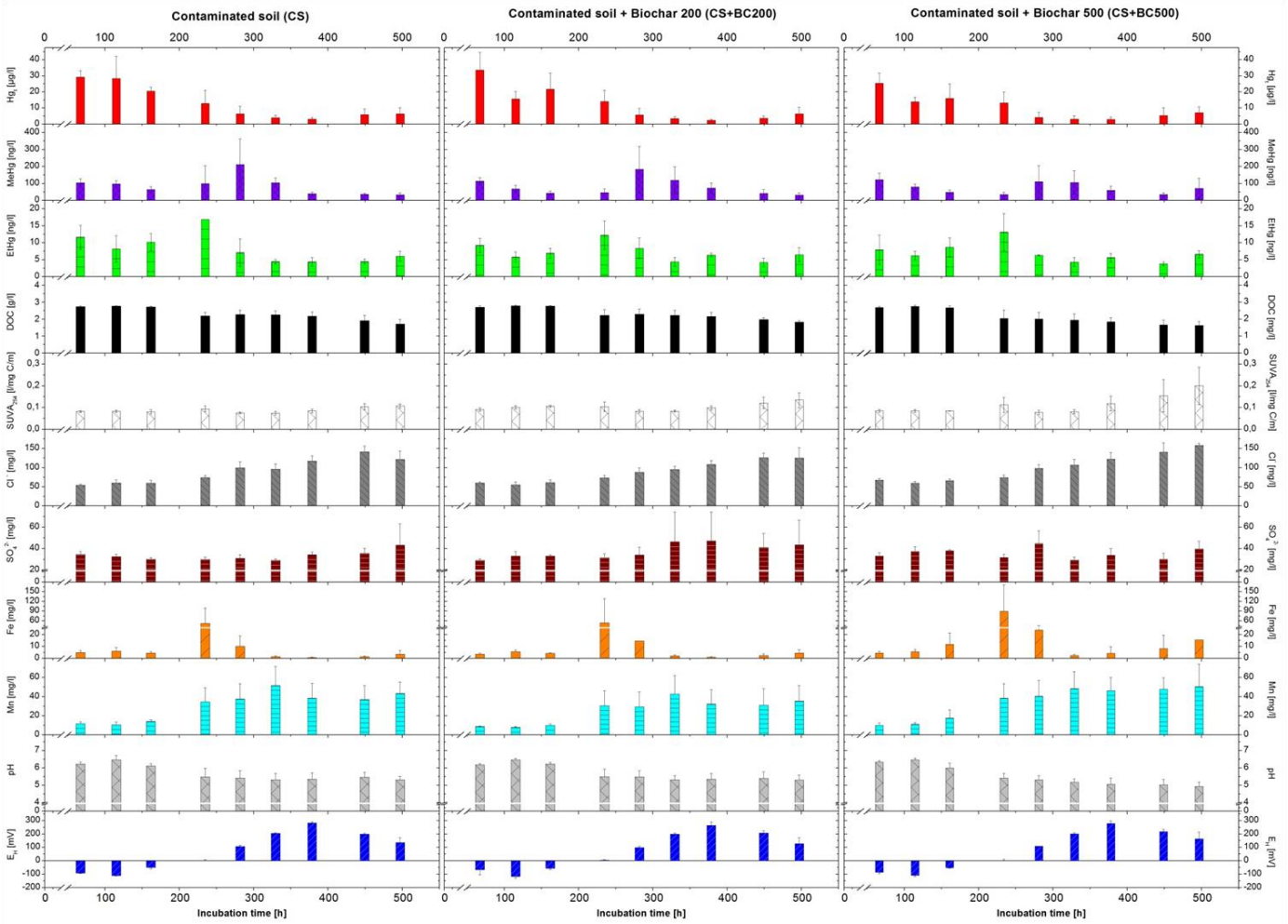

Figure 5-3: Impact of pre-defined E_H-conditions on release dynamics of dissolved total Hg (Hg_t), methylmercury (MeHg), ethylmercury (EtHg), dissolved organic carbon (DOC), specific UV absorbance at 254 nm ($SUVA_{254}$), chloride (Cl^-), sulfate (SO_4^{2-}), iron (Fe), manganese (Mn), and pH in a contaminated soil (CS) compared with a contaminated soil treated with biochar pyrolyzed at 200 °C (CS+BC200) and a contaminated soil treated with biochar pyrolyzed at 500 °C (CS+BC500). Columns represent mean and whiskers represent standard deviation of four replicates using biogeochemical microcosm systems.

In general, the pattern of Hg_t concentrations found in CS+BC200 and CS+BC500 was similar to the one observed in CS. However, under highly reduced conditions, at the second sampling, Hg_t concentrations were considerably lower in both biochar treatments (Fig. 5-3): The mean Hg_t concentration in CS was as high as 28 µg/l while those calculated for CS+BC200 (16 µg/l) and CS+BC500 (14 µg/l) constituted about half of the CS value. Even when excluding the MC with the highest Hg_t concentrations in CS the difference would be at least 4.7 µg/l. This is noteworthy since the pattern of Hg_t concentrations in CS and the biochar treatments differed by no more than 2.3 µg/l from E_H window 0 mV on. Moreover, the mean Hg_t concentration for all measurements in CS was 13 µg/l and therefore only slightly higher than those in CS+BC200 (12 µg/l) and CS+BC500 (10 µg/l) (Table 0-3). We may conclude that these small deviations were most likely caused by the variations detected under highly reduced conditions. Both biochar amendments seem to have curtailed the dissolution of Hg_t under these conditions. Similar results were found at a E_H of -122 mV when biochar based material was used to immobilize Hg (Chapter 4). To our knowledge there is no information available on changing abilities of biochars to sorb inorganic Hg at varying redox conditions. However, Xu et al. (2016) revealed that different biochars may sorb Hg via different complexation mechanisms. They found that Hg sorption by bagasse (crushed sugarcane stalks) biochar produced at 450 °C was primarily attributed to the formation of $(-COO)_2Hg$ and $(-O)_2Hg$ while hickory chip biochar produced at the same temperature sorbed Hg by the π electrons of C═C and C═O induced Hg-π binding. Liu et al. (2016) noted that Hg removal mechanisms by carbonaceous sorbents include coordination between Hg and functional groups on/within sorbents, reduction of Hg(II) to Hg(I) and precipitation, and co-precipitation with anions. However, they concluded that the chemical binding of Hg to functional groups such as thiol, hydroxyl, and carboxyl as well as to chloride on the surface of and within biochars appears to be the predominant removal mechanism. Furthermore, it was found that Hg was bound to S in biochars with high S content and to O and Cl in biochars with low S content (Liu et al., 2016). Dong et al. (2013) found that 23 to 31% of Hg sorbed by pepper biochars pyrolyzed at 300 °C and 450 °C was associated with carboxylic and 77 to 69% with phenolic hydroxyl groups. Contrarily, 91% of the Hg sorbed by pepper biochar pyrolyzed at 600 °C was associated with a graphite-like domain on an aromatic structure, with the rest being associated with phenolic hydroxyl groups. The loss of functional groups with increasing temperature due to decreasing H and O resulted in a lower Hg sorption capacity, indicating that low pyrolysis temperature was beneficial to produce biochars with higher Hg sorption potential

(Dong et al., 2013). These results are in agreement with Klüpfel et al. (2014) who produced 19 biochars from different feedstock over a range of pyrolysis temperatures and found that the pool of redox-active moieties was dominated by electron-donating, phenolic moieties at the pyrolysis temperatures 200 and 300 °C, by newly formed electron accepting quinone moieties at the pyrolysis temperatures 400 and 500 °C, and by electron accepting quinones and probably condensed aromatics at the pyrolysis temperatures 600 and 700 °C. Thus, we suggest that BC200 and BC500 had different moieties due to their distinct pyrolysis temperatures. However, the Hg_t immobilization potentials of BC200 and BC500 were marginal. Compared to CS mean Hg_t concentrations BC200 and BC500 reduced Hg_t release by 8% and 23%, respectively. The biochars primarily reduced Hg_t mobilization under highly reduced conditions around E_H -110 mV, at one specific sampling. Based on the chemistry of Hg interactions with DOC and other organic and inorganic soil components as well as on published results concerning Hg removal from aqueous solutions by means of biochar (Liu et al., 2018b) we originally hypothesized that Hg would be immobilized more efficiently by BC200 and BC500. There are several possibilities why the addition of BC200 and BC500 was not that effective in our experiment:

Typically, reduced sulfur groups are in great excess to Hg_t content in soils (Skyllberg, 2012). Thus, the majority of Hg will bind to organic matter (OM) and metal sulfides while oxygen functional groups at Fe and Al oxyhydroxides as well as the edges of phyllosilicates are indirect adsorbents (Xia et al., 1999; Skyllberg, 2012). Mercury in soil solution may be in the form of Hg^{2+}, $HgCl^{+}$, $HgCl_2^{0}$, $HgCl_3^{-}$, $HgCl_4^{2-}$, HgClOH, $Hg(OH)^{+}$, $Hg(OH)_2^{0}$, and Hg-DOC (Han, 2007). However, due to its affinity for reduced sulfur groups, complexes with thiols from DOC will dominate the speciation of Hg in soil solution (Skyllberg, 2012). Dissolved Hg concentrations measured in the course of our experiment exceeded those typically reported for natural ecosystems (Leopold et al., 2010). Therefore, it seems likely that Hg was not solely bound to the small fraction of DOC reactive thiol functional groups but also to carboxylic functional groups. Findings of Haitzer et al. (2002) indicated that the binding of Hg to DOM under natural conditions (very low Hg/DOM ratios) is controlled by a small fraction of DOM containing a reactive thiol functional group providing strong binding sites for Hg while carboxyl groups came into play at higher Hg to DOM ratios. It is noted that pH may influence the dissociation rate of carboxylic acids and thereby the number of potential binding sites.

Due to the strong binding between Hg and the reduced sulfur groups, the mobilization of Hg is rather influenced by DOC than by pH (Wallschläger et al., 1996; Xu et al., 2014).

Besides protons, other cations such as Al^{3+} may occupy biochar binding sites. Another hypothesis why biochar showed little effect on Hg sorption is the presence of dissolved complexes binding Hg and hampering the sorption to biochar. Another factor which may affect Hg adsorption in the soil environment is the formation of biofilms. They may have formed in the course of the experiment as in nature cells grow predominantly in such aggregation of soil microorganisms, especially in heavily polluted sites (Gross et al., 2007). Thus, the alteration of the biochar surface and its chemical and physical properties by the formation of biofilms on the biochar particles needs to be considered. Possibly, biofilms may reduce the interaction of Hg with the biochar surface and thereby disturb its effects on Hg immobilization. Otherwise, biofilms themselves accumulate inorganic and methylated Hg compounds (Hintelmann et al., 1993; Dranguet et al., 2017; Dranguet et al., 2018) and may also lead to a higher rate of Hg methylation compared to planktonic bacteria (Lin et al., 2013). Different mechanisms play a role in Hg uptake by biofilms, e.g. steric hindrance and electrostatic interactions, binding functional groups of the extracellular polymeric substance matrix, and adsorption by mineral fractions present in biofilms (Dranguet et al., 2017). Leclerc et al. (2015) hypothesized that Hg-thiol complexation in the extracellular fractions of biofilms can occur which may potentially affect the bioavailability of Hg and increase its methylation.

The sorption of Hg-DOC complexes at the biochars was potentially of importance as we found strong positive relations between Hg_t and DOC (Table 0-4). Considering possible interactions between Hg-DOC complexes and BC200 as well as BC500 it has to be noted that Hg_t and DOC concentrations were only slightly lower in CS+BC500 (Table 0-3). Although often used for remediation purposes biochar amendments have been shown to have the potential to increase DOC concentrations, which may be linked to enhanced mobilization of soil contaminants (Beesley et al., 2010; Qi et al., 2017; Chen et al., 2018). In contrast, it has also been reported that DOC may readily sorb to biochar (Kammann et al., 2015). However, biochar mediated changes in DOC concentration may not always be detected (Jones et al., 2012). In general, the feedstock material and pyrolysis temperature influence properties of biochars, including their potential to release DOC (Liu et al., 2015). Here, minor effects of biochar amendment on DOC concentrations were observed.

The Hg sorption capacity of both biochars increased significantly under highly reduced conditions.

One possible reason might be the cleavage of existing disulfide bonds of redox-active disulfides when they are reduced and the concomitant formation of vicinal thiol pairs which

may bind Hg (Wouters et al., 2010; Poole, 2015; Rubino, 2015). It is known that both Hg(II) and MeHg have a high affinity for reduced sulfur groups such as thiols (R-SH), monosulfides (R-S-R), and disulfides (R-SS-R) (Taube et al., 2008; Skyllberg, 2010; Skyllberg, 2012; Song et al., 2018). Moreover, both Hg species have a higher affinity for thiols than for disulfides (Yoon et al., 2005; Liem-Nguyen, 2016). We suggest that higher amounts of disulfides were present in the MCs amended with BC200 and BC500 whose disulfide bonds were reduced to the corresponding thiols leading to higher Hg_t sorption compared to CS. Following this assertion, Hg formed strong dissolved complexes with organic and inorganic ligands upon flooding while Hg was less attracted by potential binding sites of the biochars and the soil. Due to the strong attraction of the vicinal thiol pairs Hg could be removed from slurry when E_H changes induced the cleavage of existing disulfide bonds located on the surface of the biochars. This assertion is in good agreement with He et al. (2012) who indicated that a competitive complexation of Hg with DOC may limit the interactions of Hg with sorbents and who attributed rapid adsorption of Hg to the binding of one Hg to two thiols. Moreover, while carboxyl (R-COOH) and hydroxyl groups (R-OH) are generally accepted as predominant biochar binding sites for heavy metals it has been shown that thiol-functionalized sorbents, including biochars, have a higher adsorption capacity and stronger selectivity for Hg (Niu et al., 2014; Xu et al., 2016; Huang et al., 2019). Adsorption kinetics and isotherms of such studies frequently suggest that thiol-functionalization improves the Hg species removal efficiency from aqueous solution considerably (e.g. Xia et al., 2019).

The observed concentrations of Hg_t released in CS (1.8-52 µg/l) greatly exceed levels reported for natural uncontaminated fresh water systems, and are comparable to higher concentrations reported in Hg mine drainage (Rytuba, 2000; Leopold et al., 2010). Thus, flooding and the alteration of E_H resulted in a substantial Hg_t release from CS which exceeds the U.S. Environmental Protection Agency's Maximum Contaminant Level for Hg in drinking water (2 µg/l) and the trigger value for the assessment of the soil – groundwater pathway (1 µg/l) of the German BBodSchV (1999). In CS+BC200 and CS+BC500 Hg_t concentrations fell below 1 µg/l for a single measurement each (Table 0-3).

The pattern of MeHg concentrations was similar in CS and the biochar treatments (Fig. 5-3). In contrast to Hg_t no impact of biochar amendments was found under highly reduced conditions. This does not necessarily contradict the suggested cleavage of disulfide bonds

as Skyllberg (2012) noted that there are indications that Hg and MeHg may bind to different types of thiol groups.

We did not find a correlation between MeHg and E_H in CS, CS+BC200, or CS+BC500. Even though the methylation of Hg occurs primarily under anaerobic conditions, significant correlations between MeHg and E_H are not always observed (Roulet et al., 2001; DeLaune et al., 2004; Sunderland et al., 2006; Frohne et al., 2012).

A positive correlation was detected between MeHg and pH in CS+BC500 (Table 0-4). An inverse relationship between these parameters is often reported (Ullrich et al., 2001). Golding et al. (2008) indicated that increased concentrations of Hg(II) within methylating bacteria due to declining pH values would probably be reflected in enhanced methylation activity. It is generally accepted that Hg methylation is primarily driven by microbial activity. Sulfate-reducing bacteria (SRB) were identified as the principal methylators of Hg in sediments of various ecosystems and currently it is accepted that Hg methylation occurs primarily under anaerobic conditions (Moreau et al., 2015; Beckers and Rinklebe, 2017; Boyd et al., 2017). However, not all bacteria of the SRB phylogenetic tree methylate Hg (Barkay and Wagner-Döbler, 2005; Parks et al., 2013). It is suggested that SRB perform SO_4^{2-} reduction principally under highly reducing conditions at E_Hs between -100 and -1000 mV (Dominique et al., 2007; Fritsche et al., 2014). Still, MeHg concentrations determined in the course of the first three samplings under low E_H seem to be the result of soil-bound MeHg release rather than bacterial MeHg formation. Following the first sampling MeHg concentrations decreased in CS and the biochar treatments despite the lower E_H at the following sampling. Thus, MeHg that was bound to fine organic material may have initially entered the aqueous phase upon flooding, and was demethylated or sorbed over the course of the next two to three samplings. The release of sorbed MeHg when dry soils or sediments are flooded has been reported in previous studies (Bachand et al., 2014; Marvin-DiPasquale et al., 2014; Cesario et al., 2017). We found that net methylation started between the E_H windows of -50 mV and 0 mV and was highest between the E_H windows of 0 mV and 100 mV in CS and the biochar treatments (Fig. 5-3). This falls into the range of -100 to 100 mV identified by Windham-Myers et al. (2009) for high MeHg production potential rates in the San Francisco Bay-Delta.

A decreasing ratio of SO_4^{2-} to Cl^- can be used as an indicator of SO_4^{2-} reduction (Alpers et al., 2014). Clear declines in this ratio were observed between the E_H windows -50 mV and 0 mV for CS and the biochar treatments, which corresponds well with the increase of MeHg concentrations. Furthermore, the ratio of MeHg to Hg_t increased 4.0 to 7.8 fold be-

tween the E_H windows 0 mV and 100 mV in CS and the biochar treatments, which represented the highest increase. This ratio is a frequently used indicator of methylation efficiency (Frohne et al., 2012; Alpers et al., 2014). High MeHg/Hg_t rates indicate that available Hg is efficiently methylated while low MeHg/Hg_t rates indicate either low Hg methylation or high demethylation rates (Remy et al., 2006). Thus, the increase in MeHg within CS and the biochar treatments fell within the range of Fe(III) reduction while the SO_4^{2-}/Cl^- ratio indicated that SO_4^{2-} reduction might have occurred (DeLaune and Reddy, 2005). It is well established that certain strains of iron-reducing bacteria (FeRB), such as *Geobacter* sp. strain CLFeRB, are also capable of methylating Hg, while methanogens that are known to demethylate MeHg may turn into the primary methylators under specific environmental conditions (Fleming et al., 2006; Hamelin et al., 2011; Christensen et al., 2018). Concentrations of dissolved Fe increased in the range of Fe(III) reduction around 0 mV (see Appendix B) which may occur from microbial and chemical reduction of Fe(III) bearing minerals, such as Fe-oxides (Praharaj and Fortin, 2008). The microbial reduction of Fe(III) bearing minerals is related to the activity of FeRB, which relies on the availability of labile organic C substrates and the abundance and crystallinity of Fe(III) bearing minerals (Roden, 2003; Praharaj and Fortin, 2008). Abiotic Fe(III) reduction is indirectly controlled by the microbial SO_4^{2-} reduction, which is accompanied by the formation of sulfide species such as hydrogen sulfide that can act as significant reductants of Fe oxides (Li et al., 2006; Lohmayer et al., 2014; Lindsay et al., 2015). In fact, it has been frequently found that Fe(II) production was rather driven by biogenic sulfide Fe(III) reduction than by the activity of FeRB (Praharaj and Fortin, 2008; Kwon et al., 2014; Hansel et al., 2015). Moreover, even though SRB are generally described as anoxic and neutrophilic bacteria they are present (but probably not metabolically active) under aerobic conditions and can tolerate low pH (Koschorreck, 2008; Miao et al., 2012; Giloteaux et al., 2013). Praharaj and Fortin (2008) determined low SO_4^{2-} reduction rates at E_H values between 300 and 450 mV, indicating that SRB activity is not restricted to highly reduced environments. Thus, even though the increase in dissolved MeHg concentrations in our experiment did not fall into the E_H range usually considered for Hg methylation by SRB, we may conclude that the methylation of Hg in CS and the biochar treatments between -50 and 100 mV was most probably mediated by SRB. Furthermore, the increases in soluble Fe at E_H 0 mV may be attributed to abiotic Fe(III) reduction linked to SO_4^{2-} reduction. Measured MeHg concentrations are the result of ongoing methylation and demethylation processes (Lambertsson and Nilsson, 2006; Lazaro et al., 2016) and therefore MeHg concentrations determined for

the samplings following E_H window 100 mV at higher E_H in our experiment (Fig. 5-3) may in part be explained by the persistence of MeHg after major net methylation of Hg had been taken place earlier. In fact, MeHg concentrations in CS and the biochar treatments declined to approximately half between first 100 mV and first 200 mV E_H window. Most MeHg in many aquatic environments is generated in the sediments since MeHg production is basically the product of microbial activity and Hg(II) bioavailability (Hintelmann, 2010). On the other hand, demethylation rates within sediments are high as well, which leads to a standing MeHg pool that constitutes no more than 1% of the Hg_t (Hintelmann, 2010; Randall et al., 2013). However, the MeHg which is transferred from sediments into the overlying water column is very persistent, as demethylation activity is virtually absent in water (Hintelmann, 2010). Here, comparatively high MeHg concentrations were depleted within two days in the course of controlled E_H changes.

A correlation between MeHg and Hg_t was missing in CS and the biochar treatments. This might be because the amount of bioavailable Hg in Hg_t may vary and since it is suggested that the production of MeHg is limited by microbial methylation potential rather than by Hg bioavailability (Frohne et al., 2012; Feng et al., 2014; Bowman et al., 2015).

The pattern of EtHg in CS and the biochar treatments was very similar. The highest mean concentrations were determined for E_H window 0 mV (Fig. 5-3). Thereafter, there was a decline in EtHg with increasing E_H values and a slight increase when E_H was lowered again at the end of the experiment. Corresponding to this pattern, negative correlations between EtHg and E_H were determined for CS and CS+BC500 (Table 0-4). The concentrations of dissolved EtHg in the treatments amended with BC200 or BC500 were not significantly lower than those found in CS which indicates the moderate influence of the biochars on EtHg dissolution/formation (Table 0-3). Thus, the potential of BC200 and BC500 as immobilization agents for Hg_t, MeHg, and EtHg in our experiment was very limited. Considering our limited understanding of EtHg dissolution/formation, sufficient EtHg binding sites may be present in CS that would lessen the impact of the introduced biochar binding sites.

A positive correlation between EtHg and pH was only found in CS. This correlation is consistent with Pelcová et al. (2010) who observed maximum EtHg adsorption to river sediments at pH 3-4. However, calculated relations between EtHg and other parameters seemed to be influenced by the strong positive correlations found between EtHg and Hg_t in CS and the biochar treatments (Table 0-4). It appears that EtHg was either released by the

same processes as Hg_t or that a certain ratio of Hg_t was converted to EtHg. Such a correlation between dissolved Hg_t and EtHg concentrations has been observed before (Chapter 4). However, the inverse relation of these two parameters at E_H window 0 mV indicates that the conditions between the E_H windows of -50 mV and 0 mV may have favored the formation of EtHg. Following E_H window 0 mV EtHg concentrations were considerably lower again in CS and the biochar treatments. Hintelmann (2010) noted that EtHg is not very persistent and readily decomposes in the environment, which would indicate that the EtHg determined in the course of our experiment would be rather a product of EtHg formation than of the release of legacy EtHg. The process of EtHg formation and its behavior in the natural environment is not well understood; for example, data on a microbial formation of EtHg are lacking (Hintelmann, 2010; Beckers and Rinklebe, 2017). Nevertheless, Cai et al. (1997) and Mao et al. (2010) suggested that EtHg may occur widely in the environment based on detected EtHg in soil samples. Ethylmercury has been detected in soils and sediments while its concentrations in other environmental samples such as atmospheric particulates, water, plant, and fish are frequently below the detection limit (e.g. Song et al., 2013; Chen et al., 2015). Fortmann et al. (1978) showed that EtHg can form in tissues of common dwarf garden pea (*Pisum sativum*) after exposure to elemental Hg vapor and suggested that MeHg and EtHg might both be metabolites of a single Hg pathway in the peas. In fact, we found high EtHg concentrations at 0 mV preceding high MeHg concentrations at 100 mV.

5.2.3 Impact of DOC, Cl^-, SO_4^{2-}, Fe, and Mn changes on mobilization of Hg_t, MeHg, and EtHg in CS, CS+BC200, and CS+BC500

Similar to Hg_t the highest DOC concentrations were determined for those E_H windows sampled at the beginning of the experiment under low E_H conditions (Fig. 5-3). Therefore, we found positive correlations between Hg_t and DOC for CS and the biochar treatments (Table 0-4). Such correlations are frequently reported in literature (Dittman et al., 2010; Burns et al., 2013; Bravo et al., 2018) and DOC is generally regarded as the predominant ligand for both Hg_t and MeHg in oxic (sulfide-free) waters (Ravichandran, 2004; Gorski et al., 2008; Chadwick et al., 2013). However, positive relationships between Hg_t and DOC have been observed in numerous aquatic ecosystems and this link has been principally attributed to the strong affinity of Hg_t for reactive (reduced) thiol functional groups within DOC (Ravichandran, 2004; Tsui and Finlay, 2011; Frohne et al., 2012). Such a positive

correlation may not always be detected, since the binding is controlled by a small fraction of dissolved organic matter possessing these thiol groups (Ravichandran, 2004). The latter author commented that a positive correlation between Hg_t and DOC is most likely to be found when Hg_t is mainly derived from wetlands and soils, where Hg_t is discharged and co-transported bound to the organic carbon, as has been reported by Wallschläger et al. (1996). This pattern is in good agreement with our results regarding Hg_t and DOC concentrations in CS, CS+BC200, and CS+BC500. Correlations in CS and the biochar treatments between either Hg_t or DOC with Fe or Mn were either missing or negative indicating that the release of Hg_t or DOC at low E_H was not governed by the reductive dissolution of particulate Fe and Mn oxyhydroxides and the release of associated Hg or DOC (Table 0-4). Instead, the results suggest that fine biologically decomposed organic material with associated Hg entered the aqueous phase upon flooding of the soil. Figure 5-4 indicates a strong dependence of dissolved Hg_t on DOC and E_H with higher DOC concentrations and lower E_H values favoring Hg mobilization in CS, CS+BC200, and CS+BC500.

Total Hg concentrations in CS and the biochar treatments were also negatively correlated with Cl^- (Table 0-4). This relationship has been reported before (Hall et al., 2008).

Figure 5-5 shows that lower Cl^- concentrations may have promoted the mobilization of Hg in CS, CS+BC200, and CS+BC500. Higher Cl^- concentrations may provoke the formation and precipitation of Hg_2Cl_2 thereby removing dissolved Hg (Kim et al., 2004; Chen et al., 2017).

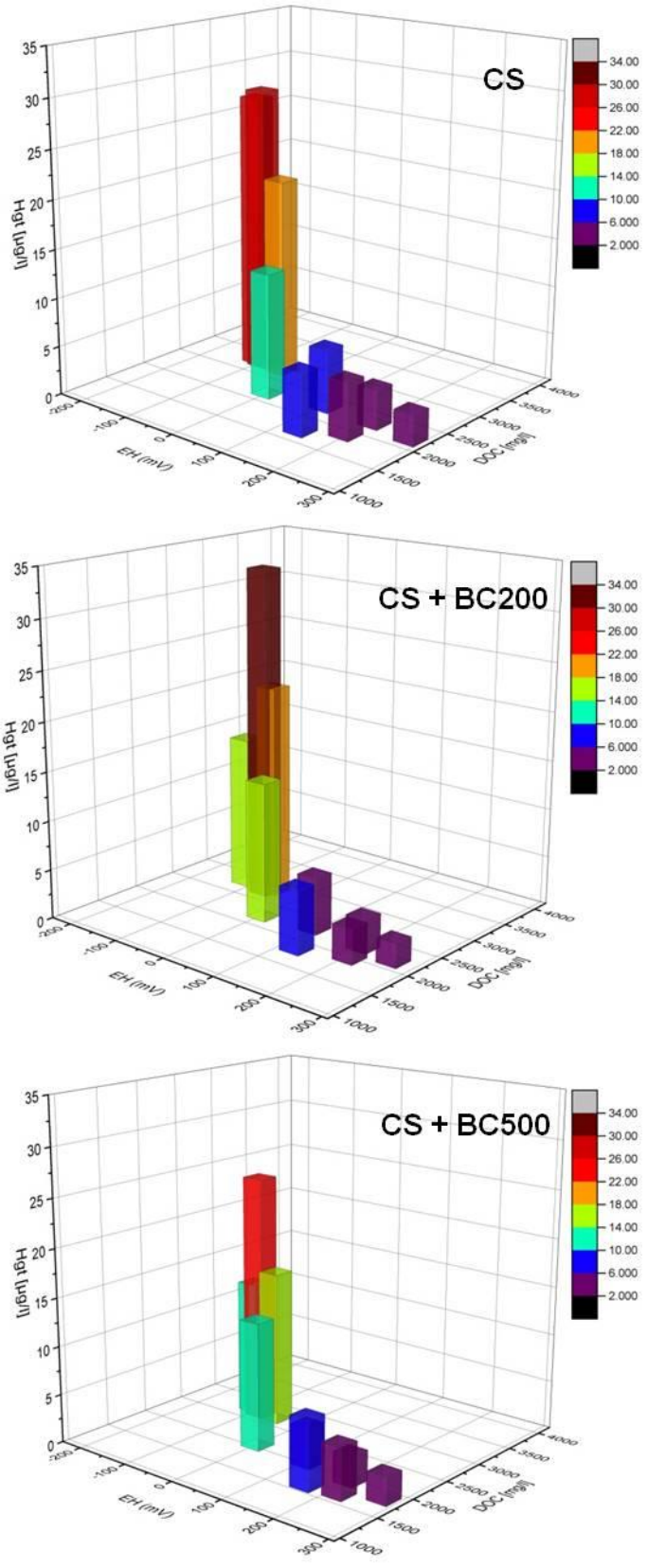

Figure 5-4: Dependency of Hg_t concentrations in soil solution from redox potential (E_H) and DOC displayed in a three-dimensional coordinate system. Bars show means of data obtained for CS, CS+BC200, and CS+BC500. Bar colors correspond to the concentrations indicated by the color scale.

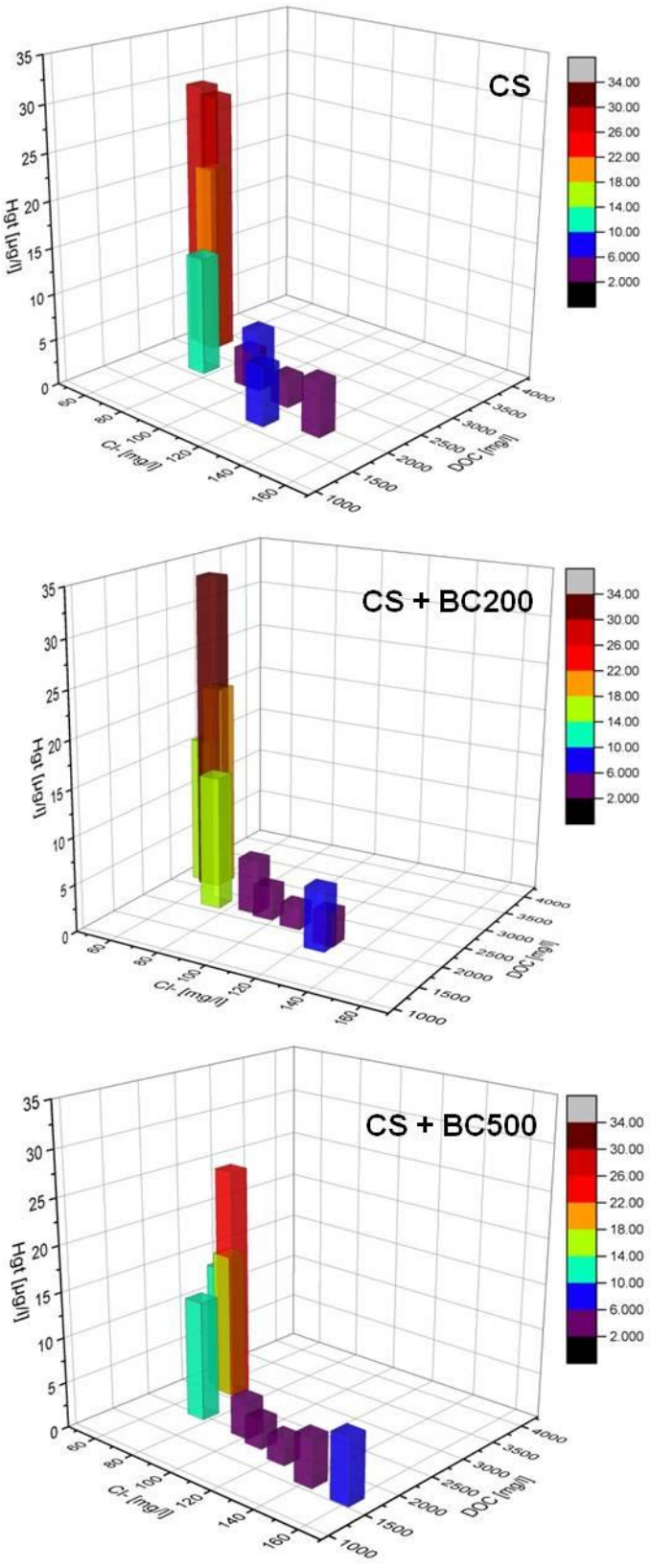

Figure 5-5: Dependency of Hg_t concentrations in soil solution from chloride concentrations (Cl^-) and DOC displayed in a three-dimensional coordinate system. Bars show means of data obtained for CS, CS+BC200, and CS+BC500. Bar colors correspond to the concentrations indicated by the color scale.

Methylmercury was positively correlated with DOC in CS and in CS+BC500 (Table 0-4). As in the case with Hg_t it has been suggested that the aromaticity of DOC, calculated as $SUVA_{254}$ values, may influence this relationship as higher aromaticity seems to enhance the Hg binding affinity or the number of strong binding sites (Tsui and Finlay, 2011). It has been hypothesized that $SUVA_{254}$ may be a suitable predictor of dissolved Hg_t concentrations in certain streams (Burns et al., 2013). $SUVA_{254}$ has been found to be a useful indicator to assess the dissolved aromatic carbon content (Ravichandran et al., 1998; Weishaar et al., 2003). Some sources of interferences in absorbance spectroscopy have to be considered (Li and Hur, 2017). Nitrate and particularly ferric iron (Fe(III)) can exert a strong influence (Weishaar et al., 2003; Poulin et al., 2014). Under our experimental E_H-pH-conditions Fe should have been present as ferrous iron (Fe(II)) predominantly (Table 0-4) (Takeno, 2005) while nitrate concentrations were frequently below the detection limit.
Positive correlations between both Hg_t and MeHg with $SUVA_{254}$ have been reported for some aquatic ecosystems and biota (Hall et al., 2008; Chasar et al., 2009), but this strong relationship is not universal (Jiang et al., 2017b; Burns and Riva-Murray, 2018). The pattern of $SUVA_{254}$ values was similar between CS and the biochar treatments (Fig. 5-3). Correspondingly, strong correlations between $SUVA_{254}$ and Hg_t, MeHg, or EtHg were neither found in CS nor in the biochar treatments (Table 0-4). In CS+BC500 $SUVA_{254}$ values increased stronger the course of the last two samplings, probably due to lower pH values as indicated by a significant negative correlation (data not shown). Such an inverse relationship has been found before (Tjerngren et al., 2012b) although the influence of pH on $SUVA_{254}$ values seems to be of minor significance (Weishaar et al., 2003). In general, $SUVA_{254}$ values were low compared to values reported for wetlands, rice fields, and lakes (Fleck et al., 2014; Poulin et al., 2014), water soluble OM (Jiang et al., 2017a), or porewater (Strickman and Mitchell, 2018).
Surprisingly, we found a positive correlation between MeHg and SO_4^{2-} in CS+BC500. Increasing concentrations of MeHg are often concomitant with decreasing SO_4^{2-} concentrations (Galloway and Branfireun, 2004; Selvendiran et al., 2008; Hellal et al., 2015). Sulfate-reducing bacteria use SO_4^{2-} as a terminal electron acceptor for the degradation of organic compounds which leads to the depletion of SO_4^{2-} as well as the production and release of sulfide and may result in the formation of MeHg provided that these SRB species are capable of Hg methylation (Muyzer and Stams, 2008; Hellal et al., 2015; Lindsay et al., 2015). However, Liu et al. (2016) found that biochars may release SO_4^{2-} to solutions, with wood-based biochars releasing lower concentrations. As such, this may explain the slightly

higher SO_4^{2-} concentrations in CS+BC200 and CS+BC500 compared to CS and the correlation found between MeHg and SO_4^{2-} in CS+BC500 (Fig. 5-3, Tables 0-3 and 0-4). The additional supply of SO_4^{2-} and labile organic carbon due to the amendment with biochar is considered to promote the growth of SRBs and may thus enhance Hg methylation (Liu et al., 2016). On the other hand, higher concentrations of SO_4^{2-} may inhibit MeHg production due to the formation of H_2S (Shao et al., 2012). Microbial SO_4^{2-} reduction can be inhibited by H_2S and organic acids which can be toxic for the SRB even though H_2S is produced by the SRB in the course of their energy metabolism (Hao et al., 1996; Koschorreck, 2008). In addition, methylation rates were found to be lower under high sulfide concentrations and the presence of FeS due to a shift from neutral Hg(II)-sulfide complexes, which are easily taken up by bacteria, to charged Hg(II)-polysulfide (Liu et al., 2008; Hellal et al., 2015). We may therefore conclude that the little additional SO_4^{2-} that was likely released due to the biochar amendments had no relevant effect on MeHg production.

Factor analyses were performed for CS and the biochar treatments (Fig. 5-4) to evaluate associations between the measured parameters and to identify hidden multivariate data structures. We extracted two factors. These factors explained 65.45% of the total variance in CS (48.86% Component No. 1 and 16.59% Component No. 2), 61.33% in CS+BC200 (46.49% Component No. 1 and 14.84% Component No. 2), and 64.32% in CS+BC500 (48.50% Component No. 1 and 15.82% Component No. 2), respectively.

Figure 5-6A shows that Hg_t, EtHg, DOC, and pH had high loadings on Component No. 1 in CS which indicates a similar biogeochemical behavior of these parameters. Manganese and E_H, in contrast, had high negative loadings on Component No. 1 which demonstrates their opposing behavior. Sulfate and $SUVA_{254}$ clustered together and had high loadings on Component No. 2. Chloride, MeHg, and Fe showed less intense loading on the two components, suggesting that they were presumably best explained by other components. In CS+BC200 (Fig. 5-6B) and CS+BC500 (Fig. 5-6C) Hg_t, DOC, and pH were again clustered together. Furthermore, Mn and E_H, which clustered with Cl^-, indicated again dissimilar biogeochemical behavior. Other parameters such as EtHg, Fe, and $SUVA_{254}$ were ungrouped. Summarizing, the results of the factor analyses indicate similarities in the biogeochemical behavior of Hg_t and DOC, while Mn was linked to E_H regardless of whether CS was amended or not. Neither amendment, BC200 or BC500, resulted in pronounced effects on the interrelationships of the parameters.

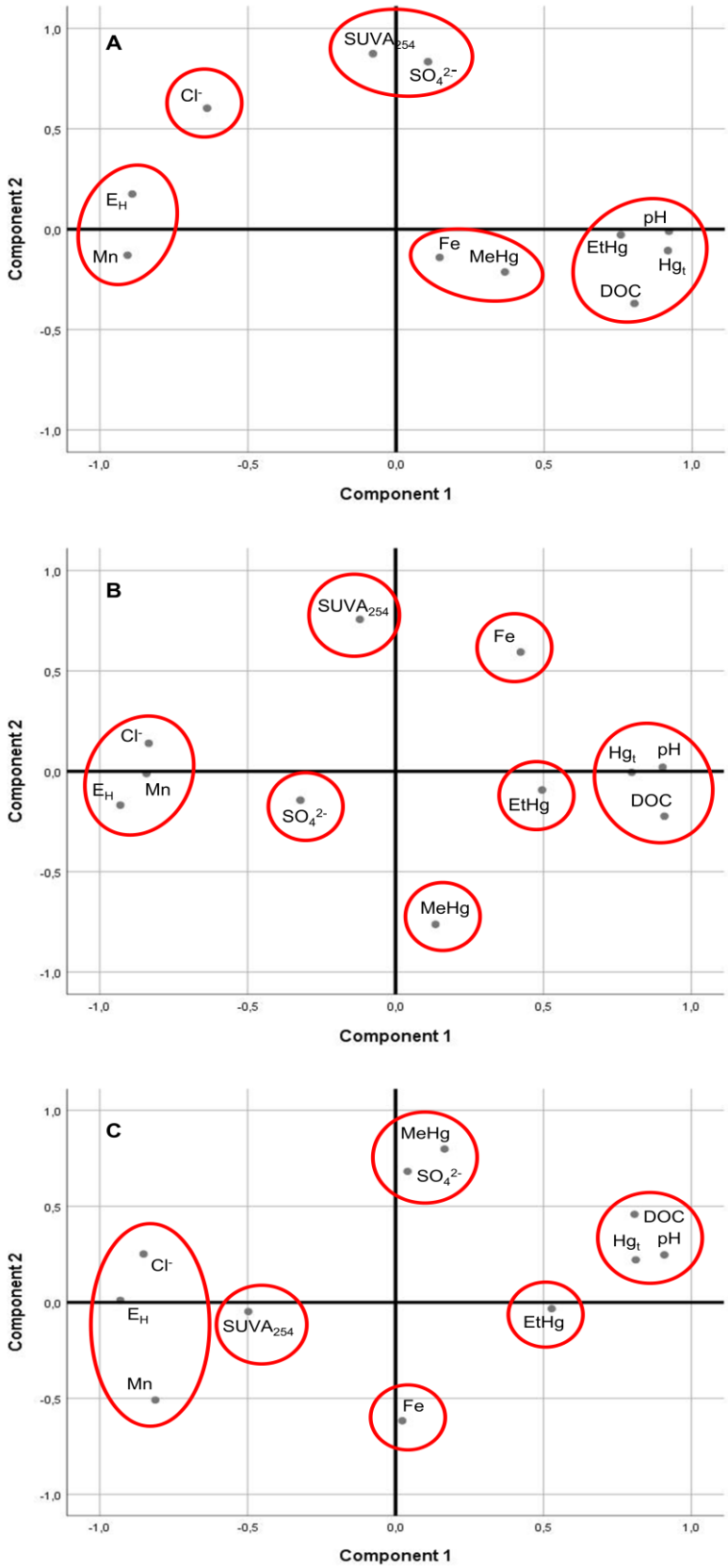

Figure 5-6: Factor analysis of the contaminated soil (CS) (A), the contaminated soil + biochar pyrolyzed at 200 °C (CS+BC200) (B), and the contaminated soil + biochar pyrolyzed at 500 °C (CS+BC500) (C). Kaiser-Meyer-Olkin (KMO) measures were 0.630 for CS, 0.599 for CS+BC200, and 0.695 for CS+BC500, respectively.

5.2.4 Impact of E_H/pH changes on the microbial community

Fifty-five PLFAs were detected. Forty-five of them had carbon numbers between C_{12} and C_{20}. Bacteria contain fatty acids mainly in this chain length range (Frostegård and Bååth, 1996; White et al., 1996; Jiang et al., 2012) (Fig. 0-4, Appendix B). In general, changes in abundances of PLFAs considered for the SRB and those with carbon numbers between C_{12} and C_{20} were similar (Figs. 0-3 and 0-4, Appendix B).

Phospholipid fatty acid abundances in the initial samples taken subsequent to the flooding of the soils when E_H was around 210 mV were slightly higher in CS compared to CS+BC200, while the amount of PLFAs detected in CS+BC500 was considerably lower (Fig. 0-3). This may, in part, be attributed to the fact that the MCs filled with CS+BC500 were sampled first and those filled with CS last. In general, rewetting of dried soils is followed by a "pulse" of soil respiration and bacterial growth rates exceed those in constantly moist soils several hours after rewetting and for a given period of time (Birch, 1958; Meisner et al., 2013; Sun et al., 2015). Strong increases in microbial CO_2 production have been found approximately one hour after rewetting and were attributed to the ability of microbes to utilize carbon substrates instantly as environmental conditions become favorable (Xu et al., 2004). However, the added BC500 seems to have had an important impact on the soil microbial community at this stage of the experiment, presumably due to its smooth surface and the shortage of nutrients which may have impeded its microbial colonization. The *Desulfobacter* biomarker fatty acid 10Me16:0 was absent in CS and the biochar treated soils over the course of the experiment (Fig. 0-3). However, the suitability of 10Me16:0 as a *Desulfobacter* specific biomarker has been questioned (Parkes et al., 1993; Chapter 4). Similarly, *Desulfovibrio* biomarker i17:1ω7c was not detected, while the considered *Desulfobulbus* indicator fatty acid 17:1ω6 could not be determined individually but as part of the summed aggregate 17:1. The abundances of PLFAs considered for the SRB were comparable between CS and the biochar treatments at the lowest sampled E_H around -110 mV. Clear changes in PLFA abundance were found for 10Me18:0 (decrease) and a15:0 (increase). Increasing E_H to 0 mV resulted in deceasing PLFA abundances in CS and CS+BC200, while this effect was not observed in CS+BC500 (Fig. 0-3). The results for the E_H windows 100 mV and 200 mV were very similar in CS and the biochar treatments. In general, PLFA abundances increased. Distinct deceases in PLFA abundance were found for CS and CS+BC500 at E_H window 300 mV. Lowering the E_H to 200 mV again resulted in PLFA abundances that were comparable to the first sampled 200 mV window in CS. However, PLFA abundances had decreased considerably in CS+BC200 and CS+BC500 at

the same time (Fig. 0-3). Abundances for the last sampling were again higher in CS and the biochar treatments.

In general, PLFA results gave no clear indication of whether SRB were the likely Hg methylators in our experiment. However, the concomitant increase in "SRB" PLFA abundance and MeHg concentrations at the first 100 mV E_H window may be seen as a sign of SRB mediated Hg methylation (Figs. 5-3 and 0-3).

5.3 Conclusions

We aimed to study the impact of two different biochars as amendments to a contaminated floodplain soil on the release of Hg_t as well as the formation and mobilization of MeHg and EtHg under dynamic E_H conditions utilizing an advanced automated biogeochemical microcosm system. Both amendments, BC200 and BC500, showed little impact on the mobilization of Hg_t, MeHg, and EtHg as well as on redox processes. Although BC500 was somewhat more effective than BC200 in controlling the mobilization of Hg_t and MeHg the results were marginal. This may reflect the formation of strong Hg complexes with dissolved organic and inorganic ligands under our experimental conditions, leading to a minor formation of chemical bonds between Hg and functional groups of the biochars. Therefore, the high Hg_t, MeHg, and EtHg concentrations at the beginning of the experiment at E_H windows ~ -80 mV and -110 mV might be interpreted as co-dissolution of Hg and DOC upon flooding, rather than a direct effect of lowering E_H at the beginning of the experiment. This assertion is supported by the strong correlations between Hg_t, MeHg, and EtHg with DOC and declining Hg concentrations despite declining E_H. Secondly, biochar is known to possess a large number of negative surfaces charges, which should actually be able to sorb Hg^{2+}. However, it could be that those potential binding sites for Hg at the biochar itself may have been occupied by other ions and/or blocked by biofilm what may have led to a mobilization of Hg and its compounds. Therefore, Hg_t could be mobilized in CS+BC200 and CS+BC500 to a similar extent as compared to CS. Overall, the mobilization of Hg_t, MeHg, and EtHg was largely impacted by the systematic changes in E_H. We found an inverse relationship between E_H and Hg_t, while the impact of E_H on MeHg and EtHg concentrations was rather characterized by specific E_H windows at which ethylation (0 mV) and methylation (between -50 and 100 mV) were favored. Presumably SRB were the principal methylators in our experiment based on PLFA results.

Future research should further clarify the impact of E_H and DOC on Hg mobilization and the role of Cl^- in influencing Hg_t immobilization. Thorough microbial analyses should be conducted to better evaluate the role of SRB. Additionally, the complex interactions between biochar and soil biogeochemical redox processes should be further elucidated. Also, various biochars, differing in feedstock and pyrolysis temperature as well as designed biochars should be tested with a view to their potential to decrease the mobilization of Hg_t, MeHg, and EtHg under dynamic redox conditions in frequently flooded soils. Finally, considering the high Hg_t release, our study highlights the necessity of conducting amendment tests under variable redox conditions in the field to evaluate the severity of environmental risk.

6. Mercury release dynamics in different soil horizons of two Saale River floodplain soils

6.1 Short introduction Chapter 6

The impact of various potential parameters such as DOC content, E_H, and pH on Hg release in soils of the Saale River floodplain were examined. The effects of flooding events and associated changes in the parameters were analyzed in different soil horizons at two different sites. The aim was to identify the parameters with the highest influence on Hg release dynamics in the field at the two specific study sites. The concept and experimental design is visualized by the following Figure 6-1.

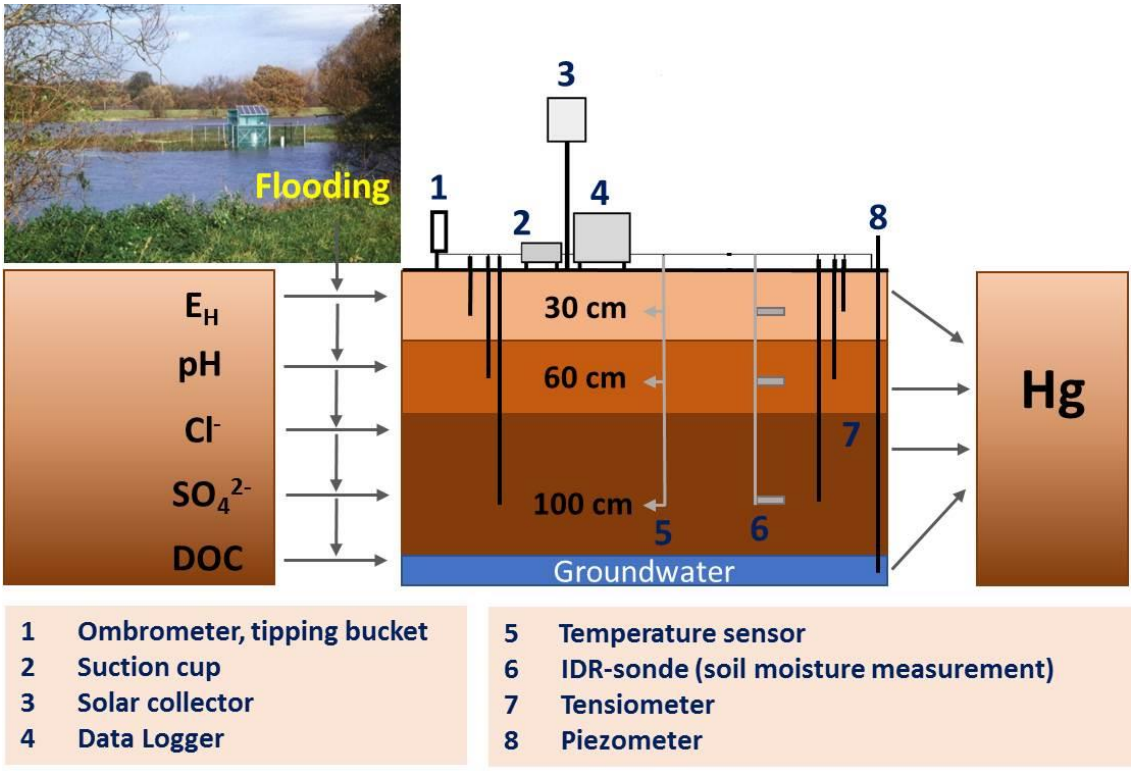

Figure 6-1: Graphical sketch illustrating the methodical concept of the field study utilizing hydrological monitoring stations acquiring data in different soil depths as indicated. Selected measured parameters are listed and the influence of floodings is implied (photograph by Jörg Rinklebe).

6.2 Results and discussion

6.2.1 Flooding events during the field experiment

The soil hydrological monitoring stations Saale 1 and Saale 2 were operated from May 23 (Saale 2) and 31 (Saale 1), 2002 until April 16, 2007. During this time period, Saale 1 was

flooded 139 days by eight flooding events, while Saale 2 was flooded nine times for 170 days in total, two of these events including only short interruptions (Fig. 6-2). The longer flooding duration at Saale 2 was due to the fact that ground surface at monitoring site Saale 1 is 43.32 metres above mean sea level, while Saale 2 is situated at lower elevation: 43.08 metres above mean sea level. No additional floodings were recorded between May 23 and 31 at Saale 2. The longest period of flooding was from March 28 until May 3 (Saale 1) and 5 (Saale 2), 2006, respectively, during Elbhochwasser 2006. Nevertheless, the highest water levels were recorded in August 2002 in the course of the 2002 European floods: At August 19, 2002 the Elbe River flooded the monitoring sites by 2.75 (Saale 1) and 2.99 (Saale 2) meters, respectively.

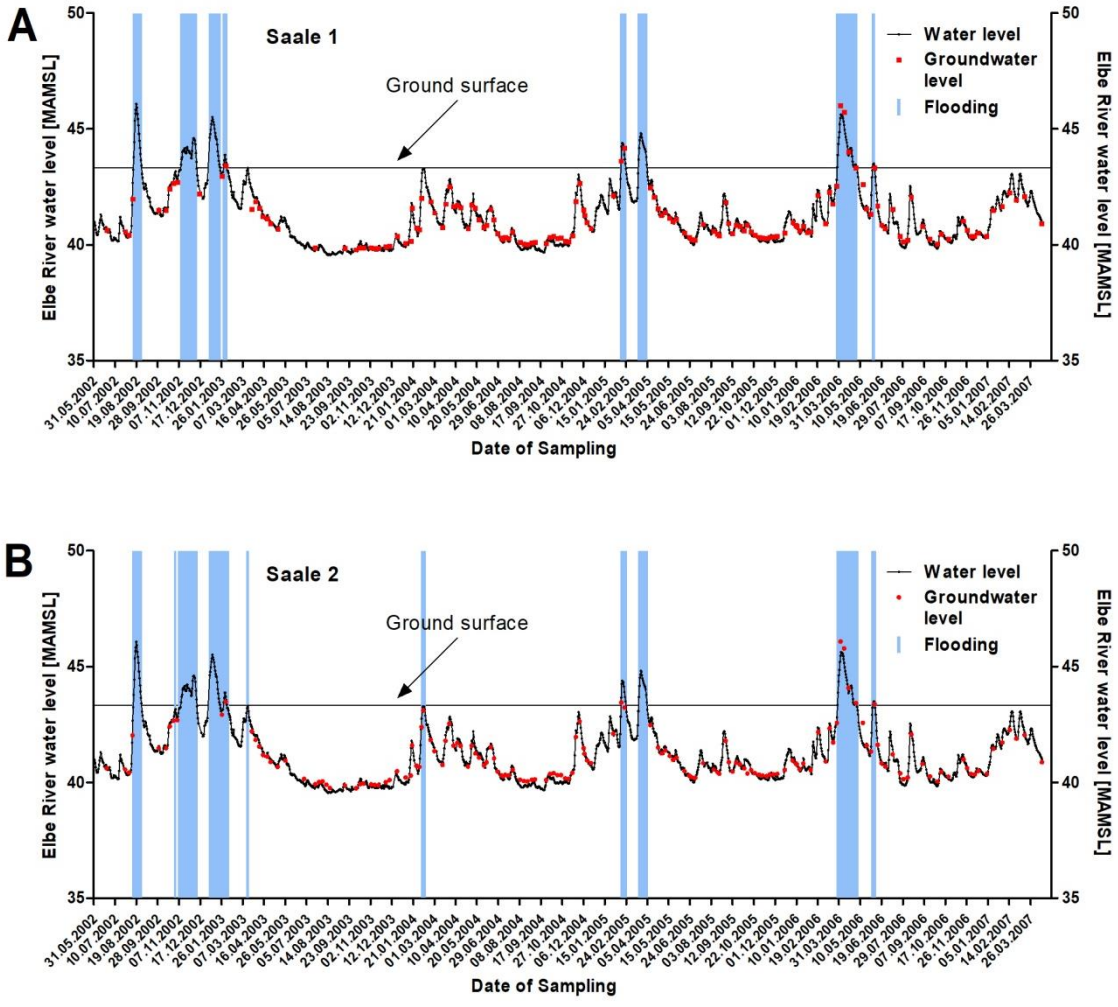

Figure 6-2: Variation of the Elbe River water level at the monitoring sites Saale 1 (A) and Saale 2 (B) as well as flooding events of the Elbe River during the operation time of the soil hydrological monitoring stations between May 31, 2002 and April 16, 2007. Saale 1 is situated 43.32 and Saale 2 43.08 metres above mean sea level (MAMSL).

6.2.2 The impact of Elbe River flooding events on soil biogeochemistry

Rising water levels of the Elbe River were accompanied by increasing soil moisture content and decreasing pore water pressure (PWP) at both sites. Significant correlations were found for both relationships which became stronger with soil depth. Similarly, rising water levels usually resulted in declining E_H within the different soil depths of the monitoring sites. This trend was more pronounced at Saale 2 and rather distinct in deeper soil depth (Fig. 6-3).

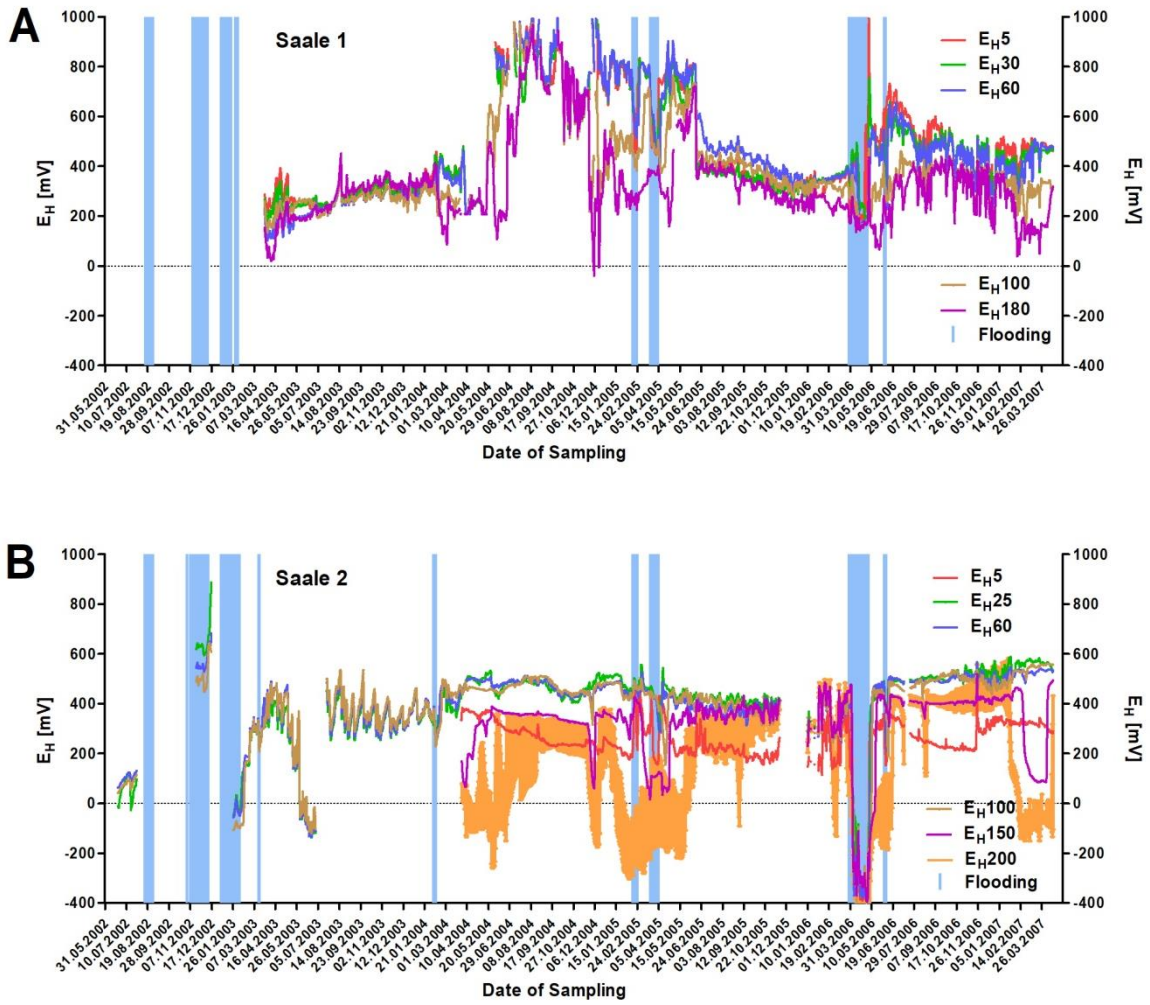

Figure 6-3: Variation of the redox potential (E_H) within soil solutions of different depths at the monitoring sites Saale 1 (A) and Saale 2 (B) as well as flooding events of the Elbe River during the operation time of the soil hydrological monitoring stations between May 23, 2002 and April 16, 2007.

Consequently, a negative relation between E_H and soil moisture content was common at both monitoring sites. Such a relation with soil moisture content was not found for pH at Saale 1 while a weak negative correlation was detected when the results of all soil depths of Saale 2 were considered. Thus, the impact of rising Elbe River water levels and soil moisture content was higher on E_H than on pH. The two last named parameters often show an inverse relationship (El-Naggar et al., 2018) which did not become apparent during the field experiment. Nevertheless, in many cases, reduction is accompanied by proton uptake while oxidation reverses this process (Alberts et al., 2008; Husson, 2013). Contrary to parameters with high temporal resolution measurement such as E_H, soil moisture content, and PWP, other parameters such as Hg(II), pH, DOC, Cl^-, and SO_4^{2-} were determined at specific dates. Considering all E_H values (E_H all) of all depths E_H at Saale 1 varied between -39 and 994 mV (Fig. 6-3). Focusing on the depths form which Hg(II) samples were collected E_H varied between 102 and 988 mV. At the times soil solution samples were taken to analyze Hg(II) and other parameters E_H in soil solution within 30, 60, and 100 cm showed moderately reduced or oxidized soils (Table 0-5, Appendix C).

The pH increased with rising soil depth when the groundwater was excluded. The pH in precipitation ranged from very strongly acid to neutral, from moderately acidic to moderately alkaline in 30 cm, and form neutral to strongly alkaline in 60 and 100 cm (Table 0-5). The pH range in groundwater was found to be high: from extremely acidic to moderately alkaline.

At the lower lying Saale 2 monitoring station considerably lower E_H values were recorded (Table 0-6, Appendix C). Particularly during Elbhochwasser 2006 a strong E_H decline was determined in soil solutions of all sampled depths (Fig. 6-3). This decline was much more pronounced compared to Saale 1 where E_H had declined as well in all probed soil solutions (Fig. 6-3). In general, differences in E_H between Saale 1 and Saale 2 became more evident in the upper soil horizons while in 100 cm depth mean E_H values were close to each other indicating again the influence of soil moisture and soil aeration on E_H values (Tables 0-5 and 0-6).

As a matter of stronger water influence E_H values at Saale 2 indicated highly reduced soils coinciding with flooding events and oxidized soils when Elbe River water levels were low (Figs. 6-2 and 6-3, Table 0-6). Redox potential varied between -435 and 887 mV when all E_H values of all sampled Saale 2 depths were considered. Thus, combining both study sites of the Saale-Elbe confluence study area E_H was in the range -435 to 994 mV which validates that the systematically controlled E_H values of the microcosm experiments were within a E_H range which can be found in nature as well.
Measured pH values at Saale 2 were similar to those determined at Saale 1 with comparable variations between soil depths (Table 0-6).

6.2.3 Mercuric mercury concentrations at the Saale-Elbe confluence

Mercuric Hg concentrations determined at the Saale-Elbe confluence study area were generally around 30 pg/ml (Tables 0-5 and 0-6). There was neither a distinct divergence between the two monitoring sites nor were pronounced differences between Hg(II) concentrations in precipitation, soil solutions or groundwater observed. Figure 6-4 shows changes in E_H and Hg(II) in soil solutions of the sampled soil depths at Saale 1 as well as the flooding events of the Elbe River. Obviously, the variations in Hg(II) concentration are hardly attributable to floodings and concomitant E_H changes. There were no significant correlations between Hg(II) and E_H (Table 0-7, Appendix C).

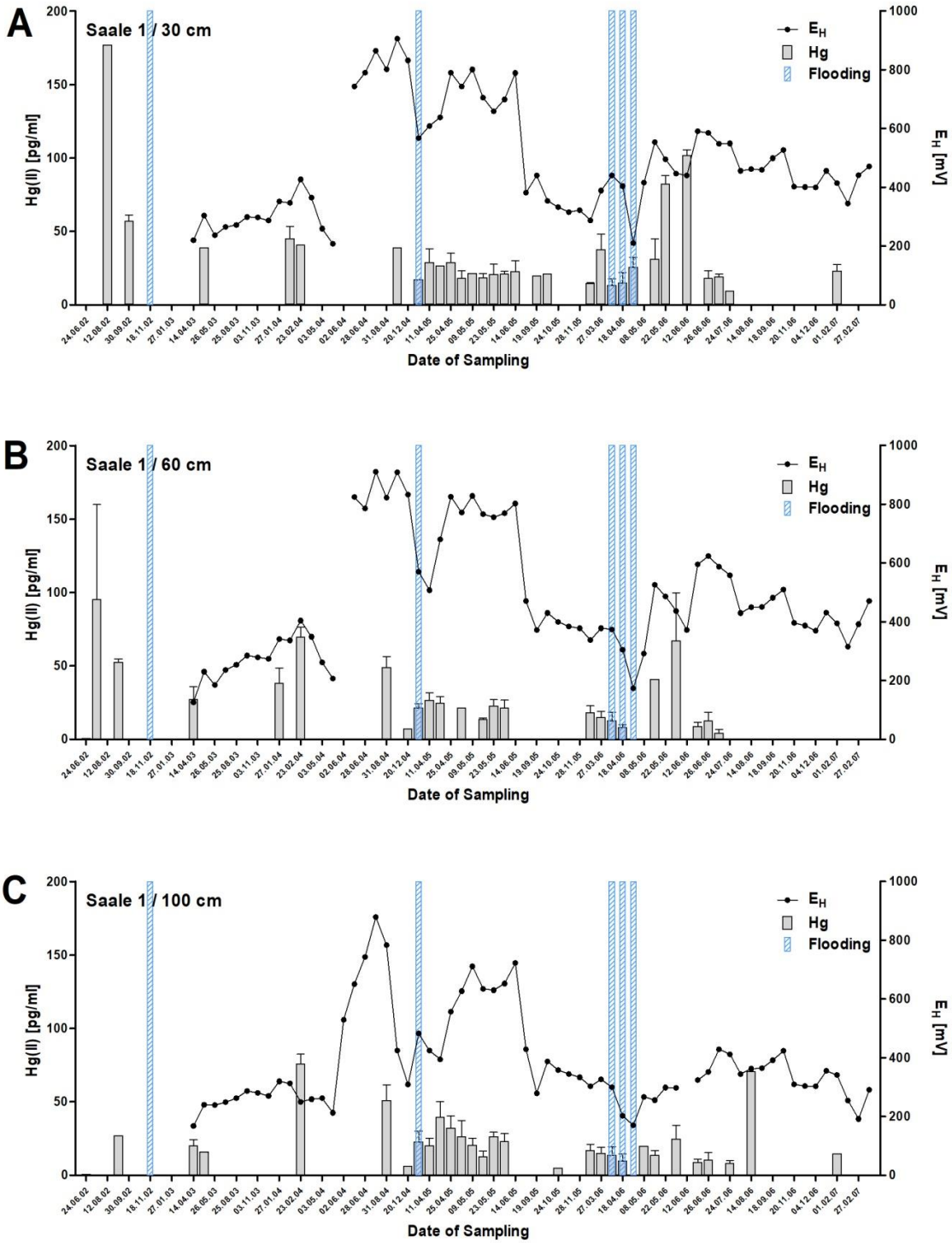

Figure 6-4: Changes in E_H and Hg(II) in soil solutions of different depths at the monitoring site Saale 1 as well as flooding events of the Elbe River.

Similarly, a clear negative relationship between E_H and Hg(II) at Saale 2 was found in the 25 cm soil solution solely (Table 0-7, Fig. 6-5).

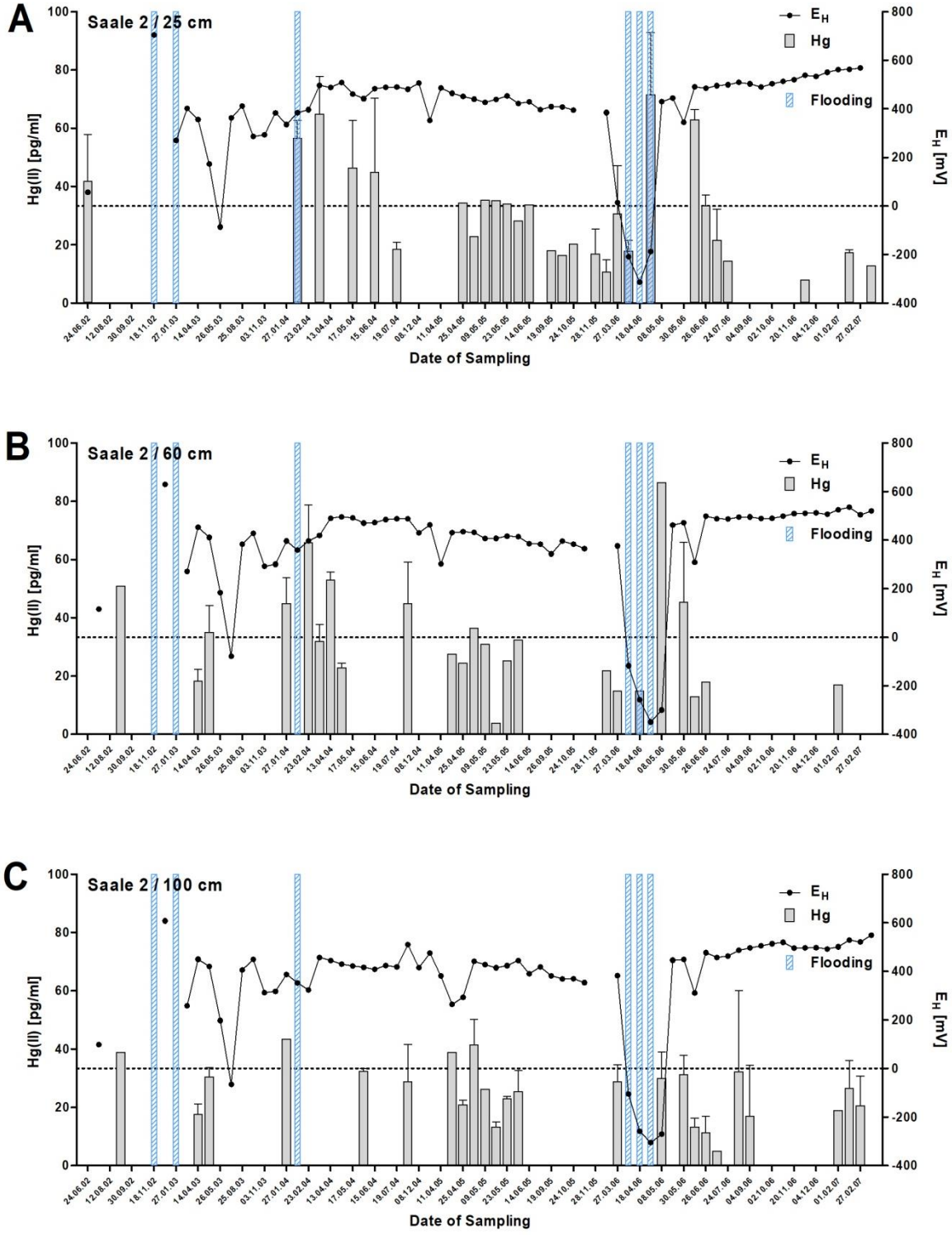

Figure 6-5: Changes in E_H and Hg(II) in soil solutions of different depths at the monitoring site Saale 2 as well as flooding events of the Elbe River.

A relation between Hg(II) and pH was missing at Saale 1 while a negative relation was found for the 100 cm soil solution at Saale 2. This negative relation is in contrast to the positive relations found between Hg_t and pH in the course of the microcosm experiments.
In general, although changes in E_H as well as pH have been identified as potential reasons for Hg release from soil (Xu et al., 2015) results for the Saale-Elbe confluence study area show strong relationships between Hg(II) and E_H or pH for individual soil depths only at the Saale 2 site (Table 0-7). The absence of strong relations between Hg_t and E_H as well as pH has also been reported by Frohne et al. (2012) who suggested that E_H and pH play subordinate roles in Hg mobilization and that E_H changes affect Hg mobilization indirectly.

6.2.4 Parameters with possible impact on mercuric mercury mobilization

Relevant parameters which may influence release or absorption of Hg(II) were compared between the sampling sites and between the different depths. In addition, interdependency between parameters was analyzed for either site or both sites in combination in order to understand potential effects on Hg(II) concentrations in the soil samples.
Average values for Hg(II), SO_4^{2-}, and Cl^- concentrations from the different sample depths show that anion concentrations increase with depth while Hg(II) appears to decrease (Fig. 6-6). This is true for both sampling sites Saale 1 and Saale 2 (Fig. 6-6). Also the DOC decreases with depth and is lowest in the groundwater (GW). The differences in the anion concentrations at the different depths is well reflected by the conductivity which is highest at 100 cm for both Saale 1 and Saale 2 samples. Interestingly, Cl^- and SO_4^{2-} molar concentrations are strongly correlated as shown here for all data from Saale 1 and Saale 2 including all depths (Fig. 6-7A). As molar concentrations are plotted in Figure 6-7A it becomes apparent that on the basis Cl^- and SO_4^{2-} concentrations are in the same range but Cl^- is on average about 1.34 times higher than SO_4^{2-}. As major anions in the samples, Cl^- and SO_4^{2-} will predominantly contribute to soil conductivity. A relationship is shown in Figure 6-7B. The plotted values are calculated from the molar concentrations of both anions considering also the net charge of the ions, i.e. the concentrations of the divalent sulfate were doubled. A significant ($P < 0.0001$) positive correlation was found and the linear regression shows an $r^2 = 0.8737$).

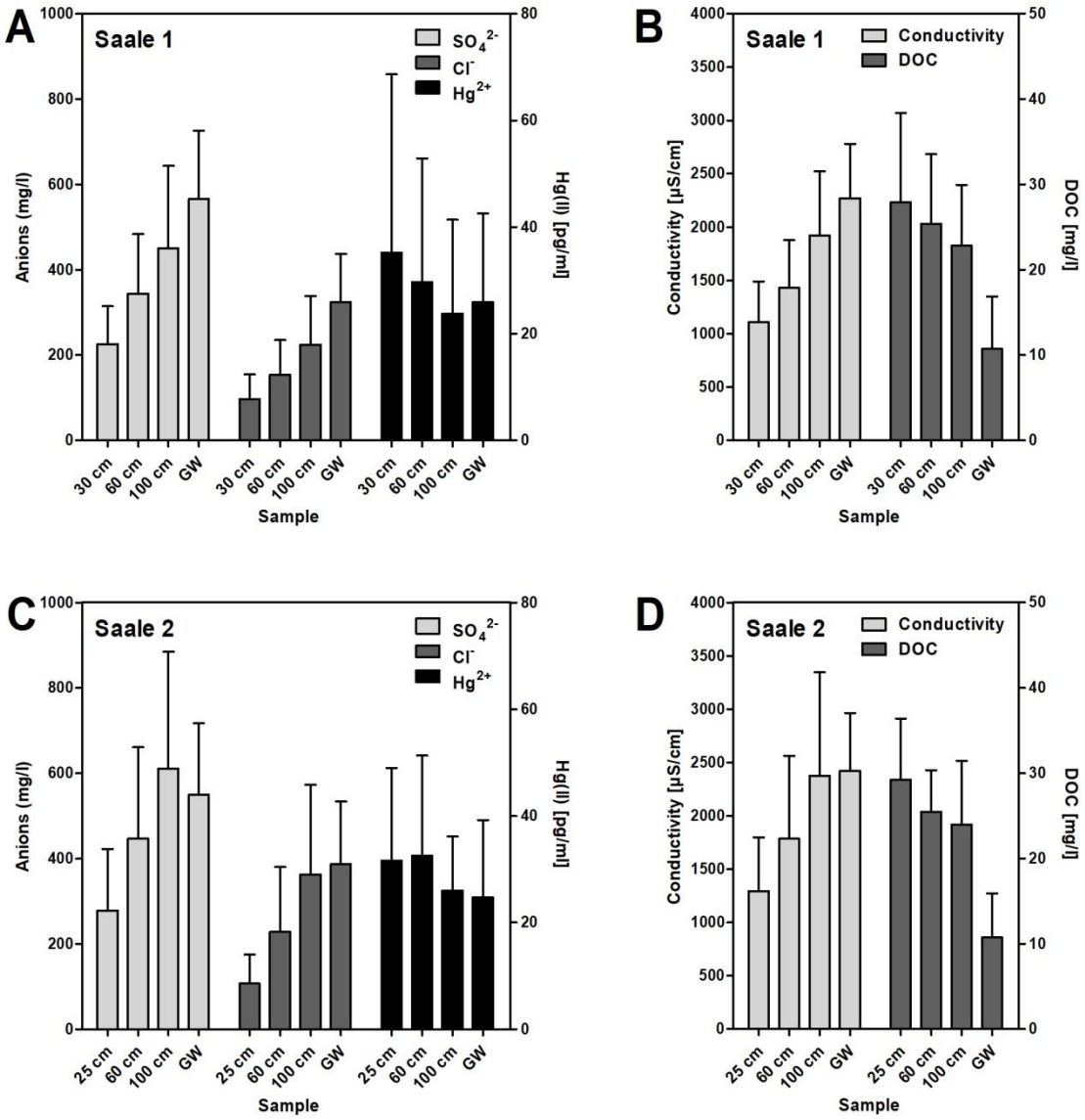

Figure 6-6: Parameters determined in different soil depths of the field study sites Saale 1 (A, B) and Saale 2 (C, D) presented as bar diagrams. Concentrations of SO_4^{2-}, Cl^-, and Hg^{2+} are shown in figures A and C. Conductivity and DOC concentrations are shown in figures B and D.

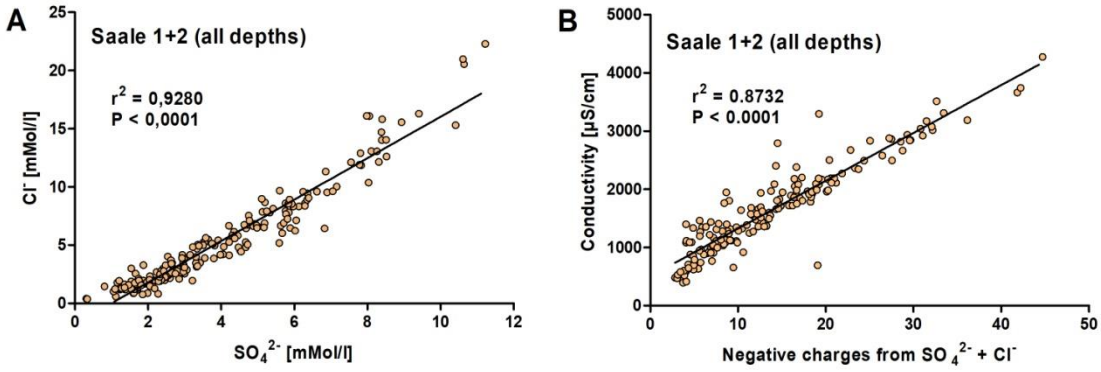

Figure 6-7: Correlation of parameters for all measurements from the Saale 1 and Saale 2 study sites including the data obtained from the different soil depths. A. Correlation between sulfate and chloride concentrations. B. Correlation between conductivity and the sum of the negative charges calculated from the molar concentrations of SO_4^{2-} and Cl^-.

Published results on the relationship between Cl^- concentrations and Hg release are inconclusive since the outcome of changing Cl^- concentrations depends on diverse parameters such as Hg species and concentration, Cl^- and sulfide concentration, OM content, and pH (Yin et al., 1996; Pelcová et al., 2010; Xu et al., 2014). As the data for Saale 1 and Saale 2 show a strong correlation between Cl^- and SO_4^{2-} concentrations, their effects on Hg(II) cannot easily be discriminated. For Saale 1 (all depths), however, we find a significant negative correlation between Hg(II) and Cl^- concentrations (Fig. 6-8A) while there is no significant correlation with SO_4^{2-} (Fig. 6-8B, Table 0-7). For Saale 2, neither Cl^- nor SO_4^{2-} significantly correlate with Hg(II) levels (Table 0-7). At least our observations partially confirm the results of others that Cl^- may have an effect on Hg release. Obviously further parameters are involved and Hg(II) release is controlled by multiple processes augmenting or impairing each other.

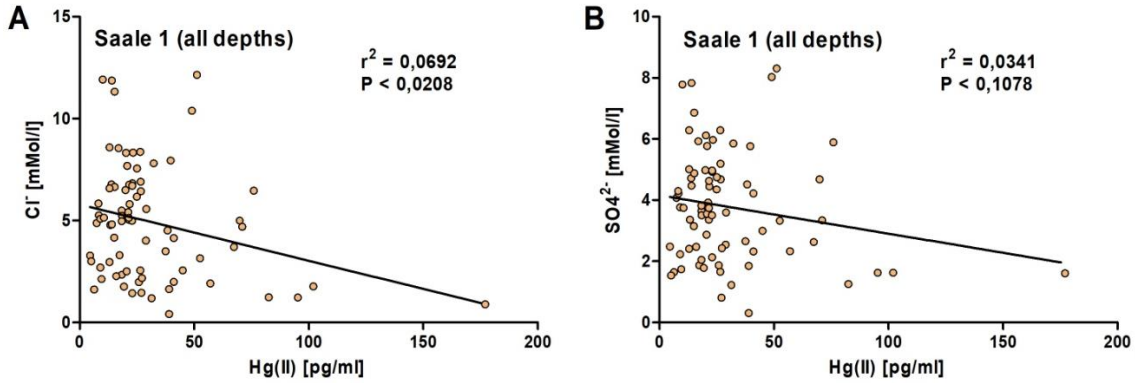

Figure 6-8: Correlation between Hg(II) concentrations and Cl^- (A) as well as SO_4^{2-} (B) for the Saale 1 study site. The negative correlation between Hg(II) and Cl^- is significant with $P < 0.0208$.

Dissolved organic carbon is well known as important parameter with possible impact on Hg mobilization due to the strong binding between Hg and the reduced sulfur groups of DOC (Wallschläger et al., 1996; Xu et al., 2014; Bravo et al., 2018). The average data from Figure 6-6 indicates that both Hg(II) and DOC concentrations decreased with soil depth. Plotting Hg(II) vs. DOC concentrations for all depths of the Saale 1 and Saale 2 sites did not reveal a significant correlation (Fig. 6-9, Table 0-7).

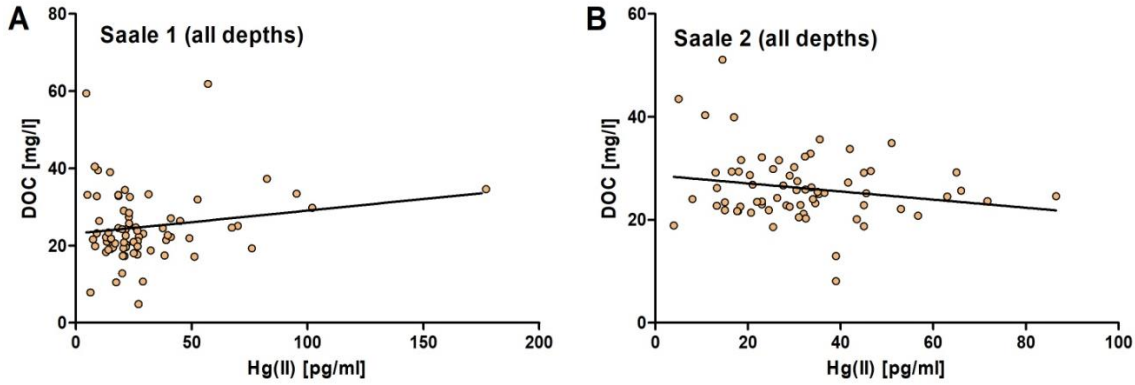

Figure 6-9: Relationship between Hg(II) and DOC concentrations for the Saale 1 and the Saale 2 study site. There is no significant correlation.

However, despite being an important ligand for Hg positive correlations between DOC and Hg may not always be found, since the reduced sulfur (i.e. thiol) groups which are the major binding sites for Hg are a small fraction of dissolved organic matter (Haitzer et al., 2002; Ravichandran, 2004). This may, in part, explain why a negative correlation was found between Hg(II) and DOC in the 100 cm soil solution of Saale 2 (Table 0-7). Such relation has been reported by Kim et al. (2015) for Hg_t and DOC as well.

Figure 6-10 shows the influence of E_H and DOC on Hg(II). A clear relationship is neither seen for the study sites Saale 1 and Saale 2 nor when results of both were combined.

Contrarily, Figure 6-11 suggests that the interplay between DOC and Cl^- may have had stronger influence on Hg(II) mobilization. The results for Saale 1, Saale 2, and both monitoring sites together indicate that a combination of higher DOC and lower Cl^- favored the release of Hg(II) (Fig. 6-11). It is interesting to notice that negative relations between Cl^- and Hg are seldom reported in literature. Hall et al. (2008) found this relation for different ecosystem types in southern Louisiana and the Gulf of Mexico region. Moreover, this relation was calculated for the BC200 & BC500 experiment as well (Chapter 5).

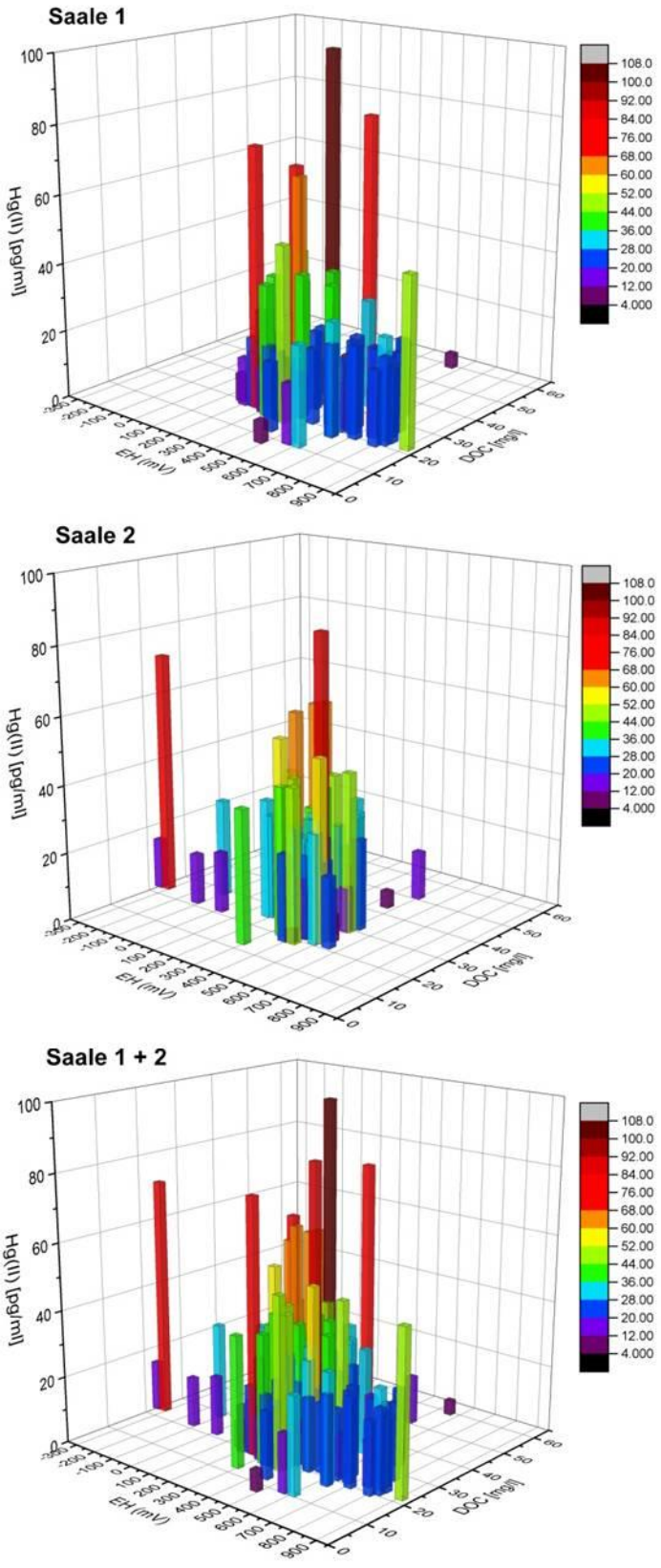

Figure 6-10: Dependency of Hg(II) concentrations in soil solution from redox potential (E_H) and DOC displayed in a three-dimensional coordinate system. Bars show means of data obtained from Saale 1 and Saale 2 and from both in combination. Bar colors correspond to the concentrations indicated by the color scale.

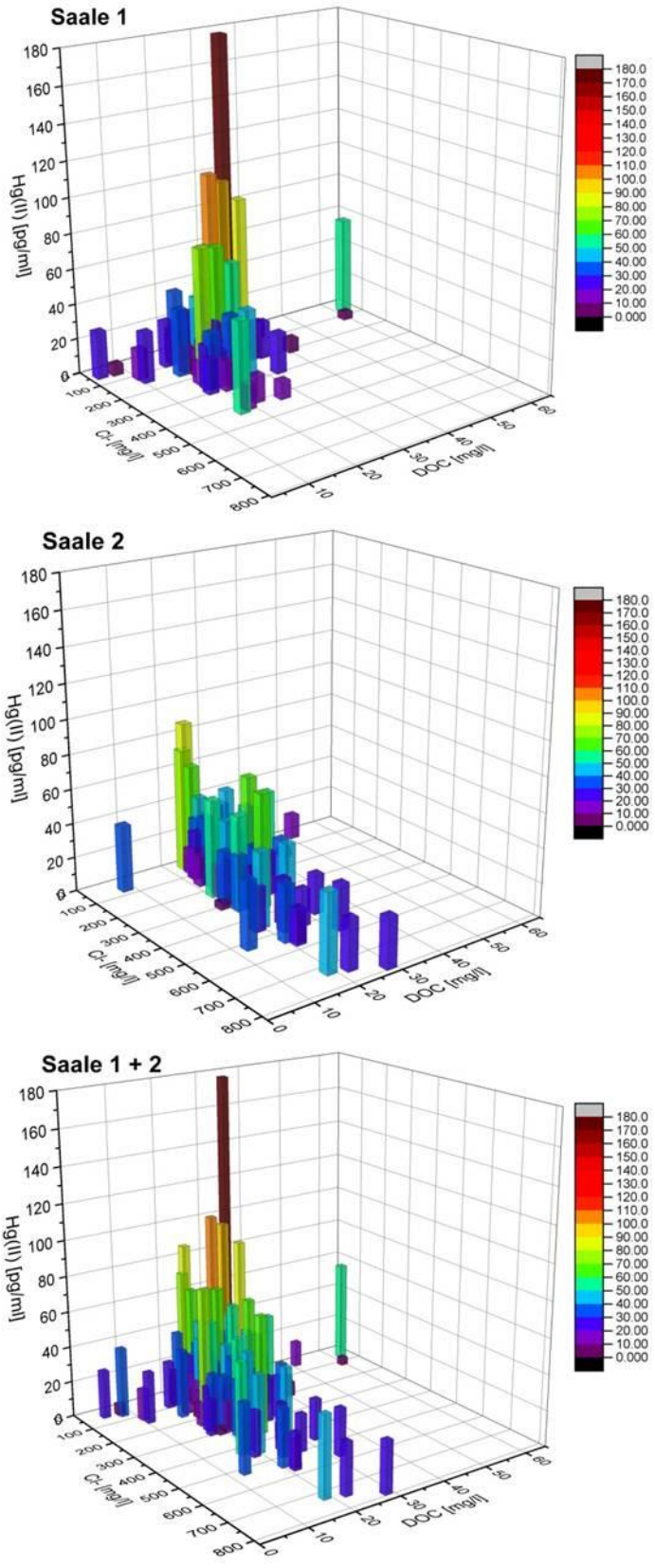

Figure 6-11: Dependency of Hg(II) concentrations in soil solution from chloride concentrations (Cl^-) and DOC displayed in a three-dimensional coordinate system. Bars show means of data obtained from Saale 1 and Saale 2 and from both in combination. Bar colors correspond to the concentrations indicated by the color scale.

A clear distinction between precipitation derived and mobilized legacy soil Hg(II) requires additional analyses. The measurement of Hg isotopes is a promising tool to identify sources and pathways of Hg (Yin et al., 2014; Sherman et al., 2015; Obrist et al., 2018). It is suggested that more than 90% of the Hg loading of surface waters can be attributed to atmospheric deposition (Leopold et al., 2010). Analysis of Hg isotope compositions in surface water of eight freshwater lakes in Ontario, Canada, indicated that about 42% ± 26 of the Hg_t determined originated from precipitation (Chen et al., 2016). Modelling by Hararuk et al. (2013) for the contiguous United States predicted increasing soil Hg pools following an increase in precipitation amounts. However, despite the potentially strong contribution of precipitation derived Hg in soil solutions and groundwater of the Saale-Elbe confluence study area research at another contaminated site indicates that precipitation may be a minor contributor (Washburn et al., 2017).

6.3 Conclusions

The results obtained by the soil hydrological monitoring stations Saale 1 and Saale 2 at the Saale-Elbe confluence study area clearly demonstrate the strong influence of rising water levels on E_H changes which have been shown to proceed within a short period of time and with appreciable intensity. A direct impact of these E_H changes on Hg(II) did not become apparent. Moreover, Hg(II) concentrations determined in precipitation samples were of similar magnitude to those measured in the different soil solutions and groundwater irrespective of monitoring site. Therefore, with regard to Hg(II) concentrations found in soil solutions and the groundwater, it is difficult to distinguish whether these concentrations result from biogeochemical changes induced by flooding events or rather reflect the seeping of precipitation derived Hg(II). However, the results indicate that Hg(II) increased with higher DOC and lower Cl^- concentrations. While the binding of Hg to thiol groups of DOC is well known the impact of Cl^- on Hg mobilization is suggested to be complex and remains an interesting field for future research. Additionally, upcoming research utilizing soil hydrological monitoring stations should consider measuring Hg isotope ratios to trace the movement of Hg. By this a clearer distinction between precipitation derived and mobilized legacy soil Hg(II) would be possible.

7. Synthesis

7.1 Influence of redox potential and amendments on the release of total mercury and mercury species

The presented work shows that the redox potential influences Hg mobility. The impact of such E_H changes on release of Hg_t and the release and formation of Hg species was complex. However, both during the microcosm experiments and in the course of the field study significant negative correlations between E_H and Hg_t as well as Hg(II) were found indicating that declining E_H favored Hg_t and Hg(II) release, while increasing E_H was accompanied by declining Hg_t and Hg(II) concentrations (Tables 0-2, 0-4, and 0-7, Figs. 4-3 and 5-3). This relation was particularly clear for the BC200 & BC500 experiment during which Hg_t concentrations were higher at the last two samplings when E_H had been lowered again (Fig. 5-3). When SBFL was used as amendment the influence of E_H became negligible. The reason is that adsorption of Hg to SBFL is governed by quite different chemical processes compared to Hg binding to biochars which will be discussed in detail below.

Redox potentials determined in the course of the field study at the Saale-Elbe confluence were in the range -435 to 994 mV. Considerably lower E_H values were found at the monitoring site Saale 2 which is situated 24 cm lower than Saale 1 and was, therefore, more affected by increasing water levels. The lowest E_H determined for Saale 1 was -39 mV. These results highlight the strong influence of soil moisture on E_H. Comparing laboratory experiments with the field study it becomes apparent that the systematically controlled E_H values of the microcosm experiments were within a E_H range which can be found in nature as well. Furthermore, the E_H values determined for Saale 2 show that the soil at this monitoring site had a higher E_H capacity than the Wupper soil used in the microcosm experiments whose E_H could not be reduced below -260 mV. Instead, E_H at Saale 2 declined from 295 to -435 mV within 32 days.

Significant positive correlations were found between pH and Hg_t in the course of the microcosm experiments. Considering published results on the relationship between Hg and pH (Wallschläger et al., 1996; Xu et al., 2014) indicating a rather small impact of pH on Hg release it may be suggested that the calculated relationship between pH and Hg_t was provoked by the strong link between E_H and pH as described in Chapter 6. Indeed, a negative correlation between Hg(II) and pH was found at the Saale-Elbe confluence solely (Tab 0-7).

The thiol groups of DOC are strong binding sites for Hg making DOC a particularly important ligand for Hg as discussed in the previous chapters. Results obtained by the microcosm experiments support the strong positive relationship (Tables 0-2 and 0-4), while no such relationship was found in the course of the field study (Table 0-7). However, the microcosm results indicate that fine biologically decomposed organic material with associated Hg entered the aqueous phase upon flooding of the soil (Fig. 5-3). Similar patterns indicating a co-release of MeHg and EtHg with DOC at the beginning of the microcosm experiments were found as well (Figs. 4-3 and 5-3).

Another parameter potentially exerting influence on Hg release is Cl^-. Considering the results of the microcosm experiments and the field study this parameter may have had stronger impact during the BC200 & BC500 experiment and the field study compared to the BC & SBFL experiment. As has been discussed in the previous chapters the effect of Cl^- on Hg release is superimposed or affected by diverse factors and it may, therefore, remain obscured in several cases. Examining the effects of Cl^- and DOC on Hg release for the BC200 & BC500 experiment and the field study results indicated that Hg release was supported by increasing DOC concentrations and decreasing Cl^- concentrations (Figs. 5-5 and 6-11).

Higher Hg concentrations at lower Cl^- concentrations may indicate that Hg_2Cl_2 formed and precipitated at higher Cl^- concentrations removing Hg from solution (Kim et al., 2004; Jeong et al., 2007; Chen et al., 2017). The formation of Hg_2Cl_2 requires the reduction of Hg(II) to Hg(I) which may take place on the surfaces of adsorbents (Lloyd-Jones et al., 2004; Kong et al., 2011; Li et al., 2017).

Based on the described results it may be concluded that comparable processes may have taken place in the course of the microcosm experiments and the field study indicating that experimental flooding in microcosms provides results similar to flooding in the field. Interactions between Hg and the considered parameters became more obvious in the course of the microcosm experiments due to laboratory conditions. However, it seems that both during microcosm experiments and in the course of the field study flooding induced E_H changes and DOC release which both contributed to the release of Hg_t or Hg(II), respectively. Furthermore, higher Cl^- concentrations may have influenced Hg concentrations in solution due to the precipitation of Hg_2Cl_2.

In conclusion, both microcosm experiments and the field study revealed potentially important processes for Hg release. However, comparing Hg results obtained in the laboratory and in the field it can be seen that, despite the fact that both floodplain soils were polluted by Hg_t to a similar degree, continuous stirring of the flooded soil in the microcosms favored the dissolution of Hg_t since Hg(II) concentrations measured in the field were significantly lower (Tables 0-1, 0-3, 0-5, and 0-6). The highest Hg(II) concentration determined for the Saale-Elbe confluence was 0.18 µg/l, while the lowest Hg_t concentration determined in the course of the microcosm experiments was 0.91 µg/l. These results demonstrate that in situ soil has a higher potential to retain Hg as might be suggested based on microcosm experiments.

Furthermore, in contrast to the microcosm experiments it was not possible to deduce whether Hg(II) in soil solution of the Saale-Elbe confluence was mobilized legacy Hg(II) or precipitation derived Hg(II). Measures to identify the source of measured Hg are discussed in Chapter 7.2.

Based on published results concerning Hg removal from aqueous solutions by means of biochar (Liu et al., 2018b) it was suggested that Hg in floodplain soils can be immobilized by amendments. Knowledge of the chemistry of Hg interactions with DOC as well as other organic and inorganic soil components will be helpful to identify suitable amendments as their interactions with Hg may depend on similar chemical reactions.

It was found that the added SBFL was particularly effective in reducing Hg dissolution from soil irrespective of prevailing E_H. Sugar beet factory lime reduced mean Hg_t concentration released during the experiment by 65%. Biochar based material as well as BC200 and BC500 showed a smaller impact on Hg_t release resulting in Hg reduction of 21%, 8% and 23%, respectively. These amendments primarily reduced Hg_t mobilization under highly reduced conditions around E_H -125 mV (BC) and -110 mV (BC200 & BC500), respectively, at one specific sampling. This effect is highlighted in Figure 7-1. Higher efficiencies in reducing Hg_t concentrations by biochars were recently reported (Liu et al., 2018a).

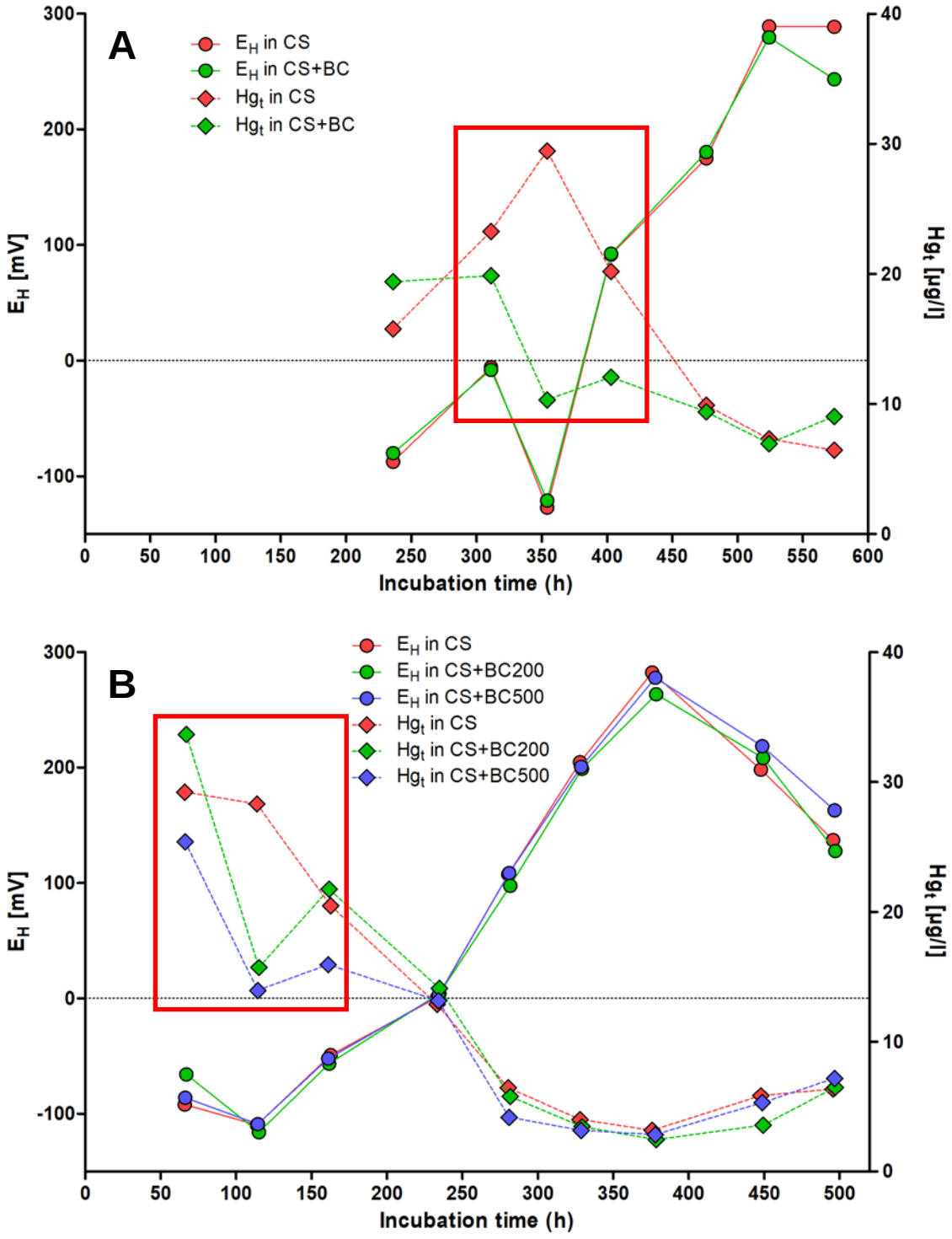

Figure 7-1: Changes of E_H values (circles) and Hg_t concentrations (rhombs) in the course of the microcosm experiments. The impact of BC (A) as well as BC200 and BC500 (B) on Hg_t concentrations under highly reduced conditions is highlighted by the red rectangles.

There are several possibilities why the amendments BC, BC200, and BC500 were not as efficient as considered in our experiment. For evaluating the potential reasons a compartment model of soil components will be used considering the specific Hg binding sites for each compartment:

In CS three compartments will be distinguished which provide binding sites for Hg; organic and mineral soil particles and the DOC. Amendments added constitute a further compartment. The biochar based material or biochar added in CS+BC, CS+BC200, and CS+BC500 provided further binding sites.

Typically, reduced sulfur groups are in great excess to Hg_t content in soils (Skyllberg, 2012). Thus, the majority of Hg will bind to OM and metal sulfides while oxygen functional groups at Fe and Al oxyhydroxides as well as the edges of phyllosilicates are indirect adsorbents (Xia et al., 1999; Skyllberg, 2012). Mercury in soil solution may be in the form of Hg^{2+}, $HgCl^{+}$, $HgCl_2^{0}$, $HgCl_3^{-}$, $HgCl_4^{2-}$, HgClOH, $Hg(OH)^{+}$, $Hg(OH)_2^{0}$, and Hg-DOC (Han, 2007). However, due to its affinity for reduced sulfur groups complexes with thiols of DOC will dominate the speciation of Hg in soil solution (Skyllberg, 2012). Dissolved Hg concentrations measured in the course of the microcosm experiments exceeded those typically reported for natural ecosystems (Leopold et al., 2010). Therefore, it seems likely that Hg was not solely bound to the small fraction of DOC reactive thiol functional groups but also to carboxylic functional groups. Research by Haitzer et al. (2002) indicated that the binding of Hg to DOM under natural conditions (very low Hg/DOM ratios) is controlled by a small fraction of DOM containing a reactive thiol functional group providing strong binding sites for Hg while carboxyl groups came into play at higher Hg to DOM ratios. It is noted that pH may influence the dissociation rate of carboxylic acids and thereby the number of potential binding sites.

As a matter of the strong binding between Hg and the reduced sulfur groups mobilization of Hg is rather influenced by DOC than by pH (Wallschläger et al., 1996; Xu et al., 2014). Therefore, it seems unlikely that biochar sorption of Hg was hampered by protons occupying binding sites. Besides protons other cations may occupy biochar binding sites. However, as Hg binding to biochars was observed at a certain E_H it doesn't seem plausible that Hg was bound to binding sites and got replaced shortly after again. Another thesis why biochar showed little effect on Hg sorption is the presence of dissolved complexes binding Hg and hampering the sorption to biochar. The presence of such complexes can't be ruled out. Still, they would have been present in the microcosms without amendment as well. Therefore, it seems unlikely that in CS Hg was released from complexes at the certain E_H and stayed in solution while the Hg released from the complexes in the amended microcosms was bound to the biochar and got complexed again after changing redox conditions. Chemical reactions which compete for Hg binding concerning organic components such as DOC

and biochars are presented in Figure 7-2. The scheme depicts some potentially important reactions which are discussed here and is thought to illustrate the interrelationships.

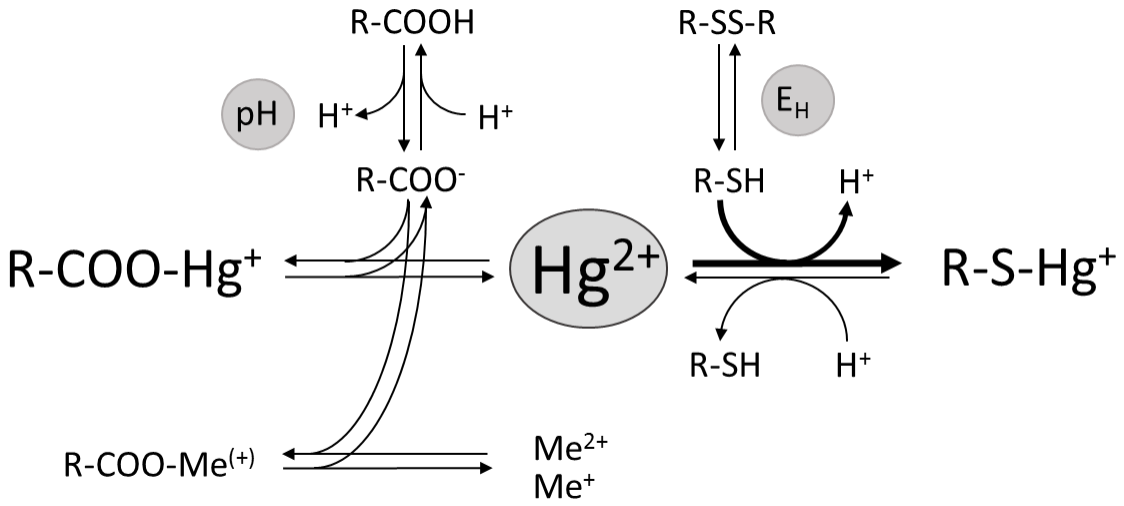

Figure 7-2: Scheme of relevant chemical reactions involved in mobilization and immobilization of Hg^{2+} by organic soil components. The concentration of dissolved Hg^{2+} is determined by the number of available binding partners and the equilibrium constants of the respective reactions. It is also indicated that binding partners can be altered in their amounts for example by pH, E_H or competitive metal ions thereby affecting potential Hg binding sites and thus the Hg^{2+}-concentration. The bold arrow should point to the fact that the reaction is driven preferentially in direction of the product R-S-Hg^+.

Another factor which may affect Hg adsorption in the soil environment is the formation of biofilms. In general, a short term redox change is unlikely to alter a possible film on the biochar so that Hg can be bound. In the course of the microcosm experiments biofilms may have formed as in nature cells grow predominantly in such aggregation of soil microorganisms especially in heavily polluted sites (Gross et al., 2007). Thus, the alteration of the biochars surface and its chemical and physical properties by the formation of biofilms on the biochar particles needs to be considered. Possibly, biofilms may reduce the interaction of Hg with the biochars surface and by that disturb its effects on Hg immobilization. Otherwise biofilms themselves accumulate inorganic and methylated Hg compounds (Hintelmann et al., 1993; Dranguet et al., 2017; Dranguet et al., 2018) and may also lead to a higher rate of Hg methylation compared to planktonic bacteria (Lin et al., 2013). Different mechanisms play a role in Hg uptake by biofilms, e.g. steric hindrance and electrostatic interactions, binding functional groups of the extracellular polymeric substance matrix, and adsorption by mineral fractions present in biofilms (Dranguet et al., 2017). Leclerc et al. (2015) hypothesized that Hg-thiol complexation in the extracellular fractions of biofilms can occur which may potentially affect the bioavailability of Hg and increase its methyla-

tion. Dranguet et al. (2017) noted that the bioavailability of Hg compounds, their transformations, and their effects depend on their concentrations and speciation, ambient water characteristics, biofilm matrix composition, and microorganism-specific characteristics. Here it seems that biofilm matrix composition and microorganism-specific characteristics had only little influence on the fate of Hg species.

The sorption of Hg-DOC complexes at the amendments was potentially of importance. Except for the microcosms amended with SBFL strong positive relations between Hg_t and DOC were found (Tables 0-2 and 0-4). In the course of the BC & SBFL experiment both Hg_t and DOC concentrations decreased due to the added BC and SBFL. The results for CS+SBFL indicate that this reduction is not exclusively attributable to concomitant binding of DOC and Hg_t. Considering possible interactions between Hg-DOC complexes and BC200 as well as BC500 it has to be noted that variations in DOC concentrations in the BC200 & BC500 experiment were less pronounced compared to the BC & SBFL experiment (Tables 0-1 and 0-3). Consistently, Hg_t and DOC concentrations were slightly lower in CS+BC500 solely (Table 0-3). Although often used for remediation purposes biochar amendment has been shown to have the potential to increase DOC concentrations which may be linked to enhanced leaching and mobility of soil contaminants (Beesley et al., 2010; Qi et al., 2017; Chen et al., 2018). Contrarily, it has also been reported that DOC may be captured by biochars (Kammann et al., 2015). However, biochar mediated changes in DOC concentration may not always be determined (Jones et al., 2012). In general, feedstocktype and pyrolysis temperature influence properties of biochars including their potential to release DOC (Liu et al., 2015). Here, minor effects of biochar amendment on DOC concentrations were determined solely.

Instead it seems likely that under highly reduced conditions when Hg got bound at the biochars disulfide bridges turned into two thiol groups providing strong binding sites for Hg lowering dissolved Hg concentrations. The redox sensitivity of such bridges explains why Hg was released with changing redox conditions again. The effectiveness of such disulfide-dithiol sites is well known for biological systems and is part of enzyme-based microbial Hg resistance (Robinson and Tuovinen, 1984; Barkay et al., 2003). Following this assumption, microcosm experiments indicated that binding site quality is potentially more relevant than binding site quantity for Hg immobilization in soil.

With respect to immobilization of Hg by means of SBFL interactions with inorganic components of the lime and also organic components of the sugar beets have to be considered. However, the components of the lime will presumably provide the dominant Hg binding sites. The chemical composition of lime is variable but its main constituent is usually calcium oxide (CaO). In addition, it contains SiO_2, Al_2O_3, Fe_2O_3, MgO, and $CaCO_3$ in variable amounts (Panda et al., 2012; Kiliç, 2013; Zumrawi and Hamza, 2014; Sarsam et al., 2017) dependent on the origin of the lime. The main constituent of carbonated lime as used in the course of the BC & SBFL experiment is $CaCO_3$ making up more than 80% of the lime (Shaheen and Rinklebe, 2017). Most of the constituents are potential binding partners for Hg. Early studies have shown, that the main component $CaCO_3$ is capable to interact with various metal ions such as Cd^{2+}, Mn^{2+}, Zn^{2+}, and Co^{2+} (Comans and Middelburg, 1987). These interactions can be resolved into two reactions, a fast primary adsorption to the $CaCO_3$ surface and a subsequent slow precipitation, i.e. a more stable incorporation of the metal into the crystal lattice (Comans and Middelburg, 1987; Papadopoulos and Rowell, 1988). A study by Hutson et al. (2008) on the removal of Hg from coal flue gas revealed that Hg^{2+} but not Hg(0) will be retained by $CaCO_3$. Fazlollahi et al. (2014) successfully applied $CaCO_3$ to remove Hg from oil field brine. Based on the high $CaCO_3$ content in SBFL, Hg binding to $CaCO_3$ is thus suspected be the major process for Hg immobilization by means of lime. Nevertheless, minor SBFL components are also capable to bind Hg. As their binding sites are still in excess compared to Hg, these components can also contribute to Hg immobilization. Silicon dioxide containing minerals as part of the lime expose hydroxyl groups (≡Si-OH) at the surface capable of Hg binding (Tiffreau et al., 1995). Similarly, iron oxides can interact with Hg^{2+} forming stable =Fe-O-HgOH (Bonnissel-Gissinger et al., 1999). Concerning CaO, density functional theory studies by Guo et al. (2007) and Sasmaz and Wilcox (2008) showed that Hg^{2+} as $HgCl_2$ binds to CaO crystalline surface while Hg(0) only weakly interacts with CaO.

Figure 7-3 summarizes the suggested binding sites in soil, those of the amendments, and those compartments for which Hg was determined in the course of the microcosm experiments and the field study.

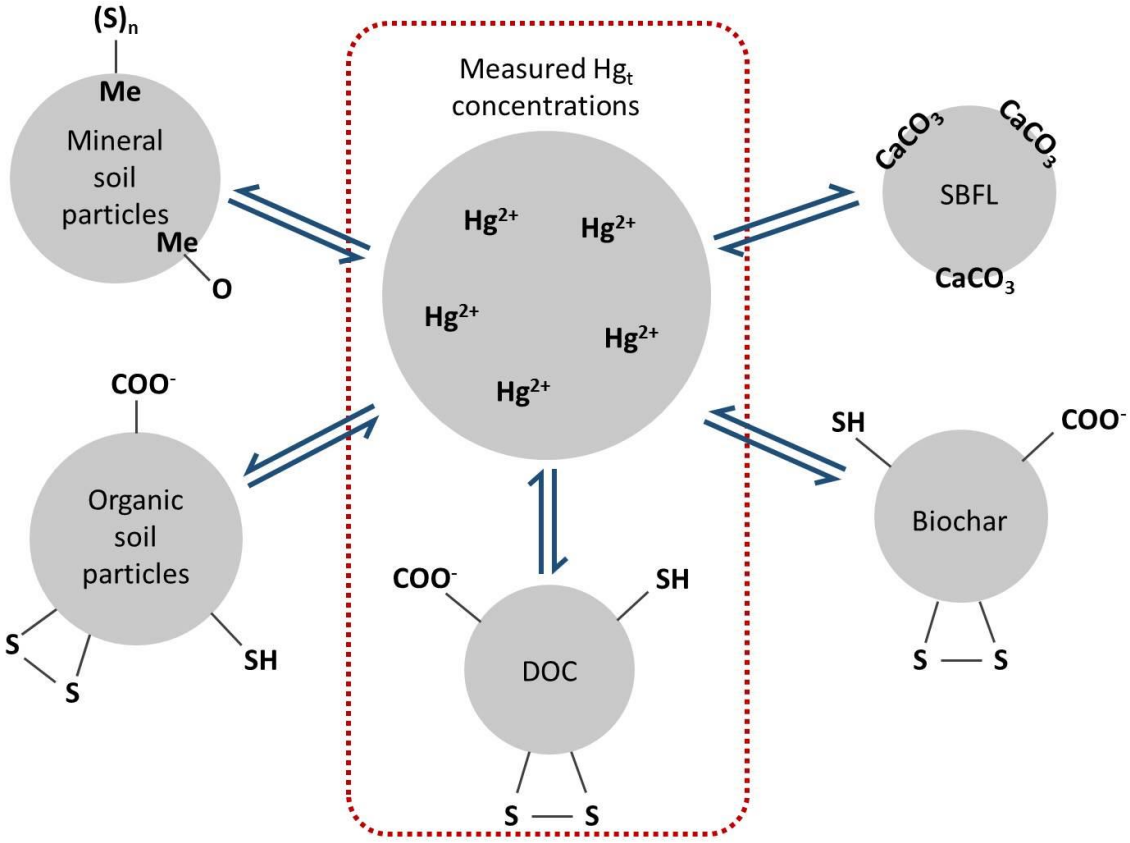

Figure 7-3: Simplified scheme illustrating the sites, considered as compartments, which interact with dissolved mercury in the course of Hg immobilization. Some typical chemical functional groups and structures involved in Hg binding and discussed here are indicated. Measured mercury concentrations in soil solution include DOC bound Hg(II) (surrounded by the red dotted line). On the left side the natural soil compartments and on the right side the amendments used in this work are depicted. The amounts and the binding strengths of the reaction partners determine the distribution of Hg^{2+} into the different compartments.

7.2 Conclusions and implications for further research

The flooding experiments conducted with the biogeochemical microcosms as well as the field study operated by means of soil hydrological monitoring stations consistently indicate that flooding with concomitant E_H reductions and the entrance of fine biologically decomposed organic material into the aqueous phase as measured by DOC concentrations resulted in higher Hg mobilization. Furthermore, laboratory and field observations suggest that Hg_2Cl_2 formed and precipitated at higher Cl^- concentrations.

The addition of BC, SBFL, BC200, and BC500 in the course of the microcosm experiments reduced mean Hg_t concentrations by 8% up to 65% compared to unamended CS. Thiols of redox sensitive disulfide bridges are suggested to be the most important additional binding sites for Hg_t of BC, BC200, and BC500. However, these suggested thiol binding

sites came into effect under highly reduced conditions solely. Therefore, the tested biochar based material as well as the biochars BC200 and BC500 showed limited potential to reduce Hg_t mobility. Furthermore, the capability of these amendments to impede the formation of MeHg and EtHg was negligible. Slightly lower MeHg concentrations were found in CS+BC500 solely. The amended SBFL was much more efficient with regard to Hg_t immobilization. One possible reason might be that Hg got incorporated into the crystal lattice of $CaCO_3$ which is the main constituent of SBFL. However, next to such stable incorporation other constituents of SBFL may bind Hg as well. Despite the lower Hg_t concentrations due to the added SBFL MeHg concentrations in CS+SBFL were similar to those of CS which can be attributed to the stimulation of microbial growth including SRB by SBFL as inferred from PLFA profiles.

In general, PLFA profiles of both microcosm experiments indicate that SRB were the primary methylators of Hg. Results of the BC200 & BC500 experiment reveal that Hg methylation may occur at comparatively high E_H (between -50 and 100 mV) as well.

The pattern of EtHg found in CS and the treatments in the course of the BC200 & BC500 experiment suggests that ethylation may be favored around E_H 0 mV. This finding might be of interest considering that limited information is available on the ethylation of Hg in the natural environment.

Future research should consider clarifying the impact of E_H and DOC on Hg mobilization separately. The microcosm results suggest that co-dissolution of Hg and DOC occurred upon flooding of the soils which may lead to an overestimation of E_H impact on Hg when E_H is lowered at the beginning of the experiment. Furthermore, additional analytics should be used for a better identification of SRB. The measurement of Hg isotopes, particularly in the field, should be considered for a better identification of Hg sources and pathways. As the role of Cl^- in influencing Hg mobilization/immobilization is not clear microcosm experiments are proposed in which Cl^- concentrations in the slurry will be varied under otherwise constant conditions (E_H, pH). It is noted that the counter cation of the applied Cl^- may have an impact on the Hg immobilization process.

References

Abel CDT, Sharma SK, Malolo YN, Maeng SK, Kennedy MD, Amy GL. Attenuation of Bulk Organic Matter, Nutrients (N and P), and Pathogen Indicators During Soil Passage: Effect of Temperature and Redox Conditions in Simulated Soil Aquifer Treatment (SAT). Water, Air, & Soil Pollution 2012; 223: 5205-5220.

Ad-hoc-Arbeitsgruppe Boden. Bodenkundliche Kartieranleitung. Hannover, 2005.

Adriano DC. Trace elements in terrestrial environments. New York Springer-Verlag, 2001.

Aguilar L, Thibodeaux LJ. Kinetics of peat soil dissolved organic carbon release from bed sediment to water. Part 1. Laboratory simulation. Chemosphere 2005; 58: 1309-1318.

Ahmad M, Lee SS, Lee SE, Al-Wabel MI, Tsang DCW, Ok YS. Biochar-induced changes in soil properties affected immobilization/mobilization of metals/metalloids in contaminated soils. Journal of Soils and Sediments 2017; 17: 717-730.

Ahmad M, Rajapaksha AU, Lim JE, Zhang M, Bolan N, Mohan D, et al. Biochar as a sorbent for contaminant management in soil and water: a review. Chemosphere 2014; 99: 19-33.

Alberts B, Johnson A, Lewis J, Raff M, Roberts K, Walter P. Molecular Biology of the Cell, 5th Edition. New York: Garland Science, 2008.

Alpers CN, Fleck JA, Marvin-DiPasquale M, Stricker CA, Stephenson M, Taylor HE. Mercury cycling in agricultural and managed wetlands, Yolo Bypass, California: spatial and seasonal variations in water quality. Science of The Total Environment 2014; 484: 276-87.

AMAP/UNEP. Technical Background Report for the Global Mercury Assessment. Arctic Monitoring and Assessment Programme/UNEP Chemicals Branch, Oslo, Norway/Geneva, Switzerland, 2013, pp. vi + 263.

Amde M, Yin Y, Zhang D, Liu J. Methods and recent advances in speciation analysis of mercury chemical species in environmental samples: a review. Chemical Speciation & Bioavailability 2016; 28: 51-65.

Antler G, Turchyn AV, Rennie V, Herut B, Sivan O. Coupled sulfur and oxygen isotope insight into bacterial sulfate reduction in the natural environment. Geochimica et Cosmochimica Acta 2013; 118: 98-117.

Arroyo-Abad U, Pfeifer M, Mothes S, Stark HJ, Piechotta C, Mattusch J, et al. Determination of moderately polar arsenolipids and mercury speciation in freshwater fish of the River Elbe (Saxony, Germany). Environ Pollut 2016; 208: 458-66.

Azevedo R, Rodriguez E. Phytotoxicity of Mercury in Plants: A Review. Journal of Botany 2012; 2012: 1-6.

Bachand PAM, Bachand SM, Fleck JA, Alpers CN, Stephenson M, Windham-Myers L. Reprint of "Methylmercury production in and export from agricultural wetlands in California, USA: The need to account for physical transport processes into and out of the root zone". Science of The Total Environment 2014; 484: 249-262.

Bakir F, Damluji SF, Amin-Zaki L, Murtadha M, Khalidi A, Al-Rawi NY, et al. Methylmercury Poisoning in Iraq. Science 1973; 181: 230-241.

Bargagli R. Moss and lichen biomonitoring of atmospheric mercury: A review. Sci Total Environ 2016; 572: 216-231.

Barkay T, Miller SM, Summers AO. Bacterial mercury resistance from atoms to ecosystems. FEMS Microbiology Reviews 2003; 27: 355-384.

Barkay T, Wagner - Döbler I. Microbial Transformations of Mercury: Potentials, Challenges, and Achievements in Controlling Mercury Toxicity in the Environment. Advances in Applied Microbiology. Volume 57. Academic Press, 2005, pp. 1-52.

Barrow NJ, Cox VC. The effects of pH and chloride concentration on mercury sorption. II. By a soil. Journal of Soil Science 1992; 43: 305-312.

BBodSchV. Federal Soil Protection and Contaminated Sites Ordinance (BBodSchV). In: Federal Government, editor. Federal Government, Bonn, 1999, pp. 60.

Beckers F, Rinklebe J. Cycling of mercury in the environment: Sources, fate, and human health implications: A review. Critical Reviews in Environmental Science and Technology 2017; 47: 693-794.

Beesley L, Moreno-Jimenez E, Gomez-Eyles JL. Effects of biochar and greenwaste compost amendments on mobility, bioavailability and toxicity of inorganic and organic contaminants in a multi-element polluted soil. Environ Pollut 2010; 158: 2282-7.

Beiyuan J, Awad YM, Beckers F, Tsang DC, Ok YS, Rinklebe J. Mobility and phytoavailability of As and Pb in a contaminated soil using pine sawdust biochar under systematic change of redox conditions. Chemosphere 2017; 178: 110-118.

Bertilsson L, Neujahr HY. Methylation of mercury compounds by methylcobalamin. Biochemistry 1971; 10: 2805-2808.

Biester H, Müller G, Schöler HF. Binding and mobility of mercury in soils contaminated by emissions from chlor-alkali plants. Science of the Total Environment 2002; 284: 191-203.

Birch HF. The effect of soil drying on humus decomposition and nitrogen availability. Plant and Soil 1958; 10: 9-31.

Blum JD, Sherman LS, Johnson MW. Mercury Isotopes in Earth and Environmental Sciences. Annual Review of Earth and Planetary Sciences 2014; 42: 249-269.

Blume H-P, Stahr K, Leinweber P. Bodenkundliches Praktikum. Eine Einführung in pedologisches Arbeiten für Ökologen, Land- und Forstwirte, Geo- und Umweltwissenschaftler. Heidelberg: Springer Spektrum, 2011.

Bohn HL. REDOX POTENTIALS. Soil Science 1971; 112: 39-45.

Bonnissel-Gissinger P, Alnot M, Lickes J-P, Ehrhardt J-J, Behra P. Modeling the Adsorption of Mercury(II) on (Hydr)oxides II: α-FeOOH (Goethite) and Amorphous Silica. J Colloid Interface Sci 1999; 215: 313-322.

Boon PI, Virtue P, Nichols PD. Microbial consortia in wetland sediments: a biomarker analysis of the effect of hydrological regime, vegetation and season on benthic microbes. Marine and Freshwater Research 1996; 47: 27.

Boschker HTS, de Graaf W, Köster M, Meyer-Reil LA, Cappenberg TE. Bacterial populations and processes involved in acetate and propionate consumption in anoxic brackish sediment. FEMS Microbiol Ecol 2001; 35: 97-103.

Bowman KL, Hammerschmidt CR, Lamborg CH, Swarr G. Mercury in the North Atlantic Ocean: The U.S. GEOTRACES zonal and meridional sections. Deep Sea Research Part II: Topical Studies in Oceanography 2015; 116: 251-261.

Boyd ES, Yu RQ, Barkay T, Hamilton TL, Baxter BK, Naftz DL, et al. Effect of salinity on mercury methylating benthic microbes and their activities in Great Salt Lake, Utah. Sci Total Environ 2017; 581-582: 495-506.

Bravo AG, Kothawala DN, Attermeyer K, Tessier E, Bodmer P, Ledesma JLJ, et al. The interplay between total mercury, methylmercury and dissolved organic matter in fluvial systems: A latitudinal study across Europe. Water Res 2018; 144: 172-182.

Brocke HJ, Wenzhoefer F, de Beer D, Mueller B, van Duyl FC, Nugues MM. High dissolved organic carbon release by benthic cyanobacterial mats in a Caribbean reef ecosystem. Sci Rep 2015; 5: 8852.

Bühring SI, Kamp A, Wörmer L, Ho S, Hinrichs K-U. Functional structure of laminated microbial sediments from a supratidal sandy beach of the German Wadden Sea (St. Peter-Ording). Journal of Sea Research 2014; 85: 463-473.

Burns DA, Aiken GR, Bradley PM, Journey CA, Schelker J. Specific ultra-violet absorbance as an indicator of mercury sources in an Adirondack River basin. Biogeochemistry 2013; 113: 451-466.

Burns DA, Riva-Murray K. Variation in fish mercury concentrations in streams of the Adirondack region, New York: A simplified screening approach using chemical metrics. Ecological Indicators 2018; 84: 648-661.

Cai Y, Jaffé R, Jones R. Ethylmercury in the Soils and Sediments of the Florida Everglades. Environ Sci Technol 1997; 31: 302-305.

Cassina L, Tassi E, Pedron F, Petruzzelli G, Ambrosini P, Barbafieri M. Using a plant hormone and a thioligand to improve phytoremediation of Hg-contaminated soil from a petrochemical plant. J Hazard Mater 2012; 231-232: 36-42.

Cesario R, Poissant L, Pilote M, O'Driscoll NJ, Mota AM, Canario J. Dissolved gaseous mercury formation and mercury volatilization in intertidal sediments. Sci Total Environ 2017; 603-604: 279-289.

Chadwick SP, Babiarz CL, Hurley JP, Armstrong DE. Importance of hypolimnetic cycling in aging of "new" mercury in a northern temperate lake. Sci Total Environ 2013; 448: 176-88.

Charlatchka R, Cambier P. Influence of Reducing Conditions on Solubility of Trace Metals in Contaminated Soils. Water, Air, and Soil Pollution 2000; 118: 143-168.

Chasar LC, Scudder BC, Stewart AR, Bell AH, Aiken GR. Mercury Cycling in Stream Ecosystems. 3. Trophic Dynamics and Methylmercury Bioaccumulation. Environ Sci Technol 2009; 43: 2733-2739.

Chen B, Wu Y, Guo X, He M, Hu B. Speciation of mercury in various samples from the micro-ecosystem of East Lake by hollow fiber-liquid-liquid-liquid microextraction-HPLC-ICP-MS. Journal of Analytical Atomic Spectrometry 2015; 30: 875-881.

Chen J, Hintelmann H, Zheng W, Feng X, Cai H, Wang Z, et al. Isotopic evidence for distinct sources of mercury in lake waters and sediments. Chemical Geology 2016; 426: 33-44.

Chen J, Wang C, Pan Y, Farzana SS, Tam NF. Biochar accelerates microbial reductive debromination of 2,2',4,4'-tetrabromodiphenyl ether (BDE-47) in anaerobic mangrove sediments. J Hazard Mater 2018; 341: 177-186.

Chen Y, Yin Y, Shi J, Liu G, Hu L, Liu J, et al. Analytical methods, formation, and dissolution of cinnabar and its impact on environmental cycle of mercury. Critical Reviews in Environmental Science and Technology 2017; 47: 2415-2447.

Chowdhury TR, Dick RP. Standardizing methylation method during phospholipid fatty acid analysis to profile soil microbial communities. J Microbiol Methods 2012; 88: 285-91.

Christensen GA, Somenahally AC, Moberly JG, Miller CM, King AJ, Gilmour CC, et al. Carbon Amendments Alter Microbial Community Structure and Net Mercury Methylation Potential in Sediments. Appl Environ Microbiol 2018; 84.

Churka Blum S, Lehmann J, Solomon D, Caires EF, Alleoni LRF. Sulfur forms in organic substrates affecting S mineralization in soil. Geoderma 2013; 200-201: 156-164.

Claus E, Kasimir P, John H-J, Möhlenkamp C, Becker B, Hillebrand G, et al. Untersuchung von Sedimenten in ausgewählten Staustufen, Nebenflüssen und Seitenstrukturen im Unterlauf der Saale. Hydrologie und Wasserbewirtschaftung 2015; 59: 305–317.

Clifford MJ, Hilson GM, Hodson ME. Tin and Mercury. In: Hooda PS, editor. Trace Elements in Soils. Blackwell Publishing Ltd., Chichester, 2010, pp. 497-513.

Comans RNJ, Middelburg JJ. Sorption of trace metals on calcite: Applicability of the surface precipitation model. Geochimica et Cosmochimica Acta 1987; 51: 2587-2591.

Compeau G, Bartha R. Methylation and demethylation of mercury under controlled redox, pH and salinity conditions. Appl Environ Microbiol 1984; 48: 1203-1207.

Compeau GC, Bartha R. Sulfate-Reducing Bacteria: Principal Methylators of Mercury in Anoxic Estuarine Sediment. Appl Environ Microbiol 1985; 50: 498-502.

Cooper RE, Eusterhues K, Wegner C-E, Totsche KU, Küsel K. Ferrihydrite-associated organic matter (OM) stimulates reduction by *Shewanella oneidensis* MR-1 and a complex microbial consortia. Biogeosciences 2017; 14: 5171-5188.

Cossa D, Averty B, Pirrone N. The origin of methylmercury in open Mediterranean waters. Limnology and Oceanography 2009; 54: 837-844.

Crump KL, Trudeau VL. Mercury-induced reproductive impairment in fish. Environmental Toxicology and Chemistry 2009; 28: 895-907.

Dadi T, Wendt-Potthoff K, Koschorreck M. Sediment resuspension effects on dissolved organic carbon fluxes and microbial metabolic potentials in reservoirs. Aquatic Sciences 2017; 79: 749-764.

DeLaune RD, Jugsujinda A, Devai I, Patrick WH. Relationship of Sediment Redox Conditions to Methyl Mercury in Surface Sediment of Louisiana Lakes. Journal of Environmental Science and Health, Part A 2004; 39: 1925-1933.

DeLaune RD, Reddy KR. REDOX POTENTIAL In: Hillel D, editor. Encyclopedia of Soils in the Environment. Elsevier, Oxford, 2005, pp. 366-371.

Derrien D, Plain C, Courty P-E, Gelhaye L, Moerdijk-Poortvliet TCW, Thomas F, et al. Does the addition of labile substrate destabilise old soil organic matter? Soil Biology and Biochemistry 2014; 76: 149-160.

Devai I, Patrick WH, Neue HU, DeLaune RD, Kongchum M, Rinklebe J. Methyl Mercury and Heavy Metal Content in Soils of Rivers Saale and Elbe (Germany). Analytical Letters 2005; 38: 1037-1048.

DIN EN 15933. Schlamm, behandelter Bioabfall und Boden – Bestimmung des pH-Werts. Deutsches Institut für Normung e. V., Berlin, 2012.

Dittman JA, Shanley JB, Driscoll CT, Aiken GR, Chalmers AT, Towse JE, et al. Mercury dynamics in relation to dissolved organic carbon concentration and quality during high flow events in three northeastern U.S. streams. Water Resources Research 2010; 46: n/a-n/a.

Dominique Y, Muresan B, Duran R, Richard S, Boudou A. Simulation of the Chemical Fate and Bioavailability of Liquid Elemental Mercury Drops from Gold Mining in Amazonian Freshwater Systems. Environ Sci Technol 2007; 41: 7322-7329.

Dong X, Ma LQ, Zhu Y, Li Y, Gu B. Mechanistic investigation of mercury sorption by Brazilian pepper biochars of different pyrolytic temperatures based on X-ray photoelectron spectroscopy and flow calorimetry. Environ Sci Technol 2013; 47: 12156-64.

Dorau K, Mansfeldt T. Comparison of redox potential dynamics in a diked marsh soil: 1990 to 1993versus2011 to 2014. Journal of Plant Nutrition and Soil Science 2016; 179: 641-651.

Dowling NJE, Widdel F, White DC. Phospholipid Ester-linked Fatty Acid Biomarkers of Acetate-oxidizing Sulphate-reducers and Other Sulphide-forming Bacteria. Microbiology 1986; 132: 1815-1825.

Dranguet P, Le Faucheur S, Slaveykova VI. Mercury bioavailability, transformations, and effects on freshwater biofilms. Environ Toxicol Chem 2017; 36: 3194-3205.

Dranguet P, Slaveykova VI, Le Faucheur S. Kinetics of mercury accumulation by freshwater biofilms. Environmental Chemistry 2018; 14: 458-467.

Duckworth OW, Rivera NA, Gardner TG, Andrews MY, Santelli CM, Polizzotto ML. Morphology, structure, and metal binding mechanisms of biogenic manganese oxides in

a superfund site treatment system. Environmental Science: Processes & Impacts 2017; 19: 50-58.

Dusek L, Svobodova Z, Janouskova D, Vykusova B, Jarkovsky J, Smid R, et al. Bioaccumulation of mercury in muscle tissue of fish in the Elbe River (Czech Republic): multispecies monitoring study 1991-1996. Ecotoxicol Environ Saf 2005; 61: 256-67.

Easton ZM, Rogers M, Davis M, Wade J, Eick M, Bock E. Mitigation of sulfate reduction and nitrous oxide emission in denitrifying environments with amorphous iron oxide and biochar. Ecological Engineering 2015; 82: 605-613.

Ebinghaus R, Kock HH, Jennings SG, McCartin P, Orren MJ. Measurements of atmospheric mercury concentrations in Northwestern and Central Europe — Comparison of experimental data and model results. Atmospheric Environment 1995; 29: 3333-3344.

Eckley CS, Blanchard P, McLennan D, Mintz R, Sekela M. Soil-Air Mercury Flux near a Large Industrial Emission Source before and after Closure (Flin Flon, Manitoba, Canada). Environ Sci Technol 2015; 49: 9750-7.

Edlund A, Nichols PD, Roffey R, White DC. Extractable and lipopolysaccharide fatty acid and hydroxy acid profiles from Desulfovibrio species. Journal of Lipid Research 1985; 26: 982-8.

Eisler R. Introduction. In: Eisler R, editor. Mercury Hazards to Living Organisms. CRC Press, 2006, pp. 3-9.

Ekström SM, Regnell O, Reader HE, Nilsson PA, Löfgren S, Kritzberg ES. Increasing concentrations of iron in surface waters as a consequence of reducing conditions in the catchment area. Journal of Geophysical Research: Biogeosciences 2016; 121: 479-493.

El-Naggar A, Shaheen SM, Ok YS, Rinklebe J. Biochar affects the dissolved and colloidal concentrations of Cd, Cu, Ni, and Zn and their phytoavailability and potential mobility in a mining soil under dynamic redox-conditions. Sci Total Environ 2018; 624: 1059-1071.

Elvert M, Boetius A, Knittel K, Jørgensen BB. Characterization of Specific Membrane Fatty Acids as Chemotaxonomic Markers for Sulfate-Reducing Bacteria Involved in Anaerobic Oxidation of Methane. Geomicrobiology Journal 2003; 20: 403-419.

Falandysz J. Mercury accumulation of three Lactarius mushroom species. Food Chem 2017; 214: 96-101.

Falandysz J, Zhang J, Wang Y, Krasinska G, Kojta A, Saba M, et al. Evaluation of the mercury contamination in mushrooms of genus Leccinum from two different regions of the world: Accumulation, distribution and probable dietary intake. Sci Total Environ 2015; 537: 470-8.

Fazlollahi F, Zarei MM, Habashi MS, Baxter LL. Method for Removal of Mercury from Oil Field Brine with Calcium Carbonate Co-precipitation. In: Carpenter JS, Bai C, Hwang J-Y, Ikhmayies S, Li B, Monteiro SN, et al., editors. Characterization of Minerals, Metals, and Materials 2014. John Wiley & Sons, Inc., Hoboken, 2014.

Feng S, Ai Z, Zheng S, Gu B, Li Y. Effects of Dryout and Inflow Water Quality on Mercury Methylation in a Constructed Wetland. Water, Air, & Soil Pollution 2014; 225.

Feng Y, Motta A, Reeves D, Burmester C, Van Santen E, Osborne J. Soil microbial communities under conventional-till and no-till continuous cotton systems. Soil Biology and Biochemistry 2003a; 35: 1693-1703.

Feng Y, Motta AC, Reeves DW, Burmester CH, van Santen E, Osborne JA. Soil microbial communities under conventional-till and no-till continuous cotton systems. Soil Biology and Biochemistry 2003b; 35: 1693-1703.

Feyte S, Gobeil C, Tessier A, Cossa D. Mercury dynamics in lake sediments. Geochimica et Cosmochimica Acta 2012; 82: 92-112.

Fike DA, Bradley AS, Rose CV. Rethinking the Ancient Sulfur Cycle. Annual Review of Earth and Planetary Sciences 2015; 43: 593-622.

Flanders JR, Turner RR, Morrison T, Jensen R, Pizzuto J, Skalak K, et al. Distribution, behavior, and transport of inorganic and methylmercury in a high gradient stream. Applied Geochemistry 2010; 25: 1756-1769.

Fleck JA, Gill G, Bergamaschi BA, Kraus TE, Downing BD, Alpers CN. Concurrent photolytic degradation of aqueous methylmercury and dissolved organic matter. Sci Total Environ 2014; 484: 263-75.

Fleming EJ, Mack EE, Green PG, Nelson DC. Mercury methylation from unexpected sources: molybdate-inhibited freshwater sediments and an iron-reducing bacterium. Appl Environ Microbiol 2006; 72: 457-64.

Fortmann L, Gay D, Wirtz K. ETHYLMERCURY: FORMATION IN PLANT TISSUES AND RELATION TO METHYLMERCURY FORMATION. EPA, Washington, D.C., 1978.

Frey B, Rieder SR. Response of forest soil bacterial communities to mercury chloride application. Soil Biology and Biochemistry 2013; 65: 329-337.

Fritsche J, Obrist D, Alewell C. Evidence of microbial control of Hg0emissions from uncontaminated terrestrial soils. Journal of Plant Nutrition and Soil Science 2008; 171: 200-209.

Fritsche J, Osterwalder S, Nilsson MB, Sagerfors J, Åkerblom S, Bishop K, et al. Evasion of Elemental Mercury from a Boreal Peatland Suppressed by Long-Term Sulfate Addition. Environmental Science & Technology Letters 2014; 1: 421-425.

Froelich PN, Klinkhammer GP, Bender ML, Luedtke NA, Heath GR, Cullen D, et al. Early oxidation of organic matter in pelagic sediments of the eastern equatorial Atlantic: suboxic diagenesis. Geochimica et Cosmochimica Acta 1979; 43: 1075-1090.

Frohne T, Diaz-Bone RA, Du Laing G, Rinklebe J. Impact of systematic change of redox potential on the leaching of Ba, Cr, Sr, and V from a riverine soil into water. Journal of Soils and Sediments 2015; 15: 623-633.

Frohne T, Rinklebe J. Biogeochemical Fractions of Mercury in Soil Profiles of Two Different Floodplain Ecosystems in Germany. Water, Air, & Soil Pollution 2013; 224.

Frohne T, Rinklebe J, Diaz-Bone RA. Contamination of Floodplain Soils along the Wupper River, Germany, with As, Co, Cu, Ni, Sb, and Zn and the Impact of Pre-definite Redox Variations on the Mobility of These Elements. Soil and Sediment Contamination: An International Journal 2014; 23: 779-799.

Frohne T, Rinklebe J, Diaz-Bone RA, Du Laing G. Controlled variation of redox conditions in a floodplain soil: Impact on metal mobilization and biomethylation of arsenic and antimony. Geoderma 2011; 160: 414-424.

Frohne T, Rinklebe J, Langer U, Du Laing G, Mothes S, Wennrich R. Biogeochemical factors affecting mercury methylation rate in two contaminated floodplain soils. Biogeosciences 2012; 9: 493-507.

Frostegård A, Bååth E. The use of phospholipid fatty acid analysis to estimate bacterial and fungal biomass in soil. Biology and Fertility of Soils 1996; 22: 59-65.

Frostegård Å, Tunlid A, Bååth E. Microbial biomass measured as total lipid phosphate in soils of different organic content. J Microbiol Methods 1991; 14: 151-163.

Frostegård Å, Tunlid A, Bååth E. Phospholipid Fatty Acid Composition, Biomass, and Activity of Microbial Communities from Two Soil Types Experimentally Exposed to Different Heavy Metals. Appl Environ Microbiol 1993; 59: 3605-3617.

Frostegård Å, Tunlid A, Bååth E. Use and misuse of PLFA measurements in soils. Soil Biology and Biochemistry 2011; 43: 1621-1625.

Gabriel MC, Williamson DG. Principal Biogeochemical Factors Affecting the Speciation And Transport of Mercury through the terrestrial environment. Environ Geochem Health 2004; 26: 421-434.

Gaida R, Radtke U. Schwermetalle in den Auensedimenten der Wupper. Decheniana 1990; 143: 434-445.

Galloway ME, Branfireun BA. Mercury dynamics of a temperate forested wetland. Science of the Total Environment 2004; 325: 239-254.

Giloteaux L, Duran R, Casiot C, Bruneel O, Elbaz-Poulichet F, Goni-Urriza M. Three-year survey of sulfate-reducing bacteria community structure in Carnoules acid mine drainage (France), highly contaminated by arsenic. FEMS Microbiol Ecol 2013; 83: 724-37.

Golding GR, Sparling R, Kelly CA. Effect of pH on intracellular accumulation of trace concentrations of Hg(II) in Escherichia coli under anaerobic conditions, as measured using a mer-lux bioreporter. Appl Environ Microbiol 2008; 74: 667-75.

Gorski PR, Armstrong DE, Hurley JP, Krabbenhoft DP. Influence of natural dissolved organic carbon on the bioavailability of mercury to a freshwater alga. Environ Pollut 2008; 154: 116-23.

Gosar M, Žibret G. Mercury contents in the vertical profiles through alluvial sediments as a reflection of mining in Idrija (Slovenia). Journal of Geochemical Exploration 2011; 110: 81-91.

Gray JE, Theodorakos PM, Fey DL, Krabbenhoft DP. Mercury concentrations and distribution in soil, water, mine waste leachates, and air in and around mercury mines in the Big Bend region, Texas, USA. Environ Geochem Health 2015; 37: 35-48.

Grigal DF. Mercury Sequestration in Forests and Peatlands. J Environ Qual 2003; 32: 393-405.

Gross R, Hauer B, Otto K, Schmid A. Microbial biofilms: new catalysts for maximizing productivity of long-term biotransformations. Biotechnol Bioeng 2007; 98: 1123-34.

Gruba P, Błońska E, Lasota J. Predicting the Concentration of Total Mercury in Mineral Horizons of Forest Soils Varying in Organic Matter and Mineral Fine Fraction Content. Water, Air, & Soil Pollution 2014; 225.

Grybos M, Davranche M, Gruau G, Petitjean P, Pédrot M. Increasing pH drives organic matter solubilization from wetland soils under reducing conditions. Geoderma 2009; 154: 13-19.

Guo X, Zheng C, Lu N. A density functional theory study of the adsorption of Hg and HgCl2 on a CaO(001) surface. Frontiers of Energy and Power Engineering in China 2007; 1: 101-104.

Gustin MS. Are mercury emissions from geologic sources significant? A status report. Science of The Total Environment 2003; 304: 153-167.

Gworek B, Bemowska-Kalabun O, Kijenska M, Wrzosek-Jakubowska J. Mercury in Marine and Oceanic Waters-a Review. Water Air Soil Pollut 2016; 227: 371.

Haitzer M, Aiken GR, Ryan JN. Binding of Mercury(II) to Dissolved Organic Matter: The Role of the Mercury-to-DOM Concentration Ratio. Environ Sci Technol 2002; 36: 3564-3570.

Hall BD, Aiken GR, Krabbenhoft DP, Marvin-Dipasquale M, Swarzenski CM. Wetlands as principal zones of methylmercury production in southern Louisiana and the Gulf of Mexico region. Environ Pollut 2008; 154: 124-34.

Hamelin S, Amyot M, Barkay T, Wang Y, Planas D. Methanogens: principal methylators of mercury in lake periphyton. Environ Sci Technol 2011; 45: 7693-700.

Han F. Biogeochemistry of Trace Elements in Arid Environments. Vol 13. Dordrecht: Springer, 2007.

Han FX, Su Y, Shi Z, Xia Y, Tian W, Philips V, et al. Mercury distribution and speciation in floodplain soils and uptake into native earthworms (Diplocardia spp.). Geoderma 2012; 170: 261-268.

Hang X, Gan F, Wang J, Chen X, Chen Y, Wang H, et al. Soil mercury accumulation and transference to different crop grains. Human and Ecological Risk Assessment: An International Journal 2016; 22: 1242-1252.

Hansel CM, Lentini CJ, Tang Y, Johnston DT, Wankel SD, Jardine PM. Dominance of sulfur-fueled iron oxide reduction in low-sulfate freshwater sediments. The ISME Journal 2015; 9: 2400-2412.

Hao OJ, Chen JM, Huang L, Buglass RL. Sulfate-reducing bacteria. Critical Reviews in Environmental Science and Technology 1996; 26: 155-187.

Hararuk O, Obrist D, Luo Y. Modelling the sensitivity of soil mercury storage to climate-induced changes in soil carbon pools. Biogeosciences 2013; 10: 2393-2407.

Hazen RM, Golden J, Downs RT, Hystad G, Grew ES, Azzolini D, et al. Mercury (Hg) mineral evolution: A mineralogical record of supercontinent assembly, changing ocean geochemistry, and the emerging terrestrial biosphere. American Mineralogist 2012; 97: 1013-1042.

HDOH. Hawaiian Islands Soil Metal Background Evaluation Report. In: Hawai‘i Department of Health, editor. HDOH, Honolulu, 2012.

He F, Wang W, Moon J-W, Howe J, Pierce EM, Liang L. Rapid Removal of Hg(II) from Aqueous Solutions Using Thiol-Functionalized Zn-Doped Biomagnetite Particles. ACS Appl Mater Interfaces 2012; 4: 4373-4379.

Heeraman DA, Claassen VP, Zasoski RJ. Interaction of lime, organic matter and fertilizer on growth and uptake of arsenic and mercury by Zorro fescue (Vulpia myuros L.). Plant and Soil 2001; 234: 215-231.

Hellal J, Guedron S, Huguet L, Schafer J, Laperche V, Joulian C, et al. Mercury mobilization and speciation linked to bacterial iron oxide and sulfate reduction: A column study to mimic reactive transfer in an anoxic aquifer. J Contam Hydrol 2015; 180: 56-68.

Hinkle SR, Bencala KE, Wentz DA, Krabbenhoft DP. Mercury and Methylmercury Dynamics in the Hyporheic Zone of an Oregon Stream. Water, Air, & Soil Pollution 2013; 225.

Hintelmann H. 11 Organomercurials. Their Formation and Pathways in the Environment. Organometallics in Environment and Toxicology: Metal Ions in Life Sciences. 7. The Royal Society of Chemistry, 2010, pp. 365-401.

Hintelmann H, Ebinghaus R, Wilken R-D. Accumulation of mercury(II) and methylmercury by microbial biofilms. Water Research 1993; 27: 237-242.

Hintelmann H, Wilken R-D. Levels of total mercury and methylmercury compounds in sediments of the polluted Elbe River: influence of seasonally and spatially varying environmental factors. Science of The Total Environment 1995; 166: 1-10.

Holmer M, Storkholm P. Sulphate reduction and sulphur cycling in lake sediments: a review. Freshwater Biology 2001; 46: 431-451.

Horowitz HM, Jacob DJ, Amos HM, Streets DG, Sunderland EM. Historical Mercury releases from commercial products: global environmental implications. Environ Sci Technol 2014; 48: 10242-50.

Hsu-Kim H, Kucharzyk KH, Zhang T, Deshusses MA. Mechanisms regulating mercury bioavailability for methylating microorganisms in the aquatic environment: a critical review. Environ Sci Technol 2013; 47: 2441-56.

Huang Y, Xia S, Lyu J, Tang J. Highly efficient removal of aqueous Hg2+ and CH3Hg+ by selective modification of biochar with 3-mercaptopropyltrimethoxysilane. Chemical Engineering Journal 2019; 360: 1646-1655.

Hunter D, Bomford RR, Russell DS. POISONING BY METHYL MERCURY COMPOUNDS. QJM: An International Journal of Medicine 1940; 9: 193-226.

Husson O. Redox potential (Eh) and pH as drivers of soil/plant/microorganism systems: a transdisciplinary overview pointing to integrative opportunities for agronomy. Plant and Soil 2013; 362: 389-417.

Hutson ND, Krzyzynska R, Srivastava RK. Simultaneous Removal of SO2, NOX, and Hg from Coal Flue Gas Using a NaClO2-Enhanced Wet Scrubber. Industrial & Engineering Chemistry Research 2008; 47: 5825-5831.

Hylander LD, Meili M. 500 years of mercury production: global annual inventory by region until 2000 and associated emissions. Science of The Total Environment 2003; 304: 13-27.

Igalavithana AD, Lee SE, Lee YH, Tsang DC, Rinklebe J, Kwon EE, et al. Heavy metal immobilization and microbial community abundance by vegetable waste and pine cone biochar of agricultural soils. Chemosphere 2017; 174: 593-603.

IMA. IMA Database of Mineral Properties. International Mineralogical Association, Available at http://rruff.info/ima/, 2018.

IUSS. World Reference Base for Soil Resources 2014, update 2015. International soil classification system for naming soils and creating legends for soil maps. FAO, Rome, 2015.

Janssen SE, Schaefer JK, Barkay T, Reinfelder JR. Fractionation of Mercury Stable Isotopes during Microbial Methylmercury Production by Iron- and Sulfate-Reducing Bacteria. Environ Sci Technol 2016; 50: 8077-83.

Jasinski SM. The materials flow of mercury in the United States. Resources, Conservation and Recycling 1995; 15: 145-179.

Jeevanaraj P, Hashim Z, Saliza ME, Zaharin Aris A. Mercury: A Review on the Target Organs and Toxic Effects. Asia Pacific Environmental and Occupational Health Journal 2016; 2: 1 - 5.

Jeong HY, Klaue B, Blum JD, Hayes KF. Sorption of Mercuric Ion by Synthetic Nanocrystalline Mackinawite (FeS). Environ Sci Technol 2007; 41: 7699-7705.

Jeremiason JD, Engstrom DR, Swain EB, Nater EA, Johnson BM, Almendinger JE, et al. Sulfate Addition Increases Methylmercury Production in an Experimental Wetland. Environ Sci Technol 2006; 40: 3800-3806.

Jernelöv A, Wennergren G. Studies of Concentrations of Methyl Mercury in Sediments from St. Clair System and Rate of Biological Methylation in Incubated Samples of Sediments. In: Luftvardsforsk IV, editor. Publ. B IVL 531, 1980.

Jiang L, Cai C, Zhang Y, Mao S, Sun Y, Li K, et al. Lipids of sulfate-reducing bacteria and sulfur-oxidizing bacteria found in the Dongsheng uranium deposit. Chinese Science Bulletin 2012; 57: 1311-1319.

Jiang T, Kaal J, Liang J, Zhang Y, Wei S, Wang D, et al. Composition of dissolved organic matter (DOM) from periodically submerged soils in the Three Gorges Reservoir areas as determined by elemental and optical analysis, infrared spectroscopy, pyrolysis-GC-MS and thermally assisted hydrolysis and methylation. Sci Total Environ 2017a; 603-604: 461-471.

Jiang T, Skyllberg U, Bjorn E, Green NW, Tang J, Wang D, et al. Characteristics of dissolved organic matter (DOM) and relationship with dissolved mercury in Xiaoqing River-Laizhou Bay estuary, Bohai Sea, China. Environ Pollut 2017b; 223: 19-30.

Jiménez-Moreno M, Perrot V, Epov VN, Monperrus M, Amouroux D. Chemical kinetic isotope fractionation of mercury during abiotic methylation of Hg(II) by methylcobalamin in aqueous chloride media. Chemical Geology 2013; 336: 26-36.

Johannesson KH, Neumann K. Geochemical cycling of mercury in a deep, confined aquifer: Insights from biogeochemical reactive transport modeling. Geochimica et Cosmochimica Acta 2013; 106: 25-43.

Jones DL, Rousk J, Edwards-Jones G, DeLuca TH, Murphy DV. Biochar-mediated changes in soil quality and plant growth in a three year field trial. Soil Biology and Biochemistry 2012; 45: 113-124.

Jurtshuk Jr. P. Chapter 4 Bacterial Metabolism. In: Baron S, editor. Medical Microbiology. University of Texas Medical Branch at Galveston, Galveston, 1996.

Kabata-Pendias A. Trace Elements in Soils and Plants. Boca Raton: CRC Press, 2011.

Kabata-Pendias A, Szteke B. Trace Elements in Abiotic and Biotic Environments. Boca Raton: CRC Press, 2015.

Kammann CI, Schmidt HP, Messerschmidt N, Linsel S, Steffens D, Muller C, et al. Plant growth improvement mediated by nitrate capture in co-composted biochar. Sci Rep 2015; 5: 11080.

Kao-Kniffin J, Zhu B. A microbial link between elevated CO2 and methane emissions that is plant species-specific. Microb Ecol 2013; 66: 621-9.

Karathanasis AD, Thompson YL, Barton CD. Long-Term Evaluations of Seasonally Saturated “Wetlands” in Western Kentucky Univ. of Kentucky Ag. Exp. Station Publ. #02-06-21. Soil Science Society of America Journal 2003; 67: 662-673.

Kiliç Ö. Impact of Physical Properties and Chemical Composition of Limestone on Decomposition Activation Energy. Asian Journal of Chemistry 2013; 25: 8116-8120.

Kim CS, Rytuba JJ, Brown GE. EXAFS study of mercury(II) sorption to Fe- and Al-(hydr)oxides. J Colloid Interface Sci 2004; 270: 9-20.

Kim MK, Lee YM, Zoh KD. Spatial and temporal variation of total mercury and methylmercury in lacustrine wetland in Korea. Environ Sci Pollut Res Int 2015; 22: 6578-89.

Kim Y, Ullah S, Moore TR, Roulet NT. Dissolved organic carbon and total dissolved nitrogen production by boreal soils and litter: the role of flooding, oxygen concentration, and temperature. Biogeochemistry 2014; 118: 35-48.

Klasson KT, Boihem LL, Uchimiya M, Lima IM. Influence of biochar pyrolysis temperature and post-treatment on the uptake of mercury from flue gas. Fuel Processing Technology 2014; 123: 27-33.

Klüpfel L, Keiluweit M, Kleber M, Sander M. Redox properties of plant biomass-derived black carbon (biochar). Environ Sci Technol 2014; 48: 5601-11.

Kodamatani H, Tomiyasu T. Selective determination method for measurement of methylmercury and ethylmercury in soil/sediment samples using high-performance liquid chromatography-chemiluminescence detection coupled with simple extraction technique. J Chromatogr A 2013; 1288: 155-9.

Kong H, He J, Gao Y, Wu H, Zhu X. Cosorption of phenanthrene and mercury(II) from aqueous solution by soybean stalk-based biochar. J Agric Food Chem 2011; 59: 12116-23.

Koschorreck M. Microbial sulphate reduction at a low pH. FEMS Microbiol Ecol 2008; 64: 329-42.

Kroppenstedt RM, Kutzner HJ. Biochemical taxonomy of some problem actinomycetes. Zentralbl. Bakteriol. Parasitenkd. Infektionskr. Hyg. Abt. I Orig. Suppl. 1978; 6: 125–133.

Krüger F. Hochwassergebundener Sediment- und Schadstoff-eintrag in die Auen der Mittelelbe. Institut für Ökologie. Leuphana Universität Lüneburg, Lüneburg, 2016.

Krüger O, Ebinghaus R, Kock HH, Richter-Politz I, Geilhufe C. Estimation of Gaseous Mercury Emissions in Germany: Inverse Modelling of Source Strengths at the

Contaminated Industrial Site BSL Werk Schkopau. In: Ebinghaus R, Turner RR, de Lacerda LD, Vasiliev O, Salomons W, editors. Mercury Contaminated Sites: Characterization, Risk Assessment and Remediation. Springer Berlin Heidelberg, Berlin, Heidelberg, 1999, pp. 377-392.

Kwon MJ, Boyanov MI, Antonopoulos DA, Brulc JM, Johnston ER, Skinner KA, et al. Effects of dissimilatory sulfate reduction on FeIII (hydr)oxide reduction and microbial community development. Geochimica et Cosmochimica Acta 2014; 129: 177-190.

Lalonde K, Mucci A, Ouellet A, Gelinas Y. Preservation of organic matter in sediments promoted by iron. Nature 2012; 483: 198-200.

Lambertsson L, Nilsson M. Organic Material: The Primary Control on Mercury Methylation and Ambient Methyl Mercury Concentrations in Estuarine Sediments. Environ Sci Technol 2006; 40: 1822-1829.

Langer U, Rinklebe J. Lipid biomarkers for assessment of microbial communities in floodplain soils of the Elbe River (Germany). Wetlands 2009; 29: 353-362.

Lavoie RA, Jardine TD, Chumchal MM, Kidd KA, Campbell LM. Biomagnification of mercury in aquatic food webs: a worldwide meta-analysis. Environ Sci Technol 2013; 47: 13385-94.

Lazaro WL, Diez S, da Silva CJ, Ignacio AR, Guimaraes JR. Waterscape determinants of net mercury methylation in a tropical wetland. Environ Res 2016; 150: 438-45.

Leclerc M, Planas D, Amyot M. Relationship between Extracellular Low-Molecular-Weight Thiols and Mercury Species in Natural Lake Periphytic Biofilms. Environ Sci Technol 2015; 49: 7709-16.

Lehnherr I. Methylmercury biogeochemistry: a review with special reference to Arctic aquatic ecosystems. Environmental Reviews 2014; 22: 229-243.

Leng G, Chen W, Wang Y. Speciation analysis of mercury in sediments using ionic-liquid-based vortex-assisted liquid-liquid microextraction combined with high-performance liquid chromatography and cold vapor atomic fluorescence spectrometry. J Sep Sci 2015; 38: 2684-91.

Leopold K, Foulkes M, Worsfold P. Methods for the determination and speciation of mercury in natural waters--a review. Anal Chim Acta 2010; 663: 127-38.

Lewicka-Szczebak D, Trojanowska A, Drzewicki W, Górka M, Jędrysek M-O, Jezierski P, et al. Sources and sinks of sulphate dissolved in lake water of a dam reservoir: S and O isotopic approach. Applied Geochemistry 2009; 24: 1941-1950.

Li H, Dong X, da Silva EB, de Oliveira LM, Chen Y, Ma LQ. Mechanisms of metal sorption by biochars: Biochar characteristics and modifications. Chemosphere 2017; 178: 466-478.

Li P, Hur J. Utilization of UV-Vis spectroscopy and related data analyses for dissolved organic matter (DOM) studies: A review. Critical Reviews in Environmental Science and Technology 2017; 47: 131-154.

Li Y-L, Vali H, Yang J, Phelps TJ, Zhang CL. Reduction of Iron Oxides Enhanced by a Sulfate-Reducing Bacterium and Biogenic H2S. Geomicrobiology Journal 2006; 23: 103-117.

Liang P, Lam C-L, Chen Z, Wang H-S, Shi J-B, Wu S-C, et al. Formation and distribution of methylmercury in sediments at a mariculture site: a mesocosm study. Journal of Soils and Sediments 2013; 13: 1301-1308.

Liem-Nguyen V. Determination of mercury chemical speciation in the presence of low molecular mass thiols and its importance for mercury methylation. Department of Chemistry. Umeå University, Umeå, 2016.

Lin TY, Kampalath RA, Lin CC, Zhang M, Chavarria K, Lacson J, et al. Investigation of mercury methylation pathways in biofilm versus planktonic cultures of Desulfovibrio desulfuricans. Environ Sci Technol 2013; 47: 5695-702.

Lindsay MBJ, Moncur MC, Bain JG, Jambor JL, Ptacek CJ, Blowes DW. Geochemical and mineralogical aspects of sulfide mine tailings. Applied Geochemistry 2015; 57: 157-177.

Liu J, Valsaraj KT, Devai I, DeLaune RD. Immobilization of aqueous Hg(II) by mackinawite (FeS). J Hazard Mater 2008; 157: 432-40.

Liu P, Ptacek CJ, Blowes DW, Berti WR, Landis RC. Aqueous leaching of organic acids and dissolved organic carbon from various biochars prepared at different temperatures. J Environ Qual 2015; 44: 684-95.

Liu P, Ptacek CJ, Blowes DW, Finfrock YZ, Gordon RA. Stabilization of mercury in sediment by using biochars under reducing conditions. J Hazard Mater 2017; 325: 120-128.

Liu P, Ptacek CJ, Blowes DW, Gould WD. Control of mercury and methylmercury in contaminated sediments using biochars: A long-term microcosm study. Applied Geochemistry 2018a; 92: 30-44.

Liu P, Ptacek CJ, Blowes DW, Landis RC. Mechanisms of mercury removal by biochars produced from different feedstocks determined using X-ray absorption spectroscopy. J Hazard Mater 2016; 308: 233-42.

Liu P, Ptacek CJ, Elena KMA, Blowes DW, Gould WD, Finfrock YZ, et al. Evaluation of mercury stabilization mechanisms by sulfurized biochars determined using X-ray absorption spectroscopy. J Hazard Mater 2018b; 347: 114-122.

Llop S, Murcia M, Aguinagalde X, Vioque J, Rebagliato M, Cases A, et al. Exposure to mercury among Spanish preschool children: trend from birth to age four. Environ Res 2014; 132: 83-92.

Lloyd-Jones PJ, Rangel-Mendez JR, Streat M. Mercury Sorption from Aqueous Solution by Chelating Ion Exchange Resins, Activated Carbon and a Biosorbent. Process Safety and Environmental Protection 2004; 82: 301-311.

Lodenius M. Use of plants for biomonitoring of airborne mercury in contaminated areas. Environ Res 2013; 125: 113-23.

Loginova K, Loginov M, Vorobiev E, Lebovka NI. Better lime purification of sugar beet juice obtained by low temperature aqueous extraction assisted by pulsed electric field. LWT - Food Science and Technology 2012; 46: 371-374.

Lohmayer R, Kappler A, Lösekann-Behrens T, Planer-Friedrich B. Sulfur Species as Redox Partners and Electron Shuttles for Ferrihydrite Reduction by Sulfurospirillum deleyianum. Appl Environ Microbiol 2014; 80: 3141-3149.

Londry KL, Jahnke LL, Des Marais DJ. Stable Carbon Isotope Ratios of Lipid Biomarkers of Sulfate-Reducing Bacteria. Appl Environ Microbiol 2004; 70: 745-751.

Longhi D, Bartoli M, Nizzoli D, Laini A, Viaroli P. Do oxic–anoxic transitions constrain organic matter mineralization in eutrophic freshwater wetlands? Hydrobiologia 2016; 774: 81-92.

Lovley DR, Giovannoni SJ, White DC, Champine JE, Phillips EJP, Gorby YA, et al. Geobacter metallireducens gen. nov. sp. nov., a microorganism capable of coupling the complete oxidation of organic compounds to the reduction of iron and other metals. Archives of Microbiology 1993; 159: 336-344.

LUA NRW. Gewässerstrukturgüte in Nordrhein-Westfalen. LUA NRW, Essen, 2005.

Lusilao-Makiese JG, Tessier E, Amouroux D, Tutu H, Chimuka L, Weiersbye I, et al. Mercury speciation and dispersion from an active gold mine at the West Wits area, South Africa. Environ Monit Assess 2016; 188: 47.

Macalady JL, Mack EE, Nelson DC, Scow KM. Sediment Microbial Community Structure and Mercury Methylation in Mercury-Polluted Clear Lake, California. Appl Environ Microbiol 2000; 66: 1479-1488.

MacDonald TC, Sylvain NJ, James AK, Pickering IJ, Krone PH, George GN. Effects of inorganic mercury on the olfactory pits of zebrafish larvae. Metallomics 2016; 8: 514-517.

Maier RM. Chapter 3 - Bacterial Growth. Environmental Microbiology (Second Edition). Academic Press, San Diego, 2009, pp. 37-54.

Manceau A, Lemouchi C, Enescu M, Gaillot AC, Lanson M, Magnin V, et al. Formation of Mercury Sulfide from Hg(II)-Thiolate Complexes in Natural Organic Matter. Environ Sci Technol 2015; 49: 9787-96.

Mancuso CA, Franzmann PD, Burton HR, Nichols PD. Microbial community structure and biomass estimates of a methanogenic Antarctic Lake ecosystem as determined by phospholipid analyses. Microb Ecol 1990; 19: 73-95.

Mansfeldt T. Redox potential of bulk soil and soil solution concentration of nitrate, manganese, iron, and sulfate in two Gleysols. Journal of Plant Nutrition and Soil Science 2004; 167: 7-16.

Mao Y, Yin Y, Li Y, Liu G, Feng X, Jiang G, et al. Occurrence of monoethylmercury in the Florida Everglades: identification and verification. Environ Pollut 2010; 158: 3378-84.

Marvin-DiPasquale M, Windham-Myers L, Agee JL, Kakouros E, Kieu le H, Fleck JA, et al. Methylmercury production in sediment from agricultural and non-agricultural wetlands in the Yolo Bypass, California, USA. Sci Total Environ 2014; 484: 288-99.

Matsuyama A, Yano S, Hisano A, Kindaichi M, Sonoda I, Tada A, et al. Distribution and characteristics of methylmercury in surface sediment in Minamata Bay. Mar Pollut Bull 2016; 109: 378-85.

Megaritis AG, Murphy BN, Racherla PN, Adams PJ, Pandis SN. Impact of climate change on mercury concentrations and deposition in the eastern United States. Sci Total Environ 2014; 487: 299-312.

Meija J, Yang L, Sturgeon RE, Mester Z. Certification of natural isotopic abundance inorganic mercury reference material NIMS-1 for absolute isotopic composition and atomic weight. Journal of Analytical Atomic Spectrometry 2010; 25: 384-389.

Meisner A, Bååth E, Rousk J. Microbial growth responses upon rewetting soil dried for four days or one year. Soil Biology and Biochemistry 2013; 66: 188-192.

Melgar MJ, Alonso J, Garcia MA. Mercury in edible mushrooms and underlying soil: bioconcentration factors and toxicological risk. Sci Total Environ 2009; 407: 5328-34.

Miao Z, Brusseau ML, Carroll KC, Carreon-Diazconti C, Johnson B. Sulfate reduction in groundwater: characterization and applications for remediation. Environ Geochem Health 2012; 34: 539-50.

MKULNV. Entwicklung und Stand der Abwasserbeseitigung in Nordrhein-Westfalen. Langfassung des Berichts mit ergänzender flußgebietsbezogener Darstellung der Abwasseranlagen und ihrer Einleitungen, Düsseldorf, 2014.

Mora A, Mahlknecht J, Baquero JC, Laraque A, Alfonso JA, Pisapia D, et al. Dynamics of dissolved major (Na, K, Ca, Mg, and Si) and trace (Al, Fe, Mn, Zn, Cu, and Cr) elements along the lower Orinoco River. Hydrological Processes 2017; 31: 597-611.

Moreau JW, Gionfriddo CM, Krabbenhoft DP, Ogorek JM, DeWild JF, Aiken GR, et al. The Effect of Natural Organic Matter on Mercury Methylation by Desulfobulbus propionicus 1pr3. Front Microbiol 2015; 6: 1389.

Morel FMM, Kraepiel AML, Amyot M. THE CHEMICAL CYCLE AND BIOACCUMULATION OF MERCURY. Annual Review of Ecology and Systematics 1998; 29: 543-566.

Morgan JJ. Kinetics of reaction between O2 and Mn(II) species in aqueous solutions. Geochimica et Cosmochimica Acta 2005; 69: 35-48.

Müller G, Furrer R. Die Belastung der Elbe mit Schwermetallen Erste Ergebnisse von Sedimentuntersuchungen. Naturwissenschaften 1994; 81: 401-405.

Munger ZW, Carey CC, Gerling AB, Hamre KD, Doubek JP, Klepatzki SD, et al. Effectiveness of hypolimnetic oxygenation for preventing accumulation of Fe and Mn in a drinking water reservoir. Water Res 2016; 106: 1-14.

Muyzer G, Stams AJ. The ecology and biotechnology of sulphate-reducing bacteria. Nat Rev Microbiol 2008; 6: 441-54.

Nagase H, Ose Y, Sato T, Ishikawa T. Mercury methylation by compounds in humic material. Science of The Total Environment 1984; 32: 147-156.

Nakamura M, Hachiya N, Murata KY, Nakanishi I, Kondo T, Yasutake A, et al. Methylmercury exposure and neurological outcomes in Taiji residents accustomed to consuming whale meat. Environ Int 2014; 68: 25-32.

Ngosong C, Raupp J, Richnow H-H, Ruess L. Tracking Collembola feeding strategies by the natural 13C signal of fatty acids in an arable soil with different fertilizer regimes. Pedobiologia 2011; 54: 225-233.

Niu Y, Qu R, Liu X, Mu L, Bu B, Sun Y, et al. Thiol-functionalized polysilsesquioxane as efficient adsorbent for adsorption of Hg(II) and Mn(II) from aqueous solution. Materials Research Bulletin 2014; 52: 134-142.

O'Driscoll NJ, Canário J, Crowell N, Webster T. Mercury Speciation and Distribution in Coastal Wetlands and Tidal Mudflats: Relationships with Sulphur Speciation and Organic Carbon. Water, Air, & Soil Pollution 2011; 220: 313-326.

Obrist D, Johnson DW, Lindberg SE, Luo Y, Hararuk O, Bracho R, et al. Mercury distribution across 14 U.S. Forests. Part I: spatial patterns of concentrations in biomass, litter, and soils. Environ Sci Technol 2011; 45: 3974-81.

Obrist D, Kirk JL, Zhang L, Sunderland EM, Jiskra M, Selin NE. A review of global environmental mercury processes in response to human and natural perturbations: Changes of emissions, climate, and land use. Ambio 2018; 47: 116-140.

Oude Elferink SJWH, Boschker HTS, Stams AJM. Identification of sulfate reducers andsyntrophobactersp. in anaerobic granular sludge by fatty-acid biomarkers and 16S rRNA probing. Geomicrobiology Journal 1998; 15: 3-17.

Overesch M, Rinklebe J, Broll G, Neue HU. Metals and arsenic in soils and corresponding vegetation at Central Elbe river floodplains (Germany). Environ Pollut 2007; 145: 800-12.

Pan F, Li Y, Chapman SJ, Yao H. Effect of rice straw application on microbial community and activity in paddy soil under different water status. Environ Sci Pollut Res Int 2016; 23: 5941-8.

Panda RK, Dhal JP, Mishra SC. Effect of sodium silicate on strengthening behaviour of fly ash compacts. International Journal of Current Research 2012; 4: 244-246.

Papadopoulos P, Rowell DL. The reactions of cadmium with calcium carbonate surfaces. Journal of Soil Science 1988; 39: 23-36.

Parkes RJ, Calder AG. The cellular fatty acids of three strains of Desulfobulbus, a propionate-utilising sulphate-reducing bacterium. FEMS Microbiology Letters 1985; 31: 361-363.

Parkes RJ, Dowling NJE, White DC, Herbert RA, Gibson GR. Characterization of sulphate-reducing bacterial populations within marine and estuarine sediments with different rates of sulphate reduction. FEMS Microbiology Letters 1993; 102: 235-250.

Parks JM, Johs A, Podar M, Bridou R, Hurt RA, Smith SD, et al. The Genetic Basis for Bacterial Mercury Methylation. Science 2013; 339: 1332-1335.

Pelcová P, Margetínová J, Vaculovič T, Komárek J, Kubáň V. Adsorption of mercury species on river sediments — effects of selected abiotic parameters. Open Chemistry 2010; 8.

Perrot V, Jimenez-Moreno M, Berail S, Epov VN, Monperrus M, Amouroux D. Successive methylation and demethylation of methylated mercury species (MeHg and DMeHg) induce mass dependent fractionation of mercury isotopes. Chemical Geology 2013; 355: 153-162.

Peter S, Isidorova A, Sobek S. Enhanced carbon loss from anoxic lake sediment through diffusion of dissolved organic carbon. Journal of Geophysical Research: Biogeosciences 2016; 121: 1959-1977.

Pezeshki SR, DeLaune RD. Soil oxidation-reduction in wetlands and its impact on plant functioning. Biology (Basel) 2012; 1: 196-221.

Picado F, Bengtsson G. Temporal and spatial distribution of waterborne mercury in a gold miner's river. Journal of Environmental Monitoring 2012; 14: 2746.

Poole LB. The basics of thiols and cysteines in redox biology and chemistry. Free Radic Biol Med 2015; 80: 148-57.

Poulin BA, Ryan JN, Aiken GR. Effects of iron on optical properties of dissolved organic matter. Environ Sci Technol 2014; 48: 10098-106.

Praharaj T, Fortin D. Seasonal variations of microbial sulfate and iron reduction in alkaline Pb–Zn mine tailings (Ontario, Canada). Applied Geochemistry 2008; 23: 3728-3740.

Qi F, Kuppusamy S, Naidu R, Bolan NS, Ok YS, Lamb D, et al. Pyrogenic Carbon and Its Role in Contaminant Immobilization in Soils. Critical Reviews in Environmental Science and Technology 2017: 00-00.

Randall PM, Yates BJ, Lal V, Darlington R, Fimmen R. In-situ subaqueous capping of mercury-contaminated sediments in a fresh-water aquatic system, Part II-evaluation of sorption materials. Environ Res 2013; 125: 41-51.

Ravichandran M. Interactions between mercury and dissolved organic matter--a review. Chemosphere 2004; 55: 319-31.

Ravichandran M, Aiken GR, Reddy MM, Ryan JN. Enhanced Dissolution of Cinnabar (Mercuric Sulfide) by Dissolved Organic Matter Isolated from the Florida Everglades. Environ Sci Technol 1998; 32: 3305-3311.

Reddy KR, DeLaune RD. Biogeochemical Characteristics. Biogeochemistry of Wetlands. CRC Press, 2008, pp. 27-65.

Reis AT, Rodrigues SM, Davidson CM, Pereira E, Duarte AC. Extractability and mobility of mercury from agricultural soils surrounding industrial and mining contaminated areas. Chemosphere 2010; 81: 1369-77.

Remy S, Prudent P, Probst J-L. Mercury speciation in soils of the industrialised Thur River catchment (Alsace, France). Applied Geochemistry 2006; 21: 1855-1867.

Rinklebe J, During A, Overesch M, Du Laing G, Wennrich R, Stärk HJ, et al. Dynamics of mercury fluxes and their controlling factors in large Hg-polluted floodplain areas. Environ Pollut 2010; 158: 308-18.

Rinklebe J, During A, Overesch M, Wennrich R, Stärk H-J, Mothes S, et al. Optimization of a simple field method to determine mercury volatilization from soils—Examples of 13 sites in floodplain ecosystems at the Elbe River (Germany). Ecological Engineering 2009; 35: 319-328.

Rinklebe J, Langer U. Microbial diversity in three floodplain soils at the Elbe River (Germany). Soil Biology and Biochemistry 2006; 38: 2144-2151.

Rinklebe J, Langer U. Soil Microbial Biomass and Phospholipid Fatty Acids. In: DeLaune RD, Reddy KR, Richardson CJ, Megonigal JP, editors. Methods in Biogeochemistry of Wetlands. Soil Science Society of America, Madison, WI, 2013, pp. 331-348.

Rinklebe J, Shaheen SM, Frohne T. Amendment of biochar reduces the release of toxic elements under dynamic redox conditions in a contaminated floodplain soil. Chemosphere 2016a; 142: 41-7.

Rinklebe J, Shaheen SM, Yu K. Release of As, Ba, Cd, Cu, Pb, and Sr under pre-definite redox conditions in different rice paddy soils originating from the U.S.A. and Asia. Geoderma 2016b; 270: 21-32.

Rinklebe J, Stubbe A, Overesch M, Neue H-U. Quantifizierung der Quecksilberausgasung aus Auenböden der Elbe. Helmholtz-Zentrum für Umweltforschung GmbH - UFZ, Halle (Saale), 2007, pp. 84.

Robinson JB, Tuovinen OH. Mechanisms of microbial resistance and detoxification of mercury and organomercury compounds: physiological, biochemical, and genetic analyses. Microbiological Reviews 1984; 48: 95-124.

Roden EE. Fe(III) Oxide Reactivity Toward Biological versus Chemical Reduction. Environ Sci Technol 2003; 37: 1319-1324.

Rogers RD. Abiological Methylation of Mercury in Soil. J Environ Qual 1977; 6: 463-467.

Rolfe MD, Rice CJ, Lucchini S, Pin C, Thompson A, Cameron AD, et al. Lag phase is a distinct growth phase that prepares bacteria for exponential growth and involves transient metal accumulation. J Bacteriol 2012; 194: 686-701.

Rothenberg SE, Feng X, Zhou W, Tu M, Jin B, You J. Environment and genotype controls on mercury accumulation in rice (Oryza sativa L.) cultivated along a contamination gradient in Guizhou, China. Sci Total Environ 2012; 426: 272-80.

Roulet M, Guimarães J-RD, Lucotte M. Methylmercury Production and Accumulation in Sediments and Soils of an Amazonian Floodplain – Effect of Seasonal Inundation. Water, Air, and Soil Pollution 2001; 128: 41-60.

Rubino FM. Toxicity of Glutathione-Binding Metals: A Review of Targets and Mechanisms. Toxics 2015; 3: 20-62.

Rytuba JJ. Mercury mine drainage and processes that control its environmental impact. Science of The Total Environment 2000; 260: 57-71.

Sarkar D, Essington ME, Misra KC. Adsorption of Mercury(II) by Variable Charge Surfaces of Quartz and Gibbsite Contribution from the Dep. of Plant and Soil Sciences, The Univ. of Tennessee. Soil Science Society of America Journal 1999; 63: 1626-1636.

Sarsam SI, Al Saidi AA, Al Taie AH. Influence of Combined Stabilization on the Structural Properties of Subgrade Soil. Journal of Geotechnical Engineering 2017; 4: 13–24.

Sasmaz E, Wilcox J. Mercury Species and SO2 Adsorption on CaO(100). The Journal of Physical Chemistry C 2008; 112: 16484-16490.

Satoh H. CHAPTER 5 Mercury. Aging and Vulnerability to Environmental Chemicals: Age-related Disorders and Their Origins in Enviromental Exposures. The Royal Society of Chemistry, 2013, pp. 125-150.

Schaller J, Böttger R, Dudel G, Ruess L. Reed litter Si content affects microbial community structure and the lipid composition of an invertebrate shredder during aquatic decomposition. Limnologica - Ecology and Management of Inland Waters 2016; 57: 14-22.

Schenk R. Verteilung und Dynamik von Schwermetallen in Sedimenten der Wupper. Heinrich-Heine Universität, Düsseldorf, 1994, pp. 229.

Schenk R, Gaida R. Die Belastung der Sedimente der Wupper (von Wuppertal-Buchenhofen bis zur Mündung) mit Schwermetallen. Natur am Niederrhein 1994; 9: 57-67.

Schinkel W. Erste Erfahrungen beim Einsatz von Falisan-Universal-Flüssigbeize (FL 398) unter praktischen Bedingungen. Archives Of Phytopathology And Plant Protection 1985; 21: 383-401.

Schlüter K. Review: evaporation of mercury from soils. An integration and synthesis of current knowledge. Environmental Geology 2000; 39: 249-271.

Schoug A, Fischer J, Heipieper HJ, Schnurer J, Hakansson S. Impact of fermentation pH and temperature on freeze-drying survival and membrane lipid composition of Lactobacillus coryniformis Si3. J Ind Microbiol Biotechnol 2008; 35: 175-81.

Schroeder WH, Munthe J. Atmospheric mercury—An overview. Atmospheric Environment 1998; 32: 809-822.

Schuster E. The behavior of mercury in soil with special emphasis of complexation and adsorption processes—A review of the literature. Water, Air, Soil Pollut. 1991; 56: 667.

Selvendiran P, Driscoll CT, Bushey JT, Montesdeoca MR. Wetland influence on mercury fate and transport in a temperate forested watershed. Environ Pollut 2008; 154: 46-55.

Shaheen SM, Rinklebe J. Impact of emerging and low cost alternative amendments on the (im)mobilization and phytoavailability of Cd and Pb in a contaminated floodplain soil. Ecological Engineering 2015; 74: 319-326.

Shaheen SM, Rinklebe J. Sugar beet factory lime affects the mobilization of Cd, Co, Cr, Cu, Mo, Ni, Pb, and Zn under dynamic redox conditions in a contaminated floodplain soil. J Environ Manage 2017; 186: 253-260.

Shaheen SM, Rinklebe J, Frohne T, White JR, DeLaune RD. Redox effects on release kinetics of arsenic, cadmium, cobalt, and vanadium in Wax Lake Deltaic freshwater marsh soils. Chemosphere 2016; 150: 740-8.

Shaheen SM, Rinklebe J, Selim MH. Impact of various amendments on immobilization and phytoavailability of nickel and zinc in a contaminated floodplain soil. International Journal of Environmental Science and Technology 2015; 12: 2765-2776.

Shao D, Kang Y, Wu S, Wong MH. Effects of sulfate reducing bacteria and sulfate concentrations on mercury methylation in freshwater sediments. Sci Total Environ 2012; 424: 331-6.

Shen B, Tian L, Li F, Zhang X, Xu H, Singh S. Elemental mercury removal by the modified bio-char from waste tea. Fuel 2017; 187: 189-196.

Sherman LS, Blum JD, Dvonch JT, Gratz LE, Landis MS. The use of Pb, Sr, and Hg isotopes in Great Lakes precipitation as a tool for pollution source attribution. Sci Total Environ 2015; 502C: 362-374.

Shu R, Dang F, Zhong H. Effects of incorporating differently-treated rice straw on phytoavailability of methylmercury in soil. Chemosphere 2016a; 145: 457-63.

Shu R, Wang Y, Zhong H. Biochar amendment reduced methylmercury accumulation in rice plants. J Hazard Mater 2016b; 313: 1-8.

Siegel SM, Siegel BZ, Barghigiani C, Aratani K, Penny P, Penny D. A contribution to the environmental biology of mercury accumulation in plants. Water, Air, and Soil Pollution 1987; 33: 65-72.

Sigler JM, Lee X. Gaseous mercury in background forest soil in the northeastern United States. Journal of Geophysical Research 2006; 111.

Singh B, Rengel Z, Bowden JW. Carbon, nitrogen and sulphur cycling following incorporation of canola residue of different sizes into a nutrient-poor sandy soil. Soil Biology and Biochemistry 2006; 38: 32-42.

Šípková A, Száková J, Hanč A, Tlustoš P. Mobility of mercury in soil as affected by soil physicochemical properties. Journal of Soils and Sediments 2016; 16: 2234-2241.

Skyllberg U. Chapter 13 - Mercury Biogeochemistry in Soils and Sediments. In: Balwant S, Markus G, editors. Developments in Soil Science. Volume 34. Elsevier, 2010, pp. 379-410.

Skyllberg U. Chemical Speciation of Mercury in Soil and Sediment. Environmental Chemistry and Toxicology of Mercury. John Wiley & Sons, Inc., 2012, pp. 219-258.

Skyllberg U, Bloom PR, Qian J, Lin C-M, Bleam WF. Complexation of Mercury(II) in Soil Organic Matter: EXAFS Evidence for Linear Two-Coordination with Reduced Sulfur Groups. Environ Sci Technol 2006; 40: 4174-4180.

Skyllberg U, Qian J, Frech W, Xia K, Bleam WF. Distribution of mercury, methyl mercury and organic sulphur species in soil, soil solution and stream of a boreal forest catchment. Biogeochemistry 2003; 64: 53-76.

Smith GA, Nichols PD, White DC. Fatty acid composition and microbial activity of benthic marine sediment from McMurdo Sound, Antarctica. FEMS Microbiology Letters 1986; 38: 219-231.

Song X, Ye M, Tang X, Wang C. Ionic liquids dispersive liquid-liquid microextraction and HPLC-atomic fluorescence spectrometric determination of mercury species in environmental waters. J Sep Sci 2013; 36: 414-20.

Song Y, Jiang T, Liem-Nguyen V, Sparrman T, Bjorn E, Skyllberg U. Thermodynamics of Hg(II) Bonding to Thiol Groups in Suwannee River Natural Organic Matter Resolved

by Competitive Ligand Exchange, Hg LIII-Edge EXAFS and (1)H NMR Spectroscopy. Environ Sci Technol 2018; 52: 8292-8301.

Stein ED, Cohen Y, Winer AM. Environmental distribution and transformation of mercury compounds. Critical Reviews in Environmental Science and Technology 1996; 26: 1-43.

Stoor RW, Hurley JP, Babiarz CL, Armstrong DE. Subsurface sources of methyl mercury to Lake Superior from a wetland-forested watershed. Sci Total Environ 2006; 368: 99-110.

Strickman RJ, Mitchell CPJ. Mercury methylation in stormwater retention ponds at different stages in the management lifecycle. Environmental Science: Processes & Impacts 2018; 20: 595-606.

Sun Q, Meyer WS, Koerber GR, Marschner P. Response of respiration and nutrient availability to drying and rewetting in soil from a semi-arid woodland depends on vegetation patch and a recent wildfire. Biogeosciences 2015; 12: 5093-5101.

Sunderland EM, Gobas FAPC, Branfireun BA, Heyes A. Environmental controls on the speciation and distribution of mercury in coastal sediments. Marine Chemistry 2006; 102: 111-123.

Sundh I, Nilsson M, Borga P. Variation in microbial community structure in two boreal peatlands as determined by analysis of phospholipid Fatty Acid profiles. Appl Environ Microbiol 1997; 63: 1476-82.

Swaton T. Böden, Schwermetallbelastung und Gefährdungspotential im NSG Biberwerder (Biosphärenreservat Mittlere Elbe). Institut für Bodenkunde und Pflanzenernährung. Martin-Luther-Universität Halle-Wittenberg, Halle (Saale), 2001, pp. 143.

Swaton T, Rinklebe J, Tanneberg H, Jahn R. Verteilungsmuster von Quecksilber und Zink in Auenböden des Saale-Eibe-Winkels. Mitteilungen der Deutschen Bodenkundlichen Gesellschaft 2003; 102: 593-594.

Takeno N. Atlas of Eh-pH diagrams. Intercomparison of thermodynamic databases In: Technology NIoAISa, editor. Open File Report No.419. Geological Survey of Japan, 2005.

Taube F, Pommer L, Larsson T, Shchukarev A, Nordin A. Soil Remediation – Mercury Speciation in Soil and Vapor Phase During Thermal Treatment. Water, Air, and Soil Pollution 2008; 193: 155-163.

Tiffreau C, Lützenkirchen J, Behra P. Modeling the Adsorption of Mercury(II) on (Hydr)oxides: I. Amorphous Iron Oxide and α-Quartz. J Colloid Interface Sci 1995; 172: 82-93.

Tipping E, Lofts S, Hooper H, Frey B, Spurgeon D, Svendsen C. Critical Limits for Hg(II) in soils, derived from chronic toxicity data. Environ Pollut 2010; 158: 2465-71.

Tjerngren I, Karlsson T, Björn E, Skyllberg U. Potential Hg methylation and MeHg demethylation rates related to the nutrient status of different boreal wetlands. Biogeochemistry 2012a; 108: 335-350.

Tjerngren I, Meili M, Bjorn E, Skyllberg U. Eight boreal wetlands as sources and sinks for methyl mercury in relation to soil acidity, C/N ratio, and small-scale flooding. Environ Sci Technol 2012b; 46: 8052-60.

Tsui MT, Finlay JC. Influence of dissolved organic carbon on methylmercury bioavailability across Minnesota stream ecosystems. Environ Sci Technol 2011; 45: 5981-7.

U.S. EPA. National Primary Drinking Water Regulations. In: U.S. Environmental Protection Agency, editor, 2009.

U.S. EPA Method 1631 RE. Mercury in Water by Oxidation, Purge and Trap, and Cold Vapor Atomic Fluorescence Spectrometry, 2002.

U.S. EPA Method 3051A. Method 3051A. Microwave Assisted Acid Digestion of Sediments, Sludges, Soils, and Oils, 2007.

UIT. Informationsblätter - Geräte- und Produktbezeichnungen. Umwelt- und Ingenieurtechnik GmbH Dresden, 2002.

Ullah A, Heng S, Munis MFH, Fahad S, Yang X. Phytoremediation of heavy metals assisted by plant growth promoting (PGP) bacteria: A review. Environmental and Experimental Botany 2015; 117: 28-40.

Ullrich SM, Tanton TW, Abdrashitova SA. Mercury in the Aquatic Environment: A Review of Factors Affecting Methylation. Critical Reviews in Environmental Science and Technology 2001; 31: 241-293.

UNEP. Summary of supply, trade and demand information on mercury, Geneva, 2006.

UNEP. Minamata Convention on Mercury. UN Publishing, Geneva, 2013, pp. 69.

Vainshtein M, Hippe H, Kroppenstedt RM. Cellular Fatty Acid Composition of Desulfovibrio Species and Its Use in Classification of Sulfate-reducing Bacteria. Systematic and Applied Microbiology 1992; 15: 554-566.

Vestal JR, White DC. Lipid Analysis in Microbial Ecology. BioScience 1989; 39: 535-541.

Vetter A, Mangelsdorf K, Wolfgramm M, Rauppach K, Schettler G, Vieth-Hillebrand A. Variations in fluid chemistry and membrane phospholipid fatty acid composition of the

bacterial community in a cold storage groundwater system during clogging events. Applied Geochemistry 2012; 27: 1278-1290.

Wallschläger D, Desai MVM, Spengler M, Wilken R. Mercury Speciation in Floodplain Soils and Sediments along a Contaminated River Transect. J. Environ. Qual. 1998a; 27: 1034-1044.

Wallschläger D, Desai MVM, Spengler M, Windmöller CC, Wilken R. How humic substances dominate mercury geochemistry in contaminated floodplain soils and sediments. J. Environ. Qual. 1998b; 27: 1044-1054.

Wallschläger D, Desai MVM, Wilken R-D. The role of humic substances in the aqueous mobilization of mercury from contaminated floodplain soils. Water, Air, and Soil Pollution 1996; 90: 507-520.

Wang J, Feng X, Anderson CW, Xing Y, Shang L. Remediation of mercury contaminated sites - A review. J Hazard Mater 2012; 221-222: 1-18.

Wang J, Feng X, Anderson CWN, Wang H, Wang L. Thiosulphate-induced mercury accumulation by plants: metal uptake and transformation of mercury fractionation in soil - results from a field study. Plant and Soil 2013; 375: 21-33.

Wang Q, Kim D, Dionysiou DD, Sorial GA, Timberlake D. Sources and remediation for mercury contamination in aquatic systems--a literature review. Environ Pollut 2004; 131: 323-36.

Wang Y, Schaefer JK, Mishra B, Yee N. Intracellular Hg(0) Oxidation in Desulfovibrio desulfuricans ND132. Environ Sci Technol 2016.

Washburn SJ, Blum JD, Demers JD, Kurz AY, Landis RC. Isotopic Characterization of Mercury Downstream of Historic Industrial Contamination in the South River, Virginia. Environ Sci Technol 2017; 51: 10965-10973.

Weber JH. Review of possible paths for abiotic methylation of mercury(II) in the aquatic environment. Chemosphere 1993; 26: 2063-2077.

Weishaar JL, Aiken GR, Bergamaschi BA, Fram MS, Fujii R, Mopper K. Evaluation of Specific Ultraviolet Absorbance as an Indicator of the Chemical Composition and Reactivity of Dissolved Organic Carbon. Environ Sci Technol 2003; 37: 4702-4708.

White D, Stair J, Ringelberg D. Quantitative comparisons ofin situ microbial biodiversity by signature biomarker analysis. Journal of Industrial Microbiology 1996; 17: 185-196.

White DC, Davis WM, Nickels JS, King JD, Bobbie RJ. Determination of the sedimentary microbial biomass by extractible lipid phosphate. Oecologia 1979; 40: 51-62.

Wichern M, Kehl O, Erbe V, Luebken M, Wilderer PA. Modelling COD and N removal in the water and in the benthic biofilm for the River Wupper in Germany. Water Science and Technology 2006; 53: 163-171.

Wilhelm SM. Estimate of Mercury Emissions to the Atmosphere from Petroleum. Environ Sci Technol 2001; 35: 4704-4710.

Willers C, Jansen van Rensburg PJ, Claassens S. Phospholipid fatty acid profiling of microbial communities--a review of interpretations and recent applications. J Appl Microbiol 2015; 119: 1207-18.

Windham-Myers L, Marvin-Dipasquale M, Krabbenhoft DP, Agee JL, Cox MH, Heredia-Middleton P, et al. Experimental removal of wetland emergent vegetation leads to decreased methylmercury production in surface sediment. Journal of Geophysical Research 2009; 114.

Wouters MA, Fan SW, Haworth NL. Disulfides as Redox Switches: From Molecular Mechanisms to Functional Significance. Antioxidants & Redox Signaling 2010; 12: 53-91.

Xia K, Skyllberg UL, Bleam WF, Bloom PR, Nater EA, Helmke PA. X-ray Absorption Spectroscopic Evidence for the Complexation of Hg(II) by Reduced Sulfur in Soil Humic Substances. Environ Sci Technol 1999; 33: 257-261.

Xia S, Huang Y, Tang J, Wang L. Preparation of various thiol-functionalized carbon-based materials for enhanced removal of mercury from aqueous solution. Environmental Science and Pollution Research 2019.

Xu J, Bravo AG, Lagerkvist A, Bertilsson S, Sjoblom R, Kumpiene J. Sources and remediation techniques for mercury contaminated soil. Environ Int 2015; 74C: 42-53.

Xu J, Kleja DB, Biester H, Lagerkvist A, Kumpiene J. Influence of particle size distribution, organic carbon, pH and chlorides on washing of mercury contaminated soil. Chemosphere 2014; 109: 99-105.

Xu L, Baldocchi DD, Tang J. How soil moisture, rain pulses, and growth alter the response of ecosystem respiration to temperature. Global Biogeochemical Cycles 2004; 18: n/a-n/a.

Xu X, Schierz A, Xu N, Cao X. Comparison of the characteristics and mechanisms of Hg(II) sorption by biochars and activated carbon. J Colloid Interface Sci 2016; 463: 55-60.

Yang J, Zhao Y, Ma S, Zhu B, Zhang J, Zheng C. Mercury Removal by Magnetic Biochar Derived from Simultaneous Activation and Magnetization of Sawdust. Environ Sci Technol 2016; 50: 12040-12047.

Yin R, Feng X, Li X, Yu B, Du B. Trends and advances in mercury stable isotopes as a geochemical tracer. Trends in Environmental Analytical Chemistry 2014; 2: 1-10.

Yin R, Feng X, Wang J, Bao Z, Yu B, Chen J. Mercury isotope variations between bioavailable mercury fractions and total mercury in mercury contaminated soil in Wanshan Mercury Mine, SW China. Chemical Geology 2013; 336: 80-86.

Yin R, Feng X, Zhang J, Pan K, Wang W, Li X. Using mercury isotopes to understand the bioaccumulation of Hg in the subtropical Pearl River Estuary, South China. Chemosphere 2016; 147: 173-9.

Yin Y, Allen HE, Li Y, Huang CP, Sanders PF. Adsorption of Mercury(II) by Soil: Effects of pH, Chloride, and Organic Matter. J Environ Qual 1996; 25: 837-844.

Yoon S-J, Diener LM, Bloom PR, Nater EA, Bleam WF. X-ray absorption studies of CH3Hg+-binding sites in humic substances. Geochimica et Cosmochimica Acta 2005; 69: 1111-1121.

Yu K, Böhme F, Rinklebe J, Neue H-U, DeLaune RD. Major Biogeochemical Processes in Soils-A Microcosm Incubation from Reducing to Oxidizing Conditions. Soil Science Society of America Journal 2007; 71: 1406.

Yu K, Rinklebe J. Advancement in soil microcosm apparatus for biogeochemical research. Ecological Engineering 2011; 37: 2071-2075.

Yu S, Ehrenfeld JG. Relationships among plants, soils and microbial communities along a hydrological gradient in the New Jersey Pinelands, USA. Ann Bot 2010; 105: 185-96.

Zerling L, Hanisch C, Junge FW, Müller A. Heavy Metals in Saale Sediments— Changes in the Contamination since 1991. Acta hydrochimica et hydrobiologica 2003; 31: 368-377.

Zhang CL, Huang Z, Li Y-L, Romanek CS, Mills GL, Gibson RA, et al. Lipid Biomarkers, Carbon Isotopes, and Phylogenetic Characterization of Bacteria in California and Nevada Hot Springs. Geomicrobiology Journal 2007; 24: 519-534.

Zhang H, Holmes CD, Wu S. Impacts of changes in climate, land use and land cover on atmospheric mercury. Atmospheric Environment 2016; 141: 230-244.

Zhang H, Lindberg SE, Marsik FJ, Keeler GJ. Mercury Air/Surface Exchange Kinetics of Background Soils of the Tahquamenon River Watershed in the Michigan Upper Peninsula. Water, Air, and Soil Pollution 2001; 126: 151-169.

Zhang H, Yin RS, Feng XB, Sommar J, Anderson CW, Sapkota A, et al. Atmospheric mercury inputs in montane soils increase with elevation: evidence from mercury isotope signatures. Sci Rep 2013; 3: 3322.

Zhao DY, Ma T, Zeng J, Yan WM, Jiang CL, Feng JW, et al. Phospholipid fatty acids analysis of the vertical distribution of microbial communities in eutrophic lake sediments. International Journal of Environmental Science & Technology 2011; 8: 571-580.

Zheng Y, Jensen AD, Windelin C, Jensen F. Review of technologies for mercury removal from flue gas from cement production processes. Progress in Energy and Combustion Science 2012; 38: 599-629.

Zhu H, Zhong H, Evans D, Hintelmann H. Effects of rice residue incorporation on the speciation, potential bioavailability and risk of mercury in a contaminated paddy soil. J Hazard Mater 2015; 293: 64-71.

Zhu W, Song Y, Adediran GA, Jiang T, Reis AT, Pereira E, et al. Mercury transformations in resuspended contaminated sediment controlled by redox conditions, chemical speciation and sources of organic matter. Geochimica et Cosmochimica Acta 2018; 220: 158-179.

Zumrawi MME, Hamza OSM. Improving the Characteristics of Expansive Subgrade Soils Using Lime and Fly Ash. International Journal of Science and Research 2014; 3: 1124-1129.

Appendix

Appendix A: Supporting information for Chapter 4

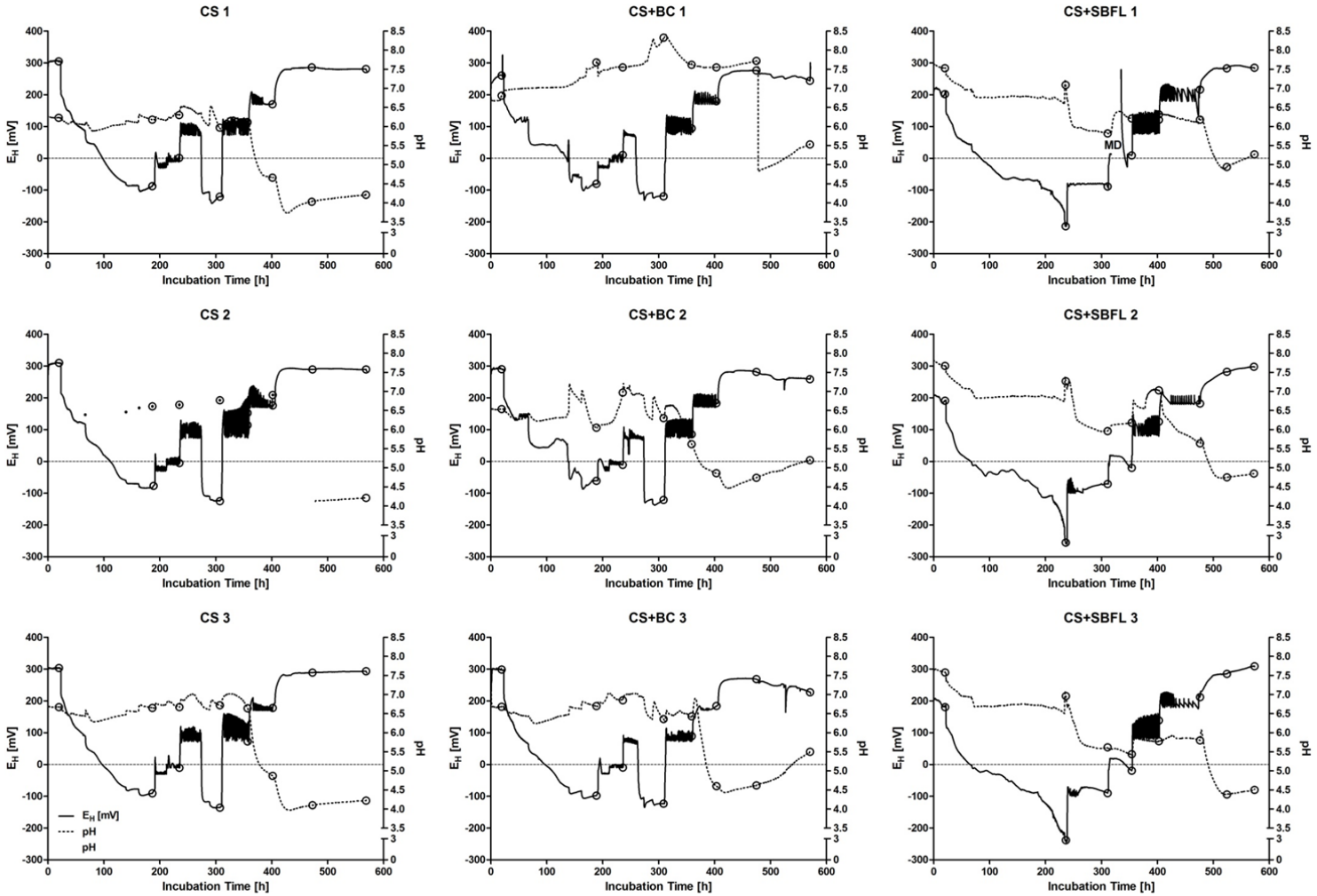

Figure 0-1: Development of redox potential E_H (solid line), pH (dashed line), and sampling points (circles) in soil slurry (data every 10 min) in the microcosms of untreated contaminated soil (CS 1; CS 2; CS 3), CS treated with biochar (CS+BC 1; CS+BC 2; CS+BC 3), and CS treated with sugar beet factory lime (CS+SBFL 1; CS+SBFL 2; CS+SBFL 3). MD = missing data.

DOC, DIC, Fe, Mn, SO_4^{2-}, and Cl^- results

Concentrations of DOC were highest in CS and decreased with increasing E_H in CS and CS+BC; therefore, the relation between DOC and E_H was negative in CS (r = -0.82) and CS+BC (r = -0.79) while this relation was missing in CS+SBFL (Fig. 4-3, Tables 0-1 and 0-2).

An inverse relationship between DOC and E_H has been observed in several studies (e.g. Grybos et al., 2009; Kim et al., 2014; Rinklebe et al., 2016b). One possible reason for the lack of this behavior in CS+SBFL might have been the considerably lower minimal E_H compared to CS and CS+BC (Table 0-1): Organic carbon-Fe chelates form mainly under anoxic conditions (Lalonde et al., 2012) which may be a reason why DOC concentrations in CS+SBFL were comparatively low at E_H -204 mV (Fig. 4-3). Diverse processes may explain why DOC concentrations were higher in CS+SBFL at E_H -80 mV as well as in CS at E_H -88 mV, and CS+BC at E_H -80 mV: Humic compounds of terrestrial organic carbon are preferentially sorbed to Fe(III) and the reductive dissolution of Fe(III) under anoxic conditions leads to a release of DOC and Fe(II) from soil (Peter et al., 2016). The simultaneous increase in DOC and Fe concentrations in CS+SBFL at E_H -80 mV may have been induced by the dissolution of OC-Fe chelates in the course of increasing E_H and decreasing pH. High DOC under reducing conditions might also have been provoked by the degradation of OM to DOC by reductive fermentation and hydrolysis (Frohne et al., 2014; Shaheen et al., 2016). The increases in DOC in CS+SBFL at E_H 116 and 184 mV may in part be explained by microbial fermentation under moderately reducing conditions (Aguilar and Thibodeaux, 2005). Similar DOC increases in CS and CS+BC are missing which may indicate that SBFL characteristics promote microbial fermentation under these E_H conditions. This is in good agreement with the finding that substrate characteristics can affect DOC production (Kim et al., 2014). It has been found that reoxygenation can remove most of before released DOC by flocculation while the remaining DOC was mineralized (Peter et al., 2016). Flocculation of DOC in the course of oxygenation occurs via co-precipitation with iron oxides (Frohne et al., 2011; Lalonde et al., 2012; Cooper et al., 2017). Lower DOC concentrations detected at higher E_H in CS and the treatments may also have been promoted by enhanced microbial carbon consumption (Yu et al., 2007; Abel et al., 2012; Husson, 2013).

Concentrations of DIC above the detection limit were solely found under reducing (< 100 mV) and highly reducing (< -100 mV) conditions in CS and the treatments (Fig. 4-3). Higher DIC release under anoxic conditions has been suggested to be linked to anaerobic

microbial communities which are responsible for OM mineralization thereby releasing DIC and that this process is impaired by oxygen penetration (Longhi et al., 2016).

The concentrations of Fe and Mn in CS and CS+BC were considerably higher under moderately reduced and acidic than under reducing and neutral to alkaline conditions (Fig. 4-3). In CS+SBFL the trend was similar although comparatively high concentrations of dissolved Fe were found at an E_H of -80 mV as well and differences in Mn concentrations were less pronounced. However, positive correlations between E_H and both Fe and Mn were found for CS and the treatments although a correlation between E_H and Fe was missing in CS+SBFL. Contrarily, negative correlations between pH and both Fe and Mn were detected in CS and the treatments. Increasing concentrations of soluble Fe and Mn in the course of reductive dissolution under low E_H were often observed in soils (Charlatchka and Cambier, 2000; Frohne et al., 2015). However, in our experiment, concentrations of dissolved Fe and Mn increased with rising E_H which was likely due to the concomitant decrease of the pH (Fig. 4-3). Thus, our results suggest that low pH values under moderately reducing conditions (100-400 mV) favor the dissolution of Fe and Mn which is in agreement with Takeno (2005) and corroborated by considerably higher concentrations of dissolved Fe and Mn in CS measured at the sampling at the lowest pH compared to CS+BC and CS+SBFL with higher pH values (Fig. 4-3).

The mean concentration of SO_4^{2-} in CS+SBFL (21.8 mg/l) was higher than in CS (14.1 mg/l) and CS+BC (7.8 mg/l) (Fig. 4-3). The sulfur contents of the three source materials alone are not able to explain these differences (Table 3-4). Contrarily, the results suggest that the addition of BC diminished the release of SO_4^{2-} from soil while the addition of SBFL increased it. Sulfate concentrations were lowest in CS+BC indicating that BC may have curtailed its release either by sorption and/or inhibiting its formation (Table 0-1). The major process of SO_4^{2-} formation in sediments is the reoxidation of reduced S compounds (Holmer and Storkholm, 2001). Thus, the increased SO_4^{2-} release in CS+SBFL under moderately reducing conditions might have been related to organic S mineralization stimulated by the amended SBFL and its subsequent oxidation (Lewicka-Szczebak et al., 2009). This hypothesis is supported by the general assumption that the influence of S forms is more significant than the S concentration regarding S mineralization (Churka Blum et al., 2013). Thus, it seems likely that both, DOC and SO_4^{2-}, show a similar pattern in CS+SBFL under moderately reducing conditions due to elevated mineralization. Contrarily, we may suggest that the added BC enhanced the sorption of sulfur forms leading to lower SO_4^{2-} concentrations in CS+BC compared to CS. Besides sorption lower SO_4^{2-} concentrations in CS+BC

might be ascribed to higher dissimilatory or assimilatory SO_4^{2-} reduction which constitute the main sink of SO_4^{2-} in freshwater systems (Lewicka-Szczebak et al., 2009). This suggestion is supported by findings of Easton et al. (2015) revealing that biochar significantly increased microbial SO_4^{2-} reduction.

In general, no consistent pattern was observed with regard to the concentrations of soluble SO_4^{2-} when CS and the treatments were considered. Negative correlations between SO_4^{2-} and E_H were found in CS and CS+BC while this relationship could not be confirmed in CS+SBFL. A relationship between pH and SO_4^{2-} was missing in CS as well as in the treatments.

Only slight differences in Cl^- concentrations were found between CS and the treatments (Fig. 4-3). Despite lower minimum and maximum concentrations in CS mean concentrations were similar. Similarly, the pattern of Cl^- was comparable. A modest increase in Cl^- concentrations was determined at higher E_H. Consequently, significant correlations were found between E_H and Cl^- in CS+BC and CS+SBFL.

Table 0-1: Redox potential (E_H), pH, concentrations of MeHg and EtHg in the slurry, as well as concentrations of Hg_t and other elements/compounds in the slurry filtrate of the contaminated soil (CS), the contaminated soil plus biochar (CS+BC), and of the contaminated soil plus sugar beet factory lime (CS+SBFL) during the experiment.

Parameter	Unit	Contaminated soil				Contaminated soil + Biochar				Contaminated soil + Sugar beet factory lime			
		N	Minimum	Maximum	Mean	N	Minimum	Maximum	Mean	N	Minimum	Maximum	Mean
E_H all	[mV]	10,261	-142	311	119	10,293	-138	303	110	10,329	-260	310	60
E_H[a]		21	-136	293	93	21	-124	283	85	21	-223	309	84
pH all		7,400	3.7	7.1	5.5[b]	10,296	4.4	8.4	6.3	10,329	4.4	7.8	6.2
pH[a]		21	4.0	6.9	5.7	21	4.6	8.2	6.3	21	4.4	7.0	5.8
Hg_t	[µg/l]	21	5.4	41.9	16.0	21	5.6	25.0	12.7	21	1.6	14.8	5.7
MeHg	[ng/l]	21	4.6	77.0	14.7	21	6.0	57.0	13.5	21	6.1	39.5	17.2
EtHg		21	4.7	66.0	15.6	21	5.7	28	14.2	21	3.2	23.0	12.7
DOC	[mg/l]	21	1,197.5	5,509.2	2,994.3	21	725.4	3,715.3	2,134.4	21	1,281.7	3,489.4	2,075.5
SO_4^{2-}		19	7.2	20.3	14.1	21	1.4	20.5	7.8	21	11.3	44.0	21.8
Cl^-		20	34.8	115.3	79.5	21	48.2	137.1	76.6	21	44.3	141.2	82.4
S		21	4.9	9.4	5.9	21	2.0	7.4	5.0	21	6.8	11.1	9.2
Fe		21	2.1	104.7	29.3	21	2.8	58.8	17.7	21	0.9	68.8	18.7
Mn		21	6.8	64	26.6	21	5.1	46.1	22.8	21	4.8	53.0	29.5

DOC: dissolved organic carbon; N: number of samplings/measurements; [a] means of data 6 hours before sampling; [b] probably to low due to dysfunction of one pH electrode

Table 0-2: Correlation coefficients (Pearson) between Hg_t, MeHg, EtHg, and factors controlling their release dynamics (E_H6, pH6, DOC, Cl^-, SO_4^{2-}, PO_4^{3-}, Fe, Mn) (n = 21) of the contaminated soil (CS), the contaminated soil + biochar (CS+BC), and the contaminated soil + sugar beet factory lime (CS+SBFL).

	Soil	E_H6	pH6	DOC	Cl^-	SO_4^{2-}	PO_4^{3-}	Fe	Mn	EtHg	MeHg
Hg_t	CS	-0.688[a]	0.690[a]	0.766[a]	n.s.[1]	n.s.[2]	-0.522[b; 1]	-0.562[a]	-0.707[a]	n.s.	n.s.
	CS+BC	-0.574[a]	n.s.	0.749[a]	n.s.	0.440[b]	n.s.[2]	-0.618[a]	-0.775[a]	0.686[a]	n.s.
	CS+SBFL	n.s.	0.511[b]	n.s.	n.s.	n.s.	n.s.[3]	-0.477[b]	n.s.	0.653[a]	0.441[b]
MeHg	CS	n.s.	n.s.	n.s.	n.s.[1]	n.s.[2]	n.s.[1]	n.s.	n.s.	n.s.	
	CS+BC	-0.590[a]	n.s.	n.s.	n.s.	n.s.	0.813[a; 2]	n.s.	n.s.	n.s.	
	CS+SBFL	n.s.	n.s.	n.s.	n.s.	n.s.	n.s.[3]	n.s.	n.s.	0.756[a]	
EtHg	CS	-0.691[a]	0.452[b]	0.533[b]	n.s.[1]	0.510[b; 2]	-0.651[a; 1]	-0.528[b]	-0.594[a]		
	CS+BC	-0.732[a]	0.526[b]	0.855[a]	n.s.	0.578[a]	n.s.[2]	-0.565[a]	-0.783[a]		
	CS+SBFL	n.s.	n.s.	n.s.	n.s.	n.s.	n.s.[3]	n.s.	n.s.		

[1]: n = 20; [2]: n = 19; [3]: n = 14

[a] Correlation significant at 0.01 level, [b] Correlation significant at 0.05 level, n.s. = not significant
DOC: dissolved organic carbon; CS: contaminated soil; BC: biochar; SBFL: sugar beet factory lime

PLFA results details

Results for PLFAs not attributed to SRB

The increases in CS and the treatments were particularly high for the two PLFAs 16:0 and 16:1. The PLFA 16:0 (palmitic acid) is found ubiquitous in most organisms and seems to tolerate metal pollution (Mancuso et al., 1990; Frostegård et al., 1993). This fatty acid is frequently among the dominating fatty acids found in the course of PLFA analysis (Feng et al., 2003a; Zhao et al., 2011; Schaller et al., 2016). Willers et al. (2015) noted that it has been repeatedly used as a general bacterial marker and indicated that this should be done with care as 16:0 has been found in plants and thus all possible plant residues should be removed from samples prior to analysis to avoid misinterpretation. In fact, Mancuso et al. (1990) used the sum of the relative abundances of i15:0 and a15:0 in their samples as representative of the bacterial component of the microbial community and divided it by the relative abundance of 16:0 as ubiquitous PLFA in most organisms to obtain an indication of the proportion of bacteria. The "unidentified" 16:1 is a summed aggregate that comprises some structurally similar fatty acids which may include fatty acids such as 16:1ω9, 16:1ω7c, and 16:1ω7t. The fatty acid 16:1ω5c is not included, since it was determined by another peak. High abundances of the fatty acids 16:0, 18:1ω9c, and 16:1ω7 were also attributed to cyanobacteria, while 16:1ω7 and 18:1ω9c, as well as C_{16}- and C_{18}-polyunsaturated acids, have been used as indicators for cyanobacteria (Zhang et al., 2007; Bühring et al., 2014). However, the fatty acids 16:1ω7c and 18:1ω7c can also be ascribed to sulfur-oxidizing bacteria (SOB) (Elvert et al., 2003; Jiang et al., 2012). According to Jiang et al. (2012) the fatty acids 16:0, 16:1ω7c, and 18:1ω7c can be found in SRB but their contents should not be higher than those of the characteristic biomarkers of SRB in this case. When attributed to SOB 16:0, 18:1ω7c, and 16:1ω7c may indicate the presence of *Beggiatoa*, *Thioploca* and other SOB (Jiang et al., 2012). The fatty acid 18:1ω9c which showed a strong increase as well is not only attributed to cyanobacteria but also to saprotrophic fungi (Chowdhury and Dick, 2012; Kao-Kniffin and Zhu, 2013; Pan et al., 2016). The fatty acid 18:1ω9t is associated with bacteria (Ngosong et al., 2011; Kao-Kniffin and Zhu, 2013).

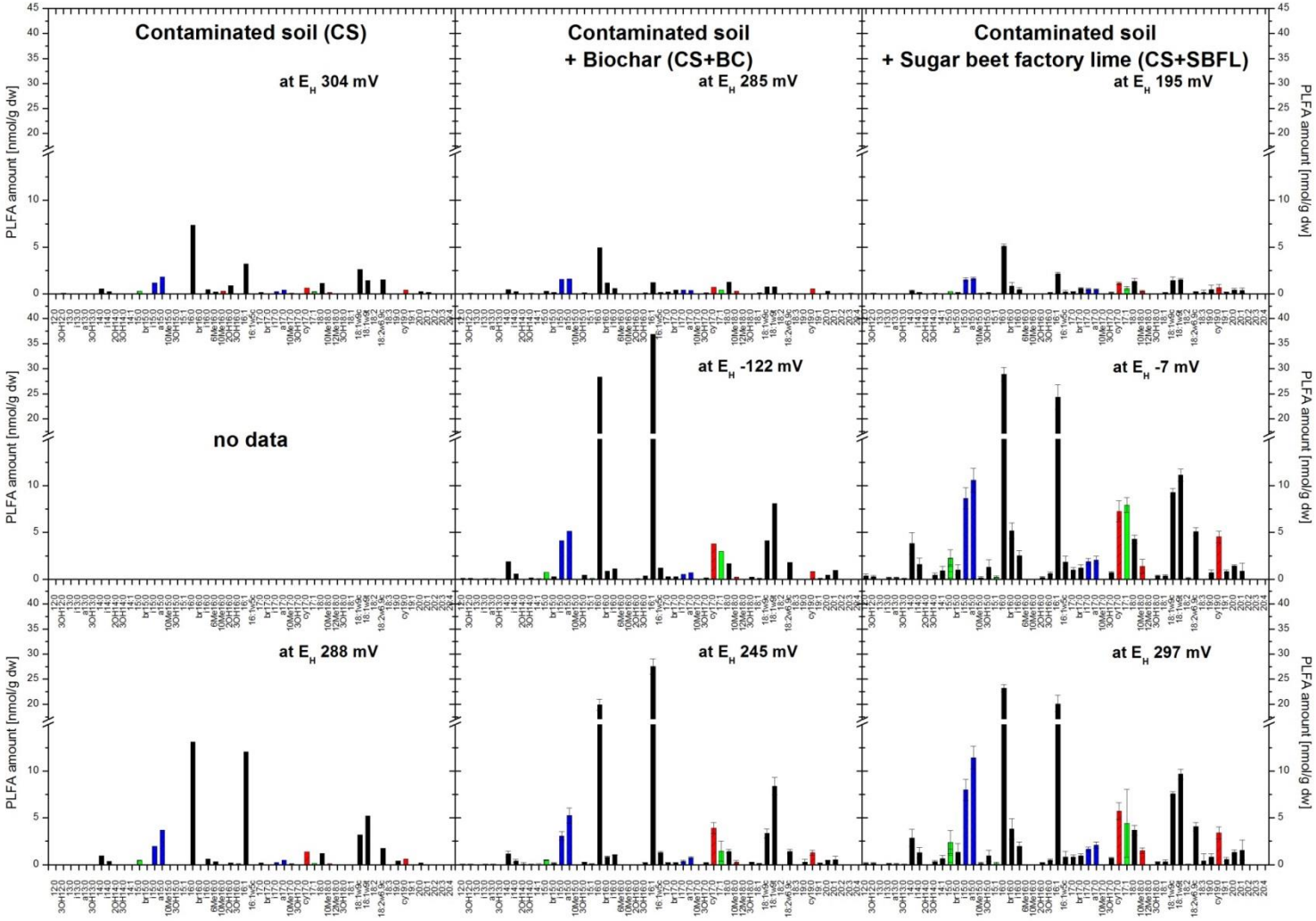

Figure 0-2: PLFA amounts as influenced by soil treatment and changing E_H/pH.

Appendix B: Supporting information for Chapter 5

DOC, Fe, Mn, and SO_4^{2-} results

Concentrations of DOC in CS and the biochar treatments showed an almost opposite behavior to E_H (Fig. 5-3). The highest concentrations (2.78, 2.79, and 2.75 g/l) were measured at the lowest E_Hs (-110, -116, and -109 mV). However, in CS and CS+BC200 slight increases in DOC were found even though E_H was increasing. Moreover, when the E_H was lowered after highest values had been reached DOC concentrations kept on declining despite decreasing E_H. Nevertheless, a strong negative correlation between DOC and E_H was found for CS and the biochar treatments ($r = -0.66$, $r = -0.71$, and $r = -0.73$). This opposing trend has been found several times (e.g. Kim et al., 2014; Rinklebe et al., 2016b; Appendix A) and may be attributed to the reductive dissolution of Fe(III) under anoxic conditions with the simultaneous release of DOC and Fe(II) from soil given the importance of Fe(III) as sorbent for humic compounds of terrestrial organic carbon (Peter et al., 2016; Dadi et al., 2017). Another explanation may be the degradation of OM to DOC by microbial reductive fermentation and hydrolysis (Aguilar and Thibodeaux, 2005; Brocke et al., 2015; Appendix A). Increasing E_H is usually accompanied by decreasing DOC concentrations in the course of flocculation (formation of stable organic complexes with Fe(III)) and mineralization (Lalonde et al., 2012; Kim et al., 2014; Peter et al., 2016).

Only modest increases in DOC release were detected as a result of the biochar amendment when maximum DOC concentrations were compared. Mean DOC concentrations in CS+BC500 were even lower than in CS (Table 0-3). Substrate characteristics exert influence on DOC production (e.g. Kim et al., 2014). The addition of biochar can intensify the microbial activity promoting respiration and fermentation processes in the substrate which may lead to a higher release of DOC (Beiyuan et al., 2017). A biochar induced increase in DOC concentrations did not become obvious in our experiment. One possible explanation for this is enhanced microbial carbon consumption (Yu et al., 2007; Abel et al., 2012; Husson, 2013). The last named process may have also exerted influence on the evolution of DOC concentrations at higher E_H, being another factor that diminishes DOC concentrations next to co-precipitation with iron oxides.

The concentrations of Fe and Mn in CS and the biochar treatments showed a similar pattern under highly reducing conditions and reducing conditions up to 0 mV. Until the third sampling at ~ -50 mV Fe and Mn concentrations were slightly increasing and significantly increased at the fourth sampling around 0 mV. This is in good agreement with literature

since bioreducible Fe and Mn compounds are in a reduced state at a E_H of 0 mV (Mansfeldt, 2004; DeLaune and Reddy, 2005; Pezeshki and DeLaune, 2012). Following E_H 0 mV dissolution behavior of Fe and Mn proceeded differently. Iron concentrations in CS and the biochar treatments were found to be highest at E_H 0 mV and were already considerably lower at the ensuing sampling at ~ 100 mV. The lowest concentrations of dissolved iron were measured at an E_H of 282 mV in CS (0.83 mg/l), an E_H of 264 mV in CS+BC200 (0.98 mg/l), and an E_H of 201 mV in CS+BC500 (2.42 mg/l). Such a decline of dissolved Fe concentrations in line with increasing E_H, particularly at higher E_H, has been repeatedly described before and is most likely provoked by the formation of Fe oxyhydroxides (Frohne et al., 2015; Munger et al., 2016). The general pattern of Fe concentrations in CS and the biochar treatments was similar. A distinct decline of Fe concentrations followed the strong increase at E_H ~ 0 mV and slight increases in Fe were found in CS+BC500 starting at E_H 278 mV, while the increases of Fe in CS and CS+BC200 begun after the highest E_H. Interestingly, it was found that in CS and CS+BC200 there was a very good agreement in the Fe concentrations measured for the first and second sampling at E_H window 200 mV indicating the influence of E_H on Fe dissolution from the substrate. This parallelism was not found for the two samplings of E_H window 100 mV, which can be attributed to a carry-over effect triggered by the strong Fe increase at E_H ~ 0 mV. However, the somewhat stronger increase of Fe concentrations found in CS+BC500 in the course of the last three samplings may have been partly induced by lower pH values as particularly strong Fe increases were observed for one microcosm (MC) in which the pH was below 4.6 during the last three samplings (data not shown). Such increases in Fe concentrations under moderately reducing conditions (100-400 mV) or comparatively high E_H at decreasing pH has been reported in earlier studies (Rinklebe et al., 2016a; Shaheen and Rinklebe, 2017; Appendix A). It is likely that Fe is dominant as Fe(II) in the dissolved phase under the prevailing E_H-pH-conditions in our experiment as indicated by (Takeno, 2005). Even though we assume that the changing pH stimulated the increase in dissolution of Fe at higher E_H a correlation between Fe and pH was missing in CS+BC500 as well as in CS and CS+BC200. In general, the BC500 amendment clearly promoted the dissolution of Fe, while the differences in Fe release between CS and CS+BC200 were less pronounced when mean concentrations were compared (Table 0-3).

In contrast to Fe no sharp decline in dissolved Mn concentrations was found following the sampling at E_H ~ 0 mV. The concentrations of Mn remained fairly constant with slightly higher concentrations found at the first sampled E_H 200 mV window which is in good

agreement with DeLaune and Reddy (2005) who indicated that oxidized manganese compounds are reduced and Mn(II) is released around E_H 200 mV (Fig. 5-2). Contrarily to CS and CS+BC200 the decline in Mn concentrations following the first 200 mV sampling was very moderate in CS+BC500 and the highest mean Mn concentration was calculated for the last sampling at the second E_H of 100 mV. This deviation in CS+BC500 was again induced by the one MC in which the pH had fallen below 4.6 during the last three samplings. Similar to Fe the more distinct shift in pH in this MC induced stronger Mn dissolution. In general, the pH was the main factor governing the dissolution of Mn in our experiment. Very strong negative correlations were calculated for Mn and pH in CS and the biochar treatments ($r = -0.94$; $p < 0.00001$; $n = 36$ in CS, $r = -0.91$; $p < 0.00001$; $n = 36$ in CS+BC200, and $r = -0.89$; $p < 0.00001$; $n = 34$ in CS+BC500). Analogous positive correlations were found between Mn and E_H ($r = 0.66$; $p < 0.00005$; $n = 36$ in CS, $r = 0.64$; $p < 0.00005$; $n = 36$ in CS+BC200, and $r = 0.75$; $p < 0.00001$; $n = 34$ in CS+BC500). Increasing concentrations of soluble Fe and Mn associated with reductive dissolution under low E_H is often observed in soils (Charlatchka and Cambier, 2000; Frohne et al., 2015). Mansfeldt (2004) detected the appearance of dissolved Mn(II) below an E_H of 350 mV, and of Fe(II) below 0 to 50 mV in soil solutions with pH values between 7.4 to 7.8. Even though we have to consider that Mn and Fe reducing conditions may develop at higher E_H in our experiment due to the influence of lower pH values (mean values (all) between 5.6 and 5.8) (Karathanasis et al., 2003; Takeno, 2005) these findings are in good agreement with our results. Similarly, Fe(II) concentrations in slurry disappeared/declined between E_H ~ 0 mV and ~ 100 mV. Probably provoked by the formation of Fe oxyhydroxides. Also, we did not detect a considerable decrease of dissolved Mn concentrations in our experiment which would indicate the formation of Mn oxyhydroxides such as Mn_2O_3, MnOOH, and MnO_x (Mora et al., 2017). Due to the lower pH in our experiment compared to Mansfeldt (2004) we may suggest that oxidation of Mn under our experimental conditions may have started at $E_H > 350$ mV leading us to conclude that the formation of Mn oxyhydroxides in our experiment with a maximum measured E_H of 307 mV is unlikely. Moreover, it is known that the reaction of Mn(II) with O_2 is slow compared to the reaction between Fe(II) and O_2. Ferrous iron rapidly precipitates under aerobic circumneutral conditions while Mn(II) oxidation is rather mediated by microorganisms and Mn(II) may therefore persist in aerobic water (Morgan, 2005; Duckworth et al., 2017). Consistently, Munger et al. (2016) found that hypolimnetic oxygenation was suitable to decrease dissolved Fe(II) concentrations in a slightly acidic to neutral (pH 5.6 to 7.5) hypolimnion,

while their results indicated that the removal of soluble Mn is also linked to the activity of Mn-oxidizing organisms and favored at neutral to alkaline pH. The strong influence of pH on Mn dissolution is supported by the strong correlations found in our experiment.

The mean concentration of SO_4^{2-} in CS+BC200 (37.5 mg/l) was higher than in CS+BC500 (35.2 mg/l) and CS (33.4 mg/l) and the maximum concentration of dissolved SO_4^{2-} was found in CS+BC200 as well (94.2 mg/l) (Table 0-3, Fig. 5-2). However, the differences between CS and the biochar treatments were not very pronounced. Sulfate concentrations in CS and the biochar treatments were fairly constant under highly reducing conditions and reducing conditions up to 0 mV. The pattern changed at higher E_H. A slight increase could be observed at the first 100 mV window in CS+BC500. A somewhat higher increase was detected in CS+BC200 at the first 200 mV window, while a perceivable increase in CS was determined for the last sampling at the second 100 mV window (Fig. 5-2). Correlations between SO_4^{2-} and E_H or pH were missing for CS and the biochar treatments. In general, the major process of SO_4^{2-} formation in sediments is the reoxidation of reduced S compounds (Holmer and Storkholm, 2001; Fike et al., 2015). For example, when organic S is mineralized or decomposed and thereafter oxidized higher SO_4^{2-} concentrations in solution can be expected (Lewicka-Szczebak et al., 2009). Research indicated that the form of sulfur (soluble sulfate and readily degradable organic S forms) present in tissues of decaying OM may be more important than total S concentrations (Singh et al., 2006; Churka Blum et al., 2013). Churka Blum et al. (2013) found that biochar amendment resulted in increasing SO_4^{2-} release. The latter authors monitored the influence of different plant residues and corn stalk biochar pyrolyzed at 450 °C added in the same amount of total S on S mineralization and immobilization in an Oxisol. Their results indicate that most of S bonded to C within corn stalks was thermally decomposed during pyrolysis, while ester-S and fractionally inorganic sulfate concentrated in the charred material. The ester-S of the biochar was then quickly converted to inorganic SO_4^{2-} which resulted in a higher initial release of SO_4^{2-} from biochar amended soil compared to other treatments (Churka Blum et al., 2013). The comparatively low increase in SO_4^{2-} resulting from the biochar amendment in our experiment may have been provoked by higher dissimilatory or assimilatory SO_4^{2-} reduction which constitute the main sink of SO_4^{2-} in freshwater systems (Lewicka-Szczebak et al., 2009). This suggestion is supported by findings of Easton et al. (2015) revealing that biochar significantly increased microbial SO_4^{2-} reduction.

Table 0-3: Redox potential (E_H), pH, concentrations of MeHg and EtHg in the slurry, as well as concentrations of Hg_t and other elements/compounds in the slurry filtrate of the contaminated soil (CS), the contaminated soil plus Biochar 200 (CS+BC200), and the contaminated soil plus Biochar 500 (CS+BC500) during the experiment.

Parameter	Unit	Contaminated soil				Contaminated soil + Biochar 200				Contaminated soil + Biochar 500			
		N	Minimum	Maximum	Mean	N	Minimum	Maximum	Mean	N	Minimum	Maximum	Mean
E_H all	[mV]	11,856	-126	300	86	11,910	-150	307	80	11,575	-119	302	90
E_H[a]	[mV]	36	-113	296	76	36	-132	300	74	34	-118	296	82
pH all		11,860	4.9	7.0	5.8	11,915	4.8	7.5	5.8	11,415	4.5	6.9	5.6
pH[a]		36	5.0	6.9	5.7	36	4.8	6.6	5.7	34	4.5	6.6	5.5
Hg_t	[µg/l]	36	1.78	52.00	12.96	36	0.99	51.81	11.88	34	0.91	35.30	10.03
MeHg	[ng/l]	35	21.30	406.00	87.74	36	11.10	392.00	80.39	34	11.20	210.00	75.49
EtHg	[ng/l]	33	3.10	17.10	7.36	34	2.30	17.90	6.93	32	2.80	20.80	6.96
DOC	[g/l]	36	1.33	2.80	2.31	36	1.66	2.82	2.33	34	1.31	2.84	2.14
$SUVA_{254}$	[l/mg C/m]	36	0.07	0.12	0.09	36	0.07	0.19	0.10	34	0.07	0.31	0.11
Cl^-	[mg/l]	36	49.98	156.26	91.48	36	46.54	157.62	88.02	34	55.11	172.72	98.42
SO_4^{2-}	[mg/l]	36	25.57	76.94	33.36	35	23.79	94.19	37.52	34	23.90	63.94	35.17
Fe	[mg/l]	36	0.56	106.94	9.46	36	0.47	183.85	10.21	34	0.39	187.66	18.68
Mn	[mg/l]	36	5.68	73.60	30.92	36	6.97	76.08	25.32	34	6.66	70.57	34.48

DOC: dissolved organic carbon; N: number of samplings/measurements; [a] means of data 6 hours before sampling

Table 0-4: Correlation coefficients (Pearson) between total dissolved mercury (Hg_t), mercury species (MeHg and EtHg), and factors controlling their release dynamics (E_H6, pH6, DOC, $SUVA_{254}$, Cl^-, SO_4^{2-}, Fe, Mn) (n = 36) of the contaminated soil (CS), the contaminated soil + Biochar 200 (CS+BC200), and the contaminated soil + Biochar 500 (CS+BC500).

	Soil	E_H6	pH6	DOC	$SUVA_{254}$	Cl^-	SO_4^{2-}	Fe	Mn	EtHg	MeHg
Hg_t	CS	-0.804[a]	0.845[a]	0.710[a]	0.559[a]	-0.603[a]	n.s.	n.s.	-0.763[a]	0.737[a; 3]	n.s.
	CS+BC200	-0.685[a]	0.664[a]	0.638[a]	0.344[b]	-0.537[a]	n.s.	n.s.	-0.618[a]	0.530[a; 2]	n.s.
	CS+BC500	-0.728[a; 2]	0.759[a; 2]	0.734[a; 2]	n.s.	-0.453[a; 2]	n.s.	n.s.	-0.786[a; 2]	0.609[a; 4]	n.s.
MeHg	CS	n.s.	n.s.	0.357[b; 1]	n.s.	n.s.	n.s.	n.s.	n.s.	0.547[a; 3]	
	CS+BC200	n.s.	n.s.	n.s.	n.s.	n.s.	n.s.	n.s.	n.s.	n.s.	
	CS+BC500	n.s.	0.343[b; 2]	0.457[a; 2]	n.s.	n.s.	0.457[a; 2]	n.s.	-0.530[a; 2]	n.s.	
EtHg	CS	-0.626[a; 3]	0.540[a; 3]	0.463[a; 3]	0.376[b; 3]	-0.530[a; 3]	n.s.	n.s.	-0.532[a; 3]		
	CS+BC200	n.s.	n.s.	n.s.	n.s.	n.s.	n.s.	0.458[a; 2]	-0.364[b; 2]		
	CS+BC500	-0.383[b; 4]	n.s.	0.367[b; 4]	n.s.	n.s.	n.s.	n.s.	-0.362[b; 4]		

[1]: n = 35; [2]: n = 34; [3]: n = 33; [4]: n = 32

[a] Correlation significant at 0.01 level, [b] Correlation significant at 0.05 level, n.s. = not significant
DOC: dissolved organic carbon; $SUVA_{254}$: specific UV absorbance at 254 nm; SO_4^{2-}: sulfate

PLFA results details

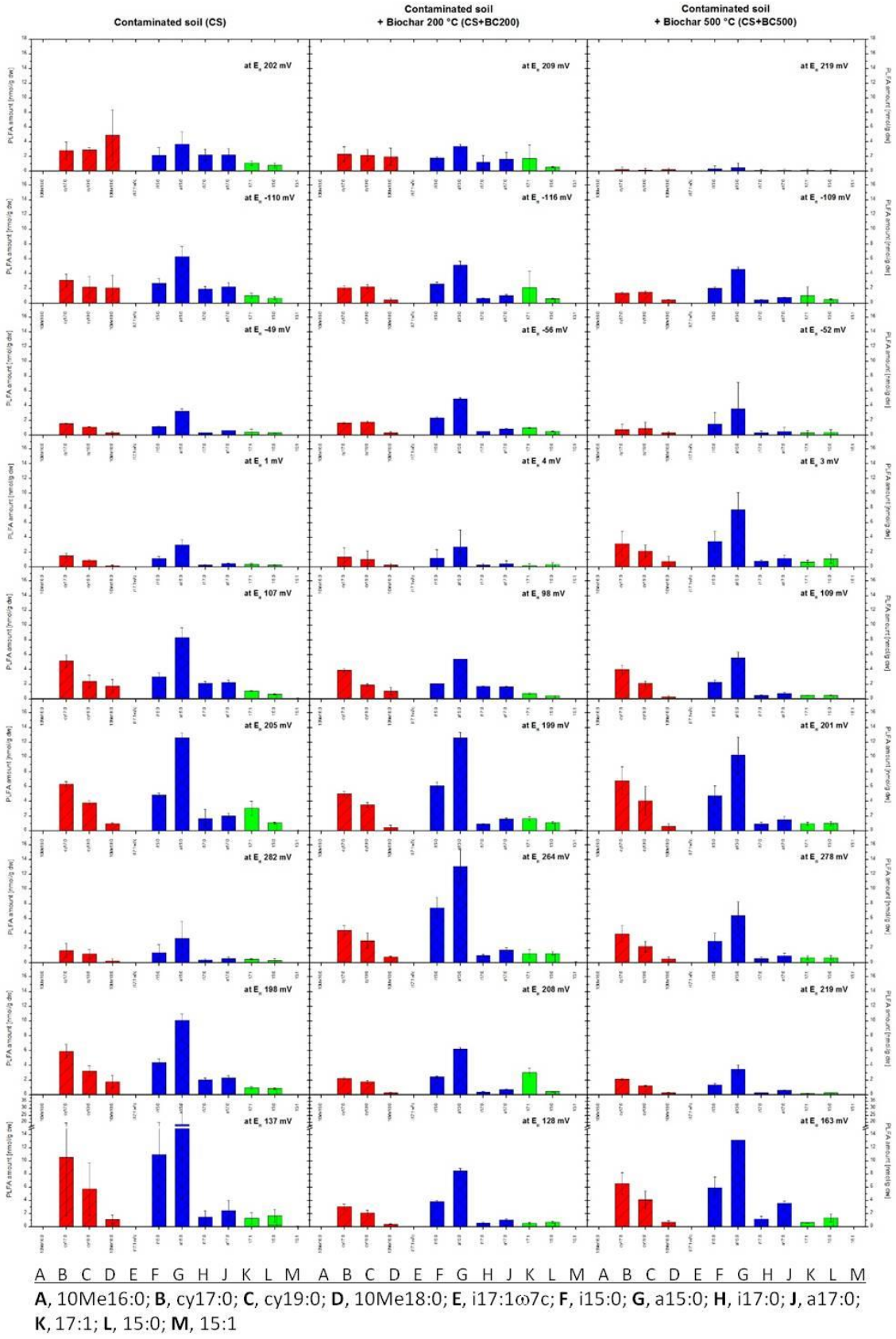

Figure 0-3: SRB PLFA amounts as influenced by soil treatment and changing E_H/pH.

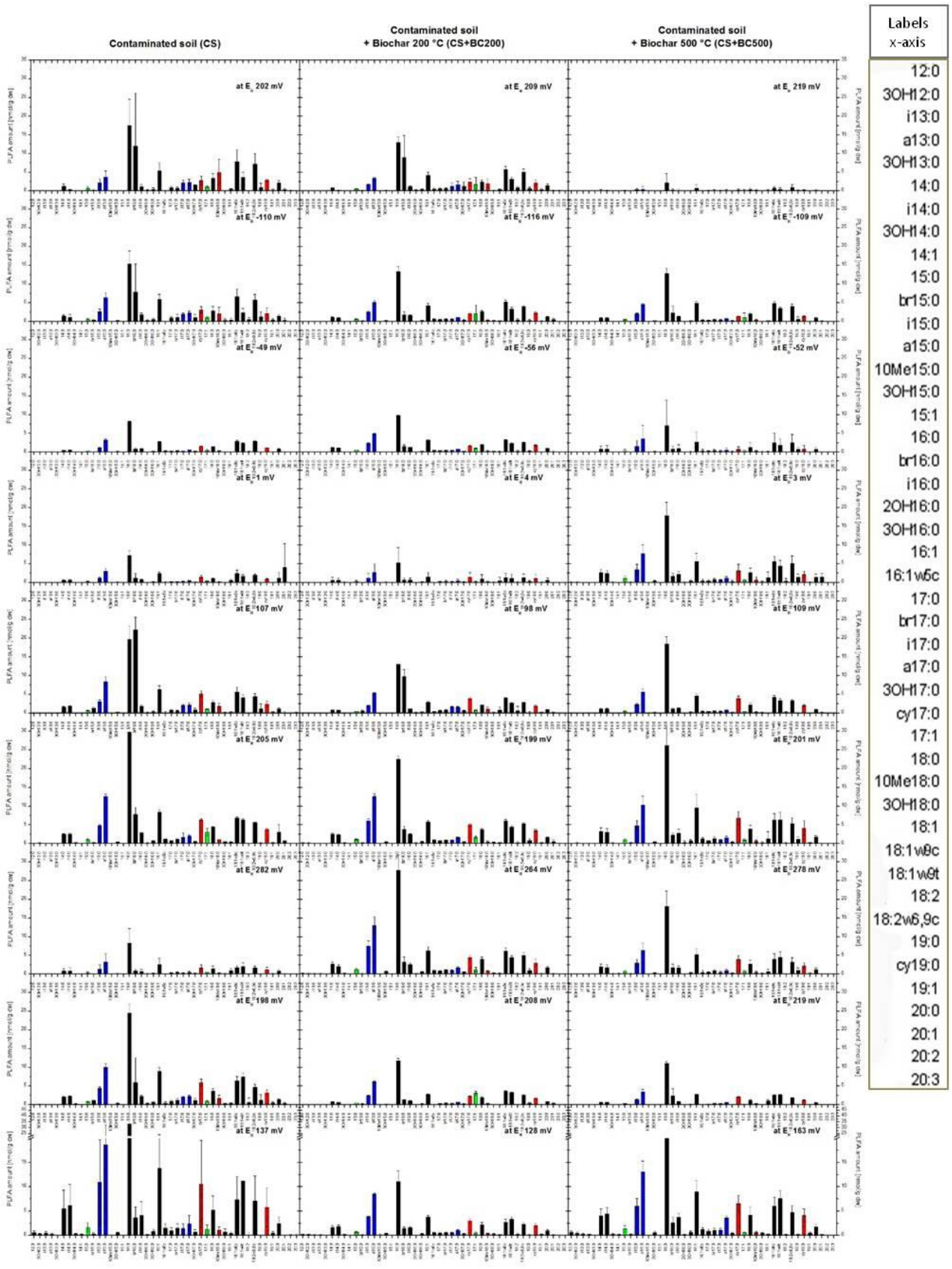

Figure 0-4: PLFA amounts as influenced by soil treatment and changing E_H/pH.

Appendix C: Supporting information for Chapter 6

Table 0-5: Concentrations of dissolved elements, compounds, as well as redox potential (E_H) and pH in sampled solutions during the experiment (Saale 1).

		Saale 1																		
Parameter	Unit	Precipitation (PCPN)				depth 30 cm				depth 60 cm				depth 100 cm				Groundwater (GW)			
		N	Minimum	Maximum	Mean	N	Minimum	Maximum	Mean	N	Minimum	Maximum	Mean	N	Minimum	Maximum	Mean	N	Minimum	Maximum	Mean
E_H	[mV]	-	-	-	-	55	208	906	485	55	174	911	485	55	170	879	386	-	-	-	-
pH		18	4.5	7.0	6.3	28	6.0	8.1	6.9	22	6.8	8.6	7.7	26	7.1	8.8	8.1	50	4.4	8.3	7.6
Hg(II)	[pg/ml]	18	12.00	73.00	33.49	30	9.50	177.00	35.21	23	4.50	95.25	29.68	27	5.00	76.00	23.75	51	4.00	80.00	25.92
DOC		18	2.13	63.00	16.51	28	10.50	61.90	27.18	22	17.47	59.45	25.16	26	4.85	40.45	22.36	51	3.55	42.90	11.00
S		18	1.49	5.72	3.01	34	10.42	139.45	81.97	26	53.86	233.47	126.13	30	24.89	236.70	161.56	49	18.07	233.80	194.93
SO_4^{2-}	[mg/l]	16	3.67	27.35	10.50	28	29.81	405.58	240.15	24	156.81	771.06	386.40	28	77.44	798.57	479.82	47	47.60	824.79	574.06
Cl^-		16	1.69	9.94	3.91	28	14.71	197.50	111.66	24	43.08	368.10	181.30	28	51.44	430.71	243.51	47	21.56	542.85	338.54
Br^-		16	0.02	0.35	0.08	27	0.02	0.35	0.08	23	0.02	0.35	0.08	27	0.02	0.35	0.09	46	0.02	0.56	0.11
EC	[µS/cm]	18	49.0	290.0	112.4	26	395.3	1847.0	1194.6	22	905.0	2576.7	1584.3	25	470.0	2860.0	1974.0	51	333.0	2850.0	2279.7
PWP	[mbar]	-	-	-	-	49	-254.7	815.8	132.1	49	-318.3	778.5	166.0	47	-340.9	766.0	171.3	-	-	-	-
Soil t	[°C]	-	-	-	-	50	0.97	17.17	9.60	50	3.28	16.94	10.22	49	4.86	14.82	10.24	-	-	-	-
Soil θ	[%]	-	-	-	-	50	19.45	53.92	30.79	50	18.49	49.61	29.15	49	17.62	49.35	28.30	-	-	-	-

DOC: dissolved organic carbon
EC: electrical conductivity
PWP: pore water pressure
Soil t: soil temperature
Soil θ: soil moisture content
N: number of samplings/measurements

Table 0-6: Concentrations of dissolved elements, compounds, as well as redox potential (E_H) and pH in sampled solutions during the experiment (Saale 2).

		Saale 2																			
Parameter	Unit	Precipitation (PCPN)				depth 25 cm				depth 60 cm				depth 100 cm				Groundwater (GW)			
		N	Minimum	Maximum	Mean	N	Minimum	Maximum	Mean	N	Minimum	Maximum	Mean	N	Minimum	Maximum	Mean	N	Minimum	Maximum	Mean
E_H	[mV]	-	-	-	-	63	-314	704	393	63	-350	630	379	63	-306	608	371	-	-	-	-
pH		19	4.6	7.6	6.3	34	4.8	7.6	6.6	31	6.6	8.7	7.6	28	7.3	8.5	7.9	61	6.5	8.4	7.6
Hg(II)	[pg/ml]	16	9.00	78.00	28.29	27	8.00	71.67	31.65	24	4.00	86.50	32.57	23	5.00	43.50	26.02	51	5.00	61.50	24.75
DOC		19	6.50	78.80	23.51	33	20.83	51.10	29.21	31	18.76	43.27	25.46	28	7.74	43.50	23.98	62	3.64	29.70	10.75
S		19	1.73	10.75	4.75	45	14.37	233.20	102.11	38	34.19	330.00	154.66	32	46.76	343.50	197.72	63	19.76	288.10	186.21
SO_4^{2-}	[mg/l]	16	5.08	28.77	13.49	32	111.30	656.52	278.19	33	101.99	1022.11	446.54	29	115.96	1077.40	611.25	56	47.60	824.50	549.17
Cl^-		16	1.52	15.49	5.76	32	27.44	236.44	107.24	33	36.34	728.23	228.53	29	68.80	789.60	362.72	56	21.56	692.16	387.25
Br^-		15	0.02	0.35	0.08	31	0.02	0.49	0.09	32	0.02	0.49	0.10	29	0.02	0.40	0.11	54	0.02	1.08	0.12
EC	[µS/cm]	19	86.3	374.0	146.0	33	413.0	2310.0	1294.3	32	531.0	3660.0	1784.2	28	646.0	4270.0	2375.0	61	415.0	3470.0	2418.8
PWP	[mbar]	-	-	-	-	50	-293.9	743.9	125.0	56	-318.4	693.9	184.8	53	-357.9	765.8	170.5	-	-	-	-
Soil t	[°C]	-	-	-	-	59	2.27	18.46	10.73	59	3.25	17.51	10.74	59	5.10	16.26	10.93	-	-	-	-
Soil θ	[%]	-	-	-	-	59	27.13	65.46	47.94	59	22.97	62.42	38.29	59	27.49	53.55	41.32	-	-	-	-

DOC: dissolved organic carbon
EC: electrical conductivity
PWP: pore water pressure
Soil t: soil temperature
Soil θ: soil moisture content
N: number of samplings/measurements

Table 0-7: Correlation coefficients (Pearson) between Hg(II) and factors potentially influencing its release at the study sites Saale 1 and Saale 2.

Hg species & location	Depth	E_H	pH	DOC	Br^-	Cl^-	SO_4^{2-}	S	EC	PWP	Soil temperature	Soil moisture
Hg(II) Saale 1	30 cm	n.s.	n.s.	n.s.	n.s.	-0.466[b; (27)]	n.s.	n.s.	n.s.	n.s.	n.s.	n.s.
	60 cm	n.s.	n.s.	n.s.	n.s.	n.s.	n.s.	n.s.	n.s.	n.s.	n.s.	n.s.
	100 cm	n.s.	n.s.	n.s.	n.s.	n.s.	n.s.	n.s.	n.s.	n.s.	n.s.	n.s.
	all	n.s.	n.s.	n.s.	n.s.	-0.263[b; (77)]	n.s.	n.s.	n.s.	n.s.	n.s.	n.s.
	GW	-	n.s.	n.s.	n.s.	n.s.	0.369[b; (47)]	0.318[b; (49)]	n.s.	-	-	-
	all + GW	n.s.	n.s.	n.s.	n.s.	-0.188[b; (124)]	n.s.	n.s.	n.s.	n.s.	n.s.	n.s.

Hg species & location	Depth	E_H	pH	DOC	Br^-	Cl^-	SO_4^{2-}	S	EC	PWP	Soil temperature	Soil moisture
Hg(II) Saale 2	25 cm	-0.463[b; (24)]	n.s.	n.s.	n.s.	n.s.	n.s.	n.s.	n.s.	-0.457[b; (24)]	n.s.	0.461[b; (25)]
	60 cm	n.s.	n.s.	n.s.	n.s.	n.s.	n.s.	n.s.	n.s.	n.s.	n.s.	n.s.
	100 cm	n.s.	-0.596[a; (21)]	-0.509[b; (21)]	n.s.	n.s.	n.s.	0.437[b; (23)]	n.s.	n.s.	n.s.	n.s.
	all	n.s.	n.s.	n.s.	n.s.	n.s.	n.s.	n.s.	n.s.	-0.257[b; (66)]	n.s.	0.274[b; (69)]
	GW	-	n.s.	n.s.	n.s.	n.s.	n.s.	n.s.	n.s.	-	-	-
	all + GW	n.s.	n.s.	n.s.	n.s.	n.s.	n.s.	n.s.	n.s.	-0.257[b; (66)]	n.s.	0.274[b; (69)]

[a] Correlation significant at 0.01 level, [b] Correlation significant at 0.05 level, [(27)] number of samples, n.s. = not significant
GW: groundwater; DOC: dissolved organic carbon; EC: electrical conductivity; PWP: pore water pressure

Proof of individual contribution

Chapter	Author (Beckers, F.)	Contributor
4	Generating research idea, conducting the microcosm experiment, generating and evaluating data, writing the manuscript	**Rinklebe, J.** Supervisor, generating research idea, selecting the floodplain soil profile and horizon, collection of soil material, soil description and soil classification, performing of a canonical discriminant analysis, and correcting the manuscript
		Mothes, S. Mercury species analyses, correcting the manuscript, and scientific advice
		Abrigata, J. PLFA analysis and scientific advice
		Zhao, J. XANES analysis, correcting the manuscript, and scientific advice
		Gao, Y. Providing resources and reviewing the manuscript
5	Generating research idea, conducting the microcosm experiment, generating and evaluating data, writing the manuscript	**Rinklebe, J.** Supervisor, generating research idea, selecting the floodplain soil profile and horizon, collection of soil material, soil description and soil classification, and correcting the manuscript
		Awad, Y.M. Conducting the microcosm experiment and reviewing the manuscript
		Beiyuan, J. Conducting the microcosm experiment and correcting the manuscript
		Abrigata, J. PLFA analysis and scientific advice
		Mothes, S. Mercury species analyses and scientific advice
		Tsang, D.C.W. Providing resources and reviewing the manuscript
		Ok, Y.S. Providing resources and reviewing the manuscript
6	Generating and evaluating data, writing the manuscript	**Rinklebe, J.** Supervisor, generating research idea, selecting the floodplain soil profile and horizon, collection of soil material, soil description and soil classification, and correcting the manuscript
		Mothes, S. Mercury species analyses and scientific advice

Acknowledgments

Diese Arbeit hätte ohne das Wohlwollen und den besonderen Rückhalt verschiedenster Personen nicht entstehen können. Mein herzlicher Dank gilt deshalb allen, die diese Dissertation ermöglicht haben.

Zunächst danke ich meinem Betreuer Herrn Professor Jörg Rinklebe für die Möglichkeit mich nach meiner Masterarbeit weiter mit dem spannenden Element Quecksilber auseinandersetzen zu können.

Furthermore, I would like to thank my co-supervisor Professor Pablo León Higueras and my committee members Professor Andreas Schlenkhoff and Professor Steffen Anders for their guidance and encouragement.

Bei Professor Anders möchte ich mich zusätzlich dafür bedanken, dass wir Proben in seinem Labor aufbereiten durften, als wir noch keine geeignete Mühle hatten. Gleichermaßen möchte ich mich bei Professor Matthias Pulsfort bedanken, dessen Waagen wir nutzen konnten. Mein Dank gilt außerdem Frau Professor Helga Mölleken und Frau Dr. Birgit Schneider, die Testungen von Aufschlussverfahren ermöglicht haben. Frau Dr. Schneider danke ich darüber hinaus für die Überlassung des Mikrowellen-Aufschluss-Systems MLS 1200 Mega, das uns nach einer Reihe von Testläufen gute Dienste erwiesen hat. Ebenfalls danke ich der DMT GmbH & Co. KG für die Überlassung der MK3 Anaerobic Work Station. Nach Instandsetzung wurde sie wertvoller Bestandteil unserer Arbeit.

Also, I would like to acknowledge Professor Yong Sik Ok, Associate Professor Daniel C.W. Tsang, Associate Professor Yuxi Gao, and Associate Professor Jiating Zhao for their cooperation, support, and encouragement. Special thanks go to Jingzi Beiyuan and Yasser Mahmoud Awad. It was a pleasure to meet you and a privilege to work with you. Thank you so much for making our microcosm experiments a success.

Ich danke Frau Dr. Sibylle Mothes ganz herzlich für die Quecksilberspeziesanalytik und die vielen angenehmen und hilfreichen Telefonate.

Bedanken möchte ich mich auch bei meinen ehemaligen Arbeitskollegen vom Lehrstuhl für Boden- und Grundwassermanagement sowie bei vielen weiteren Mitarbeitern des Institutes für Grundbau, Abfall- und Wasserwesen, oder solchen, die gute Kontakte dorthin pflegten. Es war ein großes Glück für mich, dass ich auf der Arbeit von vielen netten Menschen umgeben war, die mir geholfen haben, die gegebenen Schwierigkeiten auszublenden und die mich immer bereitwillig aufgemuntert haben.

Ein besonderer Dank gilt Melanie Sichelschmidt, die stets sehr hilfsbereit war, wenn verwaltungstechnische Fragen zu klären waren, etwas organisiert werden musste, oder ich

auch beim siebten Ausfüllen der Statuserklärung für Beschäftigungen im Niedriglohnbereich Rückfragen hatte. Was mich zu der Kollegin bringt, der ich am meisten danken möchte: Liebe Tina, Du hast mir nicht nur gezeigt wie man Messungen mit dem mercur duo plus durchführt und warst immer eine phantastische Kollegin, Du hast auch meine Rahmenbedingungen grundlegend geändert. Ohne Deine Entscheidung zu wechseln hätte ich nicht Deine Haushaltsstelle übernehmen können und wäre wahrscheinlich am 31.01.2016 nach 11 Verträgen und sehr viel harter Arbeit mit wenig Zählbarem aus dem Forscherdasein ausgeschieden. Es war mein erster Arbeitsvertrag an der Universität, mit einer Laufzeit von über einem Jahr, was enorm wichtig für meine wissenschaftliche Arbeit war.

An dieser Stelle möchte mich auch sehr herzlich bei den Entscheidungsträgern bedanken, die es mir ab dem 01.08.2015 ermöglicht haben auf 75% aufzustocken.

Meiner Familie, speziell Suna Beckers, Lucas Eyl und Anke Engelhard, möchte ich für den steten Rückhalt und die positive Energie danken. Außerordentlich danke ich von Herzen meinen Eltern Marcel und Frauke Beckers, meinen Schwiegereltern Peter Roos und Ina Hoppe-Roos sowie meiner Frau Viola Roos: Was mit der Hoffnung auf DFG-Fördergelder begann, wurde zu einer Odyssee, bei der man, nüchtern betrachtet, nicht immer auf ein gutes Ende hoffen durfte. Dass ich diese Arbeit abschließen kann, habe ich vor allem euch zu verdanken. Ich danke euch für eure Unterstützung, eure Liebe, euer Vertrauen und besonders dafür, dass ihr meine Arbeit geduldet habt. Vielen Dank, ihr seid großartig! Zu guter Letzt möchte ich mich in Liebe bei meinem Sohn Enno bedanken, der mich immer mit seiner Heiterkeit beglückt hat.

Gewidmet:

Genoveva, Gerhard, Marcel und Frauke Beckers, Gudrun und Wilhelm Engelhard

sowie

Viola & Enno

Curriculum vitae

Der Lebenslauf ist in der Online-Version aus Gründen des Datenschutzes nicht enthalten.

Declaration of originality

I herewith certify that the work presented is the result of my own independent investigation. Wherever the work is indebted to the work of others, it has been acknowledged and cited. This thesis has not been accepted in substance for any other degree, nor is it concurrently being submitted in candidature or achievement of any other degree at any other university. I further declare that I have not previously made attempts to do a doctorate at any national or international university.

Selbständigkeitserklärung

Ich erkläre hiermit, dass ich die eingereichte Dissertation mit dem Titel "Mobilization, Methylation, and Ethylation of Mercury in Contaminated Floodplain Soils under Controlled Laboratory Redox Conditions as influenced by Potential Immobilizing Agents as well as Mobilization of Mercury under Field Conditions" selbständig und ohne fremde Hilfe verfasst, andere als die von mir angegebenen Quellen und Hilfsmittel nicht benutzt und die den benutzten Werken wörtlich oder inhaltlich entnommenen Stellen als solche kenntlich gemacht habe. Die vorgelegte Dissertation wurde bisher weder im Ausland noch im Inland in gleicher oder ähnlicher Form einer anderen Prüfungsbehörde vorgelegt.

Sprockhövel, 17.02.2020